NONLINEAR FEEDBACK EQUALIZATION

NONLINEAR FEEDBACK EQUALIZATION OF DIGITAL SIGNALS TRANSMITTED OVER DISPERSIVE CHANNELS

by

Desmond Patrick Taylor, B.Sc.(Eng.), M.Sc.

A Thesis

Submitted to the Faculty of Graduate Studies

in Partial Fulfilment of the Requirements

for the Degree

Doctor of Philosophy

McMaster University

May, 1972

DOCTOR OF PHILOSOPHY (1972)
(Electrical Engineering)

McMaster University
Hamilton, Ontario

TITLE : Nonlinear Feedback Equalization of Digital Signals Transmitted Over Dispersive Channels

AUTHOR : Desmond Patrick Taylor, B.Sc.(Eng.) (Queen's University, 1963)
M.Sc. (Queen's University, 1967)

SUPERVISOR : Professor A.S. Gladwin

NUMBER OF PAGES: (xii), 266

SCOPE AND CONTENTS:

A recursive nonlinear equalizer has been developed. Bayes estimation theory has been applied to obtain an optimum, unrealizable, nonlinear receiver structure for the improved reception of pulse amplitude-modulated (PAM) signals in the presence of intersymbol interference and noise. A realizable approximation to the Bayes structure was then derived as the cascade combination of a matched filter and a nonlinear recursive equalizer. The resulting receiver is known as the estimate feedback receiver.

The equalizer has been made adaptive using a new adaptive algorithm. The algorithm incorporates an extrapolation process to accelerate convergence and to maintain the equalizers frame of reference, and is constrained to cause the equalizer's parameters to always move toward their optimum values.

Computer simulations have been used to demonstrate the properties of the estimate feedback equalizer and to compare its performance to that of presently known equalizers.

ABSTRACT

This thesis deals with the problem of digital communication over noisy dispersive channels. The dispersion causes the overlapping of successive received pulses thus creating intersymbol interference which severely limits the performance of conventional receivers designed to combat only additive interference or noise.

In this thesis Bayes estimation theory has been applied to obtain a new, optimum, unrealizable receiver structure for the improved reception of noisy, dispersed, pulse amplitude-modulated (PAM) signals. By making certain approximations, a realization of this structure, known as the estimate feedback receiver or equalizer, is obtained. It consists of the combination of a matched filter and a nonlinear, recursive equalizer having, in the case of binary signals, a hyperbolic tangent nonlinearity in the feedback path. The well known decision feedback equalizer is shown to be a small noise limiting case of the estimate feedback equalizer. A saturating limiter is also considered as an approximation to the hyperbolic tangent nonlinearity.

A new adaptive algorithm for the iterative adjustment of the estimate feedback equalizer is derived. It incorporates an extrapolation process which has the purposes of accelerating convergence of the equalizer's parameters to their optimum values and of maintaining the equalizer's frame of reference. It is constrained so that the equalizers parameters always move toward their optimum values.

Computer simulations are used to demonstrate the properties of the adaptive estimate feedback equalizer and to compare them to those of presently known equalizers. When the estimate feedback equalizer is used, without a matched filter preceding it, to equalize phase distorted channels, its performance is seen to be superior to that of existing equalizers. The performance of an equalizer using a saturating limiter in place of the optimum hyperbolic tangent nonlinearity is seen to be almost as good as that of the estimate feedback equalizer.

ACKNOWLEDGEMENTS

The author wishes to thank his supervisor Dr. A.S. Gladwin for his many helpful criticisms and suggestions during the preparation of this thesis. Thanks are also due to Dr. S.S. Haykim and Dr. J. Mark for their contribution through many helpful and stimulating discussions.

The author is grateful for the generous support of the National Research Council through the award of an NRC scholarship and through the financial support of the research through NRC grant no. A-902.

Finally, the author's special thanks go to his wife Mary without whose patience this work could not have been undertaken.

TABLE OF CONTENTS

LIST OF ILLUSTRATIONS

CHAPTER 1

Introduction

In general communication theory deals with the development of systems for reliably transmitting information or data from one point to another. In modern communications systems the information is encoded into an electrical waveform or signal, and either this signal or a functional of it is then propagated through the medium from sender to receiver. Examples of such communications systems are telephone links, microwave links and short wave radio links through both the ionosphere and the troposphere.

Generally the information to be transmitted is presented to the transmitter in one of two forms. In the first it is continuous in time (examples of this are speech or music) and the resulting encoded electrical signal is continuous in time. The transmitted signal is then continuous and the overall system is known as an analogue communications link. In the second case the information is discrete in time. That is, it is presented to the transmission system as a sequence of numbers (samples) at regularly spaced time instants. The encoding process then produces a signal consisting of a sequence of bursts or pulses, one corresponding to each number. The transmitted signal is a sequence of bursts or pulses and the overall system is known as a pulse-communications system. If also each number (sample) in the information sequence can have only a finite number of possible values, the resulting system is known as a digital communications system. This is the type of system

which is of concern in the present research.

Because the transmission medium is imperfect and because there are always sources of additive interference or noise present, the signal arriving at the receiving end of a communications link is always distorted in some fashion. Therefore, it is impossible for the receiver to reproduce exactly the transmitted information. Thus the main objective of the present research is the design of a reception system which produces at its output an approximation, optimum in some sense, to the transmitted information.

1.1 Problem Outline

A commonly occurring problem in communications is that of transmitting the values of a set of message parameters or information symbols $\{s_i\}$ from one point to another. The symbols $\{s_i\}$ are to be transmitted sequentially, one every T_s seconds where T_s is known as the symbol or signalling period. The basic problem is to reproduce these symbols, as closely as possible, at the receiver. The general form of a communications system for doing this is shown in figure 1.1.

The first step in transmission of the symbols $\{s_i\}$ is to encode each member of the sequence, as it occurs, into a low-pass signal or waveform. This function is performed by the message encoder in figure 1.1. There is a variety of methods of performing the encoding, but we shall consider only the linear analogue method known as pulse-amplitude modulation (PAM). Thus each s_i, as it occurs is multiplied by the pulse-shape $q(t)$ resulting in the low-pass waveform or signal

$$m(t) = \sum_k s_k q(t-kT_s) \qquad (1\text{-}1)$$

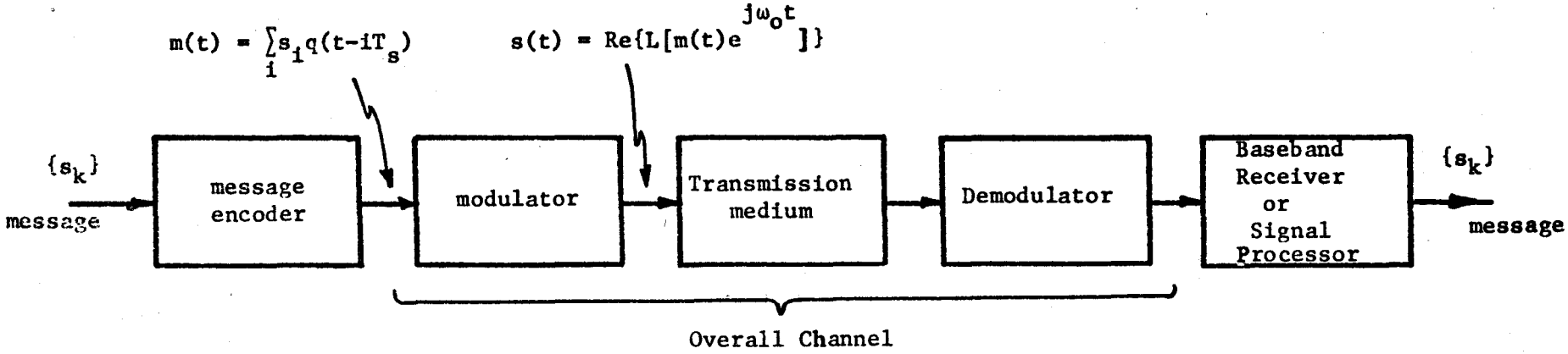

Figure 1.1 General Form of a digital communications system.

where q(t) is a finite energy pulse-shape chosen to have essentially all of its energy concentrated in a time interval T_o seconds in length where $T_o \leq T_s$. T_o is called the pulse width.

We now wish to transmit the signal m(t) over the channel, represented in figure 1.1 by the concatenation of the modulator, the transmission medium and the demodulator. In most situations of interest, it is necessary to modulate the signal m(t) onto some carrier signal for propagation through the medium. The carrier is usually a high-frequency sine wave and its frequency is dependent on the nature of the transmission medium. In this thesis we shall restrict ourselves to linear modulation processes*, and thus the transmitted signal may be written in the form

$$s(t) = \mathrm{Re}\{L[m(t)]e^{j\omega_o t}\} \qquad (1\text{-}2)$$

where $\omega_o = 2\pi f_o$ is a suitably chosen carrier frequency and L[m(t)] is a linear functional of the baseband signal m(t). By making the assumption that the modulation is linear, we may thus, in almost all cases, consider that the overall channel is linear†.

After the signal s(t) has passed through the channel, it is the task of the receiver or signal processor to recover as accurately as possible the message sequence $\{s_k\}$. In the ideal case, the signal s(t) would arrive at the demodulator completely undistorted by its passage through the medium. Demodulation and subsequent signal processing to obtain the output sequence $\{\hat{s}_k\}$ would then be a trivial operation, and

---

*We exclude, therefore, frequency and phase modulation, both of which are nonlinear.

†That is, we shall ignore any saturation or other nonlinear effects of the modulator and demodulator.

the output $\{\hat{s}_k\}$ would be identical to the transmitted sequence $\{s_k\}$.

In any realistic situation, however, the transmission medium will always distort the signal s(t), and this will cause the output sequence $\{\hat{s}_k\}$ to differ from the transmitted data sequence $\{s_k\}$. Any real transmission medium is to some extent dispersive or distorting in both time and frequency. Also in any real channel there will be additive distortion of the signal s(t). Since we have constrained the channel to be linear, it may in general be represented as the combination of a linear randomly time-varying filter and a source of additive random noise as shown in figure 1.2.

We shall represent the additive disturbance n(t) as a source of zero-mean random noise having an autocorrelation function defined as

$$R_n(t,s) = E\{n^*(t)n(s)\} \qquad (1\text{-}3)$$

where the asterisk denotes the complex conjugate. In later chapters, we will at times require n(t) to be wide sense stationary so that

$$R_n(t,s) = R_n(s-t).$$

The dispersive medium is represented by the linear time-varying filter in figure 1.2, and this filter may be represented by a randomly time-varying impulse response or weighting function

$h(t,\alpha)$ = response of the medium at time t to an impulse transmitted at time $t-\alpha$.

The medium output z(t) may then be written as the time variant convolution

$$z(t) = \int h(t,\alpha)\, s(t-\alpha)\, d\alpha \ .$$

In the time-domain the medium tends to spread or smear the signal s(t) so that a pulse in the medium output z(t) occupies a longer time

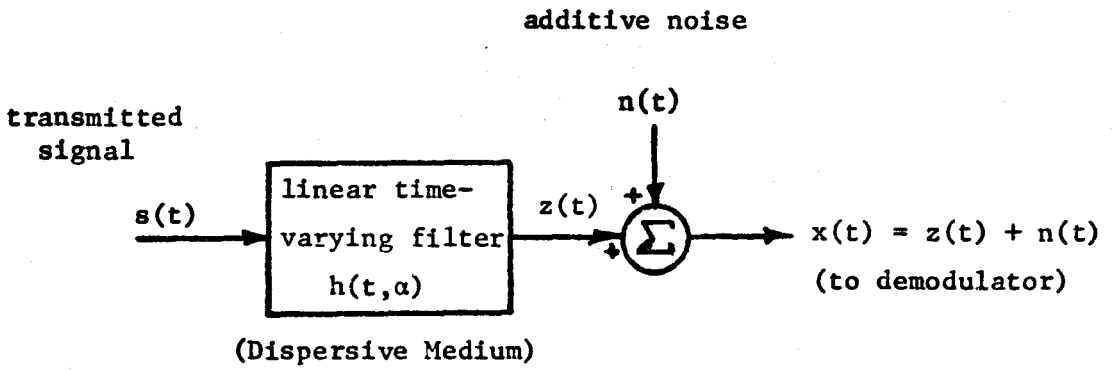

Figure 1.2 General model of a linear transmission medium or channel.

duration than the corresponding pulse in the transmitted signal s(t). This is due to the nonzero width of the channel response $h(t,\alpha)$ in the delay variable α. The pulse width was earlier specified as T_o and the symbol period as T_s. The quantity (T_s-T_o) is thus the guard space between pulses. In digital communication links when the transmission rate is high enough that the guard spaces between pulses are small $(T_s \rightarrow T_o)$ compared to the duration or delay spread of the channel pulse response, this time spreading or time dispersion will cause overlapping of two or more successive pulses. This effect is termed intersymbol interference (ISI), and it will tend to cause errors in the output sequence $\{\hat{s}_k\}$. Indeed it may be a limiting factor in the performance of the receiver since it will tend to cause errors even in the absence of additive noise.

Conceptually we may split $h(t,\alpha)$ into the sum of two components* as

$$h(t,\alpha) = h_d(t,\alpha) + h_r(t,\alpha) \qquad (1\text{-}4)$$

where we shall call $h_d(t,\alpha)$ the coherent component and $h_r(t,\alpha)$ the random component of the channel impulse response. In all cases of physical interest the term $h_d(t,\alpha)$ in equation (1-4) includes the following components of the channel impulse response:

(i) The deterministic mean-value $\bar{h}(t,\alpha)$ of $h(t,\alpha)$ which is almost always a slowly varying component, where by slowly varying we mean that it is essentially constant over time-intervals much greater than the T_s-second symbol period.

---

*We will deal with this in more detail in chapter 2.

(ii) Those randomly time varying components of $h(t,\alpha)$ which are slowly varying compared to the symbol period as explained above.

The effect of the slow time-variations in $h_d(t,\alpha)$ is to produce an aging effect in the channel response. We shall call the output signal from $h_d(t,\alpha)$ the pseudo-specular† component of the channel response. When the mean $\bar{h}(t,\alpha)$ is zero, it is actually a quasi- or pseudo-specular component, and when $\bar{h}(t,\alpha)$ is non-zero, it includes the true specular component. The effects of $h_d(t,\alpha)$ on the transmitted signal are then time dispersion causing intersymbol interference and slow aging or frequency dispersion due to its time variation.

The second component $h_r(t,\alpha)$ in equation (1-4) represents those components of $h(t,\alpha)$ which vary randomly at rates comparable to or greater than T_s^{-1}. These fluctuations tend to appear as rapid, zero-mean, random fluctuations superimposed on the pseudo-specular component $h_d(t,\alpha)$. When the signal $s(t)$ is passed through the filter represented by $h_r(t,\alpha)$ it tends to be almost completely mutilated and appears at the receiver input as signal dependent noise. Following Mark (1970) we shall call this the random scattering branch of the channel, where we include within it all severe frequency dispersive effects.

The reception problem with which we are concerned is, therefore, the recovery of the symbol sequence $\{s_k\}$ from a signal which has been transmitted through a randomly time-varying dispersive channel. From

---

†The specular component of the channel output is that component of the channel output signal which is due to the deterministic component of the channel.

the above discussion, we may summarize the limiting factors on the performance of a receiver as:

(i) intersymbol interference due to time-spread or dispersion in the channel.

(ii) slow aging or frequency dispersion due to the slowly changing nature of $h_d(t,\alpha)$.

(iii) random scattering caused by rapid random fluctuations in the random component of the channel response.

(iv) additive background noise.

The first three of these factors are signal dependent effects. They cannot be overcome by the simple expedient of increasing the transmitted signal power, since such an increase also increases the level of the interference. This is illustrated in figure 1.3 which shows curves of probability of error versus signal to additive noise ratio for both dispersive and non-dispersive channels when the receiver is a filter matched to the transmitted pulse shape.

In designing a receiver to effectively extract the message parameters $\{s_k\}$ from the received signal, the presence of intersymbol interference requires that the receiver incorporate memory or delay into its structure. Similarly the presence of Doppler-spreading or frequency dispersion requires that the receiver be time-varying in order to be able to track and compensate for time-varying effects. This last implies that in effect a good receiver should be adaptive.

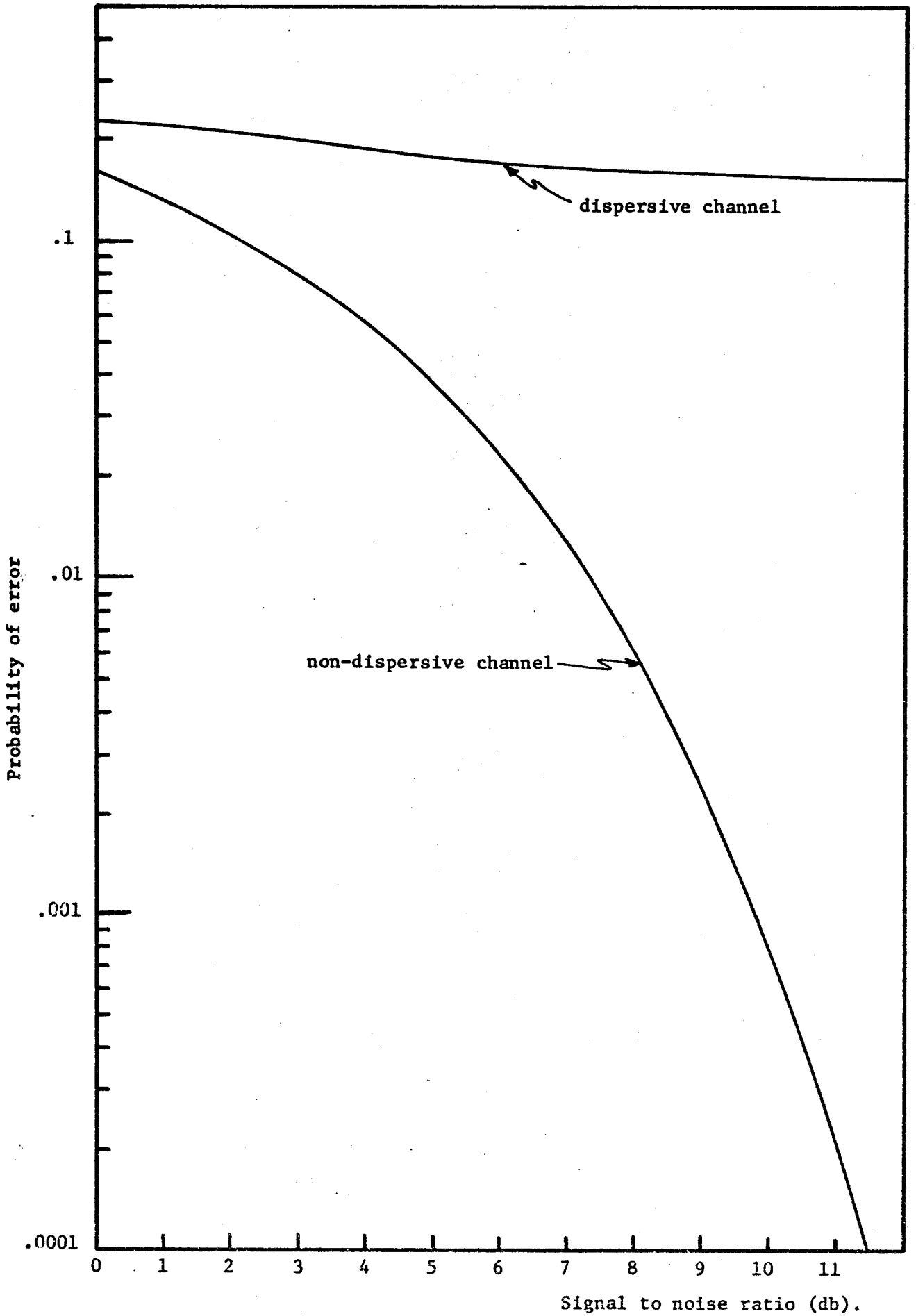

Figure 1.3 Probability of error curves for a matched filter receiver showing the effect of a dispersive channel, obtained by simulation.

1.2 Previous Work in Communication Through Random Media

The signal distortions due to additive noise and the dispersive effects of the transmission medium are inherently statistical in nature. Recognition of this fact has given rise to a mathematical theory of communication. Two approaches to the communications problem have been developed. The first is Information theory which was introduced by Shannon (1948) and the second is statistical communication theory which was introduced by Wiener (1949).

Information theory is a mathematical theory which deals in the main with mathematical models and not with physical systems or channels. Its main emphasis is on probability theory and algebraic models which are primarily concerned with coding and decoding. It has also been very useful in establishing several bounds on communication system performance, one of the most useful of which is the expression for channel capacity

$$C = B_{ch} \log_2\left(1 + \frac{P_s}{N_o B_{ch}}\right) \qquad \text{bits/sec.}$$

of a bandlimited channel where

B_{ch} is the bandwidth of the channel.

P_s is the available transmitter power.

N_o is the power spectral density of the additive noise, assumed here to be white and Gaussian. C represents the theoretical upper limit on the rate at which data can be transmitted over the channel at a vanishingly small error-rate, and one of the concerns of information theory is the construction of codes which allow a system to approach this bound.

Statistical communication theory, on the other hand deals with physical signals and channels and is concerned with the problem of extracting a signal or some function of it from a noisy, distorting background in some optimum way. Wiener's (1949) work was mainly concerned with the design of linear filters for extracting a statistically stationary signal from a stationary noise background in such a way that the mean-square error between the actual and the desired signal is minimized. This work has lead to a wide class of statistical optimization techniques and optimum systems so obtained (Zadeh and Ragazzini, 1950; Kalman, 1960; Kalman and Bucy, 1961).

In digital communications, the members of the information sequence $\{s_k\}$ can each have only one of a finite number of values, and thus in any signalling interval only one of a finite number of possible signals may be transmitted. The truly optimum receiver, in this situation, is that receiver which minimizes the probability of error at its output. In essence, such a receiver produces at its output a decision in each signalling interval as to which possible value was transmitted and the optimum receiver, therefore, minimizes the probability of decision error. The problem of synthesizing such optimum receivers is one of the main ones in communication theory, and its complexity is intimately bound up with the complexity of the channel model which is assumed.

In the classical case, the transmission medium is assumed to be non-distorting or non-dispersive. The only source of signal distortion is then the additive noise. If the noise is Gaussian and signal independent, then the minimum probability of error receiver is a parallel set of matched filters, one matched to each possible transmitted signal,

followed by a decision circuit which chooses the value of the received symbol $\hat{s}_k$ to be that which corresponds to the matched filter having the largest output. An excellent summary of the theory surrounding this derivation is given by Hancock and Wintz (1966).

For the case of randomly time-varying multipath channels Turin (1956) derived the minimum probability of error receiver under the assumption that the rate of time variation is slow compared to the length of a signal pulse. Also Turin considered only the case where the transmission rate is slow enough that channel delay-spread or time-dispersion does not cause intersymbol interference, and therefore the receiver needed to be optimized over only a single signalling interval. Kailath (1960, 1961) has generalized and extended these results to the case of any randomly time-variant channel, where the channel impulse response consists, in general, of a time-invariant mean-value or specular component and a zero-mean randomly time-variant component. Kailath also assumed that there was no intersymbol interference between the pulses in successive signalling intervals. When, in addition, both the channel and the additive noise are assumed to have Gaussian statistics, Kailath found that the minimum probability of error receiver is a parallel bank of estimator-correlator structures, of the type shown in figure 1.4, followed by suitable decision circuitry, where one estimator-correlator is required for each possible transmitted signal.

In all of the above discussion, the channel was assumed to cause no intersymbol interference, and in each case the minimum probability of error receiver could be found. However, when the transmission rate is high enough or the delay spread of the medium is great enough that

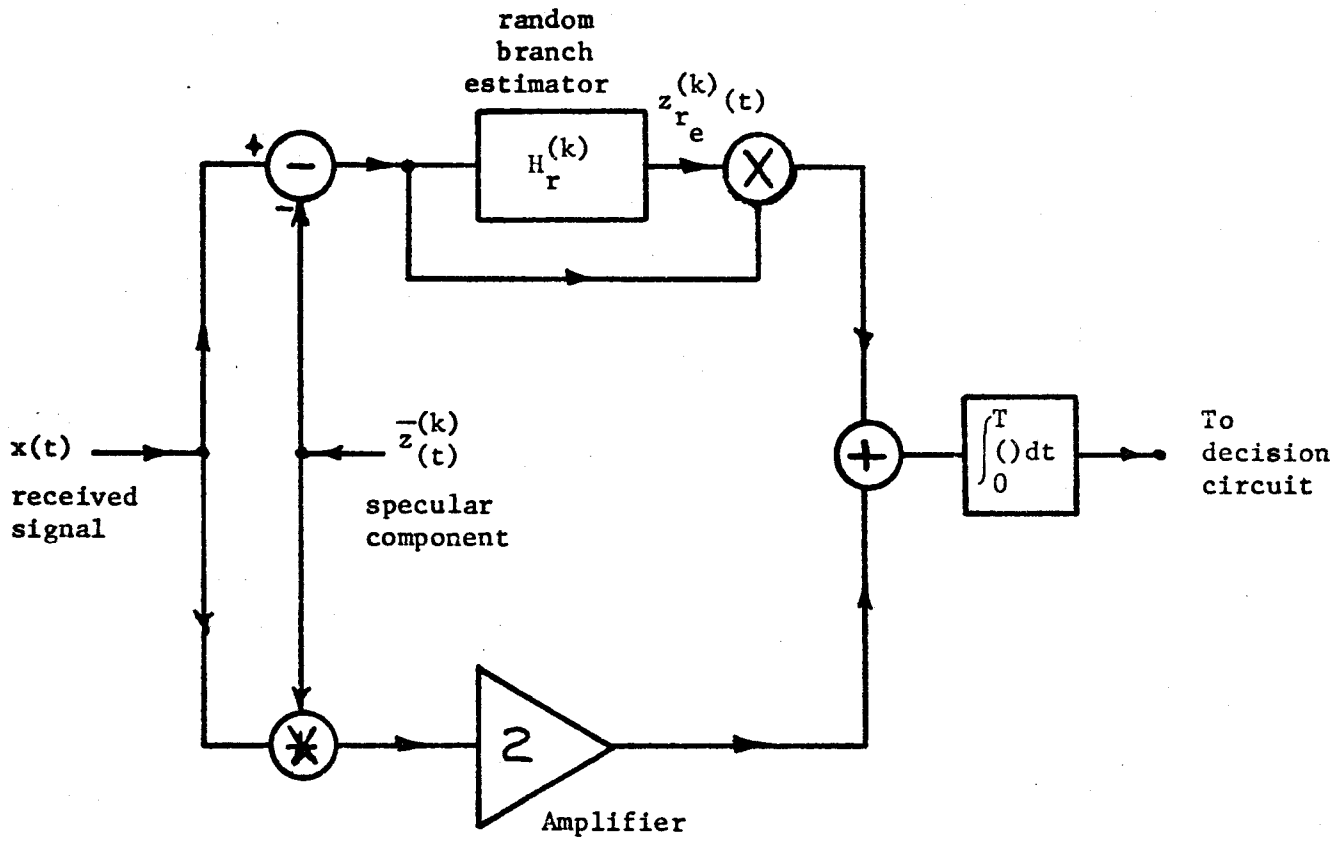

Figure 1.4 Estimator correlator structure for kth branch of receiver for randomly time-varying channels (Kailath, 1960).

significant intersymbol interference is present in the received signal, then the derivation of the minimum probability of error receiver becomes almost impossibly difficult. Under certain restrictive assumptions Bowen (1969) has derived the Baye's minimum probability of error receiver for a time-invariant dispersive channel. The resulting structure is nonlinear and very difficult to implement. Thus in order to obtain receiver structures which may readily be implemented, we are forced to place constraints on the class of allowable receiver structures, and to consider performance criteria other than the probability of error under which to optimize the receiver.

In the case of an exactly known, time-invariant, linear channel and PAM transmitted signals, Tufts (1963) and George (1965) have shown that the linear receiver which minimizes the mean-square error $E\{(s_k - \hat{s}_k)^2\}$ between the desired symbol s_k and the actual received value $\hat{s}_k$ at the times $t = kT_s$ $(-\infty < k < \infty)$ consists of a filter matched to the shape of an individual channel output pulse followed by an infinite length transversal filter having its taps spaced T_s seconds apart. Coll (1966) derived a finite form of this receiver and showed that a very good approximation to it may be obtained with the use of only a moderate number of taps on the transversal filter.

Now it can be shown that the main purpose of the matched filter is to minimize the adverse effects of the additive noise and that of the transversal filter to compensate for the intersymbol interference introduced by channel time-dispersion. The transversal filter in this situation is known as an equalizer, since, at least in the absence of noise, its function is to make the overall channel between the encoder

and the decoder look like an all-pass filter, which of course does not cause intersymbol interference. In the particular case when the desired information symbols $\{s_k\}$ are quantized such that each may have only a finite number of values, the equalizer is followed by a detection or decision circuit.

Because in most cases of interest the channel, even when it is time-invariant, is unknown and because the additive noise is small in most point-to-point communications situations, considerable work has been done on the use of an equalizer with no matched filter preceding it. The main emphasis in this work has been on the synthesis of self-adjusting or adaptive equalizers which can automatically adjust themselves to compensate for the unknown channel characteristics.

Lucky (1965) developed an equalizer of the transversal filter type which operated to force zeros in the overall channel impulse response at all points which are a multiple of T_s seconds away from the present time. Lucky derived an iterative steepest descent algorithm which when a known reference signal is transmitted automatically adjusts the equalizer to its optimum operating point. In a later paper, Lucky (1966) used the same algorithm in a decision-directed* or tracking mode to track a slowly time-varying channel. The equalizer developed by Lucky has the advantage that in the absence of noise it will completely eliminate intersymbol interference. However, its performance deteriorates

---

*In the decision-directed mode an adaptive system uses its own output to further adjust itself. This in effect provides us with a performance-feedback system.

rapidly with increased additive noise, since the performance criterion being used does not take noise into account.

Various authors, among them Lucky and Rudin (1967), Gersho (1969), Di Toro (1968) and Proakis (1969), have developed equalizers of the transversal filter type using a minimum mean-square error performance criterion. That is the tap-gains of the transversal filter are set so as to minimize the mean-square error $E\{(s_k - \hat{s}_k)^2\}$ at the times $t = kT_s$ $(-\infty < k < \infty)$. In each case an iterative steepest descent or gradient-following algorithm was used to adjust the filter gains to the optimum operating point. The use of the mean-square error performance criterion has the advantage that it takes the presence of noise into account, and therefore this equalizer is not quite as sensitive to additive noise as the zero-forcing one.

Another form of the minimum mean-square error adaptive equalizer has been obtained by Proakis (1971), who used z-transform techniques to obtain the equalizer structure as a parallel bank of comb filters. This equalizer is also used in conjunction with a steepest-descent algorithm.

Mark (1970) has made use of feedback to obtain a linear feedback equalizer. This structure has the advantage of having infinite memory into the past. Mark also developed an improved adaptive algorithm which by use of a form of learning process obtains improved convergence to the optimum, minimum mean-square error operating point.

In order to improve on the operating characteristics of the conventional linear equalizer, such as those discussed above, Austin (1967) developed the decision feedback equalizer which makes use of its

own previous decidions* to aid in making the present decision. It does this by using these previous decisions (assuming them correct) to coherently subtract out the interference due to past symbols. George et al (1971) and Monsen (1971) have since made this structure adaptive using steepest descent techniques. It has been shown that when the signal to additive noise ratio is greater than about 6 db, the decision-feedback receiver yields better error-rate performance then the linear receiver.

In the above, we have discussed briefly the development of optimum receivers for the randomly time-variant channel and for the time-invariant, time-dispersive channel. Realistically, however, any transmission medium is both randomly time-varying and time-dispersive. Because they are adaptive, the equalizers described above work very well when the channel is such that its rate of time-variation is less than the transmission rate T_s^{-1}. In terms of the channel impulse response in equation (1-5), this means the adaptive equalizer preceded by a matched filter is essentially the optimum receiver, when the channel impulse is essentially given by its (pseudo) specular component $h_d(t,\alpha)$. However, when the random scattering component $h_r(t,\alpha)$ becomes large, it must be taken into account and its presence will affect the optimum receiver structure.

As above, because the channel is time-dispersive it is very

---

*The decision feedback equalizer is constrained to operate only on digital signals; that is the members of the information sequence $\{s_k\}$ are each constrained to have only a finite number of possible values.

difficult to derive the minimum probability of error receiver, and hence most investigation has been confined to finding the optimum linear receiver, usually with a minimum mean-square error performance criterion. For the randomly time-varying, time-dispersive channel Kaye (1968) has derived the optimum linear receiver under a minimum mean-square error criterion. He has shown it to consist of a filter followed by a linear equalizer. The form of the filter is of interest. It can be seen (Kaye, 1968) to be matched to the shape of a pulse output from the specular branch of the channel in a noise background consisting of the additive background noise and the signal-dependent "noise" output from the random branch of the channel. This filter appears in the receiver following the demodulator but preceding any further signal processing. Kaye showed that it does nothing to combat the effects of time-dispersion or the slow aging of the specular component of the channel response. In a later work Mark (1970) derived an adaptive form of this filter, and thus by cascading the adaptive filter and an adaptive equalizer, a completely adaptive receiver for reception of digital signals transmitted over randomly time-invariant dispersive channels is obtained.

1.3 Scope of the Thesis

In this thesis, we shall concern ourselves with the investigation of an improved technique for the reception of digital signals. In particular, we shall derive and evaluate a new nonlinear receiver structure (the conditional Bayes receiver) for the extraction of digital information or data from signals which have been transmitted over slowly time-varying dispersive channels. We shall be mainly concerned with

compensating for or equalizing the dispersive effects of the channel. The systems required for this are known as equalizers, and the novel nonlinear equalizer which we shall consider, known as the estimate feedback equalizer is a realizable approximation to the abovementioned conditional Bayes receiver.

In chapter 2, we shall discuss briefly the transmitted signal and suitable pulse shapes for digital symbol transmission. We shall then discuss a model for the channel and the determination of those of its parameters which are pertinent to the present reception problem. We shall also discuss the demodulation of the received signal to obtain a baseband signal at the equalizer input.

Chapters 3 and 4 contain the main theoretical results of the thesis. In chapter 3, we shall apply Baye's estimation theory to obtain a novel optimum receiver structure known as the conditional Bayes receiver or estimation structure. This optimum receiver is unrealizable, and therefore we shall derive a realizable, sub-optimum approximation to it. This results in a novel, nonlinear feedback equalizer which we shall call the estimate feedback equalizer. In chapter 4, we shall derive a new adaptive algorithm for iteratively controlling the estimate feedback equalizer, and will suggest means of mechanizing this algorithm. The main contributions of the present work thus lie in the derivation of the new conditional Bayes receiver and its approximate realization and in the development of a new adaptive, nonlinear estimate feedback equalizer having performance superior to that of existing equalizers.

In chapter 5, we shall evaluate, by means of computer simulation, the performance characteristics of the adaptive estimate feedback equalizer and will compare them to those of existing equalizers.

CHAPTER 2

Signal Transmission and the Channel

Before we can deal with the problem, outlined in chapter 1, of receiving a digital signal which has been transmitted over a dispersive channel, we must first consider the form of the transmitted signal and the channel over which it is to be transmitted.

We are dealing with pulse or digital signals, and the transmitted signal may thus be represented as a sequence or train of pulses. We want to transmit these pulses at as high a rate as possible using pulses which are not too sensitive to the distorting effects of the channel, and with virtually no interference (overlap) between successive pulses at the transmitter. Therefore some attention must be given to choosing the transmitted pulse shape.

For efficient digital communication, the receiver must maintain time-synchronism and phase-coherence with the transmitted signal. To maintain phase-coherence the receiver must recover the received carrier phase and use it in demodulating the bandpass received signal to obtain a low-pass or baseband pulse-train. This is known as coherent demodulation. The maintaining of time-synchronism is essentially the maintaining of delay-lock with the low-pass envelope of the transmitted signal. To recover the digital information from the received signal, the receiver must make some form of estimate or decision once in each symbol period. By maintaining time synchronism, the receiver knows when in each symbol

period to make its estimate or decision. In the present research, we shall assume perfect time-synchronism is being independently maintained.

The maintaining of time-synchronism and phase-coherence by the receiver and the compensation for other distorting effects of the channel requires knowledge of the channel characteristics. Thus, in order to design a reliable receiver consideration must be given to developing a satisfactory model for the channel, and to determining those of its parameters which affect reception.

2.1 The Transmitted Information and the Baseband Signal

We are dealing with the communication of digital information, and thus the transmitted information may be represented as a sequence of parameters or symbols $\{s_k\}$ each of which has a value ξ_i which is a member of the finite set $(\xi_1, \ldots, \xi_m)$ of $m \geq 2$ possible values. Each symbol s_k $(-\infty < k < \infty)$ is to be transmitted during the corresponding T_s-second symbol period

$$(k - \tfrac{1}{2})T_s \leq t \leq (k + \tfrac{1}{2})T_s \quad (-\infty < k < \infty)$$

as one of the m possible values ξ_i $(i = 1,\ldots,m)$.

At the receiver, the objective during each symbol period is the recovery of the corresponding transmitted symbol. That is, during say the nth symbol period

$$(n - \tfrac{1}{2})T_s < t < (n + \tfrac{1}{2})T_s \quad (-\infty < n < \infty)$$

the receiver attempts to recover the value of the symbol s_n transmitted

in that interval. The value of each s_n is, of course, unknown a priori at the receiver, and thus for reception purposes, the symbols s_n can be specified only in a statistical sense.

We shall be concerned only with symbol by symbol reception. The receiver then treats each symbol as if it were independent of all others. We shall, therefore, assume the transmitted information $\{s_k\}$ is a sequence of statistically independent, equiprobable, m-ary symbols having the properties

$$P[s_k = \xi_i] = \frac{1}{m} \qquad \begin{matrix}(-\infty < k < \infty) \\ (i = 1,\ldots,m)\end{matrix} \tag{2-1}$$

$$E\{s_k\} = 0 \qquad (-\infty < k < \infty) \tag{2-2}$$

$$E\{s_j s_k\} = \sigma_s^2 \delta_{j,k} \qquad (-\infty < j,k < \infty) \tag{2-3}$$

where $P[\cdot]$ is a probability, $\delta_{j,k}$ is the Kronecker delta and σ_s^2 is the symbol variance.

For transmission the symbols $\{s_k\}$ must be encoded into electrical waveforms or signals. As stated in chapter 1, we are considering only the linear analogue method of encoding known as pulse-amplitude modulation (PAM). It consists of multiplying each symbol s_k by a suitable time translated pulse shape $q(t-kT_s)$. This produces the low-pass or baseband signal

$$m(t) = \sum_k s_k q(t-kT_s) \tag{2-4}$$

which is a train or sequence of amplitude modulated pulses, where the pulse $q(t-kT_s)$ corresponding to the symbol s_k in the kth symbol period

$$(k - \tfrac{1}{2})T_s \leq t \leq (k + \tfrac{1}{2})T_s \qquad (-\infty < k < \infty)$$

has the following properties:

(i) Its center of mass is located at $t = kT_s$. For all commonly used pulse shapes this implies that the peak value is located at $t = kT_s$.

(ii) It has a finite value lasting for $T_o \leq T_s$ seconds. This implies a guard space of $(T_s - T_o)$ seconds between successive pulses, T_o being known as the pulse width.

(iii) It has finite energy Eq defined as

$$Eq = \int_{kT_s - T_o/2}^{kT_s + T_o/2} q^2(t - kT_s)\,dt = \int_{-T_o/2}^{T_o/2} q^2(t)\,dt < \infty \qquad (-\infty < k < \infty) \qquad (2\text{-}5)$$

The choice of the pulse shape q(t) is of some importance, particularly since we wish to transmit at very high pulse-rates (very small or zero guard spaces), and much effort has been devoted to finding optimum* pulse shapes. The classical work in this area is due to Nyquist (1928). He recognized that a decision as to the value of each received symbol needs to be made only once in each symbol period. Thus if a pulse shape q(t) can be found which has its peak value at the time when the decision is made and is zero at all other decision times, then

---

*Optimum implies here that the pulses have been chosen so that there is minimum inter-pulse interference or overlap at the transmitter, and also the pulses are relatively insensitive to the distorting effects of the channel.

whether or not this pulse shape overlaps or interferes with other pulses is immaterial since there is zero interference at the sampling times. Nyquist showed that for the ideal bandlimited channel having the frequency response

$$H(f) = \begin{cases} 1 & |f| < \frac{1}{2T_s} \\ 0 & \text{elsewhere} \end{cases}$$

intersymbol interference free transmission can be obtained at pulse repetition frequencies up to $1/T_s$ Hz using time translates of the pulse shape

$$q(t) = \frac{\sin \pi(\frac{t}{T_s})}{\pi \frac{t}{T_s}}$$

This work was later extended to more realistic channels and pulses by Gibby and Smith (1965) who, by defining an equivalent Nyquist channel, found a set of conditions defining the "Nyquist" type of pulse (zero intersymbol interference at the sampling points) for quite general channels. Unfortunately, these pulses are usually quite difficult to generate and also tend to be subject to rather severe distortion when the channel response varies from the nominal one.

Another approach to the above problem is due to Tufts (1963) who showed that when the channel is known, its dispersive effects may be equalized or compensated for by proper choice of the pulse shape q(t). Also under certain conditions when the channel is known, it is possible to perform a joint optimization of the transmitted pulse shape and the

receiver (Tufts, 1963; George et al., 1969). However, when the channel is unknown, as it usually is, these optimizations require a nearly distortionless feedback path from receiver to transmitter. Such a path is seldom available, and the usual practice is to choose some fixed pulse-shape q(t) and to perform all equalization functions at the receiver. The main constraint on this choice of pulse shape q(t) is that it should have essentially all its energy confined to a duration or pulse width of $T_o \leq T_s$ seconds. There will then be negligible overlap or intersymbol interference between adjacent pulses in the baseband signal m(t). Typical choices of the pulse-shape q(t) are the rectangular, the Gaussian and the raised cosine shapes. These are indicated below:

(i) rectangular

$$q(t) = \begin{cases} 1 & -\frac{T_o}{2} \leq t \leq \frac{T_o}{2} \\ 0 & |t| > \frac{T_o}{2} \end{cases} \qquad (T_o \leq T_s)$$

(ii) raised cosine

$$q(t) = \begin{cases} \frac{1}{2}(1 + \cos\frac{2\pi t}{T_o}) & -\frac{T_o}{2} \leq t \leq \frac{T_o}{2} \\ 0 & |t| > \frac{T_o}{2} \end{cases} \qquad (T_o \leq T_s)$$

(iii) gaussian

$$q(t) = e^{-Bt^2} \qquad B = \text{constant.}$$

As far as most of the work in this thesis is concerned, we do not need to consider a specific pulse shape. We need only to describe q(t) as a pulse of width $T_o \leq T_s$ having finite energy Eq, as defined in

equation (2-5).

In any given symbol period say the kth,

$$(k - \tfrac{1}{2})T_s < t < (k + \tfrac{1}{2})T_s, \qquad (-\infty < k < \infty)$$

the transmitted signal is $s_k\, q(t-kT_s)$ where the value of s_k is a member of the finite set $(\xi_1,\ldots,\xi_m)$ of possible values. There are thus m signals

$$\begin{aligned} g_1(t-kT_s) &= \xi_1\, q(t-kT_s) \\ &\vdots \\ g_m(t-kT_s) &= \xi_m\, q(t-kT_s) \end{aligned}$$

which may be transmitted during the kth symbol period. These m signals may be considered as vectors in a linear vector or signal space.

For information to be transmitted we must have $m \geq 2$, and to obtain the most reliable reception we want the distance between these signals considered as members of the signal space to be as great as possible. One measure of this distance is the correlation between the various members $g_i(i=1,\ldots,m)$ of the signal set, the distance between signals being a maximum when the correlation is a minimum. In the particular case when all the signals g_i $(i=1,\ldots,m)$ have the same energy, Nuttall (1962) has derived a lower bound on this correlation as

$$\lambda \geq \frac{-1}{m-1} \tag{2-6}$$

where the correlation λ is defined as

$$\lambda = \frac{1}{E_g} \int g_i(t) g_j(t)\, dt \qquad (i,j = 1,\ldots,m)$$

Also it is known (Balakrishnan, 1960) that this bound can be achieved only with an equal energy signal set. In the case of amplitude modulated signals, an equal energy signal set can only be obtained in the case of binary signals using antipodal symbol values. For example if we use the symbol values ±1, we then have an equal energy binary signal set, and in this case the bound of equation (2-6) is met.

In this thesis, unless we state otherwise, we shall always assume that the transmitted symbols are independent and binary with the values ±1. In this case equations (2-1) to (2-3) reduce to the form

$$P[s_k = \xi_i = \pm 1] = \frac{1}{2} \qquad i = 1,2 \qquad (-\infty < k < \infty) \tag{2-7}$$

$$E\{s_k\} = 0 \qquad (-\infty < k < \infty) \tag{2-8}$$

$$E\{s_i s_j\} = \delta_{i,j} \qquad (-\infty < i,j < \infty) \tag{2-9}$$

and these are the properties which will be used throughout most of the present research.

2.2 The Transmitted Signal

In some communication links, notably coaxial cable links and short distance telephone links, the signal is transmitted through the channel at baseband. The transmitted signal is then the low-pass or baseband signal m(t) of equation (2-4). However in many situations of interest the signal m(t) must be modulated onto some carrier signal (usually a high frequency sinusoid) for propagation through the channel.

This modulation process is essentially a transformation of m(t) to a different portion of the frequency spectrum - for example the signal m(t) is transformed from the low-pass or baseband form of equation (2-4) to a bandpass form. The modulation may be a linear process as in amplitude modulation or a nonlinear process as in frequency or phase modulation. In this thesis we will restrict ourselves to linear modulation, in which case the transmitted signal may be written in the general form

$$s(t) = 2\ \mathrm{Re}\{L[m(t)]e^{j\omega_o t}\} \qquad (2\text{-}10)$$

where $\omega_o = 2\pi f_o$ is the nominal carrier frequency, L[m(t)] is a linear functional of the baseband modulating signal and the factor of 2 is included for later convenience*. Examples of the forms which L[m(t)] may take are:

(i) L[m(t)] = const + m(t) implying that s(t) is double sideband amplitude modulation (DSB-AM).

(ii) L[m(t)] = m(t) implying that s(t) is double sideband suppressed carrier amplitude modulation (DSBSC-AM).

(iii) L[m(t)] = m(t) + $j\hat{m}(t)$ where $\hat{m}(t)$ is the Hilbert transform of m(t) and s(t) is then single sideband amplitude modulation (SSB-AM).

A good summary of linear modulation schemes is given by Lucky (1968).

---

*The inclusion of this factor allows us to avoid multiplying the channel output signal by a constant factor of ½ in later equations.

In the present work, we shall assume that we are dealing with DSBSC-AM. The transmitted signal may then be written in the simple form

$$s(t) = 2\ \mathrm{Re}\{m(t)e^{j\omega_o t}\} \qquad (2\text{-}11)$$

where m(t) is real. In the case of binary antipodal symbols having the values ±1 and rectangular pulses q(t) of width $T_o = T_s$, this form of modulated signal is equivalent to a bi-phase, phase-modulated signal.

2.3 Channel Considerations

In any real communications link the effects of the channel on signals passing through it are usually unknown and uncontrollable. Therefore most communications channels can be specified only in a statistical sense. The task of the receiver is then to compensate, in some optimum fashion, for the effects of the channel so that the transmitted information can be successfully extracted from the received signal.

Considerable effort has been devoted to the problem of channel characterization and to the measurement of its parameters. Some of the more noted investigators in the field have been Turin (1956), Kailath (1960) and Bello (1963). The work of these investigators and others has recently been collated and published by Kennedy (1969).

In the classical formulation of reception problems, the channel was modelled as a linear all-pass system with constant delay and a source of additive random noise n(t). The received signal then had the form

$$y(t) = s(t) + n(t)$$

where s(t) is the transmitted signal, and from this we see that the only source of interference is the additive noise. Unfortunately, such a model conforms to reality in only a few special cases.

In this section we will consider a more realistic model for the channel. The theory to be discussed has been developed with natural media such as the ionosphere and the troposphere in mind, but it applies equally well to any linear communications channel.

Signal transmission through these natural media is unavoidably characterized by simultaneous propagation along many different and usually time-varying paths which are usually impossible to resolve. Such a channel, provided it is assumed to be linear, may be represented as a linear time-varying filter (Bello, 1963; Schwartz, Bennett and Stein, 1966). This filter may be characterized by its impulse response function

$h(t,\tau)$ = output from the channel at time t due to an impulse input applied at time $t-\tau$.

For a transmitted signal s(t) we may then write the channel output signal as

$$z(t) = \int h(t,\xi)\, s(t-\xi)\, d\xi \qquad (2\text{-}12)$$

where the limits of integration are assumed to be suitably defined.

Now we are interested only in transmission of signals s(t) of the form given by equation (2-11) where the bandwidth of the envelope m(t) is assumed to be less than the nominal carrier frequency ω_o. The transmitted signal s(t) is then a narrowband bandpass signal, and the complex signal

$$\zeta(t) = m(t)e^{j\omega_o t} \tag{2-13}$$

is analytic. We, therefore, need to define the channel impulse response $h(t,\tau)$ only over the bandwidth of $s(t)$, and we may thus write it in the same narrow-band form as

$$h(t,\tau) = \mathrm{Re}\{g(t,\tau)e^{j\omega_o \tau}\} \tag{2-14}$$

where the low-pass envelope $g(t,\tau)$ is usually complex. Then using the properties of analytic signals (Dugundji, 1958) we may write the channel output signal $z(t)$ in the form

$$z(t) = \mathrm{Re}\{e^{j\omega_o t} \int g(t,\xi)m(t-\xi)d\xi\} \tag{2-15}$$

Except for the carrier frequency ω_o contained in the exponential factor, $z(t)$ is completely determined by its complex low-pass envelope

$$\eta(t) = \int g(t,\xi)m(t-\xi)d\xi \ . \tag{2-16}$$

We may, therefore, describe the channel and analyze its properties in terms of the complex, equivalent, low-pass impulse response $g(t,\xi)$.

If a frequency-domain approach to the channel is adopted (Kailath, 1960a), an equivalent representation for $\eta(t)$ may be obtained as

$$\eta(t) = \int M(f)\ G(t,f)e^{j2\pi ft}\ df \tag{2-17}$$

where $M(f)$ is the Fourier transform of the signal envelope $m(t)$ and $G(t,f)$ is known as the equivalent low-pass, time-varying transfer function of the channel. Bello (1963) has shown that $G(t,f)$ is related to the impulse response $g(t,\xi)$ by the Fourier transform relationship

$$G(t,f) = \int g(t,\xi)e^{-j2\pi f\xi}\, d\xi \ . \qquad (2\text{-}18)$$

The manner in which $g(t,\xi)$ and $G(t,f)$ vary with time t determines the Doppler shifting and spreading properties of the channel. Similarly, the time-dispersive properties are determined by the non-zero width or spread of $g(t,\xi)$ in the delay variable ξ, or equivalently by the finite bandwidth of $G(t,f)$ in the frequency or f-domain. Bello (1963) and Kaye (1968) have defined other system functions for describing the properties of a linear, time-varying, dispersive channel, but we will not go into them here.

So far, we have described the channel in terms of system functions such as the impulse response $g(t,\xi)$ and the corresponding transfer function $G(t,f)$. In general, however, communications channels are randomly time-varying. The system functions $g(t,\xi)$ and $G(t,f)$ are then sample functions from stochastic processes and the channel can be described only in a statistical sense.

A complete statistical characterization of the channel requires the specification of multidimensional probability distributions for the channel system functions. This has been done for the case when the various propagation paths are resolvable (the discrete multipath channel) and the channel statistics can be assumed to be Gaussian (Turin, 1956). In general, however, these functions are very difficult to either measure or compute, and moreover, the channel is often non-stationary so that the distributions evolve with time.

All the systems to be considered in this thesis use a minimum mean-squared error performance criterion. This implies that only a second moment characterization of the channel is required. Therefore, in this section, we shall consider only the mean value and correlation functions of the channel system functions.

Since for any channel, we can observe only its output $z(t)$, we shall begin by finding the mean value and correlation functions of $z(t)$ assuming a deterministic transmitted signal $s(t)$ of the form given in equation (2-11). Using equation (2-15), we may write the mean value function $\bar{z}(t)$ of $z(t)$ in the form

$$\bar{z}(t) = E\{z(t)\} = E\{\mathrm{Re}[e^{j\omega_o t}\int g(t,\xi)m(t-\xi)d\xi]\}. \tag{2-19}$$

In any real channel

$$\int |g(t,\xi)|^2 d\xi < \infty \qquad (-\infty < t < \infty)$$

and if we then define

$$\bar{g}(t,\xi) = E\{g(t,\xi)\} \tag{2-20}$$

we may write the mean channel output as

$$\bar{z}(t) = \mathrm{Re}\{e^{j\omega_o t}\int \bar{g}(t,\xi)m(t-\xi)d\xi\} \tag{2-21}$$

and the corresponding complex low-pass signal as

$$\bar{\eta}(t) = \int \bar{g}(t,\xi)m(t-\xi)d\xi \tag{2-22}$$

The mean channel output $\bar{\eta}(t)$ (or $\bar{z}(t)$) is known as the specular component of the channel response. It is the channel output signal which

would be obtained if the signal m(t) (or s(t)) were transmitted through a channel having the mean impulse response $\bar{g}(t,\xi)$ (or equivalently $\bar{h}(t,\xi)$). Another representation for $\bar{\eta}(t)$ is obtained from equation (2-17) as

$$\bar{\eta}(t) = \int M(f)\ \bar{G}(t,f)e^{j2\pi ft}\ df \tag{2-23}$$

where $\bar{G}(t,f)$ is known as the mean transfer function.

Now let us find the autocorrelation function of the complex (low-pass) channel output $\eta(t)$. This function is defined by

$$R_\eta(t,s) = E\{\eta^*(t)\eta(s)\} \tag{2-24}$$

where the asterisk denotes the complex conjugate. Substituting equation (2-16) into equation (2-24) and interchanging the order of averaging and integrating, we obtain

$$R_\eta(t,s) = \iint E\{g^*(t,u)g(s,v)\}\ m^*(t-u)m(s-v)du\ dv \tag{2-25}$$

The expectation in equation (2-25) is the autocorrelation function of the complex equivalent low-pass channel impulse response $g(t,\xi)$. For notational convenience, let us write it as

$$R_g(t,s;\ u,v) = E\{g^*(t,u)g(s,v)\} \tag{2-26}$$

and then equation (2-25) becomes

$$R_\eta(t,s) = \iint R_g(t,s;\ u,v)\ m^*(t-u)m(s-v)du\ dv \tag{2-27}$$

Using the properties of analytic signals we may readily relate $R_\eta(t,s)$ to $R_z(t,s)$, the autocorrelation function of the physical channel output, by the relationship

$$R_z(t,s) = \frac{1}{2}\,\mathrm{Re}\{R_\eta(t,s)e^{j\omega_o(s-t)}\} \qquad (2\text{-}28)$$

The autocorrelation function of the equivalent low-pass transfer function $G(t,f)$ may be found from $R_\eta(t,s)$ using a Fourier transform relation due to Bello (1963), and we thus obtain

$$R_G(t,s;f,\ell) = \iint R_g(t,s;u,v)e^{j2\pi(uf-\ell v)}\,du\,dv. \qquad (2\text{-}29)$$

In principle, the mean value and autocorrelation functions derived above are sufficient to provide a second order statistical model for the channel. However, because we are interested only in the reception of digital signals, we can make certain simplifications in the model.

Digital communication systems are characterized by the fact that in each T_s-second signalling or symbol period one of a finite number of possible signals, each of maximum duration T_s seconds is transmitted. When we consider the effects of the channel on digital signal transmission, most channels may be considered to be wide sense stationary over time and frequency intervals much greater than the effective duration and bandwidth of the digital signalling waveforms (Bello, 1963). This situation arises in the following cases:

(i) In telephone and other cable links, the channel impulse response tends to be almost time-invariant with very slow and relatively small fluctuations about this constant value.

(ii) In radio links the channel usually contains slow (and possibly non-stationary) fluctuations on which are superimposed much more rapid fluctuations which are wide sense stationary in both time

and frequency.

In this context, slowly fluctuating means essentially constant over periods much greater than the symbol period of T_s seconds in the time domain and over intervals greater than the effective bandwidth* in the frequency domain. These channels are known as quasi wide sense stationary uncorrelated scattering (QWSSUS) channels (Bello, 1963). In the present work they provide the most useful model.

Now for a channel which is truly wide sense stationary the following conditions hold (Bello, 1963; Kaye, 1968)

(i) $$\bar{g}(t,\xi) = \bar{g}(\xi) \tag{2-30}$$

implying that the mean value or specular component of the channel impulse response is a function only of the delay variable ξ (i.e., is time-invariant).

(ii) $$R_g(t,s;u,v) = R'_g(s-t;u,v) = R'_g(\tau;u,v) \tag{2-31}$$

where $\tau = s-t$, or

$$R_G(t,s;f,\ell) = R'_G(s-t;f,\ell) = R'_G(\tau;f,\ell) \tag{2-32}$$

that is the autocorrelation functions of the system functions $g(t,u)$ and $G(t,f)$ are functions of the time difference τ. This

---

*For pulses which are time limited to $T_o \leq T_s$ seconds in duration there is no true band limitation. One measure of bandwidth (Schwartz, Bennet and Stein, 1966) is the quantity

$$\frac{1}{[M(0)]^2}\int |M(f)|^2 df \quad \text{which is usually of the order of } \frac{1}{T_o} \geq \frac{1}{T_s} \text{ Hz.}$$

implies that components of the channel response at different Doppler shifts are uncorrelated.

If also the channel is uncorrelated scattering, then components of its response for different values of the delay variable ξ are uncorrelated. Under this condition equation (2-31) reduces to the form

$$R'_g(\tau;u,v) = P_g(\tau,u)\delta(u-v) \quad , \tag{2-33}$$

where $\delta(\cdot)$ is the Dirac delta function, and equation (2-32) becomes

$$R_G(t,s;f,\ell) = \Phi_G(\tau,\Omega) \tag{2-34}$$

where $\Omega = \ell - f$. The function $\Phi_G(\tau,\Omega)$ is the autocorrelation function of a process which is wide sense stationary in both time and frequency. Another result which is of interest is obtained by taking the double Fourier transform of $\Phi_G(\tau,\Omega)$ to obtain

$$S(\xi,\nu) = \iint \Phi_G(\tau,\Omega)e^{j2\pi(\xi\Omega-\nu\tau)}d\tau\ d\Omega \tag{2-35}$$

where ξ is the channel delay variable and ν is the channel Doppler shift or spread variable. The function $S(\xi,\nu)$ is the well known (Bello, 1963; Kennedy, 1969) channel scattering function, and it defines the delay-Doppler energy cross-section of the channel.

Now using the mean channel output $\bar{\eta}(t)$ of equation (2-22), we may decompose the channel output signal $\eta(t)$ into the sum of two components (Kaye, 1968). If we let

$$\tilde{\eta}(t) = \eta(t) - \bar{\eta}(t) \tag{2-36}$$

we may then write the complex, low-pass channel output $\eta(t)$ as

$$\eta(t) = \bar{\eta}(t) + \tilde{\eta}(t) \tag{2-37}$$

Equation (2-37) expresses the channel output $\eta(t)$ as the sum of the mean or specular component $\bar{\eta}(t)$ and a zero-mean random component. This random component may be written as

$$\tilde{\eta}(t) = \int \tilde{g}(t,\xi)m(t-\xi)d\xi \tag{2-38}$$

where $\tilde{g}(t,\xi)$ is the zero-mean random component of the channel impulse response $g(t,\xi)$. From this we see at once that we have a decomposition for $g(t,\xi)$ which in the QWSSUS case may be written as

$$g(t,\xi) = \bar{g}(\xi) + \tilde{g}(t,\xi) \tag{2-39}$$

In many applications, particularly in the case of radio links*, the mean or specular component $\bar{g}(\xi)$ will either be zero or very small compared to the random component $\tilde{g}(t,\xi)$. In principle, if this is true, it is impossible for the receiver to perform coherent demodulation followed by filtering and equalization. The best receiver is then (Kailath 1960, 1961) an envelope detector (e.g., square-law device) followed by the usual decision circuit. However, since we are dealing with signals which are sequences of pulses, each of maximum duration T_s seconds, we can further decompose the channel response, and to some extent avoid this problem.

Let us now write the random component $\tilde{g}(t,\xi)$ of the channel impulse response as the sum of two components

---

*In particular ionospheric and tropospheric links.

$$\tilde{g}(t,\xi) = g_s(t,\xi) + g_r(t,\xi) \qquad (2\text{-}40)$$

We define the first term $g_s(t,\xi)$ of equation (2-40) to include those randomly varying components of $\tilde{g}(t,\xi)$ which vary slowly enough with time t that $g_s(t,\xi)$ appears to be time-invariant over time intervals much greater than the symbol period of T_s seconds.* We define the second term $g_r(t,\xi)$ to include all those components of $\tilde{g}(t,\xi)$ which vary randomly at rates comparable to or greater than the symbol frequency T_s^{-1}.

Now combining equations (2-39) and (2-40), we may write the overall channel impulse response in the form

$$g(t,\xi) = [\bar{g}(\xi) + g_s(t,\xi)] + g_r(t,\xi). \qquad (2\text{-}41)$$

Then let us combine the time-invariant mean-value $\bar{g}(\xi)$ and the slowly time-varying component $g_s(t,\xi)$ into the term

$$g_d(t,\xi) = \bar{g}(\xi) + g_s(t,\xi) \ . \qquad (2\text{-}42)$$

Using equation (2-42) we may now write the overall channel impulse response as

$$g(t,\xi) = g_d(t,\xi) + g_r(t,\xi) \qquad (2\text{-}43)$$

where $g_d(t,\xi)$ includes all the time-invariant and slowly varying

---

*This type of decomposition is to some extent conceptual, since the definition depends on the symbol period or data rate T_s. If the data rate is high enough (that is T_s is small enough) then all components of the channel are rapidly varying. Fortunately this is seldom the case.

components and $g_r(t,\xi)$ includes all the rapidly varying components. Thus $g_d(t,\xi)$ is a pseudo-specular component which includes the true specular component when it is non-zero. The second term $g_r(t,\xi)$ is the random scattering component mentioned in chapter 1.

The pseudo-specular component $g_d(t,\xi)$ causes two types of signal distortion. First because of its non-zero width in the delay variable ξ, it causes time-dispersion of signals passing through it. In the case of pulse or digital signals, this leads to intersymbol interference between two or more successive pulses. Second, the slow time variations in $g_d(t,\xi)$ cause a random aging of its amplitude and phase characteristics, and this causes a corresponding aging of the amplitude and phase of any signal passing through it. The pseudo-specular component $g_d(t,\xi)$ is also known as the quasi-coherent component, and in order that the receiver perform coherent demodulation followed by equalization, this component must be present and non-zero.

The random scattering component $g_r(t,\xi)$ consists of rapidly fluctuating, zero mean, wide sense stationary fluctuations superimposed on the pseudo-specular component $g_d(t,\xi)$. Because of its non-zero width in the delay variable ξ, $g_r(t,\xi)$ also causes time-dispersion, but the dominant effect in this branch of the channel is the rapid fluctuation. Signals passing through $g_r(t,\xi)$ are almost totally mutilated by these fluctuations, so that the output of this branch of the channel appears as wideband signal dependent noise, and provided the component $g_d(t,\xi)$ is also present it may be treated as such by the receiver (Kaye, 1968).

Thus far in our consideration of the channel and its effect on the signal, we have been concerned only with multiplicative effects as represented by the impulse response $g(t,\xi)$. However, in any real communications link, there is always additive interference or noise present, and in order to obtain a complete model of the channel it must be taken into account.

This additive noise is random and can be defined only in a statistical sense. As in the case of the impulse response $g(t,\xi)$, we require only a second moment characterization. Therefore, let us define it to be a source of zero mean, wide sense stationary random noise $n(t)$. Since we are dealing with narrowband signals and channels, we need to consider $n(t)$ only over the signal bandwidth, and we may therefore write any sample function $n(t)$ of the noise as

$$n(t) = 2\,\mathrm{Re}\{\mu(t)e^{j\omega_o t}\} \tag{2-44}$$

where $\mu(t)$ is a complex low-pass envelope and $\mu(t)\exp(j\omega_o t)$ is an analytic signal. Again using the properties of analytic signals (Dugundji, 1958) we may write the autocorrelation function of $n(t)$ as

$$R_n(\tau) = E\{n(t)n(t+\tau)\} \tag{2-45}$$

or

$$R_n(\tau) = \frac{1}{2}\,\mathrm{Re}\{R_\mu(\tau)e^{j\omega_o t}\} \tag{2-46}$$

where $R_\mu(\tau)$ is the complex autocorrelation function of the envelope $\mu(t)$ and is defined as

$$R_\mu(\tau) = E\{\mu^*(\tau)\mu(t+\tau)\} \tag{2-47}$$

This completes our modelling of the channel. From equations (2-15) and (2-45), we may now write the actual physical signal at the receiver input as

$$y(t) = z(t) + n(t) \tag{2-48}$$

$$= \mathrm{Re}\{e^{j\omega_o t}\int g(t,\xi)m(t-\xi)d\xi\} + \mathrm{Re}\{\mu(t)e^{j\omega_o t}\}$$

In terms of complex low-pass equivalent signals we have

$$y(t) = \int g(t,\xi)m(t-\xi)d\xi + \mu(t). \tag{2-49}$$

From these equations and from equation (2-42), we can model the channel as a parallel bank of linear filters followed by a source of additive noise. This is shown for the complex low-pass equivalent signals in the block diagram of figure 2.1 and the extension to the bandpass case is obvious.

In this thesis our primary concern is with the development of reception systems for the case when the signal dependent noise is small. This essentially means that the random scattering component $g_r(t,\xi)$ of the channel impulse response is small and the pseudo-specular component $g_d(t,\xi)$ is the main component of the channel impulse response, so that

$$g(t,\xi) \approx g_d(t,\xi)$$

When the signal dependent noise is significant, it must be taken into account in the design of the receiver (Kaye, 1968; Mark, 1970).

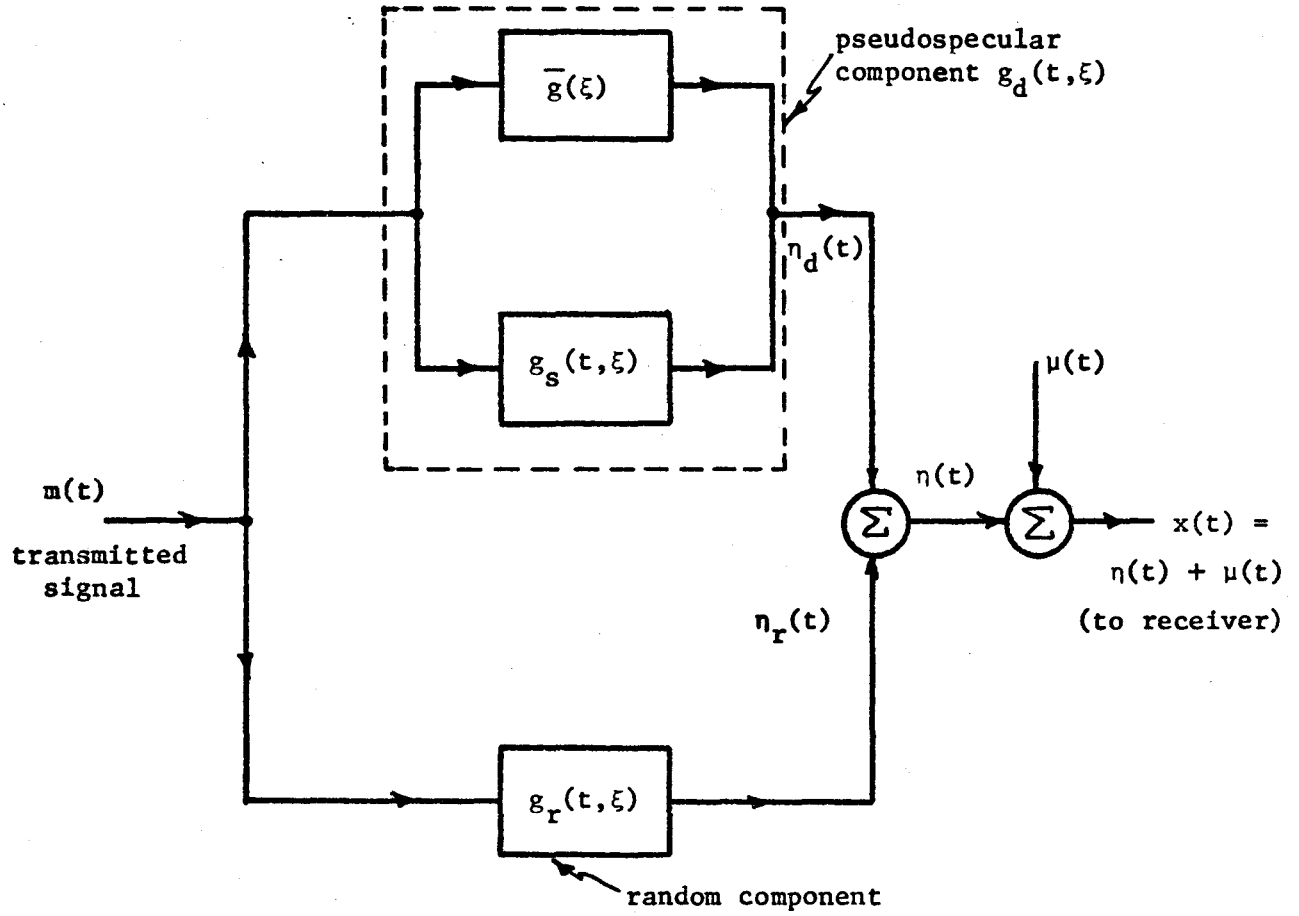

Figure 2.1 Block diagram of complex equivalent low-pass channel.

2.4 Measures of Dispersion

In the preceding section, we discussed a second order statistical model for a time-varying dispersive channel. This model characterized the channel in terms of its mean-value function and its autocorrelation function. Since the reception systems to be discussed in succeeding chapters use a minimum mean-squared error performance criterion, this second order model is sufficient to allow the optimum receiver structure to be defined.

Because the channel has memory or delay-spread, the optimum receiver includes memory within its structure. Also, because the channel is time-varying the receiver must be time-varying in order that it may follow or track the changing channel. The fact that the receiver must be time-varying leads at once to the concept of an adaptive or self-adjusting receiver. Such a receiver does not require explicit knowledge of either the mean-value or autocorrelation function of the receiver input signal, and therefore does not require explicit knowledge of the channel statistics. However, in order that the receiver be effective in adjusting itself to compensate for the channel, it must know or at least have reasonable estimates of the following parameters a priori:

(i) the channel memory size. This is synonymous with the width or spread of the channel impulse response $g(t,\xi)$ or the channel scattering function $S(\xi,\nu)$ in the delay variable ξ.

(ii) the rate of time-variation of the channel. This is equivalent to the Doppler-spread or width of the scattering function $S(\xi,\nu)$ in the Doppler variable ν.

The first of these parameters is needed in order that an estimate of the minimum receiver memory required can be made. The second one is required so that the receiver designer knows how quickly the adaptive receiver must be able to adjust itself in response to changes in the channel. Therefore, in this section, we will discuss a possible method of estimating the time and frequency spread of the channel.

In Appendix A, we have used a power series expansion of the equivalent low-pass channel transfer function to obtain the complex low-pass channel output $\eta(t)$ in the form

$$\eta(t) = \sum_{n=0}^{\infty} \Gamma_n(t) \frac{d^n}{dt^n} \{m(t-\xi_o)\} \tag{2-50}$$

where ξ_o is the mean channel or multipath delay*, and the time-varying coefficients $\Gamma_n(t)$ are defined by

$$\Gamma_n(t) = \frac{1}{n!} \int (-\xi)^n g_o(t,\xi) d\xi \tag{2-51}$$

with $g_o(t,\xi)$ being related to the channel impulse response by

$$g_o(t,\xi) = g(t,\xi+\xi_o) \tag{2-52}$$

Since the channel is randomly time-varying the $\Gamma_n(t)$ are sample functions from stochastic processes, and can be defined only in terms of their statistics.

Now the autocorrelation function of $\eta(t)$ may readily be written in the form

---

*As yet ξ_o has not been explicitly defined. We will do so in this section.

$$R_\eta(t,s) = \sum_{m=0}^{\infty} \sum_{n=0}^{\infty} E\{\Gamma_m^*(t)\Gamma_n(s)\} \frac{d^m}{dt^m}\{m^*(t-\xi_o)\} \frac{d^n}{dt^n}\{m(s-\xi_o)\} \qquad (2\text{-}53)$$

The channel correlation properties are thus defined by the correlation properties of the coefficients $\Gamma_n(t)$. Using equation (2-51), we can obtain the expectation in equation (2-53) in the form

$$E\{\Gamma_m^*(t)\Gamma_n(s)\} = \frac{(-1)^{m+n}}{m!n!} \iint \xi^m \mu^n R_g(t,s;\xi+\xi_o,\mu+\xi_o)d\xi d\mu \ ,$$

and then making use of the relationship in equation (2-52) we obtain

$$E\{\Gamma_m^*(t)\Gamma_n(s)\} = \frac{(-1)^{m+n}}{m!n!} \iint (\xi-\xi_o)^m(\mu-\xi_o)^n R_g(t,s;\xi,\mu)d\xi d\mu \ . \qquad (2\text{-}54)$$

As stated in the previous section, the channels which we are considering are QWSSUS in nature. We may, therefore, substitute equation (2-35) into equation (2-54) to obtain, after some manipulation the simplified result

$$E\{\Gamma_m^*(t)\Gamma_n(t+\tau)\} = \frac{(-1)^{m+n}}{m!n!} \int (\xi-\xi_o)^{m+n} P_g(\tau;\xi)d\xi \ . \qquad (2\text{-}55)$$

To obtain now the desired estimates or measures of dispersion, let us make the approximation that the channel exhibits linearly frequency-selective fading. This means that the complex channel output $\eta(t)$ may be approximated by the first two terms of the series in equation (2-50), yielding

$$\eta(t) \cong \Gamma_o(t)m(t-\xi_o) + \Gamma_1(t) \frac{d}{dt} m(t-\xi_o) \qquad (2\text{-}56)$$

where the first term is a flat or non-frequency-selective fading term and the second term exhibits linearly frequency selective fading.

Let us then choose as the mean channel or multipath delay ξ_o that value which minimizes in the mean-square sense the frequency-selective fading component of $\eta(t)$. From equation (2-55), the mean-square value of the flat fading coefficient $\Gamma_o(t)$ is given by

$$E\{|\Gamma_o(t)|^2\} = \int P_g(0;\xi)d\xi \tag{2-57}$$

The function $P_g(0;\xi)$ is known in the literature (Bello, 1963; Kaye, 1968) as the delay power spectral density, and is often written as $Q(\xi)$. It is related to the channel scattering function by the equation

$$Q(\xi) = \int S(\xi,\nu)d\nu \ , \tag{2-58}$$

where, as in all the preceding integrals, the limits of integration are assumed to be suitably defined. The mean-square value in equation (2-57) may then be written in the form

$$E\{|\Gamma_o(t)|^2\} = \int Q(\xi)d\xi = \iint S(\xi,\nu)d\nu d\xi \tag{2-59}$$

Similarly, the mean-square value of the linearly frequency-selective component may be found from equations (2-55) and (2-58) as

$$E\{|\Gamma_1(t)|^2\} = \int (\xi-\xi_o)^2 Q(\xi)d\xi = \iint (\xi-\xi_o)^2 S(\xi,\nu)d\nu d\xi \tag{2-60}$$

Taking the first derivative of this with respect to ξ_o, we obtain

$$\frac{\partial}{\partial \xi_o} E\{|\Gamma_1(t)|^2\} = -2 \int \xi Q(\xi)d\xi + 2\xi_o \int Q(\xi)d\xi \tag{2-61}$$

and setting this equal to zero, we may solve for the mean channel delay ξ_o as

$$\xi_o = \frac{\int \xi Q(\xi) d\xi}{\int Q(\xi) d\xi} , \tag{2-62}$$

which may be expressed in terms of the scattering function $s(\xi,\nu)$ as

$$\xi_o = \frac{\iint \xi S(\xi,\nu) d\nu d\xi}{\iint S(\xi,\nu) d\nu d\xi} \tag{2-63}$$

That this is the value of ξ_o which causes $E\{|\Gamma_1(t)|^2\}$ to be a minimum is readily verified since

$$\frac{\partial^2}{\partial \xi_o^2} E\{|\Gamma_1(t)|^2\} = 2\int Q(\xi) d\xi = 2\iint S(\xi,\nu) d\xi d\nu$$

$$\geq 0 .$$

If we now take the ratio of the mean-squared values of the frequency-selective and flat fading components, we obtain

$$\frac{E\{|\Gamma_1(t)|^2\}}{E\{|\Gamma_o(t)|^2\}} = \frac{\int (\xi-\xi_o)^2 Q(\xi) d\xi}{\int Q(\xi) d\xi} = \Delta_g^2 \tag{2-64}$$

or in terms of the channel scattering function

$$\Delta_g^2 = \frac{\iint (\xi-\xi_o)^2 S(\xi,\nu) d\xi d\nu}{\iint S(\xi,\nu) d\xi d\nu} \tag{2-65}$$

The quantity Δ_g is known as the root mean square (rms) width of $Q(\xi)$. It is a measure or estimate of the channel memory or delay spread. That is it is an estimate of the width of $g(t,\xi)$ in the delay variable ξ, and provides an estimate of the amount of receiver memory required.

Following arguments dual to those given above, we may derive the mean Doppler shift of the channel as

$$\nu_o = \frac{\int \nu P(\nu) d\nu}{\int P(\nu) d\nu} \tag{2-66}$$

and the mean square Doppler spread of the channel as

$$\beta^2 = \frac{\int (\nu-\nu_o)^2 P(\nu) d\nu}{\int P(\nu) d\nu} \quad . \tag{2-67}$$

The function $P(\nu)$ is known as the Doppler power spectral density. It is defined in terms of the scattering function $S(\xi,\nu)$ as

$$P(\nu) = S(0,\nu) \tag{2-68}$$

The quantity β is a measure of the rate of time-variation of the channel, and therefore it is indicative of how quickly the receiver must be able to adapt to and track the channel characteristics.

Typical values of the delay-spread Δ_g and the Doppler-spread β are given below for various transmission media (Richters, 1967; Niessen and Willim, 1970).

Channel	Doppler spread β(Hz)	Delay spread Δ_g(secs)
Ionospheric scatter	10	10^{-4}
tropospheric scatter	10	10^{-6}
schedule 4 data line (coaxial)	<<1	$\sim 10^{-2}$
19H88 coaxial cable	<<1	$\sim 1.2 \times 10^{-2}$

We point out that equations (2-64) and (2-67) represent only one possible way of estimating the delay and Doppler spreads for a channel. There are many other equally valid methods of defining and measuring these quantities but we will not go into them here.

2.5 The Demodulation Problem

In this thesis we are concerned with the reception of double sideband, suppressed carrier, amplitude modulated (DSBSC-AM) signals which have been transmitted over linear time-varying dispersive channels. The transmitted and received signals, s(t) and y(t) respectively are given by equations (2-5), (2-11) and (2-48) as

$$s(t) = 2\mathrm{Re}\{m(t)e^{j\omega_o t}\} = 2\mathrm{Re}\{e^{j\omega_o t}\sum_k s_k q(t-kT_s)\} \qquad (2\text{-}69)$$

and

$$y(t) = z(t) + n(t)$$

$$= \mathrm{Re}\{e^{j\omega_o t}\int g(t,\xi)m(t-\xi)d\xi\} + \mathrm{Re}\{\mu(t)e^{j\omega_o t}\} \quad . \qquad (2\text{-}70)$$

The reception problem is the recovery of the digital information or symbol sequence $\{s_k\}$ from y(t). Because of the linearity of both the

channel and the modulation, the reception process may be considered as two separate operations. The first of these is the demodulation of the bandpass signal y(t) to obtain a low-pass or baseband waveform containing the desired information. Since s(t) and therefore z(t) are both suppressed carrier signals, some form of carrier recovery operation to recover the carrier signal and its phase must be carried out. That is coherent demodulation must be used. The second operation is the compensation for the time and frequency dispersive effects of the channel so that reliable recovery of the symbols $\{s_k\}$ can be obtained. This compensation, which is usually referred to as channel equalization, is most often performed at baseband following demodulation*, and the general form of the receiver is then given by the block diagram in figure 2.2. This baseband signal processing is the main subject of this thesis and will be investigated in detail in following chapters.

In this section we will discuss the problem of demodulation. This subject has been discussed in some detail by a number of authors (Costas, 1956; Van Trees, 1964, and others). Let us consider for the moment the complex low-pass envelope of the signal component z(t). It may be written as

$$n(t) = \int g(t,\xi)m(t-\xi)d\xi \qquad (2\text{-}71)$$

The complex equivalent low-pass channel impulse response may in general be written in the form

---

*An exception to this is discussed by Lucky and Rudin (1967).

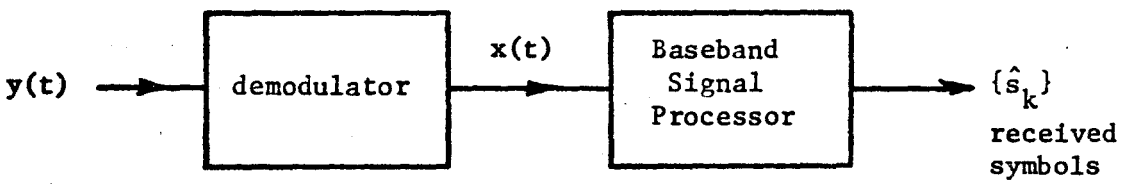

Figure 2.2 General form of the reception system.

$$g(t,\xi) = a(t,\xi)e^{j\theta(t,\xi)} \tag{2-72}$$

where

$$a(t,\xi) = |g(t,\xi)|$$

and

$$\theta(t,\xi) = \arg\{g(t,\xi)\}$$

We may then write equation (2-71) as

$$n(t) = \int a(t,\xi)e^{j\theta(t,\xi)}m(t-\xi)d\xi \ , \tag{2-73}$$

and the corresponding physical signal z(t) may be written in the form

$$z(t) = \mathrm{Re}\{e^{j\omega_o t}\int a(t,\xi)e^{j\theta(t,\xi)}m(t-\xi)d\xi\} \tag{2-74}$$

Before considering the actual demodulation, let us consider first the transmission of an unmodulated sine wave at the carrier frequency ω_o. The corresponding output signal may be written in the form

$$c(t) = \mathrm{Re}\{e^{j\omega_o t}\int a(t,\xi)e^{j\theta(t,\xi)}d\xi\} \tag{2-75}$$

and this may readily be expanded to the form

$$c(t) = [\int a(t,\xi)\cos\theta(t,\xi)d\xi]\cos\ \omega_o t$$

$$- [\int a(t,\xi)\sin\theta(t,\xi)d\xi]\sin\ \omega_o t \tag{2-76}$$

or

$$c(t) = r(t)\cos[\omega_o t + \psi(t)] \tag{2-77}$$

where

$$r(t) = \left| \int a(t,\xi) e^{j\theta(t,\xi)} d\xi \right|$$

is the envelope, and

$$\psi(t) = \tan^{-1} \frac{\int a(t,\xi)\sin\theta(t,\xi)\,d\xi}{\int a(t,\xi)\cos\theta(t,\xi)\,d\xi} \tag{2-78}$$

is known as the carrier phase. Note that $\psi(t)$ does not depend on the transmitted sine wave.

Returning now to the channel output signal $z(t)$ of equation (2-74), let us now redefine the phase process $\theta(t,\xi)$ to explicitly show the carrier phase $\psi(t)$. That is we write

$$\theta(t,\xi) = \psi(t) + \beta(t,\xi) \tag{2-79}$$

and then the signal $z(t)$ may be written in the form

$$z(t) = \mathrm{Re}\{e^{j\omega_o t} \int a(t,\xi) e^{j[\psi(t)+\beta(t,\xi)]} m(t-\xi)\,d\xi\} \ . \tag{2-80}$$

Since $a(t,\xi)$ and $m(t)$ are both real functions we may combine the exponential terms in equation (2-80) and then expand the result to obtain the signal $z(t)$ in the form

$$\begin{aligned} z(t) = {} & \left[\int a(t,\xi) m(t-\xi)\cos\beta(t,\xi)\,d\xi\right]\cos[\omega_o t + \psi(t)] \\ & - \left[\int a(t,\xi) m(t-\xi)\sin\beta(t,\xi)\,d\xi\right]\sin[\omega_o t + \psi(t)] \ . \end{aligned} \tag{2-81}$$

Recall now that the transmitted signal $s(t)$ in equation (2-69) is DSBSC, and therefore has no quadrature component. Then from equation

(2-81), we can see that the presence of a non-zero phase versus delay characteristic* $\beta(t,\xi)$ in the channel impulse response causes a portion of the available signalling energy to appear in the channel output $z(t)$ as a quadrature or orthogonal component. This means that $z(t)$ contains both amplitude and phase modulations which are dependent on the transmitted signal $s(t)$. It also has the following equivalent implications concerning the channel response

(i) the equivalent low-pass channel impulse response

$$g(t,\xi) = a(t,\xi)\exp[j(\psi(t) + \beta(t,\xi))]$$

is a complex function of the delay variable ξ.

(ii) the frequency response of the channel $H(t,\omega)$, where $H(t,\omega)$ is the Fourier transform of the actual channel impulse response $h(t,\xi)$ with respect to the delay variable ξ, is unsymmetric about the carrier frequency ω_o within the bandwidth of the transmitted signal $s(t)$. A limiting form of such a frequency response is one which totally filters out one sideband of the DSBSC signal $s(t)$, so that the channel output $z(t)$ is then single sideband in nature.

From equation (2-81), we see that coherent demodulation of $z(t)$ will produce the in-phase and quadrature components

$$v_c(t) = \int a(t,\xi)m(t-\xi)\cos\beta(t,\xi)d\xi \qquad (2\text{-}82)$$

---

*By this we mean that $\beta(t,\xi)$ is not zero or an integer multiple of π radians at all values of the delay variable ξ.

and

$$v_s(t) = \int a(t,\xi)m(t-\xi)\sin\beta(t,\xi)d\xi \qquad (2\text{-}83)$$

of its envelope. This process requires a local oscillator at the receiver producing the signals

$$\cos[\omega_o t + \psi(t)] \qquad \text{and} \qquad \sin[\omega_o t + \psi(t)]$$

which are phase-coherent with the carrier phase $\psi(t)$. The essential problem in demodulation is then the production of these local carrier signals.

It is well known (Bennett and Davey, 1965; Lucky, 1968) that coherent demodulation of any received signal having a significant quadrature component requires that an independent source of phase-coherent carrier signal be available. This local carrier may be supplied by a phase-stable, free-running oscillator as is done in many single sideband voice links, or a separate (pilot) carrier signal may be transmitted along with the signal s(t) and a phase-locked loop system may be used to produce the local carrier for demodulation.

From the information theory point of view, any communications channel has a certain capacity which imposes an upper bound on the amount of information which may be passed through the channel in a given time. In order to coherently demodulate a suppressed carrier signal using only the information in its sidebands the channel capacity must be great enough to accommodate both the transmitted information and the phase information required for coherent demodulation. If the channel capacity required for the signal information is C_s and that

required for the phase information alone is C_p, then the total channel capacity required is $C_s + C_p$. The excess channel capacity $\hat{C}$ available, over and above C_s, to establish phase lock from the sidebands alone has been found by de Buda (1970) to be

$$\hat{C} = W \log_2(1 + \frac{\rho^2}{1+2\rho}) \qquad (2\text{-}84)$$

where W is the signal bandwidth and ρ is the so-called carrier to noise ratio defined as

$$\rho = \frac{\text{In phase signal power recoverable by coherent demodulation}}{\text{Additive noise power}}$$

If the phase channel capacity C_p is greater than the excess channel capacity $\hat{C}$ which is available, then coherent demodulation cannot be performed without an independent carrier signal being transmitted.

When the channel response causes a quadrature component to be generated in its output z(t) in response to the DSBSC signal s(t), then the carrier to noise ratio ρ will be reduced and thus the excess channel capacity $\hat{C}$ available for phase lock will be reduced (de Buda, 1970). Provided that the power in this quadrature component is small (implying in equation (2-83) that $\sin\beta(t,\xi)$ is small for all ξ), then ρ will not be reduced by very much, and the excess capacity $\hat{C}$ may still be great enough that coherent demodulation is possible using only the sidebands of the received signal. This is the usual case when DSBSC signals are transmitted, and we may then represent the channel output z(t) of equation (2-81) to a good approximation by

$$z(t) = u(t)\cos[\omega_o t + \psi(t)] \tag{2-85}$$

where

$$u(t) = \int a(t,\xi)m(t-\xi)d\xi \tag{2-86}$$

is the low-pass or baseband envelope function which we wish to recover from the demodulation process.

Now let us write the instantaneous phase of z(t) in equation (2-85) as

$$\phi(t) = \omega_o t + \psi(t) \tag{2-87}$$

We may then write the received signal in the compact form

$$z(t) = u(t)\cos\phi(t). \tag{2-88}$$

Suppose now that we have available a local oscillator producing the outputs

$$u_c(t) = 2 \cos \theta(t) \tag{2-90}$$

and

$$u_s(t) = 2 \sin \theta(t) \tag{2-91}$$

Let us then multiply z(t) by each of these signals separately and then pass the resulting products through low-pass filters to remove the second harmonic components. This results in the pair of low-pass or baseband signals

$$g_c(t) = u(t) \cos \varepsilon(t) \tag{2-92}$$

and

$$g_s(t) = u(t) \sin \varepsilon(t) \tag{2-93}$$

where

$$\varepsilon(t) = \theta(t) - \phi(t) \tag{2-94}$$

is the instantaneous phase error. Then multiplying these signals together we obtain

$$w(t) = \frac{u^2(t)}{2} \sin 2\varepsilon(t) \qquad (2\text{-}95)$$

which after averaging or low-pass filtering is proportional to the sine of twice the phase error $\varepsilon(t)$. When $\varepsilon(t)$ is small, $w(t)$ is proportional to $2\varepsilon(t)$. The signal $w(t)$ may be used as the control signal for a voltage controlled oscillator which produces the local carriers $u_c(t)$ and $u_s(t)$. As the phase error $\varepsilon(t)$ approaches zero, the in-phase signal $g_c(t)$ approaches the desired envelope function $u(t)$. The resulting demodulator structure is shown in figure 2.3 and is known as the Costas Loop (Costas, 1956). This structure provides an efficient demodulator, having the noise rejection properties of a conventional phase-lock loop demodulator, provided of course that the quadrature component $v_s(t)$ of equation (2-83) is small so that $z(t)$ is well represented by equation (2-85).

In practice the received phase $\psi(t)$ in equation (2-85) may be varying rapidly enough that the time required for the Costas loop to acquire phase-lock may be prohibitively long. In such cases, improved acquisition and tracking performance may be obtained by the use of a more sophisticated loop such as the frequency controlled loop developed by Lang and Brackett (1970) in a demodulator structure similar to that shown in figure 2-3.

Thus by the use of synchronous or phase-locked detection or demodulation, we have obtained the baseband envelope signal

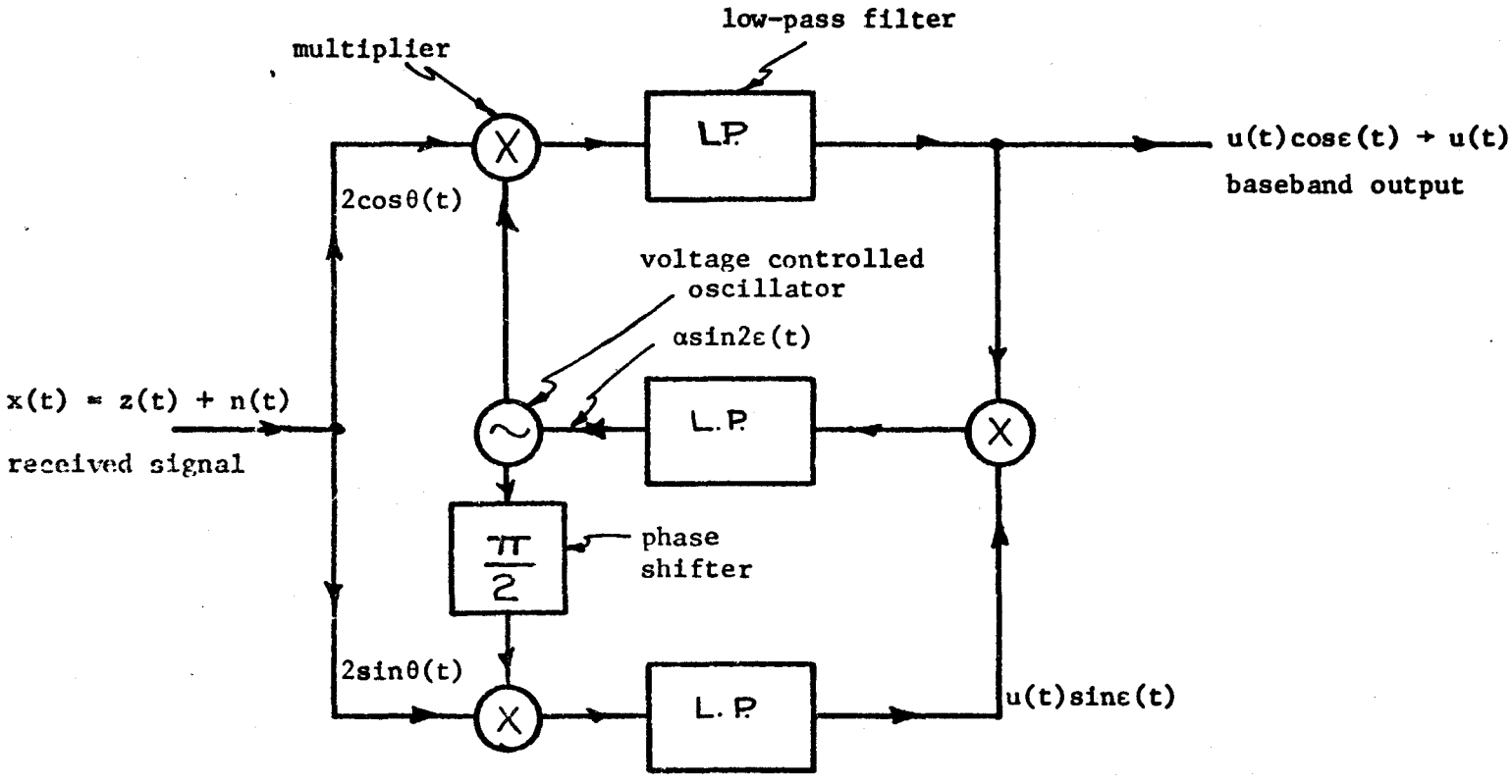

Figure 2.3 Basic structure of Costas synchronous demodulator.

$$x(t) = u(t) + n_c(t)$$

$$= \int a(t,\xi)m(t-\xi)d\xi + n_c(t) \qquad (2\text{-}96)$$

where $n_c(t)$ is the in-phase component of the additive noise defined in equation (2-45). If we substitute equation (2-5) for m(t) in this, we obtain

$$x(t) = \sum_k s_k \int a(t,\xi)q(t-kT_s-\xi)d\xi + n_c(t) \qquad (2\text{-}97)$$

and if we then define

$$r(t) = \int a(t,\xi)q(t-\xi)d\xi \qquad (2\text{-}98)$$

we may write the demodulator output as

$$x(t) = \sum_k s_k r(t-kT_s) + n_c(t) \qquad (2\text{-}99)$$

where r(t) is known as the received pulse-shape.

From equation (2-99), it can be seen that the problem now is to extract the transmitted symbols $\{s_k\}$ from the demodulator output x(t). This is known as the baseband signal processing problem (see figure 2-2), and is the subject of the remainder of this thesis.

CHAPTER 3

The Baseband Receiver

In chapter 2 we first discussed the transmitted signal and how it was distorted and interfered with by the channel. We then went on to consider the problem of demodulating the received, distorted signal to obtain the baseband signal x(t) of equation (2-99) using synchronous detection techniques.

In this chapter we shall consider the problem of how to extract the transmitted information from the baseband signal. We shall start our investigation by considering a time-domain formulation of the optimum linear receiver (George, 1965) and progress from there to the nonlinear structure which is the main subject of this thesis.

3.1 The Performance Criterion

The output from any receiver which is designed for the reception of digital signals may be regarded as a sequence of decisions. In digital signal transmission a signal is transmitted in each T_s-second signalling interval, and there is a finite number (say m) of possible signals which may be transmitted in each interval. For example in the present case the signal in the kth interval, $(k - \frac{1}{2})T_s < t \leq (k + \frac{1}{2})T_s$ is the amplitude modulated pulse $s_k q(t-kT_s)$, where the amplitude s_k is the digital symbol with values in the finite set $(\xi_1, \ldots, \xi_m)$ as described in chapter 2. The task of the receiver is to decide which of

the m symbol values was transmitted in any given signalling interval, and the best or optimum receiver is the one which makes the fewest decision errors. It is the statistically optimum receiver, and is known as the minimum probability of error receiver.

In the special case in which the channel is not dispersive the received pulse shape r(t) of equation (2-98) is identical with the transmitted pulse shape q(t). The received baseband signal may then be written as

$$x(t) = \sum_k s_k q(t-kT_s) + n_c(t) \tag{3-1}$$

where the pulses $q(t-kT_s)$ are orthogonal in the sense that

$$\int q(t-jT_s)q(t-kT_s)dt = E_q \delta_{j,k} \tag{3-2}$$

where E_q is the pulse energy and $\delta_{j,k}$ is the Kronecker delta. There is thus no overlapping or interference between pulses in disjoint signalling intervals, and therefore the only source of distortion or interference is the additive noise $n_c(t)$. We may then write the received signal in any T_s-second signalling interval, say the kth, as

$$x(t) = s_k q(t-kT_s) + n_c(t) \qquad (k - \tfrac{1}{2})T_s < t \leq (k + \tfrac{1}{2})T_s$$

$$(-\infty < k < \infty) \tag{3-3}$$

Under the assumption that the noise $n_c(t)$ is Gaussian and white, it has been shown (e.g., Turin, 1960) that the minimum probability of error receiver for extracting the symbol s_k from the signal x(t) in equation (3-3) is a filter matched to the pulse-shape q(t) followed by

a sampling and decision circuit. This sampling and decision circuit samples the filter output at time $t=kT_s$ and makes a decision as to which of the values $(\xi_1, \ldots, \xi_m)$ the symbol s_k has.

In the more general case when the channel is dispersive, the signal in any given signalling interval cannot be written in the simple form of equation (3-3). In the kth signalling interval, we may use equation (2-99) to write the received signal x(t) as

$$x(t) = s_k r(t-kT_s) + \sum_{j\neq k} s_j r(t-jT_s) + n_c(t) \qquad (3-4)$$

where now the pulses in disjoint signalling intervals are not orthogonal in the sense of equation (3-2). In fact if we sample x(t) at time $t=kT_s$, we obtain

$$x(kT_s) = s_k r(0) + \sum_{j\neq k} s_j r(kT_s-jT_s) + n_c kT_s) \qquad (3-5)$$

where the second term is non-zero. The first term in equation (3-5) represents the desired signal component. The second term is interference due to the overlapping tails of pulses in other signalling intervals and is usually known as intersymbol interference. The third and last term represents, as before, the additive noise. Because of the intersymbol interference, the derivation of the minimum probability of error receiver is a very difficult problem, and the resulting receiver is a complex nonlinear structure (Bowen, 1969).

Rather than attempt the direct minimization of the probability of error and then make the simplifying approximations required to realize the resulting structure in a form comparable in complexity to

existing receivers (e.g., Ungerboeck, 1972), we shall adopt a hybrid approach which leads to a simpler optimization problem. This approach consists essentially of considering the receiver to be made up of two parts - an estimator followed by a threshold detector or decision circuit. The estimator produces estimates $\hat{s}_k$ at the times $t=kT_s$ $(-\infty < k < \infty)$ of the corresponding transmitted symbols s_k $(-\infty < k < \infty)$. These estimates are optimized according to some performance criterion and the decision circuit then uses them to make its decisions.

Provided the values of the estimates $\hat{s}_k$ are close to the values of the corresponding symbols s_k, the decision circuit will tend to make correct decisions and the behaviour of the hybrid receiver will be close to that of the minimum probability of error receiver. Based on this argument, we must choose a performance criterion for the receiver which in some sense will make the error in the estimates $\hat{s}_k$ $(-\infty < k < \infty)$ as small as possible. If this criterion is chosen correctly, the resulting estimation error $(\hat{s}_k - s_k)$ $(-\infty < k < \infty)$ should be small, at least in an average sense, and the behaviour of the resulting receiver should be quite close to that of the minimum probability of error receiver.

The criterion which we shall employ is the so-called minimum mean-squared error criterion, which seeks to make the mean-squared estimation error

$$E\{(s_k - \hat{s}_k)^2\}$$

at the times $t=kT_s$ $(-\infty < k < \infty)$ a minimum. The use of this criterion has the following advantages:

(i) It leads to a mathematically tractable optimization problem.

(ii) It allows relatively simple iterative procedures to be used for adaptive adjustment of the receiver parameters.

It has the disadvantage that if the probability distribution of the estimation error is not relatively close to being Gaussian, the resulting receiver may be a rather poor approximation to the minimum probability of error receiver. Fortunately, this seldom happens in practice.

To employ the criterion, we shall first use it to obtain the optimum linear receiver. We shall then use it to obtain an optimum nonlinear structure which has certain exploitable similarities with the linear structure.

3.2 A Time-Domain Approach to the Optimum Linear Receiver

In this section, we consider a time-domain derivation of the optimum (minimum mean-squared error), unrealizable linear receiver for the reception of dispersed, baseband PAM signals. A frequency domain derivation which leads to an expression for the transfer function of this receiver was carried out by George (1965). The present analysis is largely based on an analysis by de Buda (1965) who carried out an analysis using the maximization of signal to noise ratio as the performance criterion.

As previously, let us consider a received signal of the form

$$x(t) = \sum_{k=-\infty}^{\infty} s_k r(t-kT_s) + n(t) \qquad (3\text{-}6)$$

where

(i) r(t) is the received pulse shape defined as

$$r(t) = \int q(\tau)c(t-\tau)d\tau$$

(ii) q(t) is the transmitted pulse-shape defined to have width T_s and normalized to unit energy so that

$$\int_0^{T_s} q^2(t)dt = 1$$

(iii) $c(\tau)$ is the channel impulse response, assumed here to be time-invariant and known a priori at the receiver.

(iv) The $\{s_k: -\infty < k < \infty\}$ are the transmitted symbols, assumed here to be independent random variables with mean

$$E\{s_k\} = 0 \qquad (-\infty < k < \infty)$$

and variance

$$E\{s_k^2\} = 1 \qquad (-\infty < k < \infty)$$

(v) n(t) is zero mean, wide sense stationary additive noise assumed here to be white with autocorrelation function

$$R_n(\tau) = N_o\delta(\tau)$$

where by white we mean that its power spectral density is constant and equal to N_o over the bandwidth of interest which is nominally equal to $(T_s)^{-1}$. The assumption of white noise makes little difference to the resulting receiver structure. Primarily it simplifies the structure of the matched filter which will be seen to be the first stage of the optimum linear

receiver. When the noise is non-white with spectral density $S_n(\omega)$, this filter has the transfer function

$$\frac{R^*(\omega)}{S_n(\omega)}$$

rather than the simple white noise form

$$\frac{R^*(\omega)}{N_o} \quad ,$$

where $R(\omega)$ is the Fourier transform of the received pulse shape $r(t)$. We shall thus assume white noise, the extension to colored noise being relatively simple.

In this section, we assume that the receiver is linear. Its output at any time $t=nT_s$ $(-\infty < n < \infty)$ may, therefore, be written as

$$\hat{s}_n = \int_{-\infty}^{\infty} x(\tau)h(nT_s - \tau)d\tau \qquad (-\infty < n < \infty) \qquad (3\text{-}7)$$

where

(i) $h(\tau)$ is the impulse response of the linear receiver

(ii) $\hat{s}_n$ is the linear estimate of the transmitted symbol s_n at time $t=nT_s$ which is the midpoint of the signalling interval $(n - \frac{1}{2})T_s \leq t \leq (n + \frac{1}{2})T_s$.

(iii) realizability constraints will be ignored at present.

Since the processes involved are wide sense stationary, and the receiver is time-invariant, the estimate at any time $t=nT_s$ will have the same form as the estimate at any other time $t=mT_s$ $(m \neq n)$. In particular the estimate $\hat{s}_o$ at $t=0$ may be written as

$$\hat{s}_o = \int_{-\infty}^{\infty} x(\tau)h(-\tau)d\tau \qquad (3\text{-}8)$$

For convenience of notation in what follows, let us define the inverse time impulse response or weighting function

$$k(\tau) = h(-\tau) \; . \qquad (3\text{-}9)$$

We may then rewrite equations (3-7) and (3-8) as

$$\hat{s}_n = \int_{-\infty}^{\infty} x(\tau)k(\tau - nT_s)d\tau \qquad (-\infty < n < \infty) \qquad (3\text{-}10)$$

and

$$\hat{s}_o = \int_{-\infty}^{\infty} x(\tau)k(\tau)d\tau \qquad (3\text{-}11)$$

Let us now consider the estimation of the symbol s_o at time t=0. The optimum linear receiver may then be found by applying the well known (Luenberger, 1969) necessary and sufficient condition for the mean squared estimation error to be a minimum, namely

$$E\{(s_o - \hat{s}_o)x(t)\} = 0 \qquad (-\infty < t < \infty) \qquad (3\text{-}12)$$

subject to the constraint that $\hat{s}_o$ be a linear functional of x(t). This may be rewritten as

$$E\{\hat{s}_o x(t)\} = E\{s_o x(t)\} \qquad (-\infty < t < \infty) \qquad (3\text{-}13)$$

and now let us evaluate the terms in this equation. The left-hand side of equation (3-13) may be written using equations (3-6) and (3-11) as

$$E\{\hat{s}_o x(t)\} = \sum_{k=-\infty}^{\infty} r(t-kT_s) \int_{-\infty}^{\infty} r(\tau - kT_s)k(\tau)d\tau + N_o k(t)$$

$$(-\infty < t < \infty) \qquad (3\text{-}14)$$

The right-hand side of equation (3-13) is then readily found to be

$$E\{s_o x(t)\} = r(t) \qquad (-\infty < t < \infty) \qquad (3\text{-}15)$$

Then substituting equations (3-14) and (3-15) into equation (2-13) we obtain the equation

$$\sum_{k=-\infty}^{\infty} r(t-kT_s) \int_{-\infty}^{\infty} r(\tau-kT_s)k(\tau)d\tau + N_o k(t) = r(t) \qquad (-\infty < t < \infty) \qquad (3\text{-}16)$$

the solution of which defines the optimum linear receiver weighting function k(t).

It can be shown (George, 1965) that a solution of the form

$$k(t) = \sum_{n=-\infty}^{\infty} g_n r(t-nT_s) \qquad (3\text{-}17)$$

satisfies equation (3-16) where the $\{g_n\}$ are constants such that

$$\sum_{n=-\infty}^{\infty} g_n^2 < \infty \quad .$$

Substituting equation (3-17) into equation (3-16) and interchanging the order of integration and summation we obtain

$$\sum_{k=-\infty}^{\infty} r(t-kT_s) \sum_{n=-\infty}^{\infty} g_n \int_{-\infty}^{\infty} r(\tau-nT_s)r(\tau-kT_s)d\tau + N_o k(t) = r(t) \qquad (-\infty < t < \infty) \qquad (3\text{-}18)$$

The integral in the first term of equation (3-18) is the time auto-correlation function of the received pulse shape r(t);

$$\phi_r[(k-n)T_s] = \int_{-\infty}^{\infty} r(\tau-nT_s)r(\tau-kT_s)d\tau \qquad (3\text{-}19)$$

Let us also define

$$\phi_r(0) = \int_{-\infty}^{\infty} r^2(t)dt = E_s < \infty \tag{3-20}$$

as the received pulse or signal energy. We may then rewrite equation (3-18) in the form

$$\sum_{k=-\infty}^{\infty} \sum_{n=-\infty}^{\infty} g_n r(t-kT_s)\phi_r[(k-n)T_s] + N_o k(t) = r(t) \qquad (-\infty < t < \infty) \tag{3-21}$$

Then letting $m = k-n$ and interchanging the order of summation, we obtain

$$\sum_{m=-\infty}^{\infty} \phi_r(mT_s) \sum_{n=-\infty}^{\infty} g_n r[t-(n+m)T_s] + N_o k(t) = r(t) \qquad (-\infty < t < \infty) \tag{3-22}$$

Now from equation (3-17), the inner summation in equation (3-22) is seen to be $k(t-mT_s)$ and we may therefore rewrite equation (3-22) as

$$\sum_{m=-\infty}^{\infty} \phi_r(mT_s)k(t-mT_s) + N_o k(t) = r(t) \qquad (-\infty < t < \infty) \tag{3-23}$$

Equation (3-23) may be solved in two ways to yield the optimum linear receiver. First it may be solved in the frequency domain. By taking the Fourier transform of both sides of equation (3-23) with respect to t, we obtain the transfer function of the optimum linear receiver as

$$K(\omega) = \frac{R(\omega)}{N_o} \cdot \frac{1}{1 + \sum_{m=-\infty}^{\infty} \frac{\phi_r(mT_s)}{N_o} e^{j\omega mT_s}} \tag{3-24}$$

From this result we see that the optimum linear receiver may be implemented as the cascade connection of a filter matched to the

received pulse shape r(t), or R(ω) in the frequency domain, and a sampled data system which compensates for channel time dispersion or intersymbol interference. This is the result obtained by George (1965).

The second way to solve equation (3-23) is to do so in the time domain. This, very simply, yields a solution for the weighting function k(t) of the optimum linear receiver as

$$k(t) = \frac{r(t)}{E_s+N_o} - \frac{1}{E_s+N_o} \sum_{m=-\infty}^{\infty}{}' \phi_r(mT_s)k(t-mT_s)$$

$$(-\infty < t < \infty) \qquad (3\text{-}25)$$

where $\sum_m{}'$ implies that the m=0 term has been excluded from the summation. Equation (3-25) is a recursive relationship for k(t). Now combining equations (3-10) and (3-11) with equation (3-25) we obtain the optimum linear estimate $\hat{s}_o$ of the symbol s_o at time t=0 as

$$\hat{s}_o = \frac{1}{E_s+N_o} \int_{-\infty}^{\infty} x(\tau)r(\tau)d\tau - \frac{1}{E_s+N_o} \sum_{m=-\infty}^{\infty}{}' \phi_r(mT_s)\hat{s}_m \qquad (3\text{-}26)$$

The first term in equation (3-26) is the result of passing the received signal x(t) through a filter matched to the shape r(t) of an individual received pulse. In the special case of no intersymbol interference it would represent the optimum receiver in a decision theoretic sense. The second term is a correction term which compensates for intersymbol interference using a weighted sum of the optimum linear estimates $\hat{s}_m$ of earlier and later symbols s_m $(m \neq 0)$.

It is of interest at this point to consider the receiver structures which are suggested by equations (3-24) to (3-26). In equation (3-24), if we carry out synthetic division of the numerator

by the denominator, we obtain the optimum transfer function $K(\omega)$ in the form

$$K(\omega) = \frac{R(\omega)}{N_o} \sum_{n=-\infty}^{\infty} a_n e^{-j\omega n T_s} \tag{3-27}$$

where the coefficients $\{a_n\}$ are constants depending on the channel correlation properties as defined in equation (3-19). Equation (3-27) may be implemented by the structure shown in figure 3.1 which consists of a matched filter followed by an infinite length transversal filter. This is the receiver structure derived by George (1965) and others (Tufts, 1963; Tufts and Berger, 1967). It is unrealizable due to the requirement of an infinite length tapped delay line.

A second receiver structure which is suggested by equations (3-24) to (3-26) consists of a filter matched to the received pulse shape r(t) followed by a recursive sampled data filter. To derive this structure, let us first define a signal to additive noise ratio ρ_n as

$$\rho_n = \frac{E_s}{N_o} \tag{3-28}$$

We may then, with a little manipulation rewrite equations (3-24) and (3-25) in the form

$$K(\omega) = \frac{R(\omega)}{N_o} \cdot \frac{(1+\rho_n)^{-1}}{1 + \frac{1}{1+\rho_n} \sum_{m=-\infty}^{\infty} \frac{\phi_r(mT_s)}{N_o} e^{j\omega m T_s}} \tag{3-29}$$

and

$$k(t) = \frac{1}{1+\rho_n} \left\{ \frac{r(t)}{N_o} - \sum_{m=-\infty}^{\infty} \frac{\phi_r(mT_s)}{N_o} k(t-mT_s) \right\}$$

$$(-\infty < t < \infty) \tag{3-30}$$

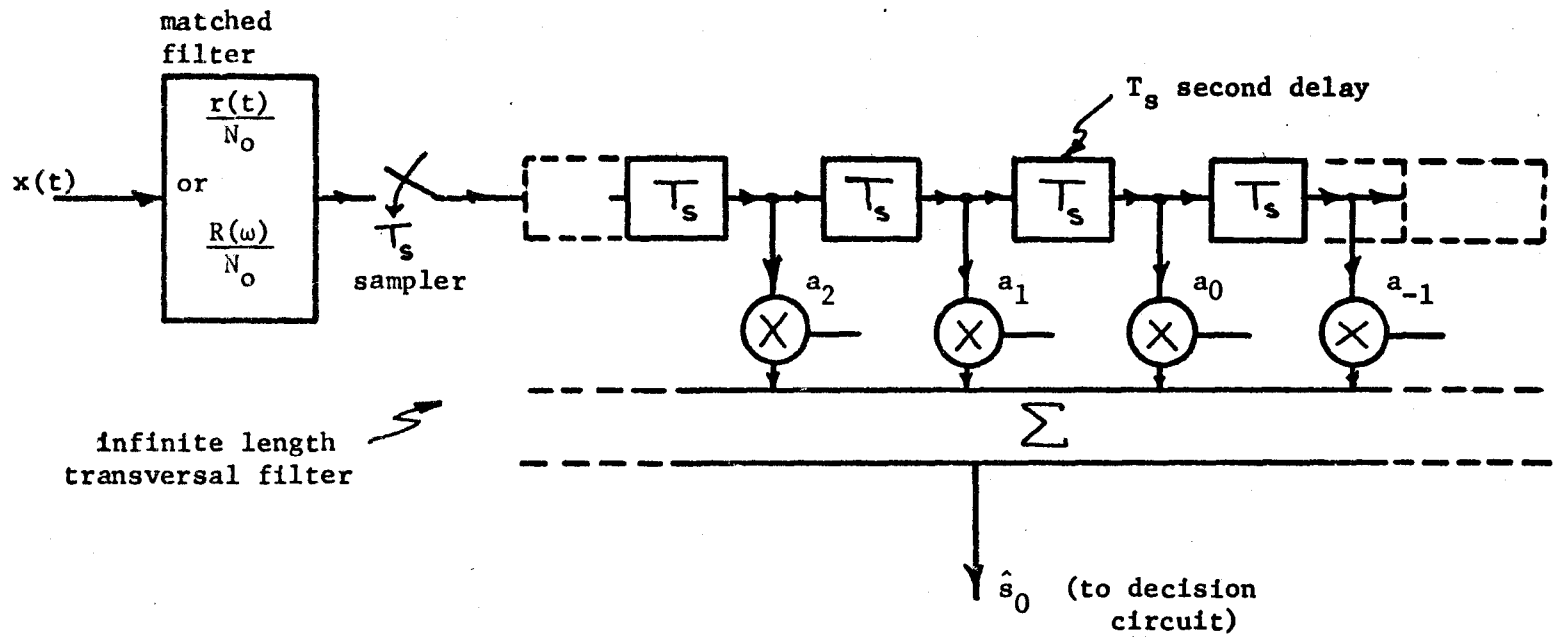

Figure 3.1 Basic unrealizable linear receiver structure. This is the structure derived by George (1965) and others.

From these, the resulting recursive receiver structure can readily be seen and it is shown in block diagram form in figure 3.2. It is an unrealizable structure because of the infinite length transversal filter

$$\sum_{m=-\infty}^{\infty}{}' \frac{\phi_r(mT_s)}{N_o} e^{j\omega mT_s}$$

which appears in the feedback path. Later in this chapter we will be concerned with obtaining realizable structures from equations (3-29) and (3-30).

In both the realizations shown in figures 3.1 and 3.2, the purpose of the systems following the matched filter is to compensate for intersymbol interference. We have shown these systems in the form of sampled data systems, but they could also be implemented in analogue form using analogue transversal filters in which case the samplers would appear at their outputs rather than at their inputs. In the present research, our main interest is in sampled data or digital implementation of the baseband receiver, and so we have represented the compensators of figures 3.1 and 3.2 as discrete time or sampled data systems.

3.3 The Nonlinear Estimate Feedback Equalizer

Using equation (3-28) we may rewrite the estimate of equation (3-26) in the form

$$\hat{s}_o = \frac{1}{1+\rho_n} \int_{-\infty}^{\infty} x(\tau) \frac{r(\tau)}{N_o} d\tau - \frac{1}{1+\rho_n} \sum_{m=-\infty}^{\infty}{}' \frac{\phi_r(mT_s)}{N_o} \hat{s}_m \qquad (3\text{-}31)$$

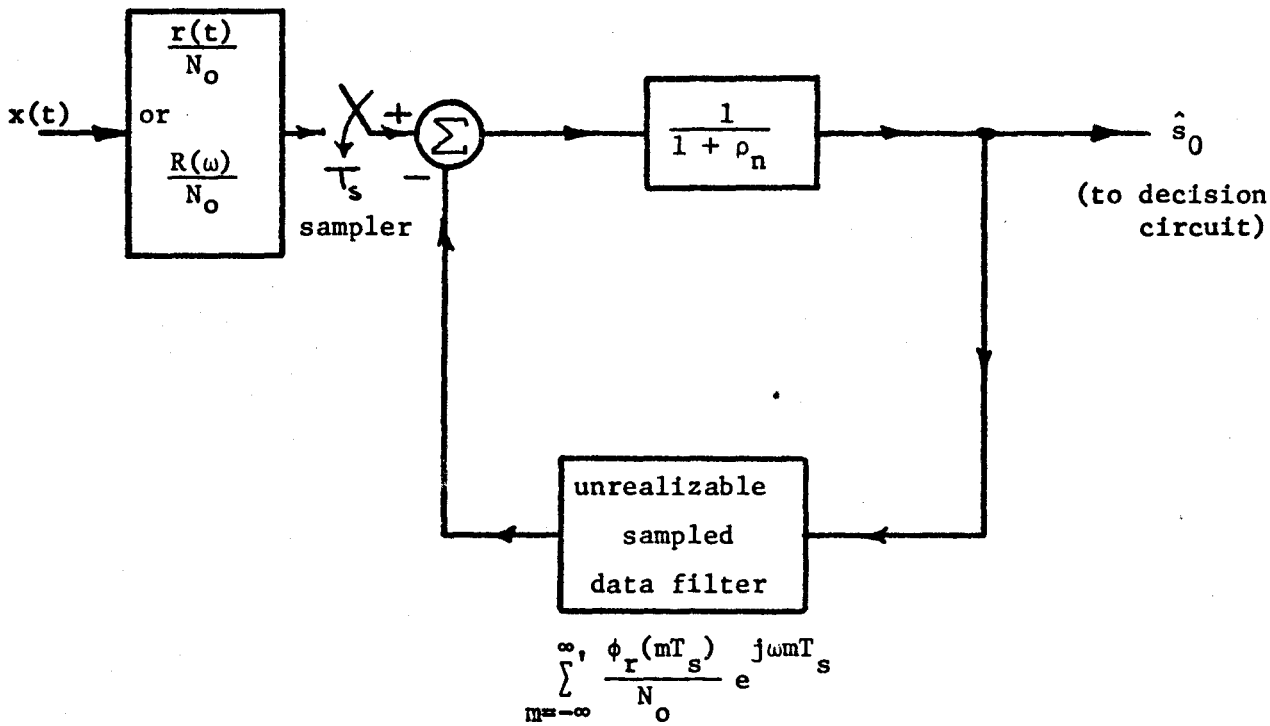

Figure 3.2 An alternate structure for the optimum unrealizable linear receiver.

If we now substitute equation (3-6) for x(t) in this we obtain $\hat{s}_o$ as

$$\hat{s}_o = \frac{\rho_n}{1+\rho_n} s_o + \frac{1}{1+\rho_n} \int_{-\infty}^{\infty} n(\tau) \frac{r(\tau)}{N_o} d\tau + \frac{1}{1+\rho_n} \sum_{m=-\infty}^{\infty}{}' \frac{\phi_r(mT_s)}{N_o} (s_m - \hat{s}_m) \quad \ldots . \quad (3\text{-}32)$$

From this we may then obtain the estimation error $(s_o - \hat{s}_o)$ at time t=0 as

$$s_o - \hat{s}_o = \frac{s_o}{1+\rho_n} - \frac{1}{1+\rho_n} \int_{-\infty}^{\infty} n(\tau) \frac{r(\tau)}{N_o} d\tau - \frac{1}{1+\rho_n} \sum_{m=-\infty}^{\infty}{}' \frac{\phi_r(mT_s)}{N_o} (s_m - \hat{s}_m) \quad \ldots . \quad (3\text{-}33)$$

The first two terms on the right-hand side of equation (3-33) are caused by the additive noise n(t) and can be reduced only by increasing the energy or power in the transmitted signal. The third term, however, is caused by errors in compensating for intersymbol interference due to errors in estimating earlier and later symbols s_k $(k \neq 0)$. This term can be reduced if the linear estimates $\hat{s}_k$ are replaced by some other estimate, say s_k^*, which has a smaller estimation error (in the mean-square sense). That is, if

$$E\{(s_k - s_k^*)^2\} \leq E\{(s_k - \hat{s}_k)^2\}$$

at all sampling times $t=kT_s$ $(k \neq 0)$ then the mean square error $E\{(s_o - \hat{s}_o)^2\}$ at t=0 will be reduced compared to that of the optimum linear receiver, and as a result improved error performance will be obtained.

The obvious answer to this is to replace the linear estimates $\hat{s}_k$ in equations (3-31) and (3-33) with the a posteriori mean values or Bayes minimum mean-square error estimates

$$s_k^* = E\{s_k|X\} \qquad (-\infty < k < \infty) \qquad (3\text{-}34)$$

where X is a realization of the received signal X: $\{x(t), -\infty < t < \infty\}$. This implies that rather than use the optimum linear receiver, we should use the Bayes receiver. The Bayes estimate s_k^* has the smallest mean-square error of any estimator whether it is linear or nonlinear (Deutsch, 1965). Now for digital transmitted symbols s_k, equation (3-34) may be expanded to the form

$$s_k^* = E\{s_k|X\} = \sum_{\underline{\xi}} s_k p(s_k|X) \qquad (-\infty < k < \infty) \qquad (3\text{-}35)$$

where $\underline{\xi}$ is the set $(\xi_1,\ldots,\xi_m)$ of m possible symbol values. Bowen (1969) has shown that the Bayes minimum probability of error receiver is a very complex nonlinear structure. This complexity arises in the computation of the a posteriori probabilities $p(s_k|X)$ and thus the Bayes minimum mean-square error receiver defined by equation (3-35) will involve the same complex nonlinear structure. Since one of our objectives in the present investigation is to design an equalizer or receiver which is comparable in complexity to conventional equalizers, we must seek some other structure than the Bayes receiver of equation (3-35).

Let us begin by recalling the received baseband signal x(t) of equation (2-99) which may be written as

$$x(t) = \sum_k s_k\, r(t-kT_s) + n(t)$$

Let us assume, as previously, the following:

(i) the symbols $\{s_k\}$ are statistically independent, equiprobable and binary with the values ± 1.

(ii) n(t) represents stationary Gaussian noise with known autocorrelation function $R_n(\tau)$.

(iii) The received pulse shape r(t) is known a priori at the receiver.

Let us concentrate our effort now on the estimation of a single symbol, say s_o. Then given a realization of the received signal X: $\{x(t), t \in I\}$ where I denotes an interval of observation stretching to both sides of $s_o r(t)$, we want to estimate s_o from X.

In the following let us suppose an interval of observation I stretching over MT_s seconds or M signalling intervals to either side of $s_o r(t)$, and let us assume for the moment that $s_j = 0$ $|j| > M$. We will, as it turns out, be able to remove this assumption later. In any event, we can by using this assumption write

$$x(t) = \sum_{k=-M}^{M} s_k r(t-kT_s) + n(t) \ . \tag{3-36}$$

Now let us make the idealizing assumption that we have available at the receiver, the sequence of symbols

$$\underline{S}' = (s_{-M},\ldots,s_{-1}, s_1,\ldots,s_M) \tag{3-37}$$

consisting of all the transmitted symbols lying within the interval of observation I except s_o which is the one we wish to estimate. Then let us define as our optimum estimate of s_o, the a posteriori conditional mean value

$$\tilde{s}_o = E\{s_o | X, \underline{S}'\} \tag{3-38}$$

This estimate is the Bayes minimum mean-square error estimate of s_o given the realization of the received signal X and the symbol sequence

$\underline{S}'$ of equation (3-37). We shall call $\tilde{s}_o$ the conditional Bayes estimate of s_o, since it is related to the Bayes estimate s_o^* of equation (3-35) by the relationship

$$s_o^* = \sum_{\underline{S}'} \tilde{s}_o \, p(\underline{S}')$$

where the summation is over all possible sequences $\underline{S}'$. In the binary case there are 2^{2M} such sequences. The conditional estimate $\tilde{s}_o$ will be a nonlinear function of X and $\underline{S}'$ unless s_o, X and $\underline{S}'$ have jointly Gaussian statistics.

Now the conditional Bayes estimate $\tilde{s}_o$ of equation (3-38) may be expanded to the form

$$\tilde{s}_o = E\{s_o|X,\underline{S}'\} = \sum_{\underline{\xi}} s_o \, p(s_o|X,\underline{S}') \tag{3-39}$$

where $p(s_o|X,\underline{S}')$ is the conditional probability function of s_o and $\underline{\xi}$ is, as before, the set $(\xi_1,\ldots,\xi_m)$ of $m \geq 2$ possible values of the symbol s_o. Now by applying Bayes rule to the probability function in equation (3-39), we obtain*

$$p(s_o|X,\underline{S}') = \frac{p_X(X|\underline{S}',s_o)p(s_o|\underline{S}')}{p_X(X|\underline{S}')} \tag{3-40}$$

Then since the transmitted symbols have been assumed to be statistically independent

$$p(s_o|\underline{S}') = p(s_o)$$

and equation (3-40) becomes

---

*We note here that the functions $p_X(X|..)$ are conditional probability density functions, not discrete probability functions.

$$p(s_o|X,\underline{S}') = \frac{p_x(X|\underline{S}',s_o)p(s_o)}{p_x(X|\underline{S}')} \tag{3-41}$$

Now the probability density function $p_x(X|\underline{S}')$ may be written as

$$p_x(X|\underline{S}') = \sum_{\underline{\xi}} p_x(X,s_o|\underline{S}')$$

and applying Bayes rule to the right hand side, we obtain the result

$$p_x(X|\underline{S}') = \sum_{\underline{\xi}} p(s_o)p_x(X|\underline{S}',s_o) \tag{3-42}$$

Then substituting equations (3-42) and (3-41) into equation (3-40) we obtain the estimate $\tilde{s}_o$ as

$$\tilde{s}_o = \frac{\sum_{\underline{\xi}} s_o p(s_o)p_x(X|\underline{S}',s_o)}{\sum_{\underline{\xi}} p(s_o)p_x(X|\underline{S}',s_o)} \tag{3-43}$$

In the case of binary (m=2) symbols having the values ±1, this last result may be rewritten in the form

$$\tilde{s}_o = \frac{p_x(X|\underline{S}',s_o=1) - p_x(X|\underline{S}',s_o=-1)}{p_x(X|\underline{S}',s_o=1) + p_x(X|\underline{S}',s_o=-1)} \tag{3-44}$$

which is the desired result. The problem of finding the optimum estimate $\tilde{s}_o$ has now been reduced to that of evaluating the conditional probability density function $p_x(X|\underline{S}',s_o)$ as a function of s_o.

Let us now define the sequence

$$\underline{S} = (\underline{S}',s_o) = (s_{-M},\ldots,s_1, s_o, s_1,\ldots,s_M)$$

as the sequence of all transmitted symbols lying within the observation interval I, so that

$$p_x(X|\underline{S}',s_o) = p_x(X|\underline{S}) \ .$$

Then if we know X and $\underline{S}$ we may regard

$$N_s: \ \{n_s(t) = x(t) - \sum_{k=-M}^{M} s_k r(t-kT_s)\} \tag{3-45}$$

as a realization of a Gaussian noise signal with autocorrelation function $R_n(\tau)$. Then using abstract vector space notation (Vulikh, 1963), where the inner product of any two functions $\mu(t)$ and $\eta(t)$ is defined as

$$[\mu,\eta] = \int_I \mu(t)\eta(t)dt \ ,$$

we may write the probability density function $p_x(X|\underline{S})$ as

$$p_x(X|\underline{S}) = p_n(N_s) = C\exp\{-\frac{1}{2}[n_s, R_n^{-1} * n_s]\} \tag{3-46}$$

where

(i) C is a constant

(ii) $*$ denotes convolution

(iii) R_n^{-1} is the inverse kernel (Van Trees, 1968) where

$$R_n * (R_n^{-1} * n_s) = n_s$$

Now let us define the shorthand notations

$$y_i = [x(t), R_n^{-1} * r(t-iT_s)] \tag{3-47}$$

and

$$\phi_k = [r(t), R_n^{-1} * r(t-kT_s)] = \phi_{-k} \tag{3-48}$$

We may then rewrite equation (3-46) in the form

$$p_x(X|\underline{S}) = C'\exp\{\sum_{i=-M}^{M} s_i(y_i - \frac{1}{2}\sum_{k=-M}^{M} s_k\phi_{k-i})\} \tag{3-49}$$

which is the desired conditional probability density function.

In order to obtain the optimum estimate $\tilde{s}_o$, let us write the exponent in equation (3-49) to explicitly show s_o, the symbol which we wish to estimate. We may then write after some manipulation

$$p_x(X|\underline{S}) = C'\exp\{s_o y_o - s_o \sum_{k=-M}^{M}{}' s_k\phi_k - \frac{1}{2} s_o^2 \phi_o + \sum_{i=-M}^{M}{}' s_i y_i - \frac{1}{2} \sum_{i=-M}^{M}{}' \sum_{k=-M}^{M}{}' s_i s_k \phi_{k-i}\} \qquad (3\text{-}50)$$

where $\sum_k'$ implies that the k=0 term has been removed from the various summations. Substituting equation (3-50) into equation (3-44), and cancelling those terms common to both the numerator and the denominator, we obtain the optimum estimate $\tilde{s}_o$ at time t=0 as

$$\tilde{s}_o = \frac{\exp\{y_o - \sum_{k=-M}^{M}{}' s_k\phi_k\} - \exp\{-y_o + \sum_{k=-M}^{M}{}' s_k\phi_k\}}{\exp\{y_o - \sum_{k=-M}^{M}{}' s_k\phi_k\} + \exp\{-y_o + \sum_{k=-M}^{M}{}' s_k\phi_k\}} \qquad (3\text{-}51)$$

Equation (3-51) may then be rewritten to obtain the optimum estimate $\tilde{s}_o$ in closed form as

$$\tilde{s}_o = \tanh\{y_o - \sum_{k=-M}^{M}{}' s_k\phi_k\} \qquad (3\text{-}52)$$

This expression specifies the operations which must be performed on the received signal x(t) to obtain the conditional Bayes estimate $\tilde{s}_o$ at time t=0, given the availability of the symbol sequence $\underline{S}'$ at the receiver. The problem now is to interpret this estimate so that we can obtain a receiver structure from it.

The estimate $\tilde{s}_o$ in equation (3-52) is specifically the estimate of the symbol s_o at time t=0. The optimum estimate of the transmitted symbol in any other T_s second symbol period, say the nth, may be found by simply shifting the observation interval I by nT_s seconds. Thus the conditional Bayes estimate $\tilde{s}_n$ of the symbol s_n may be written as

$$\tilde{s}_n = \tanh(y_n - \sum_{k=-M}^{M'} s_{k+n}\phi_k) \quad (-\infty < n < \infty) \tag{3-53}$$

where now the observation interval I extends MT_s seconds to either side of $t=nT_s$.

Thus far in this analysis we have assumed a finite observation interval I. In practice the response of any physical channel will extend to infinity, although it will be negligibly small after a finite time. For any physical channel of interest the series

$$\lim_{M\to\infty} \{ \sum_{k=-M}^{M} \phi_k \}$$

will thus converge, since the ϕ_k represent the sampled autocorrelation properties of the received pulse shape r(t). There are thus no difficulties in extending the observation interval I to infinity, and we may, therefore, write

$$\tilde{s}_o = \tanh(y_o - \sum_{k=-\infty}^{\infty'} s_k\phi_k) \tag{3-54}$$

or in a more general form

$$\tilde{s}_o = \tanh(y_o - \sum_{k\in I}' s_k\phi_k) \tag{3-55}$$

where I is the observation interval of any desired length.

The optimum conditional Bayes estimate $\tilde{s}_o$ of s_o at time t=0 has been derived under the assumption that the sequence $\underline{S}'$ of transmitted symbols in all other symbol periods is available to the receiver. In practice of course this assumption will never be fulfilled, and therefore in order to obtain a receiver which can be implemented, we must, to some extent, sacrifice the optimality of equation (3-55). What we do have available (in principle) are the estimates $\{\tilde{s}_n\}$ of the symbols $\underline{S}'$. We may, therefore replace the symbol sequence $\underline{S}'$ in equation (3-55) with the estimates $\{\tilde{s}_n\}$ to obtain the sub-optimum estimate.

$$\tilde{s}_o = \tanh(y_o - \sum_{k\epsilon I}{}' \tilde{s}_k \phi_k) \qquad (3\text{-}56)$$

Provided that the estimates $\{\tilde{s}_n\}$ are good estimates of the corresponding symbols $\underline{S}'$, the behaviour of the sub-optimum estimate in equation (3-56) will be very close to that of the optimum estimate in equation (3-55). The sub-optimum estimate in equation (3-56) has the very attractive property of being recursive, and as a result any resulting receiver may be implemented as a feedback structure as we will now show.

Let us start with the quantity y_o in equation (3-56). From equation (3-47) it may be written as

$$y_o = [x(t), R_n^{-1} * r(t)] \qquad (3\text{-}57)$$

and this is seen to be the result of passing the received signal x(t) through a filter matched to the pulse-shape r(t) in a background of additive Gaussian noise with autocorrelation function $R_n(\tau)$. The weighting function of this filter is defined as

$$g(t) = R_n^{-1} * r(t) \qquad (3\text{-}58)$$

and in the particular case when the noise is white with power spectral density N_o, as in the preceding section, we have

$$g(t) = \frac{r(t)}{N_o} \tag{3-59}$$

Equation (3-57) may then be written in the form

$$y_o = \int_I x(\tau)\, \frac{r(\tau)}{N_o}\, d\tau \tag{3-60}$$

In a similar manner, the quantities ϕ_k in equation (3-56) are given by equations (3-48) and (3-58) as

$$\phi_k = [r(t),\, g(t-kT_s)] \qquad (k \in I)\ . \tag{3-61}$$

When the noise is white so that equation (3-59) applies, we may write

$$\phi_k = \frac{1}{N_o} \int_I r(t)r(t-kT_s)dt = \frac{\phi_r(kT_s)}{N_o} \qquad (k \in I) \tag{3-62}$$

where $\phi_r(kT_s)$ is the sampled autocorrelation function of the received pulse shape r(t) defined in equation (3-19).

Let us now substitute equations (3-60) and (3-62) into equation (3-56) to obtain the estimate $\tilde{s}_o$ as

$$\tilde{s}_o = \tanh\Big(\frac{1}{N_o} \int_I x(\tau)r(\tau)d\tau - \sum_{k\in I}{}' \frac{\phi_r(kT_s)}{N_o}\, \tilde{s}_k \Big) \tag{3-63}$$

when the additive noise is white with power spectral density N_o. Comparing the quantity

$$\frac{1}{N_o} \int_I x(\tau)r(\tau)d\tau - \sum_{k\in I}{}' \frac{\phi_r(kT_s)}{N_o}\, \tilde{s}_k \tag{3-64}$$

in equation (3-63) with the optimum linear estimate of equation (3-31),

we see that except for the multiplying factor $(1+\rho_n)^{-1}$ in equation (3-31) and the nonlinear estimates $\tilde{s}_k$ $(k \neq 0)$ in equation (3-64), the two are identical. We, therefore, see that the nonlinear estimate $\tilde{s}_o$ of equation (3-63) may be implemented as a feedback structure similar to that shown for the linear estimate in figure 3.2. The only difference between the two structures is that in the nonlinear case, there is a zero-memory nonlinearity tanh(·) included in the feedback path as shown in figure 3.3. This structure which we shall call the (nonlinear) estimate feedback receiver is very similar to that suggested by de Buda (1965). de Buda suggested replacing the linear estimates $\hat{s}_m$ $(m \neq 0)$ in equation (3-31) with the a posteriori mean values $E\{s_m|\hat{s}_m\}$ $(m \neq 0)$ to obtain improved performance compared to the linear receiver. In the case of binary, anti-podal, transmitted symbols $\{s_m\}$ having the values ±1, de Buda then obtained the tanh(·) nonlinearity which we have derived in this section, however, he did not show that the resulting receiver is an approximation to the conditional Baye's estimator $E\{s_o|X,\underline{S}'\}$. He did, however, show that the resulting estimation error is always less than that obtained from the corresponding linear receiver and hence the performance of the estimate feedback receiver is better than that of the linear receiver. The structure of figure 3.3 is unrealizable because of the requirement of delay into the future in the feedback path. We will deal with this problem in a later section.

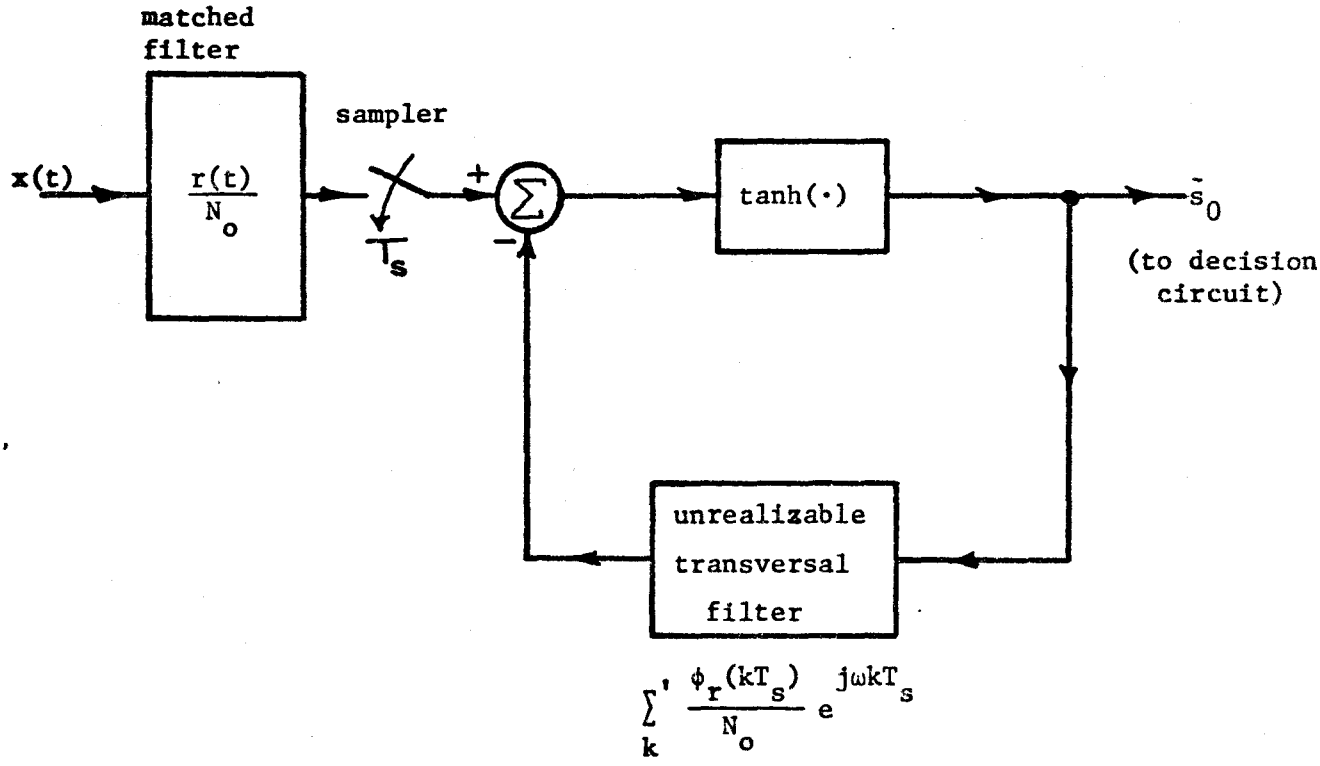

Figure 3.3 Basic (unrealizable) structure of nonlinear estimate feedback receiver.

3.4 The Decision Feedback Receiver

Let us first examine the function

$$y_c = \tanh\left(\frac{x}{c}\right) \qquad (c > 0)$$

where c is a positive constant. If we now take the limit as c approaches zero, we obtain the result

$$\lim_{c\to 0} y_c = \lim_{c\to 0} \tanh\left(\frac{x}{c}\right) = \mathrm{sgn}(x) \tag{3-65}$$

where sgn(x) is the signum function defined by

$$\mathrm{sgn}(x) = \begin{cases} 1 & x > 0 \\ 0 & x = 0 \\ -1 & x < 0 \end{cases} \tag{3-66}$$

If we then apply equation (3-65) to the nonlinear estimate in equation (3-63) we obtain the result as the noise power spectral density N_o approaches zero

$$\tilde{s}_o\Big|_{N_o\to 0} \to \mathrm{sgn}\left\{ \int_I x(\tau)r(\tau)d\tau - \sum_{k\in I}{}' \phi_r(kT_s)\mathrm{sgn}(\tilde{s}_k)\right\} \tag{3-67}$$

The righthand side of equation (3-67) is the decision feedback receiver developed by Austin (1967). It may be implemented by the same structure as that shown in figure 3-3 except that in this case the tanh(x) nonlinearity is replaced by the sgn(x) nonlinearity of equation (3-66). In other words the decision-feedback equalizer is a small noise limiting approximation to the sub-optimum nonlinear estimate feedback equalizer described by equation (3-63).

The implication of equation (3-67) is that at low additive noise levels the decision feedback and the nonlinear estimate feedback receivers

are essentially equivalent in performance. However, at high levels of additive noise (N_o large) the approximation of equation (3-67) tends to fail and as a result the nonlinear estimate feedback structure exhibits superior performance. In later chapters where we carry out simulations of the two structures, we shall see that this is essentially true.

3.5 Realization of the Receiver Structure

In the foregoing, we have developed a nonlinear feedback receiver structure which has been shown to be an approximation to a conditional Baye's estimation structure. Because of the requirement of negative delay (delay into the future) within the feedback path, this structure is not physically realizable. The problem now, therefore, is to find a physically realizable approximation to this optimum structure which, hopefully, is comparable in complexity to conventional (transversal filter) equalization receivers.

Let us start with the recursive unrealizable nonlinear estimate $\tilde{s}_o$ at time t=0 which is given by equation (3-63) as

$$\tilde{s}_o = \tanh\left(\frac{1}{N_o} \int_I x(\tau) r(\tau) d\tau - \sum_{k \in I}{}' \frac{\phi_r(kT_s)}{N_o} \tilde{s}_k \right) \qquad (3\text{-}63)$$

Now let us call the input to the tanh(·) nonlinearity* $\hat{s}_o$. It may be written as

---

*We use the same notation here as for the optimum linear estimate of equation (3-31). We do this because if the parameters of the optimum linear receiver are found, the optimum input to the nonlinearity will be identical to the linear estimate s except for the replacement of the linear estimates $\hat{s}_k$ ($k \neq 0$) by the nonlinear estimates $\tilde{s}_k$ ($k \neq 0$). Also in chapter 4, we will find the optimum parameters for the nonlinear receiver using the same linear algorithm as would be used for the linear receiver.

$$\hat{s}_o = \int_I x(\tau) \frac{r(\tau)}{N_o} d\tau - \sum_{k\epsilon I}' \frac{\phi_r(kT_s)}{N_o} \tilde{s}_k \qquad (3\text{-}68)$$

which except for the nonlinear estimates $\tilde{s}_k$ $(k \neq 0)$ in the second term is identical in form to the linear estimate of equation (3-31). The observation interval I is the time interval extending to either side of t=0 over which our observation of x(t) is considered to extend. In theory it may be infinite in length. It may also be considered equivalent to the set of integers over which the index k in equation (3-68) extends. Now let us split I into the sum of two parts I_+ and I_- where

I_+ : $\{k: k > 0\}$ corresponding to those signalling intervals which occur after t=0

and

I_- : $\{k: k < 0\}$ corresponding to those signalling intervals in I which occur prior to t=0.

We may then rewrite equation (3-68) in the form

$$\hat{s}_o = \int_I x(\tau) \frac{r(\tau)}{N_o} d\tau - \sum_{k\epsilon I_+} \frac{\phi_r(kT_s)}{N_o} \tilde{s}_k - \sum_{k\epsilon I_-} \frac{\phi_r(kT_s)}{N_o} \tilde{s}_k \qquad (3\text{-}69)$$

The second term in equation (3-69) compensates for intersymbol interference caused by symbols (or pulses) in signalling intervals occurring after t=0 using a weighted sum of future nonlinear estimates $\tilde{s}_k$ $(k > 0)$. The third term performs a similar compensation for intersymbol interference due to symbols in previous signalling intervals using a weighted sum of previous estimates $\tilde{s}_k$ $(k < 0)$.

Neither $\tilde{s}_o$ of equation (3-63) nor $\hat{s}_o$ of equation (3-69) represent physically realizable systems since the future nonlinear estimates $\tilde{s}_k$ ($k > 0$) cannot be made available at t=0. However, the previous nonlinear estimates $\tilde{s}_k$ ($k < 0$) can be made available at t=0 by means of a nonlinear feedback system. We may, therefore, implement (unrealizably) the nonlinear estimate $\tilde{s}_o$ of equation (3-63) or equivalently $\hat{s}_o$ of equation (3-69) by the system shown in figure 3.4. This configuration is equivalent to the one derived earlier in figure 3-3.

In the structure of figure 3-4 the block

$$\frac{r(-\tau)}{N_o} \qquad \text{or equivalently} \qquad \frac{R^*(\omega)}{N_o}$$

represents a filter matched to the received pulse-shape r(t). Such a filter may always be realized, at least approximately, to any desired degree of accuracy (e.g., Coll, 1966). Also the nonlinear feedback system of figure 3.4 may be realized as shown provided of course the range of k is kept finite.

In practice the index k may always be constrained to a finite range, since for any real pulse shape r(t) the corresponding auto-correlation function $\phi_r(\tau)$ will be negligible for τ outside some finite range. In fact for almost all channels of physical interest

$$\phi_r(\tau) \approx 0 \qquad |\tau| > \frac{\Delta_g}{2}$$

where Δ_g is the rms channel delay spread* defined by equation (2-64).

---

*We use $\Delta_g/2$ here because by its definition Δ_g is an estimate of the total delay spread symmetrically located about the mean channel delay.

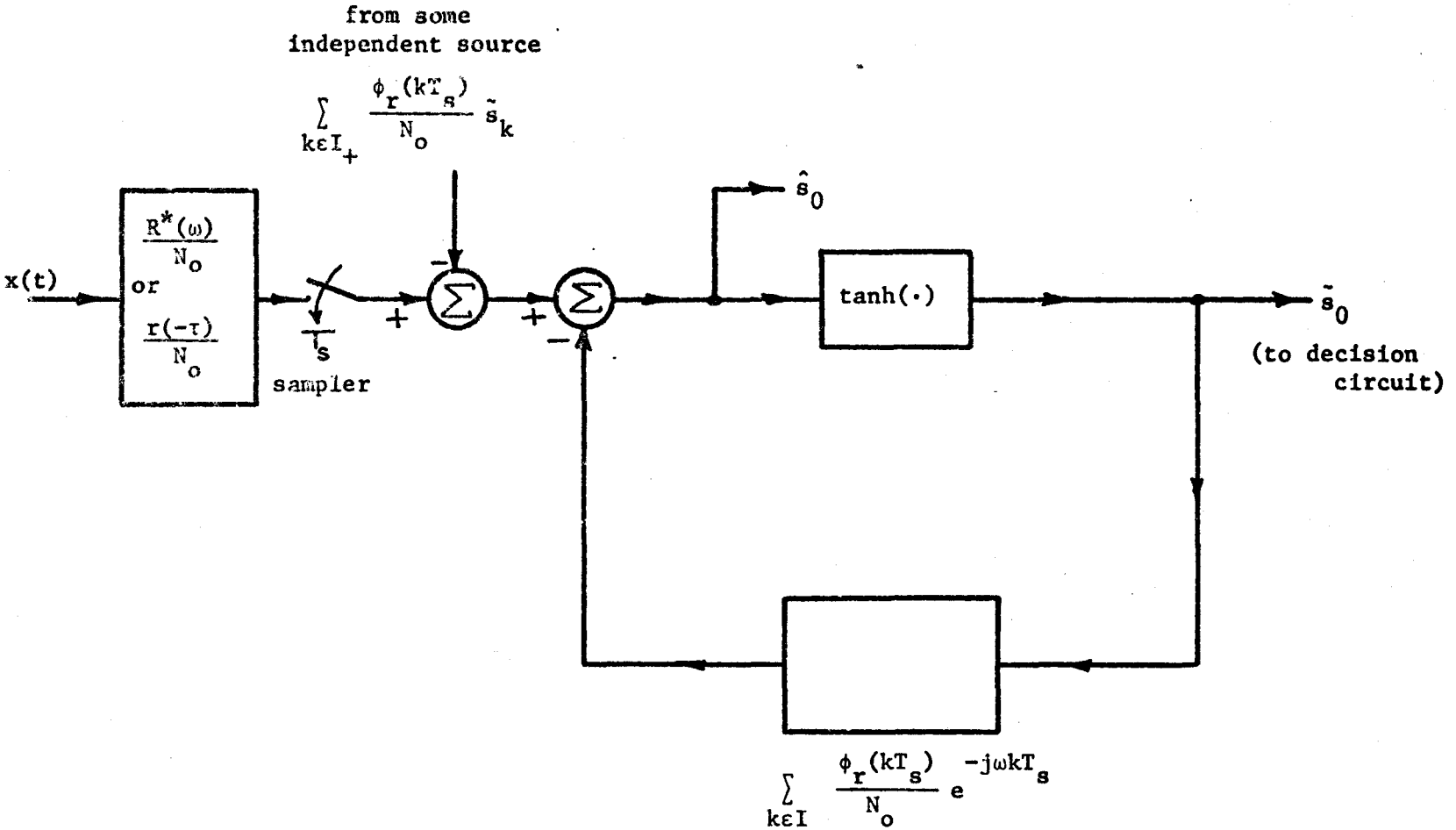

Figure 3.4 Unrealizable nonlinear receiver configuration equivalent to figure 3.3.

We may, therefore restrict the range of k in equation (3-69) such that

$$k \leq L = \left[\frac{\Delta_g}{2T_s} \right] \tag{3-70}$$

where [x] implies the nearest larger integer to x. By so restricting the range of k, we obtain a similar restriction on the observation interval I and on the index sets I_+ and I_- which now become

$$I_+ : \{k : k=1,\ldots,L\}$$

$$I_- : \{k : k=-1,\ldots,-L\} .$$

Equation (3-69) may then be rewritten in the form

$$\hat{s}_o = \int_I x(\tau) \frac{r(\tau)}{N_o} d\tau - \sum_{k=1}^{L} \frac{\phi_r(kT_s)}{N_o} \tilde{s}_k - \sum_{k=-1}^{-L} \frac{\phi_r(kT_s)}{N_o} \tilde{s}_k \tag{3-71}$$

We point out here that because Δ_g is only an estimate of the channel delay spread, L is only an estimate of the range over which k must extend. In practice, one would normally choose a range for k which is somewhat greater than L.

The first and third terms of equation (3-71) represent essentially realizable quantities. The problem now, therefore, is how to realize, at least approximately, the term

$$\sum_{k=1}^{L} \frac{\phi_r(kT_s)}{N_o} \tilde{s}_k$$

which represents the compensation for intersymbol interference due to symbols in future signalling periods.

Let us begin by imposing a delay of LT_s seconds (L signalling intervals) on each term of $\hat{s}_o$. We may then write the delayed estimate

corresponding to $\hat{s}_o$ as

$$\hat{s}'_o = \int_I x(\tau) \frac{r(\tau+LT_s)}{N_o} d\tau - \sum_{k=1}^{L} \frac{\phi_r(kT_s)}{N_o} \tilde{s}_{k-L} - \sum_{k=-1}^{-L} \frac{\phi_r(kT_s)}{N_o} \tilde{s}_{k-L} \qquad (3\text{-}72)$$

and from this we can see that if some way is found to approximate the nonlinear estimates $\tilde{s}_k$ $(k > 0)$ in equation (3-71), then the receiver may be realized by the inclusion of a delay of LT_s seconds within its structure. In most of our analysis there is no need to explicitly show this delay provided that it is understood to be present in any implementation.

At this point let us digress for a moment. If the signal x(t) is passed through a filter matched to the received pulse shape r(t), then at time t=0, the filter output, which we shall call y_o, may be written as

$$y_o = \int_I x(\tau) \frac{r(\tau)}{N_o} d\tau \quad .$$

If we then substitute for $x(\tau)$ in this, we obtain

$$y_o = \sum_m s_m \int_I r(\tau-mT_s) \frac{r(\tau)}{N_o} d\tau + \int_I n(\tau) \frac{r(\tau)}{N_o} d\tau \qquad (3\text{-}73)$$

or on substituting equation (3-19) for the integral in this first term

$$y_o = \sum_m s_m \frac{\phi_r(mT_s)}{N_o} + w(0) \qquad (3\text{-}74)$$

where

$$w(0) = \int_I n(\tau) \frac{r(\tau)}{N_o} d\tau$$

is the additive noise at t=0 appearing at the filter output. Using the signal to noise ratio ρ_n defined in equation (3-28), we may rewrite equation

(3-74) as

$$y_o = \rho_n s_o + \sum_{m\neq 0} \frac{\phi_r(mT_s)}{N_o} s_m + w(0) \qquad (3\text{-}75)$$

where we note that

$$\left|\frac{\phi_r(mT_s)}{N_o}\right| \leq \frac{\phi_r(0)}{N_o} = \rho_n \,. \qquad (m \neq 0)$$

Now let us pass the L signals $x(t+kT_s)$ $k=1,\ldots,L$ through the same matched filter as above. If we call the L filter outputs $\{y_k: k=1,\ldots,L\}$, we may write

$$y_k = \int_I x(\tau+kT_s) \frac{r(\tau)}{N_o} d\tau \qquad (k=1,\ldots,L) \,. \qquad (3\text{-}76)$$

Then let us substitute for $x(\tau+kT_s)$ in equation (3-76) and expand the result in the same manner as equation (3-75) to obtain

$$y_k = \rho_n s_k + \sum_{m\neq k} \frac{\phi_r[(k-m)T_s]}{N_o} s_m + w(kT_s)$$

$$(k=1,\ldots,L) \qquad (3\text{-}77)$$

The set of filter outputs $(y_o, y_1,\ldots,y_L)$ may be realizably produced by the cascade combination of the above matched filter and a tapped delay line having L+1 taps as shown in figure 3.5. The use of the overall delay of LT_s seconds allows us to produce all L+1 outputs simultaneously.

Now let us define a set of (L+1) tap-gains $(g_o, g_1,\ldots,g_L)$ for this delay line. Then summing the weighted tap outputs, we obtain at time t=0, the quantity

$$u_o = \sum_{i=0}^{L} g_i y_i \qquad (3\text{-}78)$$

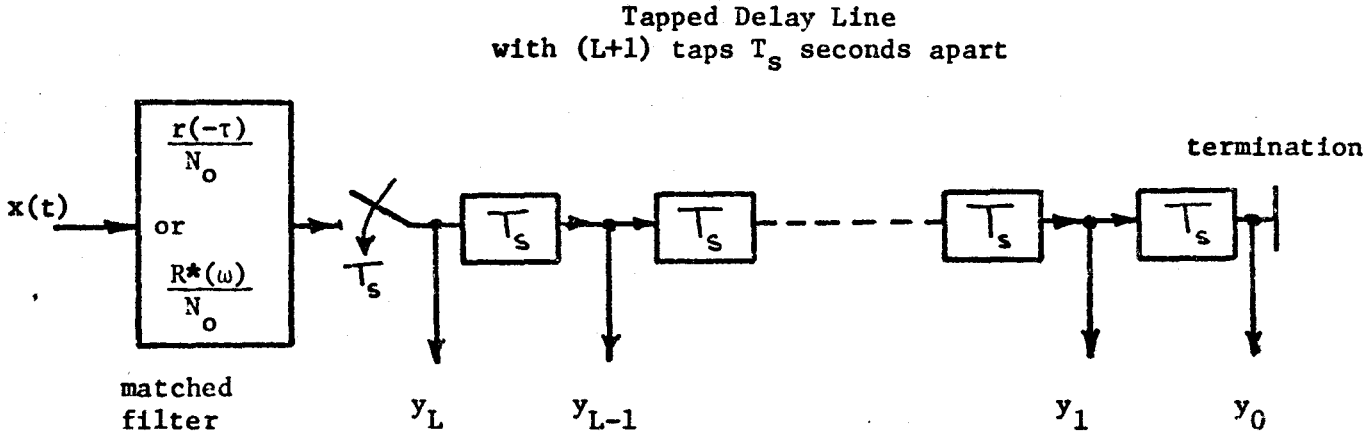

Figure 3.5 Configuration of system to produce set of filter outputs $(y_0, y_1, \ldots y_L)$. Note the use of a delay of LT_s seconds used to produce them simultaneously.

If we next define the values of these tap-gains as

$$g_o = 1$$

$$g_k = \frac{-\phi_r(kT_s)}{\rho_n N_o} \qquad (k=1,\ldots,L) \tag{3-79}$$

we may rewrite equation (3-78) in the form

$$u_o = \int_I x(\tau)\frac{r(\tau)}{N_o}d\tau - \sum_{k=1}^{L}\frac{\phi_r(kT_s)}{N_o}s_k$$

$$- \sum_{k=1}^{L}\frac{\phi_r(kT_s)}{\rho_n N_o}\left[\sum_{m\neq k}\frac{\phi_r[(k-m)T_s]}{N_o}s_m + w(kT_s)\right] \tag{3-80}$$

The first two terms in u_o are identical in form with the first two terms of $\hat{s}_o$ in equation (3-71). In fact the first two terms are identical with the corresponding terms in the Bayes optimum unrealizable estimate of equation (3-52). The third term of equation (3-80) represents an undesired interference component or noise term where we note that

$$\left|\frac{\phi_r(kT_s)}{\rho_n N_o}\right| = \left|\frac{\phi_r(kT_s)}{\phi_r(0)}\right| \leq 1 \qquad (k=1,\ldots,L)$$

We thus see that u_o is a linear approximation to the forward (present and future) components of the Bayes optimum unrealizable estimate of equation (3-52). Equation (3-80) may, therefore, be used as a realizable linear approximation to the first two terms of $\hat{s}_o$ in equation (3-71) or equivalently to the corresponding terms of $\tilde{s}_o$ in equation (3-63).

Thus, if we use equation (3-78) or (3-80) in equation (3-63) we obtain a realization of the nonlinear estimate feedback receiver as

$$\tilde{s}_o = \tanh\left(\int_I x(\tau)\frac{r(\tau)}{N_o}d\tau + \sum_{i=1}^{L} g_i y_i - \sum_{k=-1}^{-L}\frac{\phi_r(kT_s)}{N_o}\tilde{s}_k\right) \tag{3-81}$$

or equivalently

$$\hat{s}_o = \sum_{i=0}^{L} g_i \int_I x(\tau+iT_s) \frac{r(\tau)}{N_o} d\tau - \sum_{k=-1}^{-L} \frac{\phi_r(kT_s)}{N_o} \tilde{s}_k \qquad (3\text{-}82)$$

where in equation (3-82) we have made use of the definition of the $\{y_i: i=1,\ldots,L\}$ given by equation (3-76) and where the gains g_i $(i=0,1,\ldots,L)$ are defined by equations (3-79). The receiver structure implied by equations (3-81) and (3-82) may be implemented by the combination of a matched filter and two transversal filters shown in figure 3-6. In the diagram we have shown a sampler directly following the matched filter since in succeeding chapters we intend to employ sampled data transversal filters.

In the above we have described a realization of the nonlinear estimate feedback receiver in which a linear approximation to the optimum compensation for intersymbol interference due to future symbols was used. We will now discuss a realization of the receiver which uses a nonlinear approximation to this component of the compensation.

Suppose we take the hyperbolic tangent of the quantities y_k $(k=1,\ldots,L)$ defined in equations (3-76) and (3-77) to produce

$$\tilde{y}_k = \tanh(y_k) \qquad (k=1,\ldots,L) \qquad (3\text{-}83)$$

The $\tilde{y}_k$ $(k=1,\ldots,L)$ are a set of nonlinear estimates of the future symbols s_k $(k=1,\ldots,L)$. In the absence of the interference term

$$\sum_{m\neq k} \frac{\phi_r[(k-n)T_s]}{N_o} s_m$$

and under the assumption that the noise terms $w(kT_s)$ $(k=1,\ldots,L)$ are uncorrelated, the estimates $\tilde{y}_k$ $(k=1,\ldots,L)$ are the optimum Bayes estimates (Appendix B) of the future symbols s_k $(k=1,\ldots,L)$. They may

thus be used in equation (3-71) as an approximation to the nonlinear estimates $\tilde{s}_k$ (k=1,...,L) so that we now obtain

$$\hat{s}_o = \int_I x(\tau) \frac{r(\tau)}{N_o} d\tau - \sum_{k=1}^{L} \frac{\phi_r(kT_s)}{N_o} \tilde{y}_k - \sum_{k=-1}^{-L} \frac{\phi_r(kT_s)}{N_o} \tilde{s}_k \qquad (3\text{-}84)$$

We may also rewrite the corresponding nonlinear estimate $\tilde{s}_o$ of equation (3-63) as

$$\tilde{s}_o = \tanh\left(\int_I x(\tau) \frac{r(\tau)}{N_o} d\tau - \sum_{k=1}^{L} \frac{\phi_r(kT_s)}{N_o} \tilde{y}_k - \sum_{k=-1}^{-L} \frac{\phi_r(kT_s)}{N_o} \tilde{s}_k\right) \qquad (3\text{-}85)$$

The receiver structure implied by equations (3-84) and (3-85) may be realized by the nonlinear feedback structure of figure 3.7 which thus represents another possible implementation of the nonlinear estimate feedback receiver.

In practice, because of the unwanted interference term in the y_k (k=1,...,L), the tap-gain values which minimize the mean-square error in the forward (non-recursive) sections of both the above receiver structures will vary from the nominal values used in the above arguments. We will deal with this problem in chapter 4.

In this section we have derived two realizable approximations to the nonlinear estimation structure defined by equation (3-63). In the remainder of this thesis, we shall consider only the structure of figure 3.6 which uses a linear compensation term for intersymbol interference due to symbols in future signalling periods. We shall do this for the following reasons:

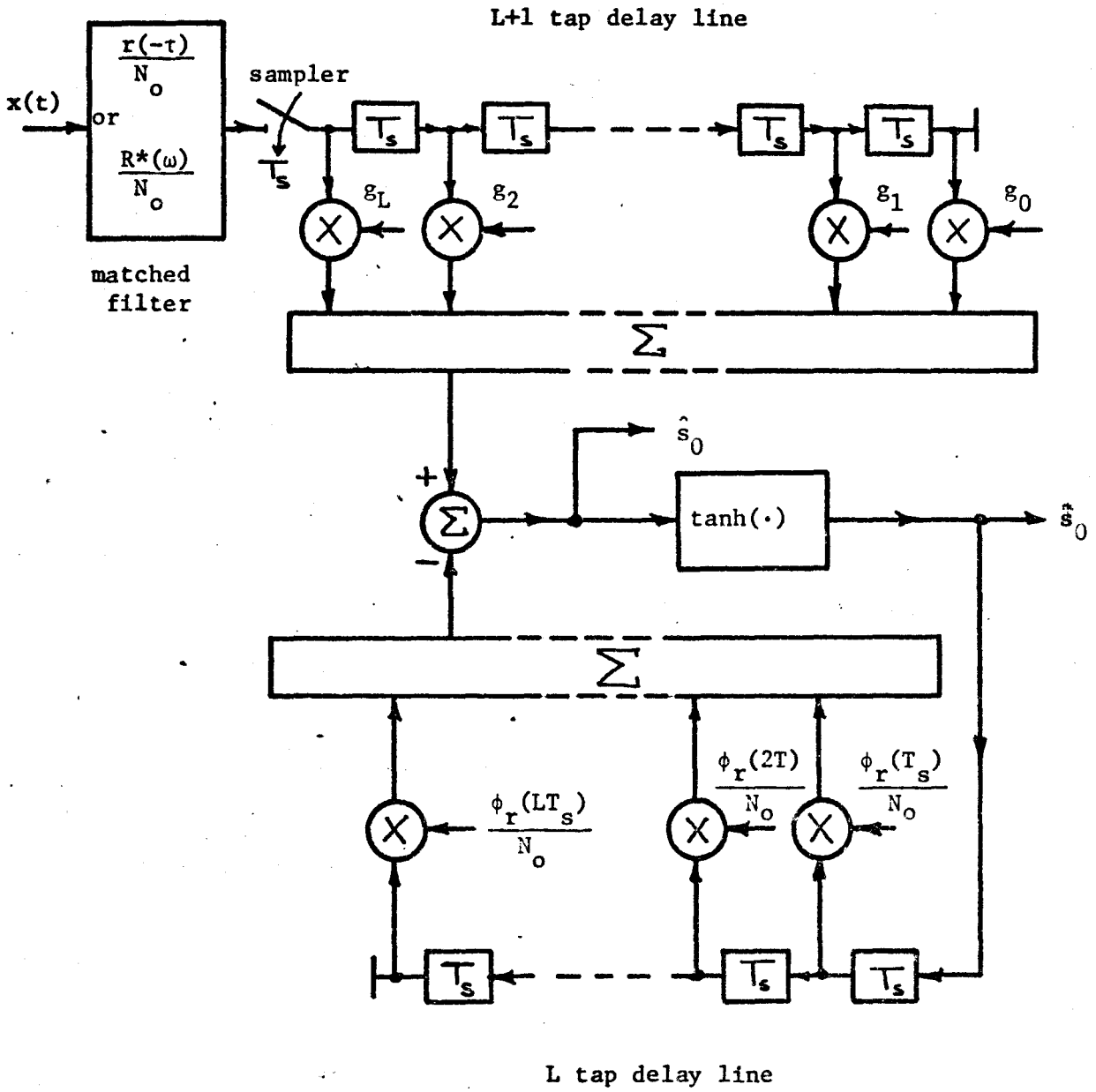

Figure 3.6 Basic structure of realizable nonlinear receiver using linear approximation in forward section.

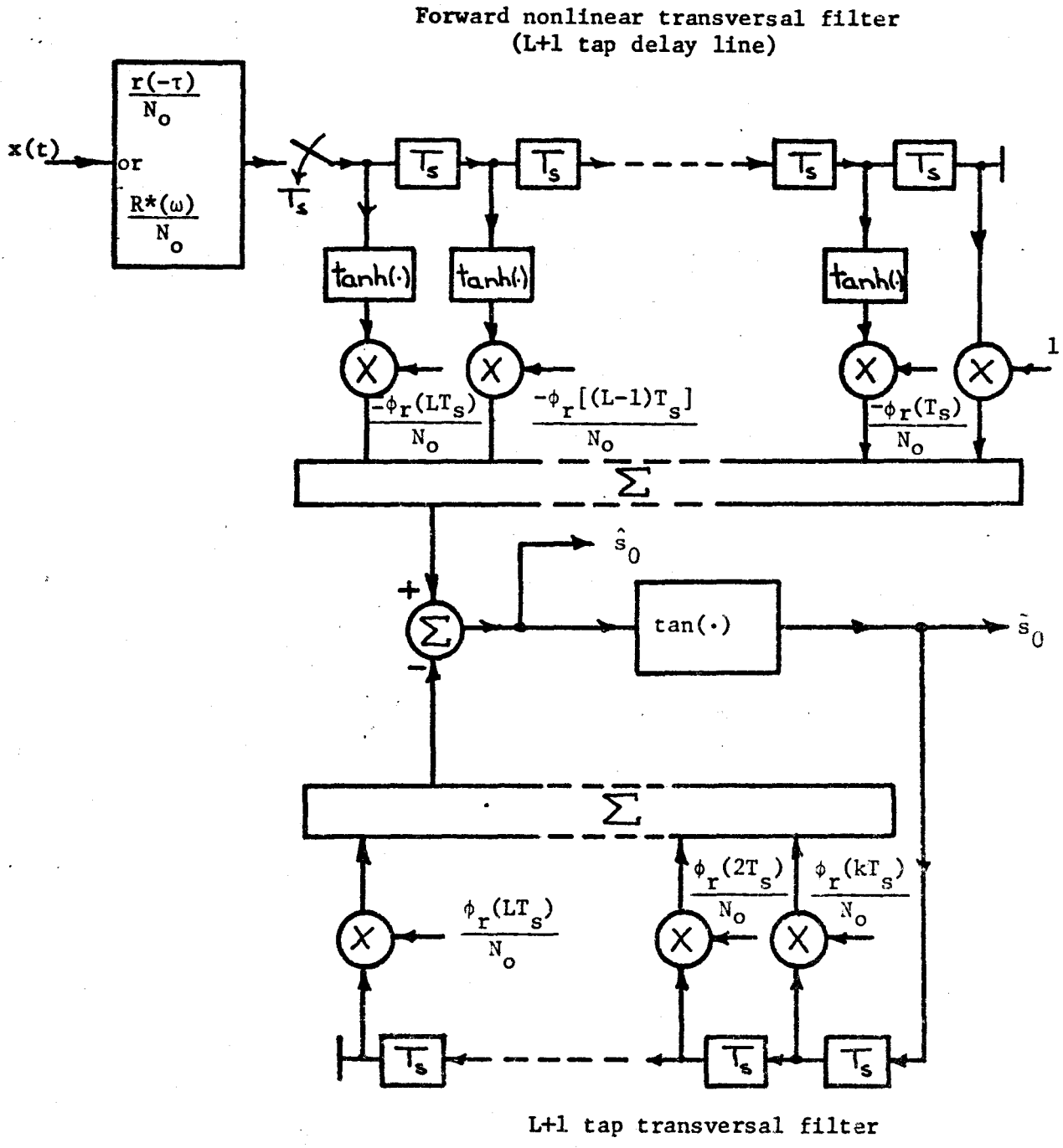

Figure 3.7 Basic structure of realizable nonlinear receiver using a nonlinear approximation in the forward section.

(i) The structure of figure 3.6 is simpler to implement because the forward section is linear rather than nonlinear, and one of our objectives is the development of receiver structures which are comparable in complexity to existing linear equalization receivers.

(ii) Except for the form of the nonlinearity in the feedback path, the structure of figure 3.6 is identical to the decision feedback receiver (Austin, 1967). We, therefore, can and will in later chapters obtain a direct measure of the change in performance induced by the use of the tanh(·) nonlinearity rather than the threshold detector used by Austin.

(iii) It is simpler, at least mathematically, to apply linear adaptive algorithms to the structure of figure 3.6. In chapter 4, we shall embed the receiver in an adaptive structure which uses these linear techniques.

3.6 The Use of a Saturating Limiter

In some applications, particularly if an analogue implementation of the receiver is used, the use of the tanh(·) nonlinearity may be both difficult and costly. At the same time, however, we may wish to preserve its properties, in particular its high noise properties. We note that when the noise power spectral density N_o is large the input to the tanh(·) nonlinearity is small in magnitude. As a result the tanh(·) nonlinearity when N_o is large tends to behave as a linear device and the feedback system in figure 3.6 as a linear filter. This tends to

avoid the small "signal suppression effect" (Davenport and Root, 1958) normally associated with zero-memory nonlinearities (for example the threshold detector or hard limiter sgn(·)). In the interests of simplicity, we would therefore like, in some cases, to replace the tanh(·) nonlinearity, by some other form of limiter having most of its favorable properties.

Recalling now that the slope of the function tanh(x) in the region of x small ($x \approx 0$) is close to unity, an obvious form of nonlinearity with which to replace tanh(x) is a saturating limiter defined by the relationship

$$\tilde{x} = \begin{cases} -1 & x \leq -\alpha \\ x & -\alpha < x < \alpha \\ 1 & x \geq \alpha \end{cases} \qquad (0 \leq \alpha \leq 1) \qquad (3\text{-}86)$$

where α, the limiter saturation value, lies between zero and one. We note that for $\alpha = 0$, we have the nonlinearity sgn(x) and the receiver is the decision feedback equalizer. The best value of α appears to be to some extent arbitrary, and should be determined by experiment in a particular application. We will discuss this in a later chapter.

CHAPTER 4

The Adaptive Equalizer

In chapter 3, we applied Bayes estimation theory to derive a nonlinear estimate feedback receiver for the extraction of binary antipodal transmitted symbols from a noisy, dispersed received signal or pulse train. This structure was derived under the assumption that the overall channel impulse response or equivalently the received pulse shape was time-invariant and known a priori at the receiver. This assumption and the additional assumption of wide sense stationary additive noise with known autocorrelation function lead to a time-invariant optimal receiver structure.

In practice, the received pulse shape is almost always unknown at the receiver, and in addition is usually randomly time-varying. Because of this, we shall, in this chapter, formulate an adaptive receiver using as its basis the nonlinear estimate feedback structure developed in chapter 3. The adaptive receiver has the ability to iteratively adjust itself to an unknown channel response (or received pulse shape), and in addition can track or follow the random time variations in the channel response.

4.1 The Fixed Optimum Equalizer

The basic receiver structure which we shall consider in this chapter is the one shown in figure 3-6 and defined by equations (3-81) and (3-82). It consists of the cascade connection of the following

three stages:

(i) a linear filter matched to the received pulse shape r(t). This filter maximizes the signal to additive noise ratio at its output and also equalizes or compensates for phase distortion in the frequency spectrum of the received signal.

(ii) a linear transversal filter which linearly compensates for intersymbol interference (time dispersion) due to symbols or pulses occurring after the present symbol.

(iii) a nonlinear feedback system having a zero-memory nonlinearity (ideally tanh(·)) followed by a transversal filter in the feedback path. It provides compensation for the intersymbol interference due to symbols in signalling intervals occurring prior to the present one.

The subsystem formed by (ii) and (iii) which compensates for intersymbol interference or channel time dispersion is known as an equalizer. It will be our primary concern in this chapter.

In any real communications system, the received pulse shape r(t) is usually both unknown and time-varying. Therefore the use of a fixed matched filter as shown in figure 3-6 is not feasible*. The usual practice, and one which we shall follow, is to replace the matched filter

---

*In some recent work Mark (1970) has developed an adaptive filter whose performance approaches that of a matched filter as it iteratively adjusts itself. In most point-to-point links, however, the signal to additive noise ratio is high enough that the processing gain of a matched filter is not required.

with some suitable time-invariant, bandlimiting filter which limits the additive noise power. This of course causes some loss in overall receiver performance but in most cases this loss is small. One often-used choice for this filter (Proakis, 1969) is one which is matched to the transmitted pulse shape.

Let us suppose that this filter is defined by its impulse response $a(\tau)$. Then for a receiver input signal of the form

$$y(t) = \sum_k s_k \, r(t-kT_s) + w(t) \tag{4-1}$$

where

(i) the s_k $(-\infty < k < \infty)$ are the binary information symbols which we wish to detect.

(ii) $r(t)$ is the unknown, time-varying received pulse shape.

(iii) $w(t)$ is wide sense stationary additive noise.

we may write the output of the filter $a(\tau)$ or equivalently the equalizer input as

$$x(t) = \sum_k s_k \int a(\tau) r(t-\tau-kT_s) d\tau + \int a(\tau) w(t-\tau) d\tau \tag{4-2}$$

where the limits of integration are assumed to be suitably defined. If we then define

$$h(t) = \int a(\tau) r(t-\tau) d\tau$$

and

$$n_c(t) = \int a(\tau) w(t-\tau) d\tau$$

we may rewrite equation (4-2) as

$$x(t) = \sum_k s_k h(t-kT_s) + n_c(t) \tag{4-3}$$

where h(t) is the effective overall channel impulse response* or received pulse shape at the equalizer input and $n_c(t)$ is the additive noise.

In the receiver structure of figure 3-6, we showed a sampler operating on the matched filter output at the times $t=nT_s$ $(-\infty < n < \infty)$. The equalizer is then a sampled data system. Equivalently, we could have shown the overall receiver as an analogue system with a sampler at its output producing the sequence of estimates $\{\tilde{s}_n\}$ or equivalently $\{\hat{s}_n\}$ at the times $t=nT_s$ $(-\infty < n < \infty)$. But, because we are mainly interested in the implementation of the equalizer using digital circuitry, we have placed the sampler preceding the equalizer. It then operates on the signal x(t) to produce the sample sequence $\{x(nT_s)\}_{n=-\infty}^{\infty}$ where the sample at time $t=nT_s$ has the form

$$x(nT_s) = \sum_k s_k h(nT_s - kT_s) + n_c(nT_s) \qquad (-\infty < n < \infty) \quad (4\text{-}4)$$

If we normalize the sampling period T_s to unity†, this may be written in the simple form

$$x(n) = \sum_k s_k h(n-k) + n_c(n) \qquad (-\infty < n < \infty) \qquad (4\text{-}5)$$

Now let us consider the estimation of an arbitrary symbol, say s_n at time $t=nT_s$ $(-\infty < n < \infty)$. In chapter 3, we derived a fixed, optimum equalizer structure having the nominally optimum tap gain values shown in equations (3-81) and (3-82). However, in practice the received pulse-

---

*By doing this we have lumped the filter response $a(\tau)$ in with the channel response.

†We do this both for convenience of notation, and because it provides a natural way to simulate $\{x(n)\}$ on a computer.

shape h(t) and its autocorrelation function are usually unknown, and also the pulse shape h(t) changes with time. The optimum equalizer tap-gain values will, therefore, be unknown and time-varying. In order now to avoid having to know explicitly these optimum values, we shall make the equalizer adaptive or self-adjusting. Then if we define $\{g_i(n);\ i=0,1,\ldots M\}$ and $\{f_j(n);\ j=1,\ldots,L\}$ as the current values (not in general optimum), at the nth sampling time, of the non-recursive and recursive gains respectively, we may rewrite the nonlinear estimate $\tilde{s}_n$ of equation (3-81) in sampled form as

$$\tilde{s}_n = \tanh\left(\sum_{i=0}^{M} g_i(n)x(n+i) - \sum_{j=1}^{L} f_j(n)\tilde{s}_{n-j}\right). \qquad (4\text{-}6)$$

Equivalently, we may write the input to the tanh(·) nonlinearity as

$$\hat{s}_n = \sum_{i=0}^{M} g_i(n)x(n+i) - \sum_{j=1}^{L} f_j(n)\tilde{s}_{n-j} \qquad (4\text{-}7)$$

which since it is a linear combination of the available data $\{x(n+i);\ i=0,1,\ldots,M\}$ and $\{\tilde{s}_{n-j};\ j=1,\ldots,L\}$, we shall refer to as the linear estimate of s_n.

We have made the number of taps on the non-recursive and recursive delay lines different (note the values M and L in equations (4-6) and (4-7)). We have done so because a matched filter is not being used preceding the equalizer, and hence the overall channel impulse response at the equalizer input cannot be guaranteed to be symmetric about its peak value as it can when such a filter is used.

The problem now is to find those values of both the non-recursive gains $\{g_i(n)\}$ and the recursive gains $\{f_j(n)\}$, at each sampling time n, which are optimum in the sense that the mean-square error $E\{(s_n-\tilde{s}_n)^2\}$

is a minimum. These optimum tap gain values are defined by the simultaneous solution of the M+L+1 equations*

$$\frac{\partial}{\partial g_k(n)} E\{(s_n - \tilde{s}_n)^2\} = 0 \qquad (k=0,1,\ldots,M)$$

$$\frac{\partial}{\partial f_m(n)} E\{(s_n - \tilde{s}_n)^2\} = 0 \qquad (m=1,\ldots,L)$$

at each sampling time n. For the estimate feedback equalizer these equations may readily be written in the form

$$-2E\{[1 - \tanh^2(\hat{s}_n)][(s_n - \tanh(\hat{s}_n)) \frac{\partial}{\partial g_k(n)} \hat{s}_n]\} = 0 \qquad (k=0,1,\ldots,M)$$

$$-2E\{[1 - \tanh^2(\hat{s}_n)][(s_n - \tanh(\hat{s}_n)) \frac{\partial}{\partial f_m(n)} \hat{s}_n]\} = 0 \qquad (m=1,\ldots,L)$$

where

$$\tilde{s}_n = \tanh(\hat{s}_n) \ .$$

But these equations do not have a unique solution for the (optimum) tap gain values. That is the mean square error is not a unimodal function of the tap gains $\{g_i(n)\}$ and $\{f_j(n)\}$, and thus the equations have more than one solution. One solution occurs when the tap gains become very large in magnitude so that

$$\hat{s}_n \to \infty$$

and

---

*These equations provide only necessary and not sufficient conditions for the mean-square error to be a minimum.

$$\tilde{s}_n = \tanh(\hat{s}_n) \rightarrow \pm 1$$

In this case no compensation for intersymbol interference takes place and the equalizer does not decrease the error-rate.

We note that this effect was actually observed in some computer simulations, using these derivatives in a steepest descent algorithm to adjust the tap gains. In these tests we found that the tap gains grew without limit, and eventually forced the equalizer output very close to the values ±1, but that virtually no compensation for intersymbol interference took place.

In the present work, in order to avoid this problem, we shall minimize the mean-square error $E\{(s_n-\hat{s}_n)^2\}$ in the linear estimate $\hat{s}_n$ at the input to the tanh(·) nonlinearity*. The mean-square error $E\{(s_n-\hat{s}_n)^2\}$ is a unimodal, convex (in fact quadratic) function of the tap gains $\{g_i(n)\}$ and $\{f_j(n)\}$ and the necessary conditions

$$\frac{\partial}{\partial g_k(n)} E\{(s_n-\hat{s}_n)^2\} = -2E\{(s_n-\hat{s}_n)\frac{\partial}{\partial g_k(n)}\hat{s}_n\} = 0 \qquad (k=0,1,\ldots,M)$$

$$\frac{\partial}{\partial f_m(n)} E\{(s_n-\hat{s}_n)^2\} = -2E\{(s_n-\hat{s}_n)\frac{\partial}{\partial f_m(n)}\hat{s}_n\} = 0 \qquad (m=1,\ldots,L)$$

for it to be a minimum, have a unique solution for the optimum tap gain values. The use of this criterion also allows us to use a linear adaptive algorithm for iterative adjustment of the equalizer tap gains, and as we shall see in chapter 5, very satisfactory performance is

---

*In the case of decision feedback, we recall that this nonlinearity must be replaced by a hard limiter.

obtained using this criterion.

Now let us consider $E\{(s_n-\hat{s}_n)^2\}$ in somewhat more detail. Substituting equation (4-7) into it and expanding the result, we obtain

$$E\{e_n^2\} = E\{(s_n-\hat{s}_n)^2\}$$

$$= E\{s_n^2\} - 2\sum_{i=0}^{M} g_i(n)E\{x(n+i)s_n\} - 2\sum_{j=1}^{L} f_j(n)E\{\tilde{s}_{n-j}s_n\}$$

$$+\sum_{i=0}^{M}\sum_{j=0}^{M} g_i(n)g_j(n)E\{x(n+i)x(n+j)\} - 2\sum_{i=0}^{M}\sum_{j=1}^{L} g_i(n)f_j(n)E\{x(n+i)\tilde{s}_{n-j}\}$$

$$+\sum_{i=1}^{L}\sum_{j=1}^{L} f_i(n)f_j(n)E\{\tilde{s}_{n-i}\tilde{s}_{n-j}\} \qquad (4\text{-}8)$$

We now want to minimize $E\{e_n^2\}$ with respect to the two sets of tap-gains $\{g_i(n)\}$ and $\{f_j(n)\}$.

A necessary condition for $E\{e_n^2\}$ to be a minimum is given (as stated above) by the equations

$$\frac{\partial E\{e_n^2\}}{\partial g_k(n)} = 0 \qquad (k=0,1,\ldots,M) \qquad (4\text{-}9)$$

and

$$\frac{\partial E\{e_n^2\}}{\partial f_m(n)} = 0 \qquad (m=1,\ldots,L) \qquad (4\text{-}10)$$

which are equivalent to saying that for $E\{e_n^2\}$ to be a minimum, its gradient with respect to the tap-gains must be zero. Now let us consider the matrix

$$Q = \left[\begin{array}{c|c} \dfrac{\partial^2 E\{e_n^2\}}{\partial g_i(n)\partial g_k(n)} & \dfrac{\partial^2 E\{e_n^2\}}{\partial g_i(n)\partial f_m(n)} \\ \hline \dfrac{\partial^2 E\{e_n^2\}}{\partial f_\ell(n)\partial g_k(n)} & \dfrac{\partial^2 E\{e_n^2\}}{\partial f_\ell(m)\partial f_m(n)} \end{array}\right] \quad \begin{array}{l}(i,k=0,1,\ldots,M) \\ (\ell,m=1,\ldots,L)\end{array}$$

This matrix is symmetric about its main diagonal with positive diagonal terms. It is, therefore, at least positive semidefinite, and this ensures that $E\{e_n^2\}$ is a convex function of the tap gains $\{g_i(n)\}$ and $\{f_j(n)\}$. This implies that steepest descent and other related techniques may be used to find the minimum mean-square error point (Gersho, 1969a), where equations (4-9) and (4-10) are satisfied. In most cases, Q is positive definite. Its inverse then exists, and we may, at least in principle, solve equations (4-9) and (4-10) directly to obtain the optimum tap gains which we shall call $\{g_{i_o}(n)\}$ and $\{f_{j_o}(n)\}$.

Now let us obtain the equations which define the optimum tap gains in more explicit form. Taking the derivatives of $E\{e_n^2\}$ as indicated in equations (4-9) and (4-10), we obtain

$$\frac{\partial E\{e_n^2\}}{\partial g_k(n)} = -2E\{s_n x(n+k)\} + 2\sum_{i=0}^{M} g_i(n)\, E\{x(n+i)x(n+k)\}$$

$$-2\sum_{j=1}^{L} f_j(n)\, E\{\tilde{s}_{n-j}x(n+k)\}$$

$$= -2E\{(s_n-\hat{s}_n)x(n+k)\}$$

$$= -2E\{e_n x(n+k)\} \qquad (k=0,1,\ldots,M) \qquad (4\text{-}11)$$

and

$$\frac{\partial E\{e_n^2\}}{\partial f_m(n)} = 2E\{s_n\tilde{s}_{n-m}\} - 2\sum_{i=0}^{M} g_i(n)\, E\{x(n+i)\tilde{s}_{n-m}\} + 2\sum_{j=1}^{L} f_j(n)\, E\{\tilde{s}_{n-j}\tilde{s}_{n-m}\}$$

$$= +2E\{(s_n-\hat{s}_n)\tilde{s}_{n-m}\}$$

$$= +2E\{e_n\tilde{s}_{n-m}\} \qquad (m=1,\ldots,L) \qquad (4\text{-}12)$$

Then substituting these last equations into equations (4-9) and (4-10) respectively, we obtain the M+L+1 equations

$$\sum_{i=0}^{M} g_i(n)E\{x(n+i)x(n+k)\} - \sum_{j=1}^{L} f_j(n)E\{\tilde{s}_{n-j}x(n+k)\} - E\{s_n x(n+k)\} = 0$$

$$(k=0,1,\ldots,M) \qquad (4\text{-}13)$$

and

$$\sum_{j=1}^{L} f_j(n)E\{\tilde{s}_{n-j}\tilde{s}_{n-m}\} - \sum_{i=0}^{M} g_i(n)E\{x(n+i)\tilde{s}_{n-m}\} + E\{s_n\tilde{s}_{n-m}\} = 0$$

$$(m=1,\ldots,L) \qquad (4\text{-}14)$$

which define the optimum tap-gains $\{g_{i_o}(n)\}$ and $\{f_{j_o}(n)\}$.

It is of interest at this point to compute the minimum mean-square error $E\{e_n^2\}_{min}$. If equations (4-13) and (4-14) are substituted into equation (4-8), we obtain

$$E\{e_n^2\}_{min} = E\{s_n^2\} - \sum_{i=0}^{M} g_{i_o}(n)E\{x(n+i)s_n\} + \sum_{j=1}^{L} f_{j_o}(n)E\{\tilde{s}_{n-j}s_n\} \qquad (4\text{-}15)$$

This may readily be put in the form

$$E\{e_n^2\}_{min} = E\{e_{n_o} s_n\} \tag{4-16}$$

where e_{n_o} is the estimation error $(s_n - \hat{s}_n)$ when the tap gains have their optimum values. Equation (4-16) is the standard form obtained for the minimum mean-square error in all linear minimum mean-square error estimation problems (Luenberger, 1969).

In this section, we have derived equations which define the optimum tap gain values for the equalizer at any arbitrary sampling time n ($-\infty < n < \infty$). In the next section we will develop iterative procedures for adaptively finding these values.

4.2 The Adaptive Algorithm

In theory the optimum tap gain values $\{g_{i_o}(n)\}$ and $\{f_{j_o}(n)\}$ at any arbitrary sampling time - say the nth - may be found by the simultaneous solution of equations (4-13) and (4-14). However, this calculation requires a priori knowledge of the correlation properties of the available data $\{x(n+i)\}_{i=0}^{M}$ and $\{\tilde{s}_{n-j}\}_{j=1}^{L}$, and in practice this information is seldom available. It is therefore desirable to develop some form of iterative or adaptive procedure which in effect learns these correlation properties as it goes along and uses this learned information to adjust the tap gains to their optimum values.

One such iterative algorithm or procedure which has been widely used in implementing adaptive equalizers* is the steepest descent or

---

*See for example Lucky (1964, 1965) Lucky and Rudin (1967), Proakis (1969), George (1970), Niessen (1970) and others.

gradient following algorithm (Widrow, 1966; Gersho, 1969a). This algorithm uses estimates of the gradient components or first derivatives of the mean-square error with respect to the tap gains to iteratively adjust each tap gain to within a small neighborhood of its optimum value. At the end of any iteration cycle, say the (m+1)st, the value of an arbitrary tap gain, say $c_j(m+1)$ is given by the steepest descent algorithm as

$$c_j(m+1) = c_j(m) + \frac{\alpha}{2} \frac{\partial E\{e_m^2\}}{\partial c_j(m)} \quad \text{(all gains j)} \qquad (4\text{-}17)$$

where $c_j(m)$ is the value of the jth gain after the mth iteration and $(\alpha/2)$ is a constant which must be chosen so that the algorithm (4-17) is stable and converges.

In adaptive equalization, the basic idea is that the equalizer should adjust itself so that its response is approximately the inverse of the channel impulse response modified of course by the additive noise which must be fairly small for effective equalization. Thus at any sampling time, say the nth, the desired output is the symbol s_n, uncontaminated by interference from other symbols. This implies that one tap gain, denoted the reference gain, and usually the gain corresponding to the data sample x(n), should be the dominant gain. The only reason that any other tap gains should be non-zero is to attempt to compensate for intersymbol interference caused by channel time dispersion. This is readily seen from equation (3-82).

In implementing the gradient following algorithm, a problem arises as to which gain is the dominant or reference gain. Each tap gain performs a non-stationary random walk which, provided the algorithm is

correctly specified, converges in the mean to the optimum value. However, the random walks of the various tap gains are related only through the estimation error e_n at each time n, and if all tap gains have the same initial value, then each is equally likely to become the reference gain. In such a case the equalizer may not converge, since there is no preferred reference gain.

In most adaptive equalizers employing the gradient following algorithm, this problem is at least partially avoided by initially defining one gain to be the reference tap gain, setting its value to unity and setting all other gains initially to zero. During adaptation of the equalizer, however, there is still a finite non-zero probability that one of the other gains will overtake the defined reference gain and thus become the reference gain. This causes the equalizer time reference frame to shift and large numbers of output decision errors to occur.

In the formulation of the nonlinear estimate $\tilde{s}_n$ of equation (4-6) or equivalently the linear estimate $\hat{s}_n$ of equation (4-7) we have implicitly assumed that the reference gain is $g_o(n)$ $(-\infty < n < \infty)$. Using an auxiliary function concept developed by Mark (1970), we shall now develop an adaptive algorithm which rigorously defines $g_o(n)$ as the reference gain. The resulting algorithm will be seen to be similar to that developed by Mark (1970), but there are some novel differences in the manner in which convergence is assured.

The derivation of the algorithm will be carried out in two steps. We shall first derive a procedure for adjusting the non-recursive gains

$\{g_i(n);\ i=0,1,\ldots,M\}$, and then we shall derive one for adjusting the recursive gains $\{f_j(n);\ j=1,\ldots,L\}$. This two part development is possible even though (as equations (4-13) and (4-14) indicate) the two sets of gains are interdependent because the resulting adaptive procedure requires, in both instances, a measurement of the error $e_n = (s_n - \hat{s}_n)$ at each iteration time n. The error e_n includes the effect of the interdependence of the two sets of gains thus making possible the separate derivation of procedures for iteratively adjusting them.

4.2a Adaptive Procedure for Adjusting the Non-recursive Gains

In this section, we shall derive an adaptive procedure for iteratively adjusting the non-recursive gains $\{g_i(n)\}$ to their optimum values. By iteratively adjusting we mean that as each new input sample $x(n)$ $(-\infty < n < \infty)$ is received and processed by the equalizer, a small adjustment is made to each of the tap-gains in such a way that the mean-square error $E\{(s_n - \hat{s}_n)^2\}$ tends to be decreased. The procedure which we shall consider will define the gain $g_o(n)$ $(-\infty < n < \infty)$ as the reference gain by making the increments in the remaining gains $\{g_i(n);\ i=1,\ldots,M\}$ dependent on the increment in $g_o(n)$ at each iteration.

Now let us write the linear estimate of equation (4-7) at the nth iteration (or sampling) time as

$$\hat{s}'_n = \sum_{i=0}^{M} g_i(n)x(n+i) - \sum_{j=1}^{L} f_j(n)\tilde{s}_{n-j} \qquad (-\infty < n < \infty) \qquad (4\text{-}18)$$

where the $\{g_i(n)\}$ and the $\{f_j(n)\}$ are the current (not in general optimum) values of the tap gains arrived at by some iterative procedure, and where we have included the prime on $\hat{s}_n'$ for reasons which will shortly become clear. We shall refer to $\hat{s}_n'$ as the basic estimate.

The problem now is to find some means at each iteration (or sampling) time n of adjusting or incrementing each of the gains $\{g_i(n); i=0,1,\ldots,M\}$ in such a way that as n increases, the mean-square error $E\{e_n^2\}$ decreases and approaches its optimum, minimum value. To aid in this process, let us augment $\hat{s}_n'$ with an auxiliary function (Mark, 1970) $h[x(n),x^*(n)]$ at each time n where $x^*(n)$ is an extrapolated or learned value of $x(n)$. We then obtain

$$\hat{s}_n = \hat{s}_n' + h[x(n),x^*(n)] \qquad (-\infty < n < \infty) \qquad (4\text{-}19)$$

which we shall refer to as the augmented estimate. Because of the linear form of $\hat{s}_n'$, we shall assume that $h[x(n),x^*(n)]$ is a linear function, and because we are considering here only the non-recursive gains $\{g_i(n)\}$ we shall assume that it is a function only of the data $\{x(n+i); i=0,1,\ldots,M\}$ in the non-recursive section of the equalizer. Let us then write it in the form

$$h[x(n),x^*(n)] = \sum_{i=0}^{M} \partial g_i(n)\, x(n+i) \qquad (4\text{-}20)$$

where the weights $\{\partial g_i(n); i=0,1,\ldots,M\}$ are some set of increments in the current (non-optimum) values of the non-recursive tap-gains $\{g_i(n); i=0,1,\ldots,M\}$.

Using equations (4-18) and (4-20), we may write the augmented estimate $\hat{s}_n$ at the nth iteration time as

$$\hat{s}_n = \sum_{i=0}^{M} (g_i(n) + \partial g_i(n))\, x(n+i) - \sum_{j=1}^{L} f_j(n)\, \tilde{s}_{n-j} \qquad (4\text{-}21)$$

Then since the equalizer is being iteratively adjusted toward its optimum point, let us require that the incremental gains $\{\partial g_i(n)\}$ at the nth iteration time be such as to make the current (non-optimum) overall gain values $\{(g_i(n) + \partial g_i(n));\ i=0,1,\ldots,M\}$ equal to the gain values $\{g_i(n+1)\}$ at the (n+1)st iteration. This implies the definition

$$g_i(n+1) = g_i(n) + \partial g_i(n) \qquad (i=0,1,\ldots,M) \qquad (4\text{-}22)$$

and we may then write the augmented estimate of equation (4-21) in the form

$$\hat{s}_n = \sum_{i=0}^{M} g_i(n+1)x(n+i) - \sum_{j=1}^{L} f_j(n)\tilde{s}_{n-j}\ . \qquad (4\text{-}23)$$

But this equation represents a non-causal system in that at the nth iteration time it requires a knowledge of the non-recursive gains $\{g_i(n+1)\}$ at the (n+1)st iteration time. We will attempt to overcome this difficulty by introducing a learning or extrapolation process into the equalizer structure.

Let us begin by considering the conditions which define the optimum, minimum mean-square error point. For the basic estimate $\hat{s}'_n$ of equation (4-18) the optimum values $\{g_{i_o}(n)\}$ and $\{f_{j_o}(n)\}$ of the tap gains at the nth iteration (or sampling) time are defined by equations (4-13) and (4-14) as

$$\sum_{i=0}^{M} g_i(n)E\{x(n+i)x(n+k)\} - \sum_{j=1}^{L} f_j(n)E\{\tilde{s}_{n-j}x(n+k)\} - E\{s_n x(n+k)\} = 0$$

$$(k=0,1,\ldots,M) \qquad (4\text{-}13)$$

and

$$\sum_{j=1}^{L} f_j(n)E\{\tilde{s}_{n-j}\tilde{s}_{n-m}\} - \sum_{i=0}^{M} g_i(n)E\{x(n+i)\tilde{s}_{n-m}\} + E\{s_n\tilde{s}_{n-m}\} = 0$$

$$(m=1,\ldots,L) \qquad (4\text{-}14)$$

Similarly for the augmented estimate $\hat{s}_n$ of equation (4-23) the optimum values $\{g_{i_o}(n+1)\}$ of the non-causal gains $\{g_i(n+1)\}$ and the optimum values $\{f_{j_o}(n)\}$ of the recursive gains are defined by the equations

$$\sum_{i=0}^{M} g_i(n+1)E\{x(n+i)x(n+k)\} - \sum_{j=1}^{L} f_j(n)E\{\tilde{s}_{n-j}x(n+k)\} - E\{s_n x(n+k)\} = 0$$

$$(k=0,1,\ldots,M) \qquad (4\text{-}24a)$$

and

$$\sum_{j=1}^{L} f_j(n)E\{\tilde{s}_{n-j}\tilde{s}_{n-m}\} - \sum_{i=0}^{M} g_i(n+1)E\{x(n+i)\tilde{s}_{n-m}\} + E\{s_n\tilde{s}_{n-m}\} = 0$$

$$(m=1,\ldots,L) \qquad (4\text{-}24b)$$

But equations (4-13), (4-14) and (4-24) clearly define the same optimum point. We may thus equate the left hand sides of equations (4-13) and (4-24a) to obtain, with the aid of equation (4-22), the result

$$\sum_{i=0}^{M} \partial g_i(n)\ E\{x(n+i)x(n+k)\} = 0 \qquad (k=0,1,\ldots,M) \qquad (4\text{-}25)$$

Equations (4-25) are a set of (M+1) homogeneous equations in the (M+1) incremental tap gains $\{\partial g_i(n)\}$. Now it can be shown that the matrix defined by

$$E\{x(n+i)x(n+j)\} \qquad (i,j=0,1,\ldots,M)$$

is positive definite (Appendix C), and therefore the only solution to equations (4-25) is the null solution

$$\partial g_i(n) = 0 \qquad (i=0,1,\ldots,M) \qquad (4\text{-}26)$$

This is, of course, the condition to which we wish the adaptive equalizer to converge, since it corresponds to the gains $\{g_i(n)\}$ having their optimum values and implies that

$$g_{i_o}(n+1) = g_{i_o}(n) \qquad (i=0,1,\ldots,M) \text{ for all iterations } n$$

so that no further iteration of an adaptive procedure need take place.

However, initially at least, and in practice virtually all of the time the tap gains will not have their optimum values and at each iteration time n some adjustment of their values will take place. We want now to specify the incremental gains $\{\partial g_i(n)\}$ such that at the nth iteration time the overall non-recursive gains have the values belonging to the (n+1)st iteration time. Since the gain values are never exactly optimum, then at the nth iteration time at least one of the $\partial g_i(n)$ will be non-zero and we have the (M+1) inequalities

$$\sum_{i=0}^{M} \partial g_i(n)\, E\{x(n+i)x(n+k)\} \neq 0 \qquad (k=0,1,\ldots,M)$$

Let us assume that $\partial g_o(n)$, the increment in the gain $g_o(n)$ is non-zero. Then if we delete the k=0 inequality from the above and require that

$$\sum_{i=1}^{M} \partial g_i(n)\, E\{x(n+i)x(n+k)\} = -\partial g_o(n)\, E\{x(n)x(n+k)\} \qquad (k=1,\ldots,M) \qquad (4\text{-}27)$$

we have a set of M non-homogeneous equations in M unknowns from which we can obtain a solution for the M gain increments $\{\partial g_i(n);\ i=1,\ldots,M\}$ as a function of the increment $\partial g_o(n)$ in the gain $g_o(n)$. This dependence defines $g_o(n)$ to be the reference gain, since at each iteration the gains $\{g_i(n);\ i=1,\ldots,M\}$ are iterated by the amounts $\{\partial g_i(n);\ i=1,\ldots,M\}$ which depend on $\partial g_o(n)$.

The solution of equations (4-27) for the gain increments $\{\partial g_i(n);\ i=1,\ldots,M\}$ causes the M equations

$$\sum_{i=0}^{M} \partial g_i(n)\ E\{x(n+i)x(n+k)\} = 0 \qquad (k=1,\ldots,M)$$

to be satisfied at each iteration - that is M of the (M+1) equations (4-25) are satisfied at each iteration time n. Later in this analysis, we will find a value for $\partial g_o(n)$ such that as n increases the reference gain $g_o(n)$ approaches its optimum value and $\partial g_o(n)$ approaches zero. This will mean that in the limit as n becomes large the (M+1) equations (4-25) will be satisfied and the optimum, minimum mean-square error point will be reached.

The object of the adaptive procedure is to cause the gains $\{g_i(n)\}$ to converge, as n increases, to their optimum values $\{g_{i_o}(n)\}$ where the mean-square error is a minimum. Now in order that the gain increments $\{\partial g_i(n);\ i=1,\ldots,M\}$ cause this process to be accelerated, the mean-square error in the augmented estimate $\hat{s}_n$ must, at each iteration, be less than or equal to the mean square error in the corresponding basic estimate $\hat{s}'_n$, with equality occurring at the optimum point. In other words, we must have at each iteration time n, the condition

$$E\{e_n^2\} = E\{(\hat{s}_n - s_n)^2\} \leq E\{(\hat{s}_n' - s_n)^2\} = E\{e_n^2\}' \tag{4-28}$$

or equivalently

$$\Delta_{e_n} = E\{e_n^2\}' - E\{e_n^2\} \geq 0 \tag{4-29}$$

fulfilled, where Δ_{e_n} is known as the error increment. This means that the tap gain increments $\{\partial g_i(n);\ i=0,1,\ldots,M\}$ must be found such that inequality (4-29) is satisfied. If we assume for the moment that $\partial g_o(n)$ is known and that it causes the constraint (4-29) to be satisfied, then we are left with the problem of finding the $\{\partial g_i(n);\ i=1,\ldots,M\}$ such that the constraint is satisfied.

We shall do this by first finding an explicit form for the $\{\partial g_i(n);\ i=1,\ldots,M\}$ in terms of $\partial g_o(n)$ without regard to the constraint (4-29). We shall then calculate Δ_{e_n} as an explicit function of the $\{\partial g_i(n)\}$ from which we will find that a very simple modification to the unconstrained $\{\partial g_i(n)\}$ causes the inequality (4-29) to be satisfied at each iteration.

In equations (4-27), we note that the reference sample x(n) appears only in the correlations on the right hand side. These correlations may be learned by a linear extrapolation of x(n) using the data samples x(n+1),...,x(n+M). This extrapolation or learned value of x(n) may be written in the form

$$x^*(n) = \sum_{i=1}^{M} \alpha_i(n)\, x(n+i) \tag{4-30}$$

where $\{\alpha_i(n);\ i=1,\ldots,M\}$ is a set of learning or extrapolation weights which must be determined. We shall find them such that the mean square

learning error

$$E\{\varepsilon_n^2\} = E\{(x(n) - x^*(n))^2\} \tag{4-31}$$

is minimized.

The weights $\{\alpha_i(n)\}$ which minimize $E\{\varepsilon_n^2\}$ at each time n may be found by setting the first derivatives of $E\{\varepsilon_n^2\}$ with respect to the $\{\alpha_i(n)\}$ equal to zero to obtain the M equations

$$\frac{\partial E\{\varepsilon_n^2\}}{\partial \alpha_k(n)} = 0 \qquad (k=1,\ldots,M) \tag{4-32}$$

Substituting equation (4-30) into equation (4-31), expanding and taking the derivatives indicated in equation (4-32) we obtain

$$\frac{\partial E\{\varepsilon_n^2\}}{\partial \alpha_k(n)} = -2E\{x(n)x(n+k)\} + 2\sum_{i=1}^{M} \alpha_i(n)E\{x(n+i)x(n+k)\}$$

$$= -2E\{(x(n) - x^*(n))x(n+k)\}$$

$$= -2E\{\varepsilon_n x(n+k)\} \qquad (k=1,\ldots,M) \tag{4-33}$$

Then substituting equations (4-33) into equations (4-32) we obtain the M equations

$$\sum_{i=1}^{M} \alpha_i(n)E\{x(n+i)x(n+k)\} = E\{x(n)x(n+k)\} \qquad (k=1,\ldots,M) \tag{4-34}$$

which define the optimum learning weights.

Now substituting equations (4-34) into equations (4-27) we obtain

$$\sum_{i=1}^{M} \partial g_i(n)\, E\{x(n+i)x(n+k)\} = -\partial g_o(n) \sum_{i=1}^{M} \alpha_i(n)\, E\{x(n+i)x(n+k)\}$$

$$(k=1,\ldots,M) \qquad (4\text{-}35)$$

and then equating the coefficients of like terms, we obtain the explicit form

$$\partial g_i(n) = -\partial g_o(n)\alpha_i(n) \qquad (i=1,\ldots,M) \qquad (4\text{-}36)$$

for the increments $\{\partial g_i(n)\}_{i=1}^{M}$ in the non-recursive gains $\{g_i(n)\}_{i=1}^{M}$. Equation (4-36) shows explicitly the dependence of these increments on the increment $\partial g_o(n)$ in the reference gain $g_o(n)$ when the constraint (4-29) is ignored. Substituting now equations (4-36) into equations (4-22) we obtain

$$g_i(n+1) = g_i(n) - \partial g_o(n)\alpha_i(n) \qquad (i=1,\ldots,M) \qquad (4\text{-}37)$$

which provides an explicit relationship for iteratively adjusting all the non-recursive gains except the reference gain $g_o(n)$.

Now substituting equation (4-37) into equation (4-23) we obtain the augmented estimate $\hat{s}_n$ as

$$\hat{s}_n = g_o(n+1)x(n) + \sum_{i=1}^{M} (g_i(n)-\partial g_o(n)\alpha_i(n))x(n+i) - \sum_{j=1}^{L} f_j(n)\tilde{s}_{n-j} \qquad (4\text{-}38)$$

which with the use of equations (4-22) and (4-30) may be rewritten in the form

$$\hat{s}_n = \sum_{i=0}^{M} g_i(n)x(n+i) - \sum_{j=1}^{L} f_j(n)\tilde{s}_{n-j} + \partial g_o(n)(x(n)-x^*(n)) \qquad (4\text{-}39)$$

Equations (4-39) together with equations (4-30) and (4-37) form the basis for the adaptive equalizer, as far as the non-recursive section is

concerned, when the inequality constraint of equation (4-29) is ignored.

So far we have assumed that the increment $\partial g_o(n)$ in the reference gain $g_o(n)$ is known and available at each iteration time n. In practice, this quantity will not be available at time n, since in a causal system, input must precede output. We are therefore constrained to use

$$\partial g_o(n-1) = g_o(n) - g_o(n-1)$$

in place of

$$\partial g_o(n) = g_o(n+1) - g_o(n)$$

and to accept some loss of optimality. This loss will be small, provided the adaptive algorithm is converging, since then

$$\partial g_o(n-1) \to \partial g_o(n) \to 0$$

as n increases. We will now consider how to adaptively adjust the reference gain $g_o(n)$.

From equation (4-11) we obtain at time n the derivative of the mean-square estimation error with respect to the reference gain $g_o(n-1)$ in the form

$$\frac{\partial E\{e_{n-1}^2\}}{\partial g_o(n-1)} = -2E\{e_{n-1}x(n-1)\} \qquad (4\text{-}40)$$

This derivative has the same form for both the basic estimate $\hat{s}_n'$ and the augmented estimate $\hat{s}_n$. When the equalizer is at the optimum point it must be zero. Therefore, we may adjust $g_o(n)$ using a recursive steepest descent algorithm of the form

$$g_o(n) = g_o(n-1) + \frac{\alpha}{2} \frac{\partial E\{e_{n-1}^2\}}{\partial g_o(n-1)} \tag{4-41}$$

or

$$g_o(n) = g_o(n-1) - \alpha E\{e_{n-1} x(n-1)\} \tag{4-42}$$

which implies

$$\partial g_o(n-1) = -\alpha E\{e_{n-1} x(n-1)\} \tag{4-43}$$

where α is a constant which must be chosen so that the algorithm is stable. The range of values which α may have when the algorithm is stable is investigated in Appendix D-II and is found to be

$$\frac{-2}{\lambda_{max}} < \alpha < 0$$

where λ_{max} is the largest eigenvalue of a positive definite matrix $[R_{ij}]$ defined in the appendix.

Summarizing now we have the adaptive algorithm for adjusting the forward gains given by equations (4-37), (4-42) and (4-43) as

$$g_i(n+1) = g_i(n) - \partial g_o(n)\alpha_i(n) \qquad (i=1,\ldots,M) \tag{4-37}$$

$$g_o(n) = g_o(n-1) - \alpha E\{e_{n-1} x(n-1)\} \tag{4-42}$$

and

$$\partial g_o(n-1) = -\alpha E\{e_{n-1} x(n-1)\} \tag{4-43}$$

where the last two represent a practicable realizable approximation to the non-causal ideal which is given by

$$g_o(n+1) = g_o(n) - \alpha E\{e_n x(n)\} \tag{4-44}$$

and

$$\partial g_o(n) = -\alpha E\{e_n x(n)\} \quad . \tag{4-45}$$

However, equation (4-37) has been obtained without applying the constraint of equation (4-29), and we must now consider what effects it will have on the algorithm.

Let us begin by defining the output of the recursive section of the equalizer at time n as

$$y_n = \sum_{j=1}^{L} f_j(n)\tilde{s}_{n-j} \ .$$

Then using equation (4-8) we may write the mean square error $E\{e_n^2\}'$ for the basic estimate $\hat{s}_n'$ as

$$E\{e_n^2\}' = E\{s_n^2\} - 2\sum_{i=0}^{M} g_i(n)\ E\{s_n x(n+i)\} + 2E\{s_n y_n\}$$

$$+ \sum_{i=0}^{M}\sum_{j=0}^{M} g_i(n)g_j(n)\ E\{x(n+i)x(n+j)\}$$

$$- 2\sum_{i=0}^{M} g_i(n)\ E\{x(n+i)y_n\} + E\{y_n^2\} \qquad (4\text{-}46)$$

Similarly the mean-square error $E\{e_n^2\}$ at time n for the augmented estimate $\hat{s}_n$ may be found in the same form as

$$E\{e_n^2\} = E\{s_n^2\} - 2\sum_{i=0}^{M} g_i(n+1)\ E\{x(n+i)s_n\} + 2E\{s_n y_n\}$$

$$+ \sum_{i=0}^{M}\sum_{j=0}^{M} g_i(n+1)g_j(n+1)\ E\{x(n+i)x(n+j)\}$$

$$- 2\sum_{i=0}^{M} g_i(n+1)\ E\{x(n+i)y_n\} + E\{y_n^2\} \qquad (4\text{-}47)$$

Now let us form the error difference Δ_{e_n} defined in equation (4-29). It may be written as

$$\Delta_{e_n} = -2 \sum_{i=0}^{M} [g_i(n) - g_i(n+1)]\, E\{x(n+i)s_n\}$$

$$+ \sum_{i=0}^{M} \sum_{j=0}^{M} [g_i(n)g_j(n) - g_i(n+1)g_j(n+1)]\, E\{x(n+i)x(n+j)\}$$

$$- 2 \sum_{i=0}^{M} [g_i(n) - g_i(n+1)]\, E\{x(n+i)y_n\} \qquad (4\text{-}48)$$

Using equation (4-22), we may reduce this last equation to the form

$$\Delta_{e_n} = 2 \sum_{i=0}^{M} \partial g_i(n)\, E\{x(n+i)(s_n+y_n)\}$$

$$- 2 \sum_{i=0}^{M} \partial g_i(n) \sum_{j=0}^{M} g_j(n)\, E\{x(n+j)x(n+i)\}$$

$$- \sum_{i=0}^{M} \sum_{j=0}^{M} \partial g_i(n)\partial g_j(n)\, E\{x(n+i)x(n+j)\} \qquad (4\text{-}49)$$

Because of the products $\partial g_i(n)\partial g_j(n)$, the last term of equation (4-49) will be (in practice at least) very small in comparison to the first two terms, and therefore it may be neglected. We may then write the error difference Δ_e as

$$\Delta_{e_n} \cong 2 \sum_{i=0}^{M} \partial g_i(n)\, E\{(s_n - \hat{s}_n)x(n+i)\}$$

$$= 2 \sum_{i=0}^{M} \partial g_i(n)\, E\{e_n x(n+i)\} \qquad (4\text{-}50)$$

Making use of equations (4-37), this last result may be written as

$$\Delta_{e_n} \cong 2\partial g_o(n)\, E\{e_n x(n)\} - 2\partial g_o(n) \sum_{i=1}^{M} \alpha_i(n)\, E\{e_n x(n+i)\} \qquad (4\text{-}51)$$

and substituting equation (4-30) into this we obtain the error difference Δ_e in the form

$$\Delta_{e_n} \cong 2\partial g_o(n)\ E\{e_n x(n)\} - 2\partial g_o(n)\ E\{e_n x^*(n)\} \qquad (4\text{-}52)$$

In order to guarantee that the constraint (4-29) is fulfilled, we must have, as stated in equation (4-29), the condition

$$\Delta_{e_n} \geq 0$$

fulfilled at each iteration. Now using equation (4-45) the first term in equation (4-52) may be written as

$$2\partial g_o(n)\ E\{e_n x(n)\} = -2\alpha E^2\{e_n x(n)\} \qquad (4\text{-}53)$$

The term is always positive or zero provided α is negative which it must be for the algorithm of equations (4-42) or (4-44) to be stable. The second term of equation (4-52) may similarly be written as

$$-2\partial g_o(n)\ E\{e_n x^*(n)\} = -2\alpha E\{e_n x(n)\}\ E^*\{e_n x^*(n)\} \qquad (4\text{-}54)$$

and we see that there is no way to ensure that this term is either positive or negative and smaller in magnitude than the first term. There is thus no guarantee that the constraint of equation (4-29) is satisfied.

The first term in equation (4-52) is the incremental change in the mean-square error due to adjusting the reference gain $g_o(n)$, and the second term is the incremental error change due to adjusting the remaining non-recursive gains $\{g_i(n)\}_{i=1}^{M}$. In order to guarantee that the constraint $\Delta_e \geq 0$ of equation (4-29) is fulfilled at each iteration, all that we must do is to test the sign of the second term

$$\beta(n) = -2\partial g_o(n)\ E\{e_n x^*(n)\}$$

in equation (4-52) at each iteration time. If $\beta(n) \geq 0$ we iterate the gains $\{g_i(n)\}_{i=1}^{M}$ as

$$g_i(n+1) = g_i(n) - \partial g_o(n)\alpha_i(n) \qquad (i=1,\ldots,M)$$

as in the unconstrained case, and if $\beta(n) < 0$ we iterate them as

$$g_i(n+1) = g_i(n) + \partial g_o(n)\alpha_i(n) \qquad (i=1,\ldots,M)$$

This guarantees that $\Delta_e \geq 0$ and that the non-recursive gains $\{g_i(n)\}_{i=1}^{M}$ are always being iterated in a direction to decrease the mean-square error. These last two equations may be summed up in the single relationship

$$g_i(n+1) = g_i(n) - \partial g_o(n)\alpha_i(n)\mathrm{sgn}(\beta(n)) \qquad (i=1,\ldots,M) \qquad (4\text{-}55)$$

which is more convenient for visualizing the implementation of the equalizer.

From equation (4-23) the augmented estimate $\hat{s}_n$ may be written as

$$\hat{s}_n = \sum_{i=0}^{M} g_i(n+1)x(n+i) - \sum_{j=1}^{L} f_j(n)\tilde{s}_{n-j}$$

Substituting equation (4-55) into this and rearranging we obtain

$$\hat{s}_n = \sum_{i=0}^{M} g_i(n)x(n+i) + \partial g_o(n)\{x(n)-x^*(n)\mathrm{sgn}(\beta(n))\} - \sum_{j=1}^{L} f_j(n)\tilde{s}_{n-j} \qquad (4\text{-}56)$$

which together with equations (4-42), (4-43) and (4-55) describes the adaptive equalizer as far as the non-recursive portion is concerned. We will now develop an adaptive algorithm for the recursive portion.

4.2b Adaptive Algorithm for the Recursive Section

In equations (4-12) we found that the derivatives of the mean-square error with respect to the recursive gains $\{f_j(n)\}_{j=1}^{L}$ were given by

$$\frac{\partial E\{e_n^2\}}{\partial f_m(n)} = 2E\{e_n \tilde{s}_{n-m}\} \qquad (m=1,\ldots,L)$$

We also found that the minimum mean-square error point with respect to the recursive gains was defined by the L equations

$$\frac{\partial E\{e_n^2\}}{\partial f_m(n)} = 0 \; . \qquad (m=1,\ldots,L)$$

Using these results, we may then define a recursive steepest descent algorithm for adaptively adjusting the recursive gains to their optimum values as

$$f_j(n+1) = f_j(n) + \frac{\gamma}{2} \frac{\partial E\{e_n^2\}}{\partial f_j(n)} \qquad (j=1,\ldots,L) \qquad (4\text{-}57)$$

where γ is a constant which must be chosen so that the algorithm remains stable. Substituting for the derivatives in equation (4-57), we may write

$$f_j(n+1) = f_j(n) + \gamma E\{e_n \tilde{s}_{n-j}\} \quad (j=1,\ldots,L) \qquad (4\text{-}58)$$

The stability properties of this algorithm are investigated in Appendix D-I, and it is found that a sufficient condition for stability is to constrain γ lie in the range

$$\frac{-2}{\mu_{max}} < \gamma < 0$$

where μ_{max} is the largest eigenvalue of the matrix defined by

$$E\{\tilde{s}_{n-j} \tilde{s}_{n-k}\} \qquad (j,k=1,\ldots,L) \; .$$

4.2c Adaptive Algorithm for the Learning Weights

In the preceding analysis, we implicitly assumed that the optimum values of the learning or interpolation weights $\{\alpha_i(n)\}_{i=1}^{M}$ had been found and were available at each iteration time n. However, their calculation requires much of the same a priori knowledge as the calculation of the optimum values of the non-recursive gains $\{g_i(n)\}_{i=0}^{M}$. Therefore, as in the case of the equalizer gains, we shall use an adaptive algorithm to find the optimum learning weights.

The learning weights $\{\alpha_i(n)\}$ may be adaptively adjusted to their optimum values using a recursive steepest descent or gradient following algorithm of the form

$$\alpha_i(n+1) = \alpha_i(n) + \frac{\delta}{2} \frac{\partial E\{\epsilon_n^2\}}{\partial \alpha_i(n)} \qquad (i=1,\ldots,M) \qquad (4\text{-}59)$$

where $\alpha_i(n+1)$ is the ith learning weight at the (n+1)st iteration time and δ is a small constant which must be chosen so that the algorithm is stable. From equations (4-33), the derivatives required in equations (4-59) are obtained as

$$\frac{\partial E\{\epsilon_n^2\}}{\partial \alpha_i(n)} = -2E\{\epsilon_n x(n+k)\} \qquad (k=1,\ldots,M) \qquad (4\text{-}60)$$

These may be substituted into equations (4-59) to obtain the algorithm for adaptively adjusting the learning weights as

$$\alpha_i(n+1) = \alpha_i(n) - \delta E\{\epsilon_n x(n+i)\} \qquad (i=1,\ldots,M) \qquad (4\text{-}61)$$

The stability properties of this algorithm are investigated in Appendix D-III. There it is found that a sufficient condition for stability is that δ lie in the range

$$\frac{-2}{\sigma_{max}} < \delta < 0$$

where σ_{max} is the largest eigenvalue of the positive definite correlation matrix

$$E\{x(n+i)x(n+j)\} \qquad (i,j=1,\ldots,M) \ .$$

This completes our derivation of the adaptive equalizer. In the next section we will consider its implementation.

4.3 Implementation of the Adaptive Feedback Equalizer

The operation of the adaptive feedback equalizer is described by equations (4-30), (4-42), (4-55), (4-56), (4-58) and (4-61). These are repeated below as a convenient summary

$$x^*(n) = \sum_{i=1}^{M} \alpha_i(n)x(n+i) \qquad (4\text{-}30)$$

$$g_o(n) = g_o(n-1) - \alpha E\{e_{n-1}x(n-1)\} \qquad (4\text{-}42)$$

$$g_i(n+1) = g_i(n) - \partial g_o(n)\alpha_i(n)\mathrm{sgn}(\beta(n)) \qquad (i=1,\ldots,M) \qquad (4\text{-}55)$$

with

$$\beta(n) = -2\partial g_o(n)\ E\{e_n x^*(n)\}$$

$$\hat{s}_n = \sum_{i=0}^{M} g_i(n)x(n+i) + \partial g_o(n)\{x(n) - x^*(n)\mathrm{sgn}(\beta(n))\} - \sum_{j=1}^{L} f_j(n)\tilde{s}_{n-j} \qquad (4\text{-}56)$$

$$f_j(n+1) = f_j(n) + \gamma E\{e_n \tilde{s}_{n-j}\} \qquad (j=1,\ldots,L) \qquad (4\text{-}58)$$

and

$$\alpha_i(n+1) = \alpha_i(n) - \delta E\{\epsilon_n x(n+i)\} \qquad (i=1,\ldots,M) \qquad (4\text{-}61)$$

In implementing the equalizer, we must first decide which of the three nonlinearities discussed in chapter 3 is to be used in the recursive section to generate the $\{\tilde{s}_{n-j};\ j=1,\ldots,L\}$. The optimum nonlinearity was seen in chapter 3 to have the form

$$\tilde{s}_n = \tanh(\hat{s}_n) \qquad (-\infty < n < \infty) \qquad (4\text{-}62)$$

Two approximations to it, which were considered, are the threshold detector or decision device

$$\tilde{s}_n = \operatorname{sgn}(\hat{s}_n) = \begin{cases} 1 & \hat{s}_n > 0 \\ 0 & \hat{s}_n = 0 \\ -1 & \hat{s}_n < 0 \end{cases} \qquad (-\infty < n < \infty) \qquad (4\text{-}63)$$

and the saturating limiter

$$\tilde{s}_n = \begin{cases} \pm 1 & \hat{s}_n \geq \alpha \\ \hat{s}_n & -\alpha < \hat{s}_n < \alpha \\ -1 & \hat{s}_n \leq -\alpha \end{cases} \qquad \begin{matrix} (-\infty < n < \infty) \\ (0 \leq \alpha \leq 1) \end{matrix} \qquad (4\text{-}64)$$

Equations (4-62) and (4-64) lead to novel estimate feedback equalizers whose performance we shall examine in chapter 5. Equation (4-63) leads to the well known decision feedback equalizer (Austin, 1967; George et al., 1971 and Monsen, 1971) to which we shall, in chapter 5, compare the performances of the estimate feedback equalizers.

Examining now the equations describing the adaptive algorithm (4-42, 4-55, 4-58 and 4-61) we see that the explicit computation of several different cross-correlations is required at each iteration time. In practice this is, of course, impossible. The best that can be done is to form estimates of them, and to use these estimates as if they were the true values.

One method of doing this is to replace the expected values by unbiased estimates in the form of sample means taken over the previous $K \geq 1$ samples*. The equations describing the adaptive algorithm then become

$$g_o(n+1) = g_o(n) - \frac{\alpha}{K} \sum_{j=n-K+1}^{n} e_j x(j) \qquad (n \geq K) \qquad (4\text{-}65)$$

$$\beta(n) = -2\partial g_o(n) \cdot \frac{1}{K} \sum_{j=n-K+1}^{n} e_j x^*(j) \qquad (4\text{-}66)$$

$$f_j(n+1) = f_j(n) + \frac{\gamma}{K} \sum_{\ell=n-K+1}^{n} e_j \tilde{s}_{\ell-j} \qquad (n \geq K) \quad (j=1,\ldots,L) \qquad (4\text{-}67)$$

and

$$\alpha_i(n+1) = \alpha_i(n) - \frac{\delta}{K} \sum_{j=n-K+1}^{n} \varepsilon_j x(j+1) \qquad (n \geq K) \quad (i=1,\ldots,M) \qquad (4\text{-}68)$$

where in all cases K is an integer specifying the number of samples over which averaging is to be carried out. This type of implementation has been described by Gersho (1968, 1969a) and by Widrow (1966) who used $K = 1$.

An alternative technique for implementing the various equations requiring correlations has been suggested by Lender (1970). In using this technique, the polarity of the instantaneous correlation is used as an estimate of the true correlation. To explain this, let us consider equation (4-42) which describes the adaptive behaviour of the reference gain. The correlation required at the nth iteration is $E\{e_n x(n)\}$, but it

---

*In forming this type of estimate, we are implicitly assuming that the random signal sequences are wide sense stationary over any $K \geq 1$ samples.

is impossible to obtain this. By the instantaneous correlation we mean just the product $e_n x(n)$ which is an unbiased estimate of $E\{e_n x(n)\}$. By taking only its polarity, we obtain

$$\text{sgn}(e_n x(n)) = \text{sgn}(e_n)\ \text{sgn}(x(n)) \ ,$$

and if we now use this in equation (4-42) we obtain a recursive equation for adjusting the reference gain as

$$g_o(n+1) = g_o(n) - \alpha \text{sgn}(e_n)\text{sgn}(x(n)) \qquad (4\text{-}69)$$

where as before α is a small constant which must be chosen so that the algorithm is stable. If we use similar polarity estimates in place of the correlations in the remaining equations of the adaptive algorithm, we obtain

$$\beta(n) = -2\partial g_o(n)\ \text{sgn}(e_n)\ \text{sgn}(x^*(n)) \qquad (4\text{-}70)$$

$$f_j(n+1) = f_j(n) + \gamma \text{sgn}(e_n)\text{sgn}(\tilde{s}_{n-j}) \quad (j=1,\ldots,L) \qquad (4\text{-}71)$$

and

$$\alpha_i(n+1) - \alpha_i(n) - \delta \text{sgn}(\varepsilon_n)\text{sgn}(x(n+i)) \quad (i=1,\ldots,M) \ . \qquad (4\text{-}72)$$

Gersho (1968a) has examined the convergence properties of such quantized algorithms, and has shown that for α, γ and δ sufficiently small, they will converge to a small neighborhood of the optimum point. He has also pointed out that this convergence may tend to be slower than that of the linear type of algorithm described in equations (4-65) to (4-68). However, Lender (1970) in applying the quantized type of algorithm to adaptive equalization, obtained very rapid convergence which, as we will see later, we have also obtained using the quantized implementation

of equations (4-69) to (4-72). It appears, in fact, that provided the transmitted symbols are quantized to some finite number of values, very rapid convergence may be obtained using a quantized algorithm.

In the use of the linear form of the algorithm described in equations (4-65) to (4-68), there are several disadvantages when compared with the quantized version of equations (4-69) to (4-72). First, the linear version requires accumulators (or memory) to store the sum of products over K samples, whereas in the discrete or quantized version no storage is required, the gains being incremented by a fixed amount ($\pm\alpha$, $\pm\delta$ or $\pm\gamma$) as each new data sample is received. Second, the linear version requires multipliers to form the correlation products in equations (4-65) to (4-68) and to multiply the estimated correlations by the constants α, δ and γ. In the discrete or quantized version the first set of multiplications may be performed by a hardlimiting and gating operation, and the second set of multiplications is avoided altogether as the gains in equations (4-69) to (4-72) are incremented by adding the small fixed quantities $\pm\alpha$, $\pm\delta$ or $\pm\gamma$ to the present values of the gains.

In implementing either version of the adaptive algorithm, we see that measures of the learning error $\varepsilon_n = x(n)-x^*(n)$ and the estimation error $e_n = s_n-\hat{s}_n$ are required at each iteration. The learning error ε_n is directly available at each iteration as the difference $x(n)-x^*(n)$ but the estimation error e_n is not, and thus some method of measuring it must be devised. One method of measuring the estimation error e_n is provided by the technique known as decision-directed error measurement. This involves passing the estimate $\hat{s}_n$ (or equivalently the

nonlinear estimate $\tilde{s}_n$) at each iteration or sampling time through a decision circuit, and then treating the decision circuit output as if it were the true value s_n of the corresponding symbol. Provided that most of the decisions are correct, which they are in most point-to-point communications systems, this provides a quite satisfactory method of measuring the estimation error e_n. The alternative to this is to provide an independent known reference or training signal with which to adjust the equalizer. This method is often used, in practice, during initial adaptation of the equalizer.

In view of the above discussion and the resulting simplifications in implementation, we shall use the discrete or quantized version of the algorithm throughout the remainder of this thesis. We shall also conduct much of our investigation using decision directed error measurement.

In chapter 5, we will investigate the performance characteristics of the estimate feedback equalizer and will compare them to those of the known decision feedback equalizer.

CHAPTER 5

Performance of the Nonlinear Estimate Feedback Equalizer

In this chapter, we shall investigate the performance characteristics of the adaptive, nonlinear, estimate feedback equalizer, when it is controlled by the new adaptive algorithm of chapter 4. The fixed optimum decision feedback equalizer which was shown in chapter 3 to be a high signal to noise ratio approximation to the estimate feedback structure has been investigated by Austin (1967) and was later made adaptive by George et al. (1971) and Monsen (1971). We shall, concurrently with our tests of the estimate feedback equalizer, carry out the same tests on the decision feedback equalizer. The results for the decision feedback structure, whose behaviour is essentially known will provide a standard to which the performance of the estimate feedback equalizer may be compared.

The analytical evaluation of the performance of any of these nonlinear, adaptive equalizers is almost hopelessly difficult, although in section (5.3), we will obtain some limited results for the decision feedback case. In the main, however, we will resort to Monte Carlo simulation techniques as a means of evaluating performance.

In section 5.1, we will discuss the input signal to the equalizer, its simulation and the measurement of signal conditions at the equalizer input. Then, in the remainder of the chapter we will discuss the performance of the estimate feedback equalizer and how it compares with that of the decision feedback equalizer.

5.1 Signal Conditions at the Equalizer Input

In order to demonstrate the adaptive equalizer of the preceding chapters and to investigate its performance characteristics, we decided to simulate it, using Monte Carlo techniques, on a digital computer - in this case a CDC-6400*. The simulation of the equalizer structure itself presents few problems since essentially all that is required is the mechanization, in the computer, of the various equations developed in the analysis of the preceding chapter. However, some consideration must be given to how the equalizer input signal, namely the sample sequence $\{x(n)\}$ of equation (4-5), is to be generated, and this we now discuss.

5.1a Simulation of the Equalizer Input Signal

From equation (4-3), we may write the equalizer input signal as

$$x(t) = \sum_k s_k h(t-kT_s) + n_c(t) \qquad (5\text{-}1)$$

where as before

(i) the $\{s_k\}_{k=-\infty}^{\infty}$ are the transmitted digital (binary) symbols.

(ii) $h(t)$ is the received pulse shape at the equalizer input. It consists of the convolution of the transmitted pulse shape with first the channel impulse response and then with whatever

---

*The CDC-6400 is a batch processing machine, and thus the simulations could not be performed in real time. However, provided we keep in mind that the symbol period of T_s seconds has been normalized to unity, the results are quite general.

filtering, $a(\tau)$, that is used in the receiver preceding the equalizer.

(iii) $n_c(t)$ is the additive Gaussian background noise.

In the simulation, we shall assume that $x(t)$ is essentially bandlimited to the frequency band

$$\frac{-1}{2T_s} < f < \frac{1}{2T_s}$$

where T_s seconds is the length of an individual symbol period, and that time synchronism is being maintained between the equalizer and the transmitted signal.

Using these assumptions we may sample $x(t)$ once every T_s seconds at the times $t=mT_s$ to produce at the equalizer input the sequence of samples

$$x(mT_s) = \sum_k s_k h(mT_s - kT_s) + n_c(mT_s) \qquad (-\infty < m < \infty) \qquad (5\text{-}2)$$

If the symbol period T_s is then normalized to unity, we may write equation (5-2) in the simple form

$$x(m) = \sum_k s_k h(m-k) + n_c(m) \qquad (-\infty < m < \infty) \qquad (5\text{-}3)$$

At the mth sampling time the transmitted symbol is s_m. Also the pulse shape $h(t)$ is in practice effectively time limited. That is each sample $x(m)$ $(-\infty < m < \infty)$ includes only some finite number, say 2L, of non-negligible components due to preceding and following data symbols s_k $(k \neq m)$. We may, therefore write each $x(m)$ in the form

$$x(m) = \sum_{k=m-L}^{m+L} s_k h(m-k) + n_c(m) \qquad (-\infty < m < \infty) \qquad (5\text{-}4)$$

where a measure of L is provided by equation (3-70). This is the form we shall use for simulation of the equalizer input samples.

In order to simulate the transmitted symbols $\{s_k\}$ where each s_k equals ± 1, we shall use a pseudo-random binary sequence. Such a sequence is a periodic sequence of binary digits where the digits within a period behave in a random-like manner. Such sequences, having any desired length or period, are readily generated using shift registers, and the procedures for doing this have been widely discussed (Peterson, 1961). In the present work, we shall use a sequence having a period of 2^8-1 or 255 binary symbols, which is readily generated, at the desired rate of one symbol every T_s seconds, by an eight stage shift register. Its period of $(2^8-1)T_s$ seconds is much longer than either the channel memory of $(2L+1)T_s$ seconds or the equalizer memory of $(M+L+1)T_s$ seconds, and thus the periodicity of the sequence will have almost no effect on the equalizer's performance.

In the simulations, we shall slowly and randomly vary the received pulse shape h(t). To do this, after approximately every 100 symbols have been passed through the channel, we shall add to each sample $\{h(k); k=-L,\ldots,0,\ldots,L\}$ a zero-mean random number generated by a Gaussian random number generator which is resident within the computer. The additive noise samples $\{n_c(m); -\infty < m < \infty\}$ in equation (5-4) are also obtained from this random number generator. The signal samples $\{x(m); -\infty < m < \infty\}$ are then generated by convolving the pseudo-random sequence $\{s_n\}$ with the

sampled pulse shape {h(k); k=-L,...,0,...,L} and then adding the Gaussian noise samples $\{n_c(m)\}$ to the result.

5.1b Measurement of Conditions at the Equalizer Input

In this section, we shall discuss some measures of signal versus interference conditions at the input to any equalization system.

From equation (5-4), we may write the noise-free input sample at an arbitrary mth sampling time as

$$x(m) = s_m h(0) + \sum_{\substack{k=m-L \\ k\neq m}}^{k=m+L} s_k h(m-k) \qquad (-\infty < m < \infty) \quad (5\text{-}5)$$

The symbol we want to detect is s_m, and we thus see that the second term in equation (5-5) is intersymbol interference or distortion caused by time dispersion or spread in the channel. One convenient way to characterize this is the so-called peak distortion

$$D = \frac{1}{|h(0)|} \sum_{\substack{k=-L \\ k\neq 0}}^{L} |h(k)| \qquad (5\text{-}6)$$

which is defined by Lucky (1965). The peak distortion D is closely related to the so-called binary eye opening (Lucky, 1968). When $D < 1$, the eye is open and binary symbols may be transmitted and received at low error rates without an equalizer. But when $D \geq 1$, the binary eye is closed, and some form of compensation for intersymbol interference is required to make possible the reception of binary symbols at acceptably low error rates.

The peak distortion D does not include the effects of additive

noise. In any real situation some noise is always present. It will always be one limiting factor on system performance and thus should be taken into consideration. Let us begin by rewriting x(m) of equation (5-4) so as to isolate the desired symbol s_m:

$$x(m) = s_m h(0) + \sum_{\substack{k=m-L \\ k\neq m}}^{m+L} s_k h(m-k) + n_c(m) \ . \qquad (-\infty < m < \infty) \quad (5\text{-}7)$$

The first term in x(m) is the desired signal component. The second term is an interference or distortion component due to the intersymbol interference caused by channel dispersion. The third term is due to the additive background noise. The intersymbol interference component depends on the transmitted symbols $\{s_n\}$ but the additive noise is signal independent.

One possible measure of signal conditions at the equalizer input is the signal to interference ratio which we shall define as

$$\rho_{in} = \frac{\text{received signal energy in each sample}}{\text{total interference energy in each sample}} \qquad (5\text{-}8)$$

From equation (5-7), we may write the signal energy in each x(m) as

$$h^2(0)\ E\{s_m^2\}$$

and the total interference energy as

$$\sum_{\substack{k=m-L \\ k\neq m}}^{m+L} \sum_{\substack{\ell=m-L \\ \ell\neq m}}^{m+L} h(m-k)h(m-\ell)E\{s_k s_\ell\} + E\{n_c^2(m)\} \ .$$

Then substituting these in equation (5-8), we obtain the signal to interference ratio as

$$\rho_{in} = \frac{h^2(0)\ E\{s_m^2\}}{\sum_{\substack{k=m-L \\ k\neq m}}^{m+L} \sum_{\substack{\ell=m-1 \\ \ell\neq m}}^{m+L} h(m-k)h(m-\ell)E\{s_k s_\ell\} + E\{n_c^2(m)\}} \tag{5-9}$$

where we have implicitly assumed that the samples $\{h(k);\ k=-L,\ldots,0,\ldots,L\}$ of the received pulse shape are non-random in nature. If we than assume that

$$E\{s_i s_j\} = \delta_{i,j} \qquad (-\infty < i,j < \infty)$$

and that the noise is stationary and white over the bandwidth of interest with variance

$$E\{n_c^2(m)\} = N_o \qquad (-\infty < m < \infty)$$

we may rewrite equation (5-9) in the simple form

$$\rho_{in} = \frac{h^2(0)}{\sum_{\substack{k=-L \\ k\neq 0}}^{L} h^2(k) + N_o} \tag{5-10}$$

When the channel is non-dispersive ρ_{in} reduces to the well known signal to noise ratio

$$\rho_n = \frac{h^2(0)}{N_o} \tag{5-11}$$

We also note that as the additive noise becomes very small, ρ_{in} approaches a limiting non-zero value given by

$$\rho_{in} \underset{N_o \to 0}{\to} \frac{h^2(0)}{\sum_{\substack{k=-L \\ k\neq 0}}^{L} h^2(k)} \tag{5-12}$$

While D and ρ_{in} are useful measures of input signal conditions, the most meaningful measurement when considering the reception of digital symbols, is the probability of error $P_e(\rho_{in})$ which would be obtained if each input sample x(m) were just threshold detected with no attempt being made to compensate for intersymbol interference. Under the following assumptions:

(i) the symbols $\{s_k\}$ are independent, equiprobable and binary with the values ±1,

(ii) the sampled received pulse shape {h(k): k=-L,...,0,...,L} is time-invariant and known,

(iii) the additive noise is white and Gaussian with zero mean and variance N_o,

we may use some results due to Shimbo et al (1971) to obtain the desired error probability as

$$P_e(\rho_{in}) = \frac{1}{2}[1 - \mathrm{erf}(\frac{\rho_{in}}{2})] + \frac{e^{-\rho_{in}/2}}{\sqrt{2\pi}} \sum_{n=2}^{\infty} b_{2n}(-1)^n H_{2n-1}(\sqrt{\rho_{in}}) \qquad (5\text{-}13)$$

In equation (5-13), $H_n(x)$ is the nth Hermite polynomial

$$H_n(x) = e^{-x^2/2} \{(-1)^n \frac{d^n}{dx^n} (e^{-x^2/2})\}$$

which may be generated by the recursion relation

$$H_o = 1 \quad , \qquad H_1(x) = x$$

$$H_{n+1}(x) = xH_n(x) - nH_{n-1}(x)$$

The coefficients b_{2n} of the series in equation (5-13) may be computed from

$$[\alpha u - \sum_{k=1}^{\infty} \alpha_k \tan \alpha_k u] = \sum_{\ell=1}^{\infty} d_{2\ell-1} u^{2\ell-1}$$

where the left hand side is a generating function for the coefficients $d_{2\ell-1}$, and the recursion relation

$$b_{2n} = \frac{1}{2n} \sum_{\ell=1}^{n} b_{2n-2\ell} d_{2\ell-1}$$

where

$$\alpha_k = \frac{h(k)}{\sigma_x}, \qquad \alpha = \sum_k \alpha_k^2 = \frac{1}{\sigma_x^2} \sum_k h^2(k)$$

and

$$\sigma_x^2 = E[(\sum_{\substack{k=-L \\ k\neq 0}}^{L} h(k) s_{m-k} + n_c(m))^2] \qquad (-\infty < m < \infty)$$

is the variance of the input sample x(m).

Equation (5-13) is often approximated by

$$P_e(\rho_{in}) = \frac{1}{2}[1 - \mathrm{erf}(\frac{\rho_{in}}{2})] \qquad (5\text{-}14)$$

which is the probability of error that is obtained when the total interference in equation (5-7) is assumed to be Gaussian. In most cases this assumption is valid only when the interference due to additive noise is comparable to or greater than that due to intersymbol interference. Equations (5-13) and (5-14) are plotted in figure 5.1 for the typical sampled received pulse shape of figure 5-2. Also shown is the probability of error

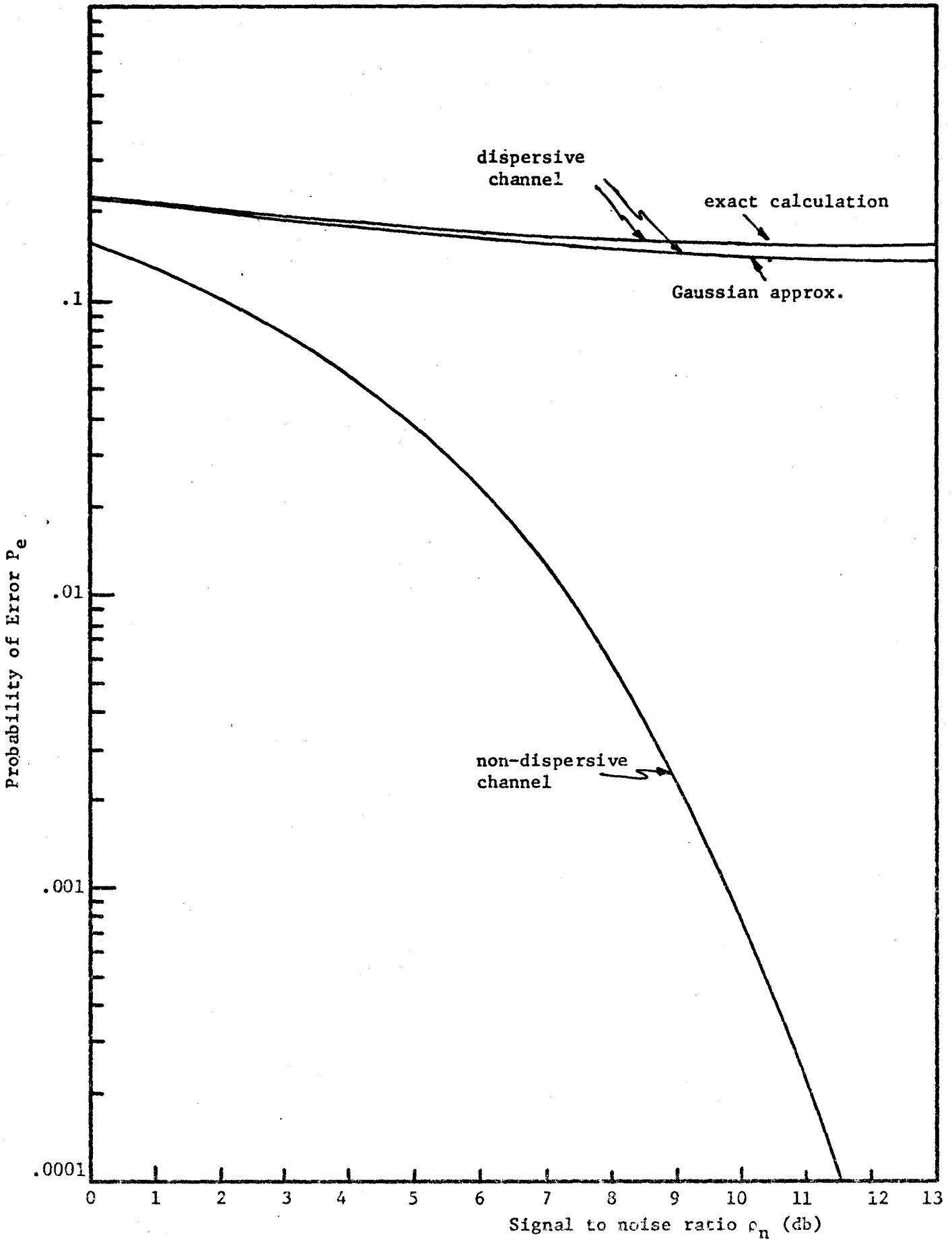

Figure 5.1 Probability of Error Curves showing effects of dispersive channel of Fig. 5.2.

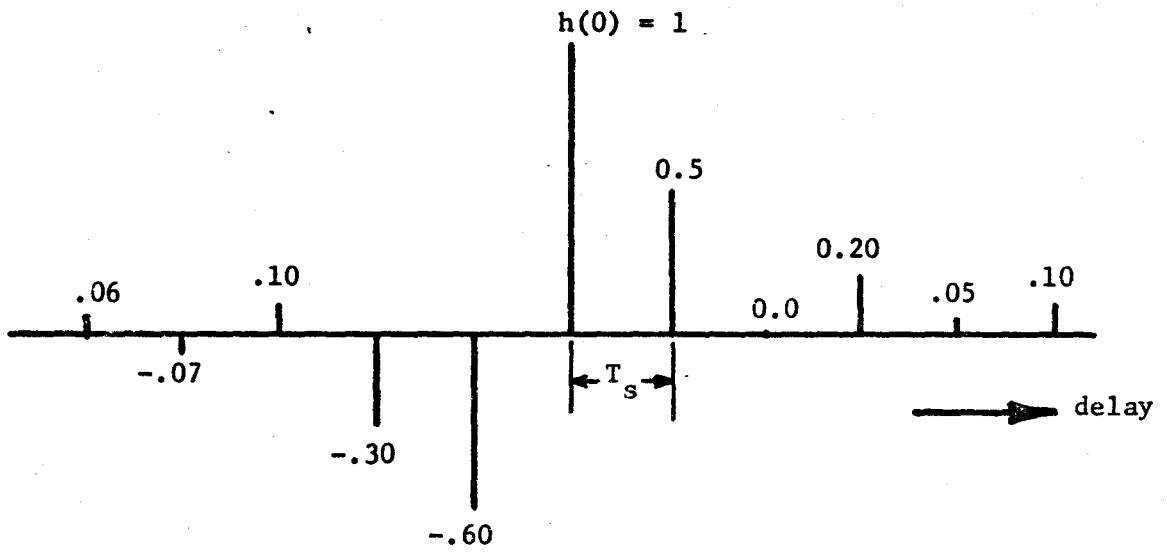

Figure 5.2 Sampled channel impulse response used to illustrate $P_e(\rho_{in})$ in figure 5.1.

$$P_e(\rho_n) = \frac{1}{2}[1 - \text{erf}(\frac{\rho_n}{2})] \qquad (5\text{-}15)$$

as a function of the signal to noise ratio ρ_n, which would be obtained if the channel were non-dispersive. The important point here is that as ρ_n increases or equivalently as the signal to interference ratio ρ_{in} approaches the limiting value of equation (5-12), $P_e(\rho_{in})$ approaches a limiting non-zero value. It is then the function of the equalizer to compensate for the intersymbol interference such that this limiting value of $P_e(\rho_{in})$ is forced to be very small.

5.2 Convergence Properties of the Estimate Feedback Equalizer

In this section, we shall evaluate by means of computer simulation, the convergence and tracking characteristics of the estimate feedback equalizer, and will compare them to those of the decision feedback equalizer when both equalizers are operated under the control of the adaptive algorithm developed in chapter 4.

For all our simulation work, we shall specify both these equalizers to have M=11 non-recursive and L=6 recursive delay line taps. There is no particular constraint on the number of non-recursive taps, but the number of recursive taps must be at least as great as the number of signalling intervals over which the channel impulse response extends into the past.

The transmitted symbols $\{s_k\}$ were simulated by repeated transmission of the 255 bit pseudorandom binary sequence discussed earlier. The received samples $\{x(m)\}$ were generated according to equation (5-7). For the

moment at least the sampled received pulse shape {h(k); k=-L,..,0,...,L} was made almost time-invariant. The samples {h(k)} were varied randomly every 100 symbols by adding to each of them a zero mean Gaussian random number from a distribution having a standard deviation of $\sigma_c = 0.001$, where σ_c is known as the channel standard deviation.

5.2a Decision Directed Convergence Tests

This first set of tests was designed to investigate the convergence properties of the adaptive estimate feedback equalizer. Since one of our concerns is the capability of the equalizer to adapt itself to compensate for the channel concurrently with the reception of data, these tests were conducted with the adaptive algorithm operating in the decision directed mode. That is the output estimate $\hat{s}_m$ (or equivalently the nonlinear estimate $\tilde{s}_m$) at each sampling time m was passed through a threshold detector to obtain the decisions s_m^* ($\text{sgn}(\hat{s}_m)$ or $\text{sgn}(\tilde{s}_m)$ in the binary case). The difference $(s_m^* - \hat{s}_m)$ was then used as if it were the actual error $(s_m - \hat{s}_m)$. This is known as decision directed error measurement.

The convergence tests were all conducted at a signal to additive noise ratio of $\rho_n = 30\text{db}$, so that the predominant source of interference was the intersymbol interference caused by channel time dispersion or spread. This was done because the main aim of equalization is the compensation for intersymbol interference and not the suppression of additive noise, and in these tests we wanted to investigate the capability of the equalizer to perform this compensation.

For test purposes, a group of nine different sampled channel impulse responses $\{h(k);\ k=-L,\ldots,0,\ldots,L\}$ was chosen. These are shown in figures 5.3 to 5.11. In each case, for convenience in the simulations, we have set the initial value of h(0) to unity. We note that Lucky et al. (1968) have shown that h(0) may have any arbitrary value without affecting the equalizer's performance. The responses of figures 5.3 and 5.7 to 5.9 were chosen because they represent in sampled form typical impulse responses which might be encountered in practice. Those of figures 5.7 to 5.9 are typical of schedule 4 data lines (Niessen et al., 1970), and that of figure 5.3 is also typical of a coaxial cable link. The responses of figures 5.4, 5.5 and 5.11 were used because they are symmetric about h(0), and therefore, they represent the situation in which a matched filter has been used preceding the equalizer. The responses of figures 5.6 and 5.10 were obtained by merely reversing the sign of some of the samples in the responses of the above symmetric channels. They are included in order to show the difference in the equalizer's behaviour for symmetric and unsymmetric, but otherwise equivalent channel responses.

Convergence of the equalizer to its optimum operating point was measured by computing the root mean square (rms) estimation error

$$e_{rms} = E\{e_n^2\} = E\{(s_n-\hat{s}_n)^2\}$$

as a function of time (number n of samples processed). By making a number of simulation runs for each channel, we obtained average convergence properties for the estimate feedback equalizer. In figures 5.3 to

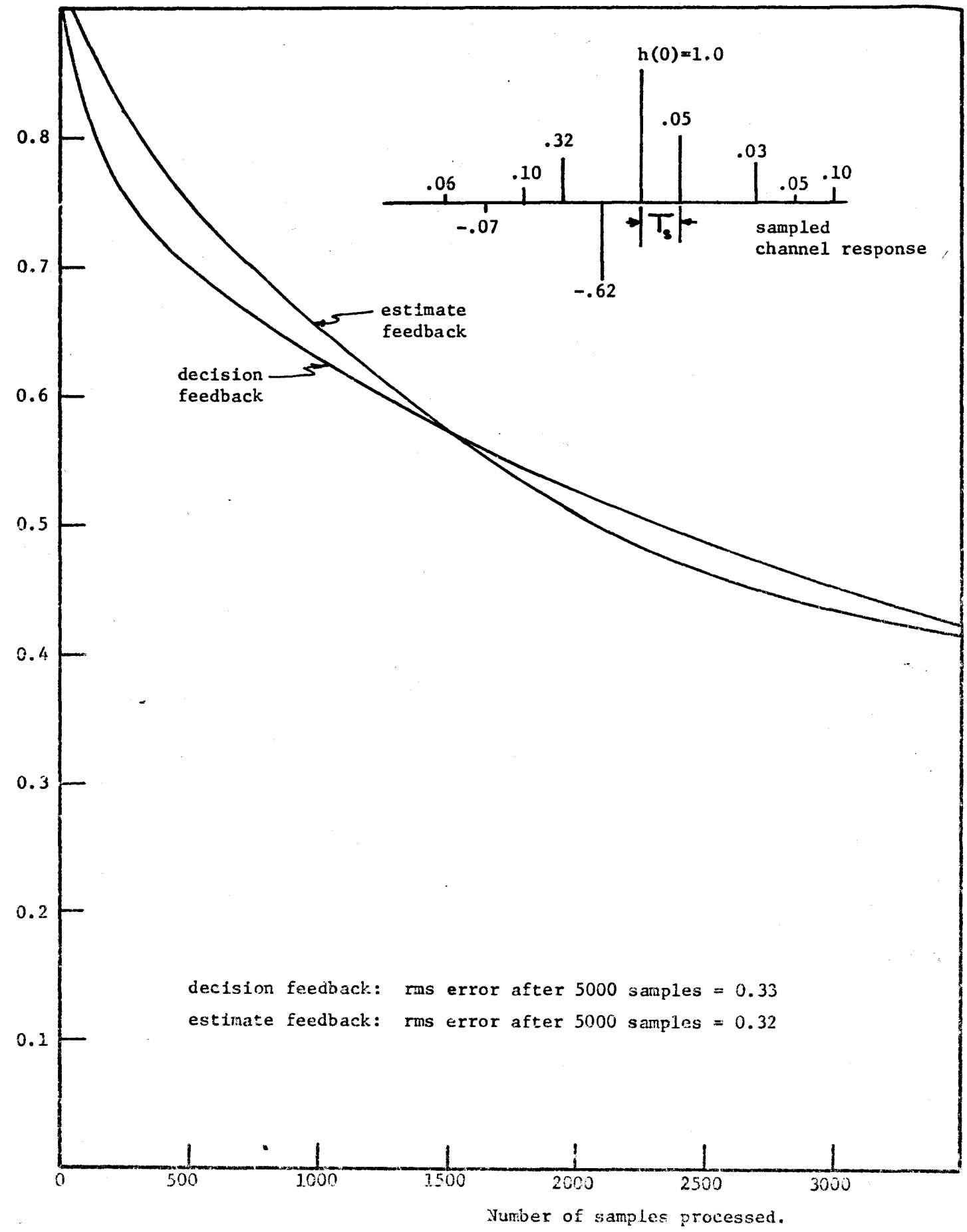

Figure 5.3 Decision directed convergence curves for channel response shown. Initial peak distortion D = 2.12 and signal to interference ratio ρ_{in} = 1.17.

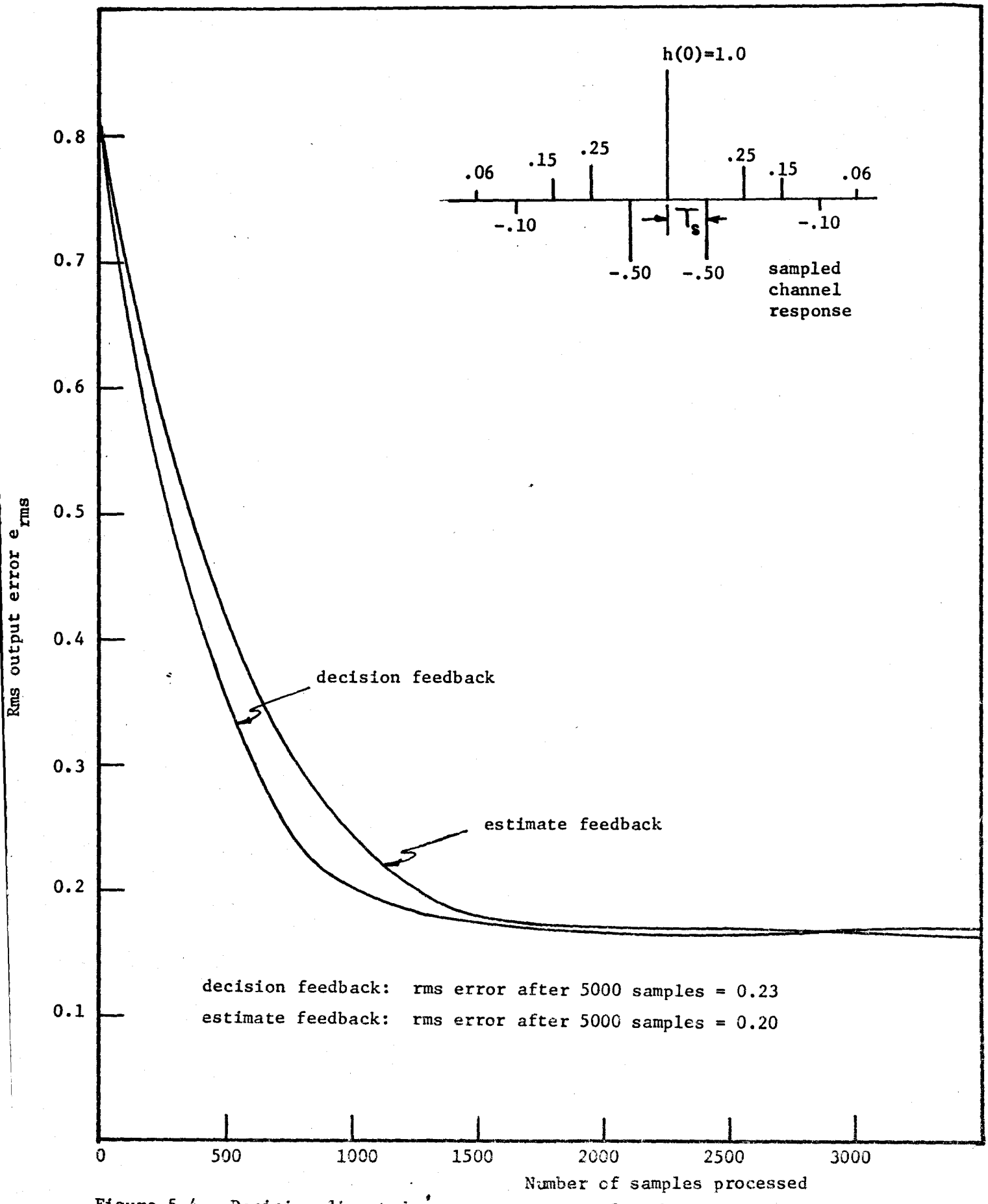

Figure 5.4 Decision directed convergence curve for channel response shown. Initial peak distortion D=2.12 and signal to interference ratio ρ_{in}=1.487.

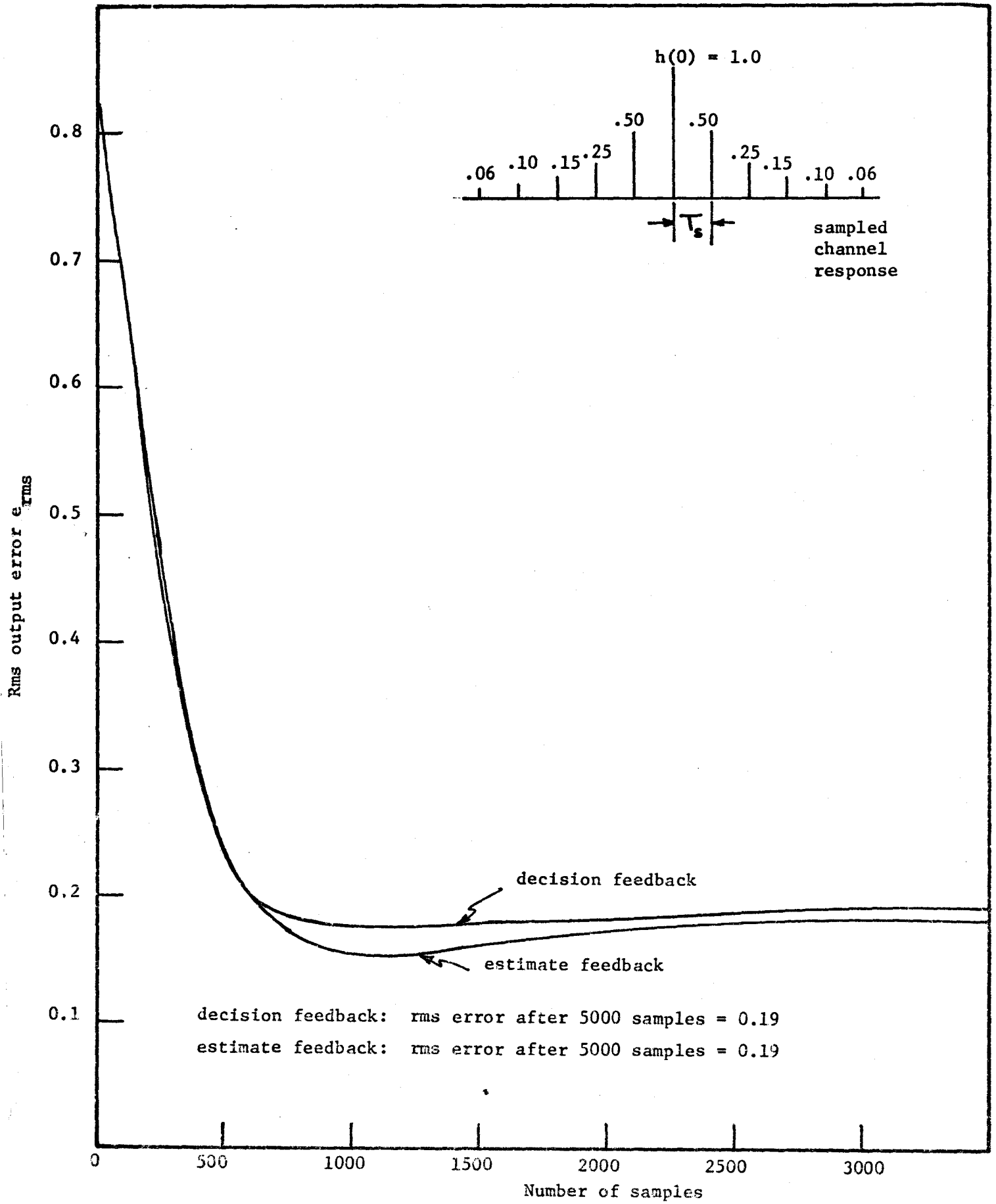

Figure 5.5 Decision directed convergence curve for channel shown. Initial peak distortion D=2.12 and signal to interference ratio ρ_{in}=1.487.

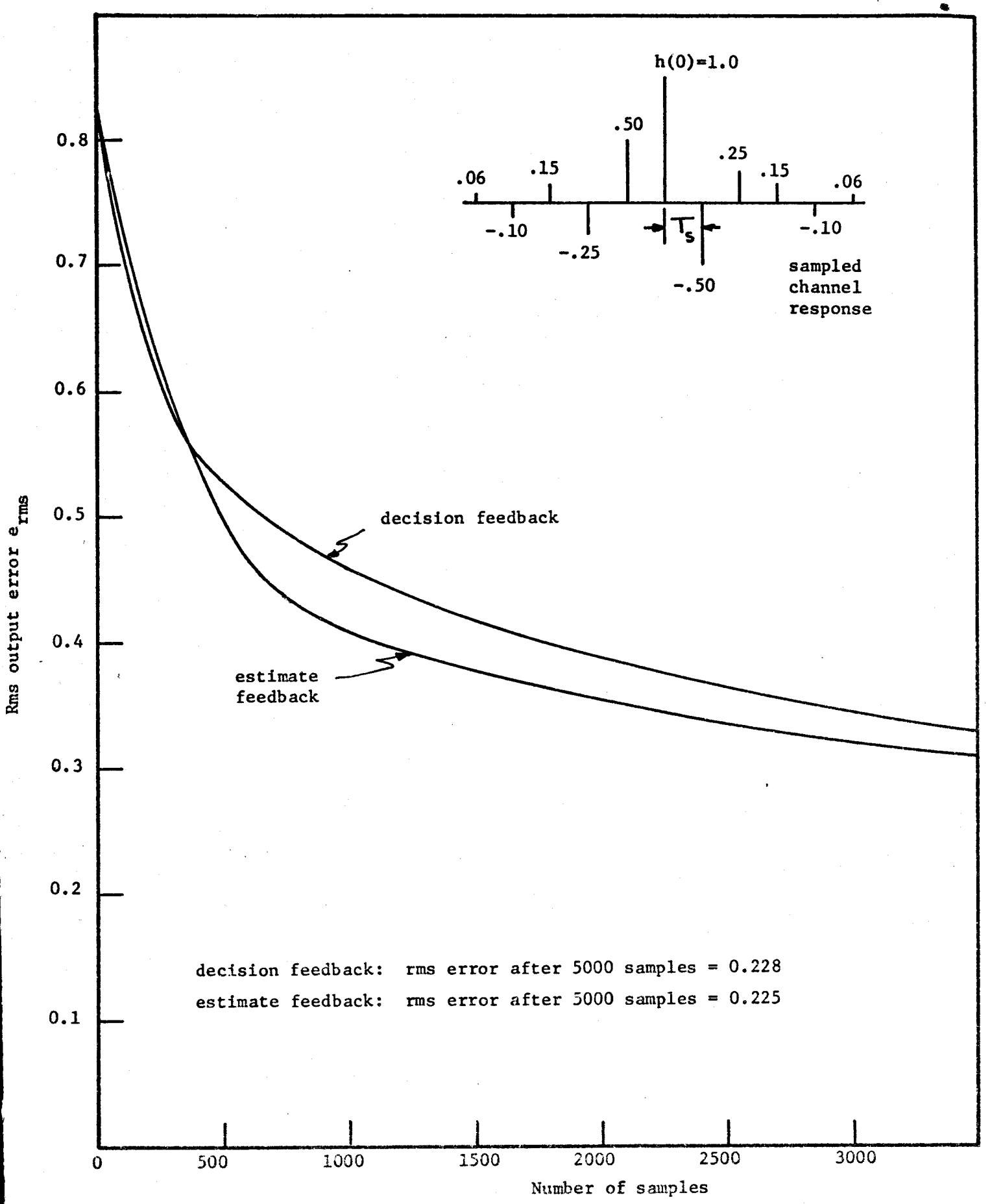

Figure 5.6 Decision directed convergence curve for channel response shown. Initial peak distortion D=2.12 and signal to interference ratio ρ_{in}=1.487.

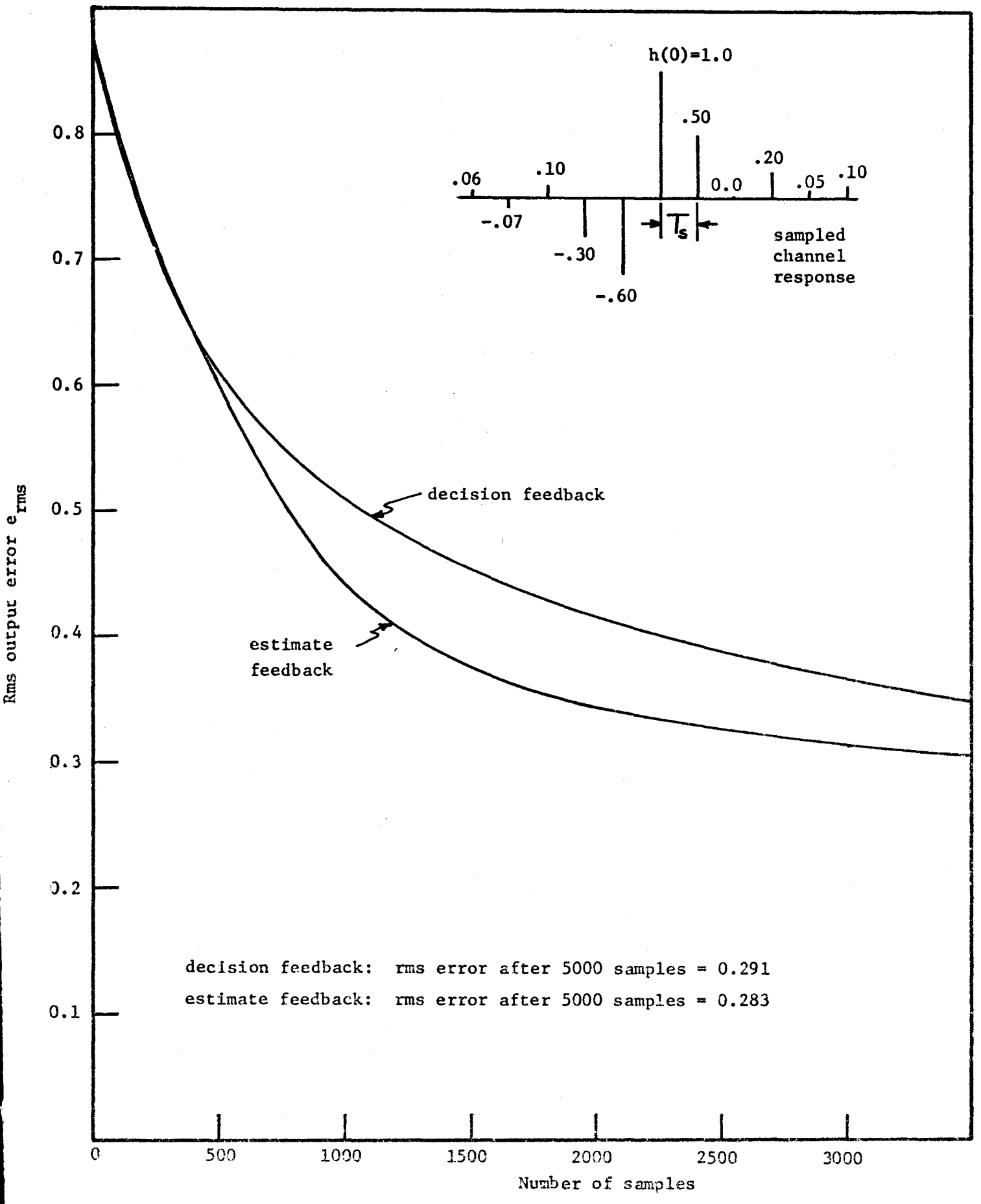

Figure 5.7 Decision directed convergence curves for channel response shown. Initial peak distortion D=1.98 and signal to interference ratio ρ_{in}=1.295.

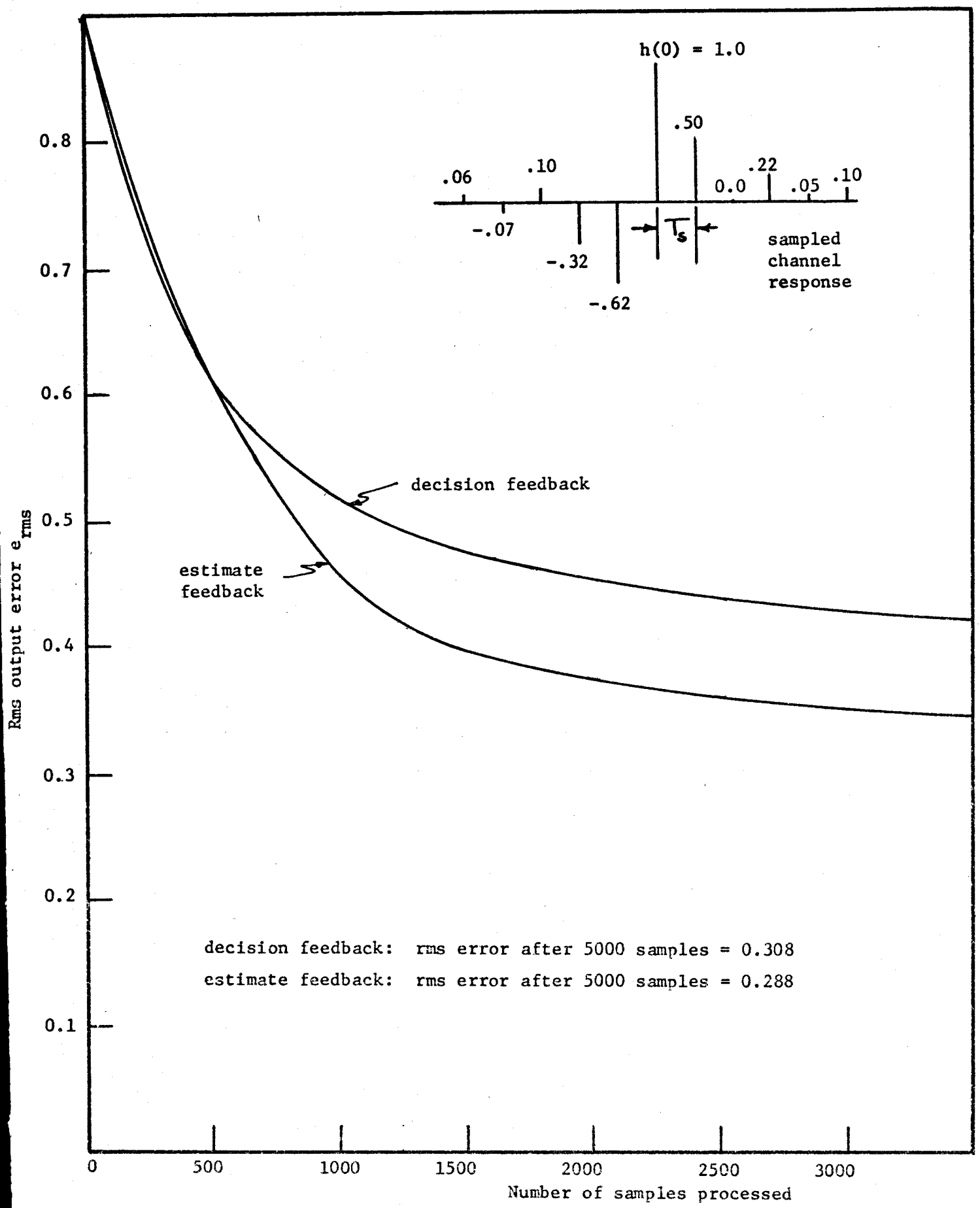

Figure 5.8 Decision directed convergence curves for channel response shown. Initial peak distortion $D=2.04$ and signal to interference ratio $\rho_{in}=1.225$.

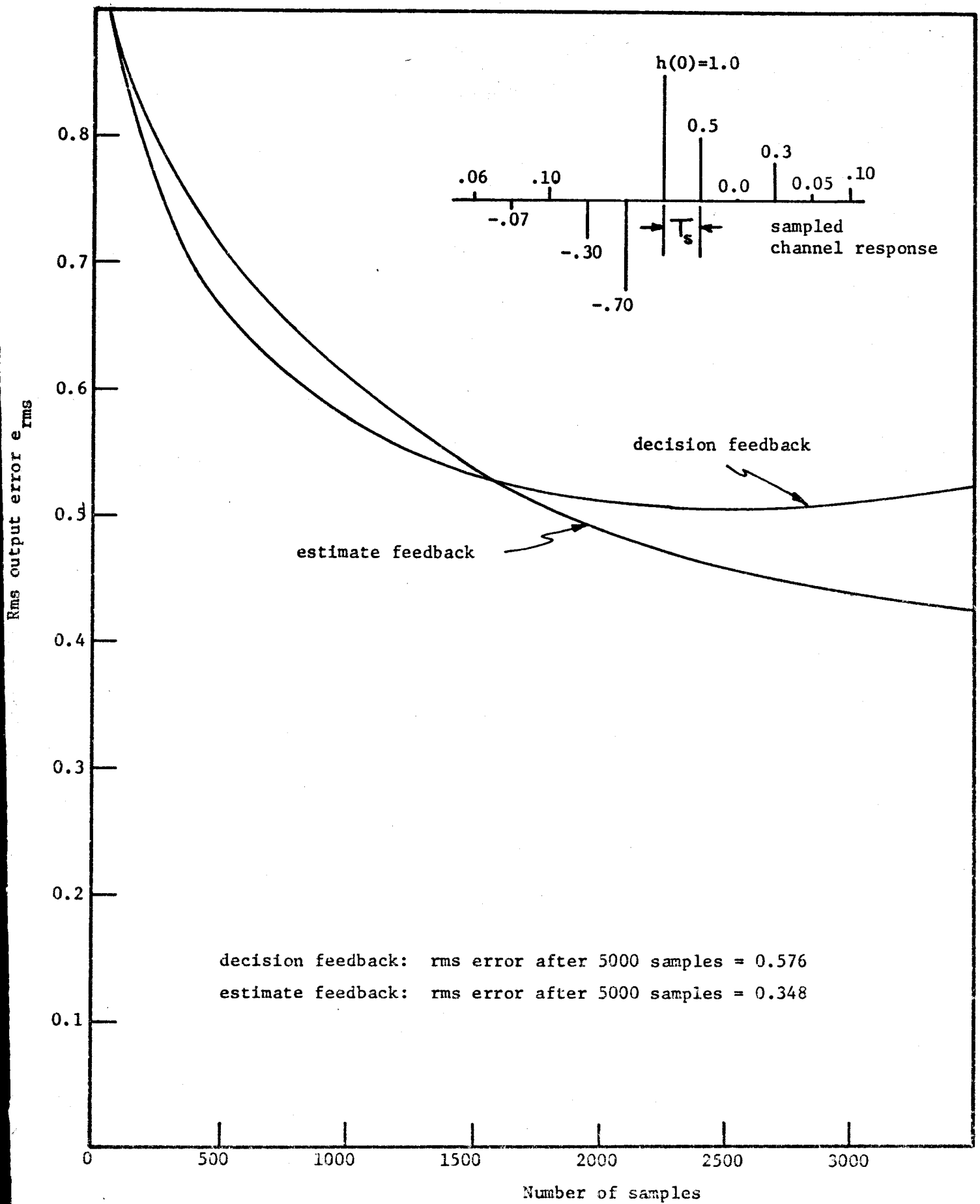

Figure 5.9 Decision directed convergence curves for channel response shown. Initial distortion D=2.18 and signal to interference ratio $\rho_{in} = 1.05$.

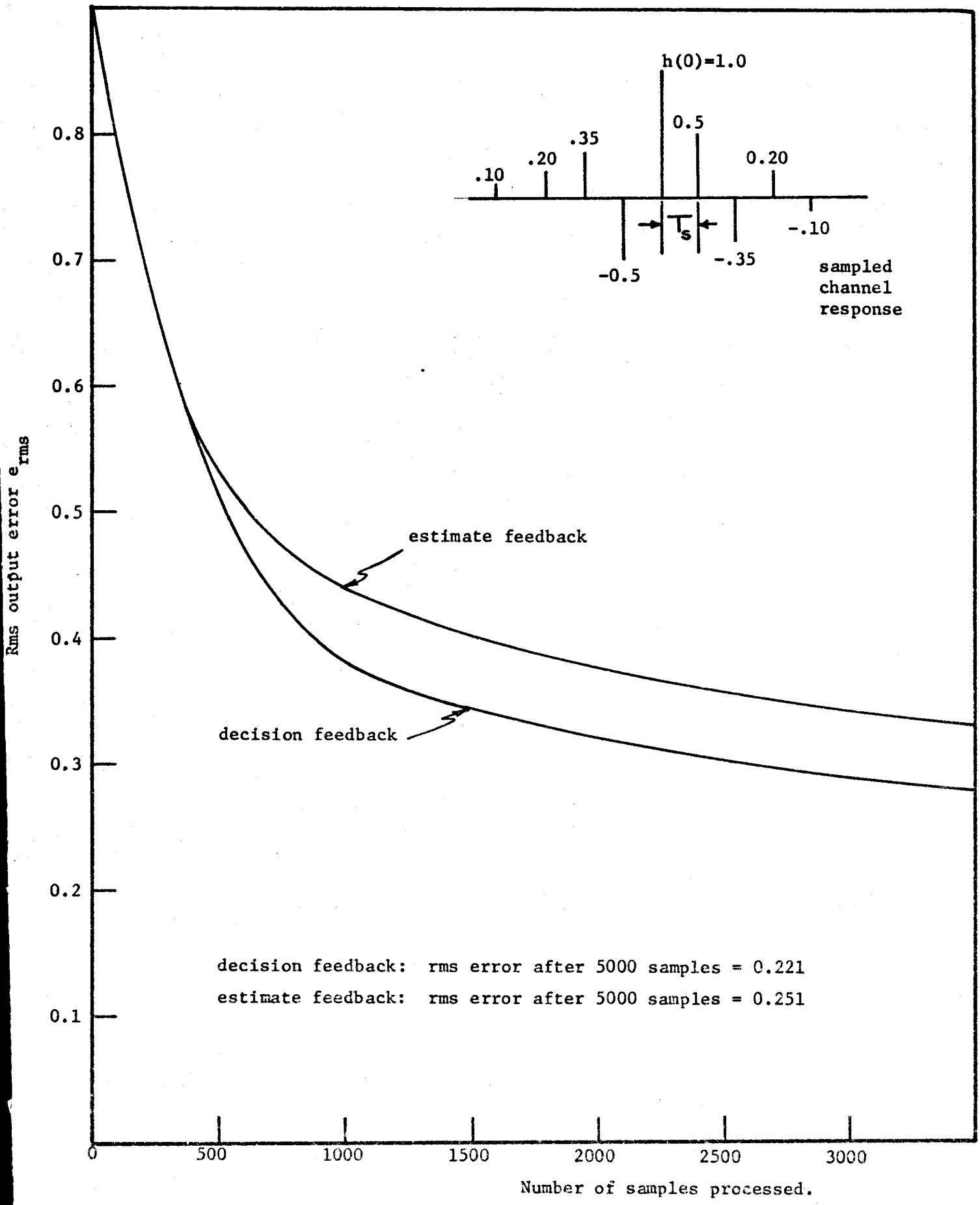

Figure 5.10 Decision directed convergence curves for channel response shown. Initial peak distortion D=2.30 and signal to interference ratio ρ_{in} = 1.18.

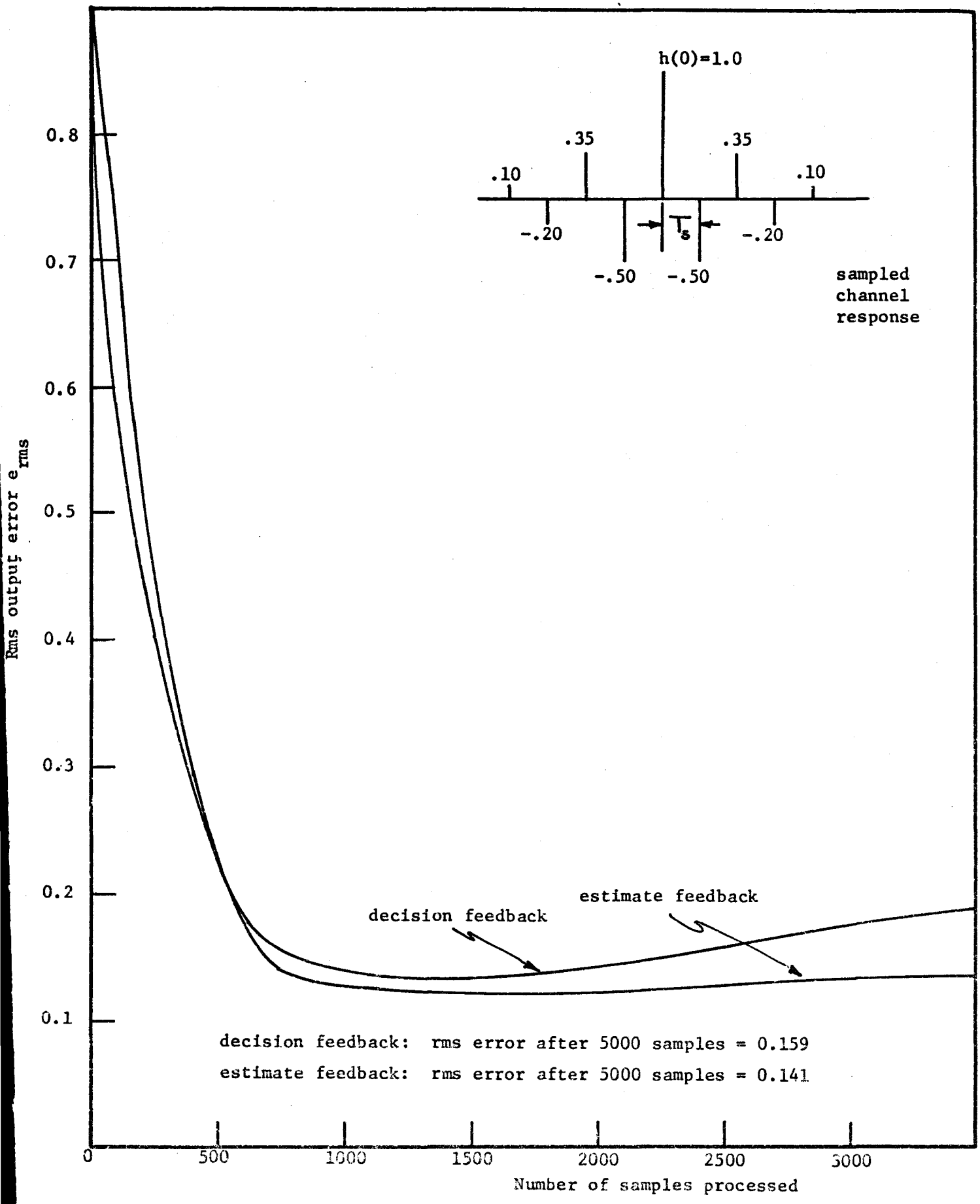

Figure 5.11 Decision directed convergence curve for channel shown. Initial peak distortion D=2.30 and signal to interference ratio ρ_{in}=1.18.

5.11 we have shown these properties by plotting, for each channel, the rms estimation error e_{rms} versus the number of samples processed. These curves are the ones labelled "estimate feedback". For comparison purposes, we have also simulated the decision feedback equalizer under the control of the same adaptive algorithm, and the corresponding convergence curves are shown in figures 5.3 to 5.11 as the ones labelled "decision feedback". Each of the curves in figures 5.3 to 5.11 represents the average over 5 independent simulation runs.

From the curves of figures 5.3 to 5.11, we may make the following observations concerning the estimate feedback equalizer:

(i) Convergence to some minimal value of the rms error e_{rms} always occured. We note that for the channel of figure 5.9, the decision feedback equalizer did not converge with the adaptive algorithm operating in the decision directed mode. Rather, in this case, the value of e_{rms} appeared to drift aimlessly between about 0.5 and 0.7.

(ii) There was a wide variation in the number of samples (symbols) required for the equalizer to achieve error-free reception over different channels.

(iii) Convergence was always fastest when the sampled channel impulse response $\{h(k);\ k=-L,\ldots,0,\ldots,L\}$ was symmetric about $h(0)$.

(iv) We found that the fastest convergence times and the smallest (average) values of e_{rms} after convergence, for any of the channels

under test, were obtained with the iteration constants α, δ and γ lying in the ranges

$$-2^{-8} < -.004 \leq \alpha \leq -.002 < -2^{-9}$$

$$-2^{-5} < -.035 \leq \delta \leq -.015 \approx -2^{-6}$$

$$-2^{-7} < -.005 \leq \gamma \leq -.002 < -2^{-9}$$

(v) For some of the channels which we tested (see figures 5.4, 5.5 and 5.11) the convergence curves exhibit a bottoming effect. That is the rms error decreases to some minimum value and then increases slightly after which it may or may not decrease again. This effect has been noted by previous investigators (George et al., 1969) and it appears to be a slow overshoot effect due to the transient properties of the adaptive algorithm.

The convergence curves of figures 5.3 to 5.11 were all obtained using the values $\alpha = -.004$, $\delta = -.025$ and $\gamma = -.005$. From the above ranges of values for these constants, we see that in an all digital implementation of the equalizer, we should maintain between 8 and 9 bits of accuracy in the recursive and non-recursive gains and about 6 bits of accuracy in the learning or extrapolation weights.

As in all adaptive system studies, we are faced with the problem of trying to relate the convergence and tracking properties of the adaptive algorithm to the signal conditions at the system input. This is a very complex problem, and there does not appear to be any simple, general solution to it, although we can draw some tentative conclusions

from the simulations. In Table (5.1) we have tabulated, for the estimate feedback equalizer, two measures of speed of convergence together with the corresponding values of the input peak distortion D, the signal to interference ratio ρ_{in} and the input probability of error $P_e(\rho_{in})$. We have also shown the corresponding measures of convergence speed for the adaptive decision feedback equalizer. From the table, we may make the following observations:

(i) As the input error probability $P_e(\rho_{in})$ increases beyond 0.15, there is a significant increase in the average number of samples required for the equalizer to adapt to a condition of essentially zero output error-rate†.

(ii) For channel 5.9 the adaptive decision feedback equalizer never converged with the adaptive algorithm operating in the decision directed mode. For this same channel the estimate feedback equalizer converged to essentially zero output error-rate in about 6000 samples. In fact we never observed a channel for which decision directed convergence of the estimate feedback equalizer could not be achieved.

(iii) Convergence was always faster when the sampled channel response $\{h(k);\ k=-L,\ldots,0,\ldots,L\}$ is symmetric about $h(0)$.

---

†Whenever we refer to the output error-rate, we shall mean the measured or estimated output probability of error.

Channel (numbers refer to figures)	Input Conditions (ρ_n=30db)			Measures of Convergence			
				Decision feedback		Estimate feedback	
	Peak Distortion D	Signal to Interference ratio ρ_{in}	Input error rate $P_e(\rho_{in})$	no. of samples for $e_{rms}<0.5$	no. of samples for $E_r = 0$	no. of samples for $e_{rms}<0.5$	no. of samples for $E_r = 0$
5.3	2.12	1.165	0.155	2250	3000	2150	3450
5.4(s)	2.12	1.487	0.129	300	300	350	500
5.5(s)	2.12	1.487	0.129	250	250	250	250
5.6	2.12	1.487	0.129	650	650	500	500
5.7	1.98	1.295	0.147	1050	1400	750	920
5.8	2.04	1.225	0.151	1150	3400	800	1220
5.9	2.18	1.052	0.173	$>10^4$	$>10^4$	1800	6000
5.10	2.30	1.18	0.148	500	710	600	3000
5.11(s)	2.30	1.18	0.148	200	200	200	200

E_r = measured output error rate or probability of error.

(s) implies channel impulse response is symmetric about h(0).

Table 5.1: Input signal conditions and convergence rates.

(iv) Generally speaking the convergence properties of the estimate feedback equalizer are comparable to those of the decision feedback equalizer. When the channel response is symmetric about h(0), there is little difference between the two, although there is a slight tendency for the decision feedback equalizer to be faster. When the channel response is unsymmetric about h(0), we found that with two exceptions, the estimate feedback equalizer tended to be faster. These two exceptions are channels 5.3 and 5.10. For channel 5.3, the rms error decreases slightly faster but the error-rate more slowly for the estimate feedback equalizer. For channel 5.10 the estimate feedback equalizer was found to be slower in both senses.

In observation (iii) above, we noted that convergence was always fastest when the sampled channel response {h(k)} was symmetric about h(0). This was true for both equalizer structures. The symmetry in {h(k)} implies that the channel causes only amplitude and no phase or delay distortion* of the transmitted signal. Thus the nonlinear feedback equalizers exhibit their best convergence properties when the channel causes only amplitude distortion.

The phase distortion caused by the channel may be removed by preceding the equalizer with a filter matched to the channel response. If the channel transfer function is $H(j\omega)$, then the required matched

---

*We are considering here distortion as a function of frequency.

filter has the transfer function $H^*(j\omega)$, where the asterisk implies the complex conjugate. When this filter is used, then as far as the equalizer is concerned, the channel transfer function is $|H(j\omega)|^2$. This function is purely real, and thus as far as the equalizer is concerned the channel causes only amplitude distortion. Such a filter is called for in the derivation of the optimum receiver in chapter 3. In practice, however, the used of a matched filter is not feasible since the channel response is unknown. It is, therefore, important that the equalizer have the capability to converge to a low error-rate when the channel causes both amplitude and phase distortion.

5.2b Effect of the Learning Algorithm

When the signals being processed by a system are stochastic in nature, the use of an adaptive algorithm to adjust the system implies that its performance will always be sub-optimum. An adaptive algorithm can adjust a system only to within a small, stochastically defined neighborhood of its optimum operating point. The objectives of the adaptive algorithm are to adjust the system to within as small a neighborhood as possible and to do so as quickly as possible. Unfortunately, these are usually conflicting objectives (Widrow, 1966), and thus some compromise between the speed of convergence and the size of the neighborhood about the optimum must be reached.

In conducting some further tests of the adaptive, nonlinear, feedback equalizer structures, we found that by using the algorithm developed in chapter 4, the adaptive behaviour, in terms of both the convergence speed and the size of the resulting neighborhood, could be improved by

increasing the speed of adaptation of the algorithm which adjusts the learning weights $\{\alpha_i(n);\ i=1,\ldots,M\}$. By increasing the speed of adaptation, we mean increasing the magnitude $|\delta|$ of the adjustments to the weights $\{\alpha_i(n)\}$ at each iteration.

Tests were conducted for the channels of figures 5.3 and 5.8 using the two values $\delta = -.025$ and $\delta = -.03$, and average convergence curves were obtained. The resulting curves are shown in figures 5.12 and 5.13 for the estimate feedback equalizer. For both channels, we see that the speed of convergence of the adaptive algorithm is increased by increasing the magnitude of the extrapolation process constant δ from 0.025 to 0.030. We also found for both channels that when $\delta = -.03$, the rms error e_{rms} always remained smaller than when $\delta = -.025$. This is indicated below by the values of e_{rms} after 5000 samples have been processed.

Channel	$\delta = -.025$ e_{rms} (5000)	$\delta = -.03$ e_{rms} (5000)
fig. 5.12	0.32	0.23
fig. 5.13	0.288	0.255

The above two channels were chosen as examples. We found that the same behaviour as a function of δ held for all the channels which we tested. The use of a larger magnitude for the iteration constant δ, therefore appears to result in improved adaptive behaviour of the estimate feedback equalizer. In fact, this improvement was observed with increasing values of δ up to the point* at which the learning process

---

*This point is of course dependent on the particular channel response which is being equalized.

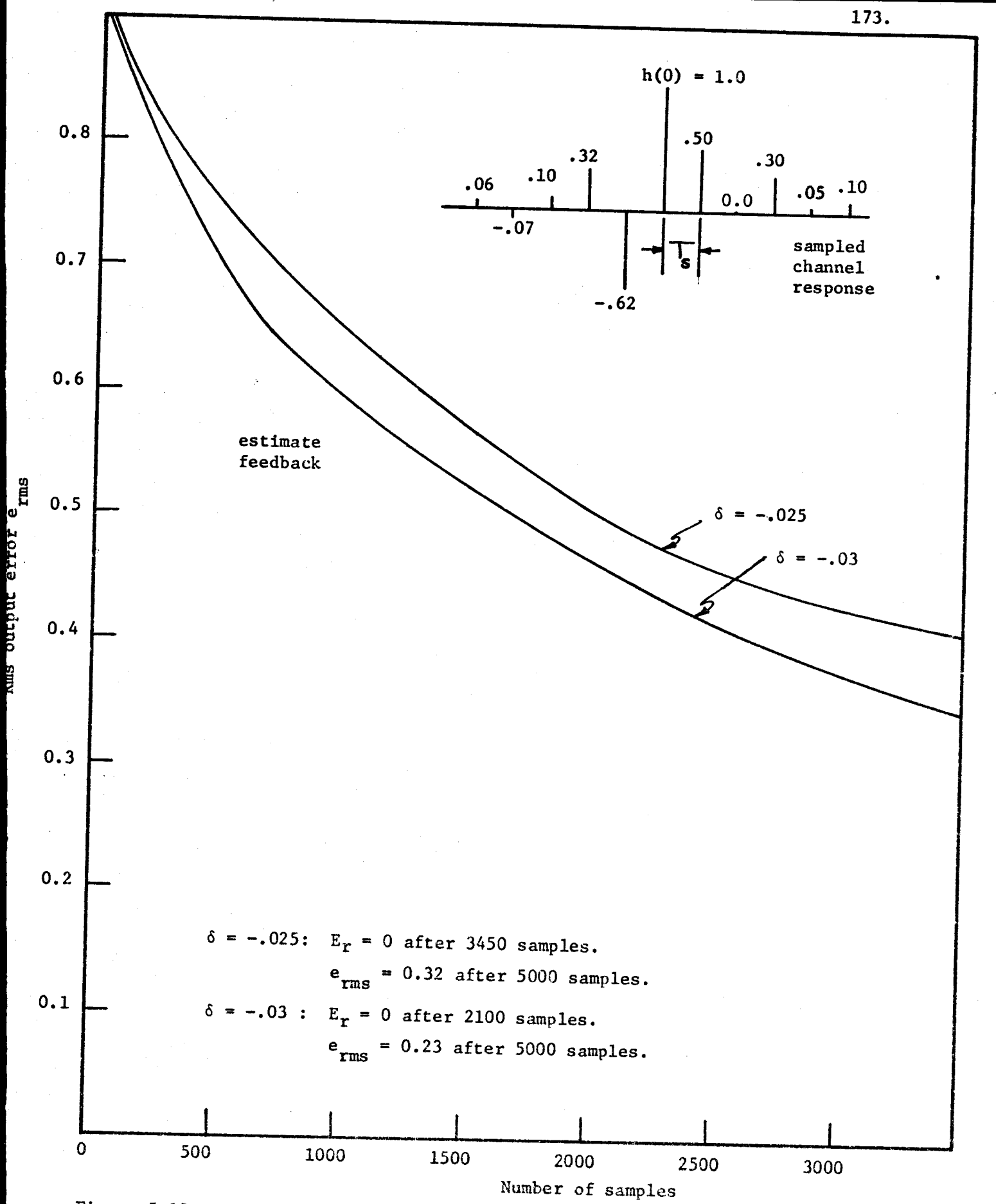

Figure 5.12 Estimate feedback, decision directed convergence curves for channel response shown and 2 values of learning constant δ.

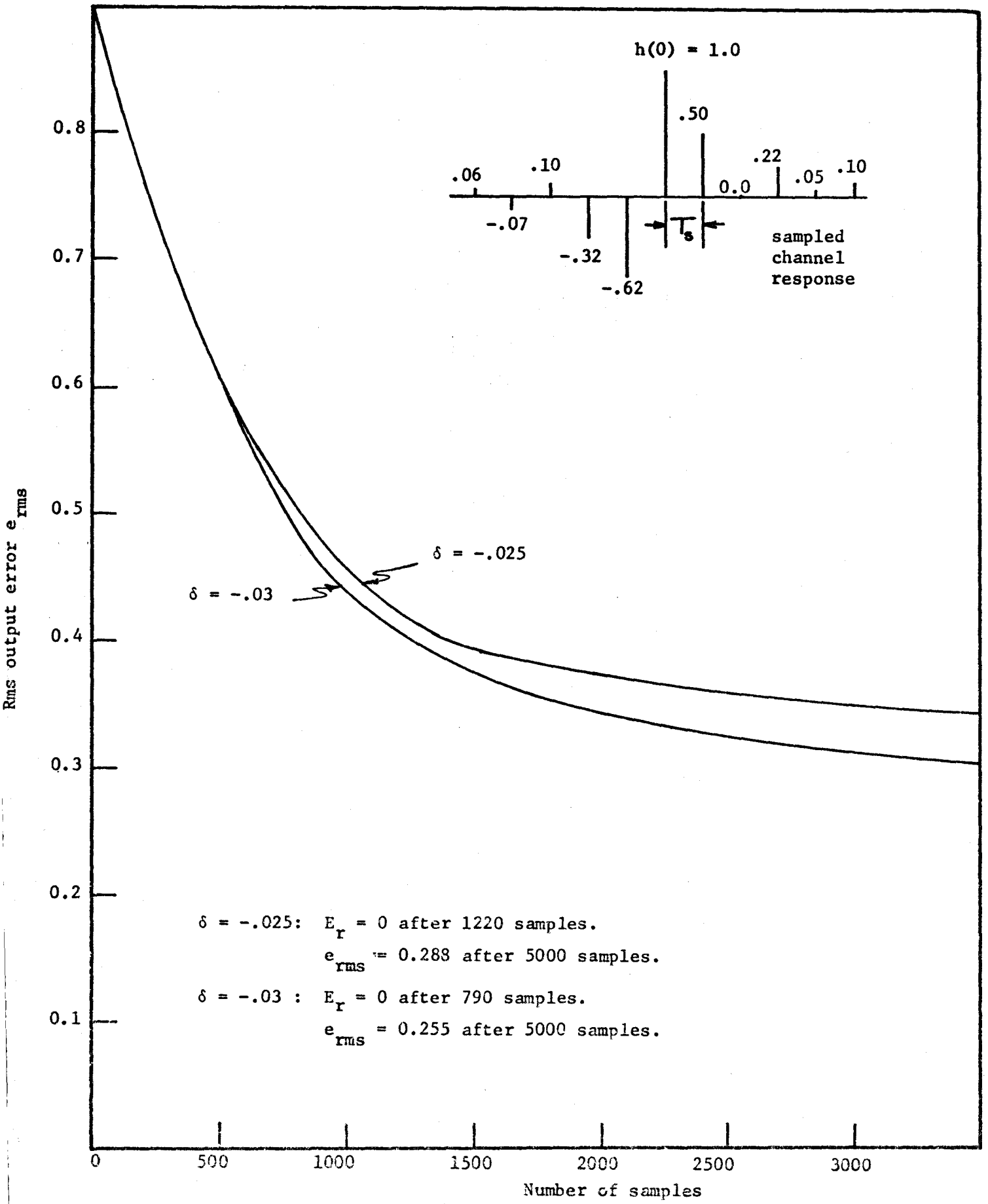

Figure 5.13 Estimate feedback, decision directed convergence curves for channel response shown and 2 values of δ.

adaptive algorithm becomes unstable.

We conducted these same tests for the decision feedback equalizer and obtained similar results to those given above. They are shown in figures 5.14 and 5.15.

5.2c The Use of a Training Sequence

We next examined the effect of training the equalizer. By training we mean that a known symbol sequence is transmitted, and that the receiver has available a copy of this sequence which it uses for adaptation purposes. The measurements of the output error used to iterate the adaptive algorithm are then made as $(s_n - \hat{s}_n)$, where s_n is the known symbol rather than as the decision directed measurements $(s_n^* - \hat{s}_n)$ where s_n^* is the output of the threshold detector or decision device. The purpose of these tests was to determine whether or not a relatively short training sequence has much of an effect on the convergence speed of the adaptive estimate feedback equalizer.

The first training test was conducted using the sampled channel impulse response shown in figure 5.3. A 255 symbol training sequence was used and an average convergence curve (averaged over 5 runs) was obtained. This curve is shown in figure 5.16, where we have also plotted, for purposes of comparison, the decision directed convergence curves of figures 5.3 and 5.12. From these curves, it is immediately obvious that the use of the relatively short 255 symbol training sequence has greatly increased the speed at which the equalizer converges to its optimum operating point. It is of interest to note that convergence to

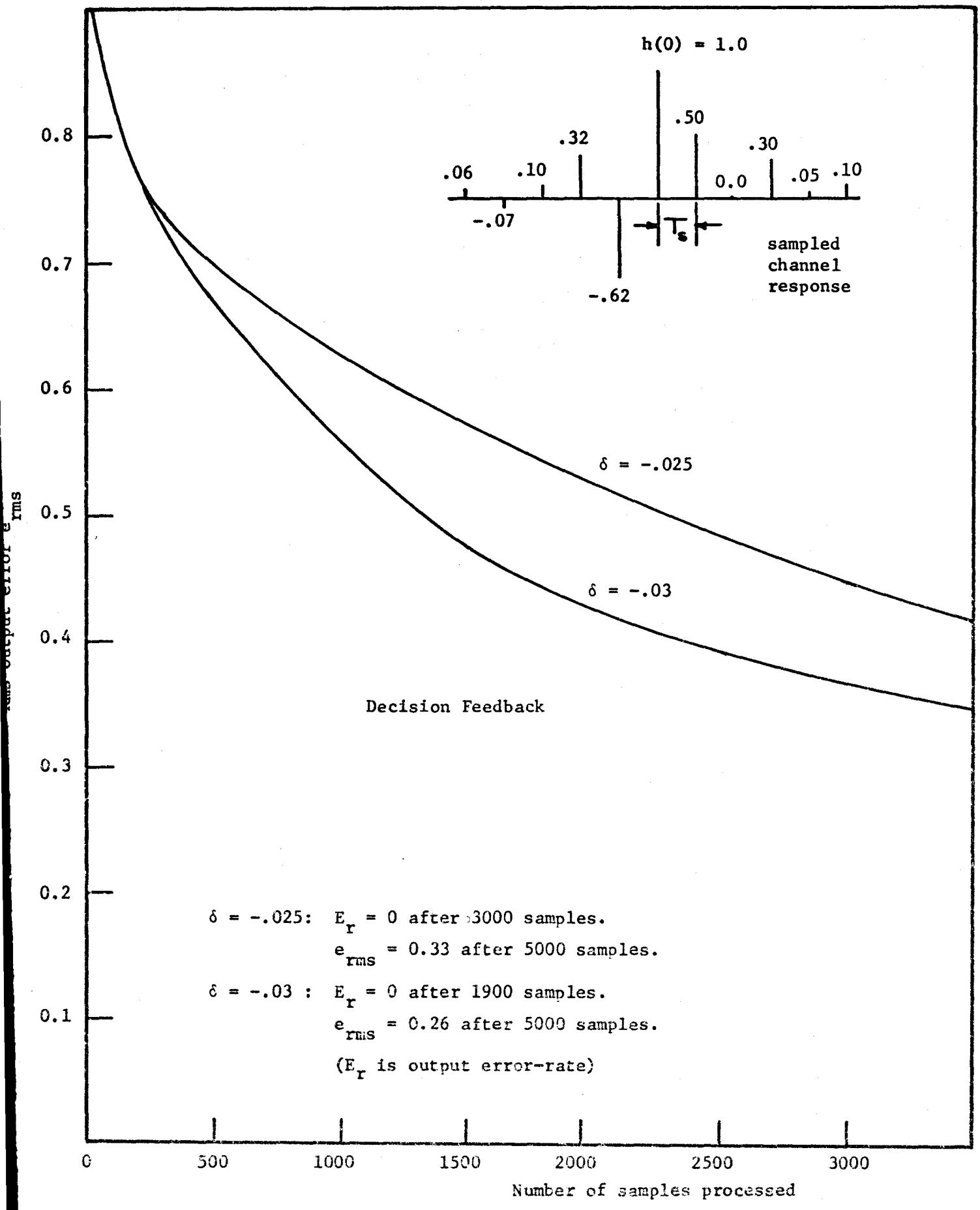

Figure 5.14 Decision directed convergence curves for channel response shown for 2 values of δ.

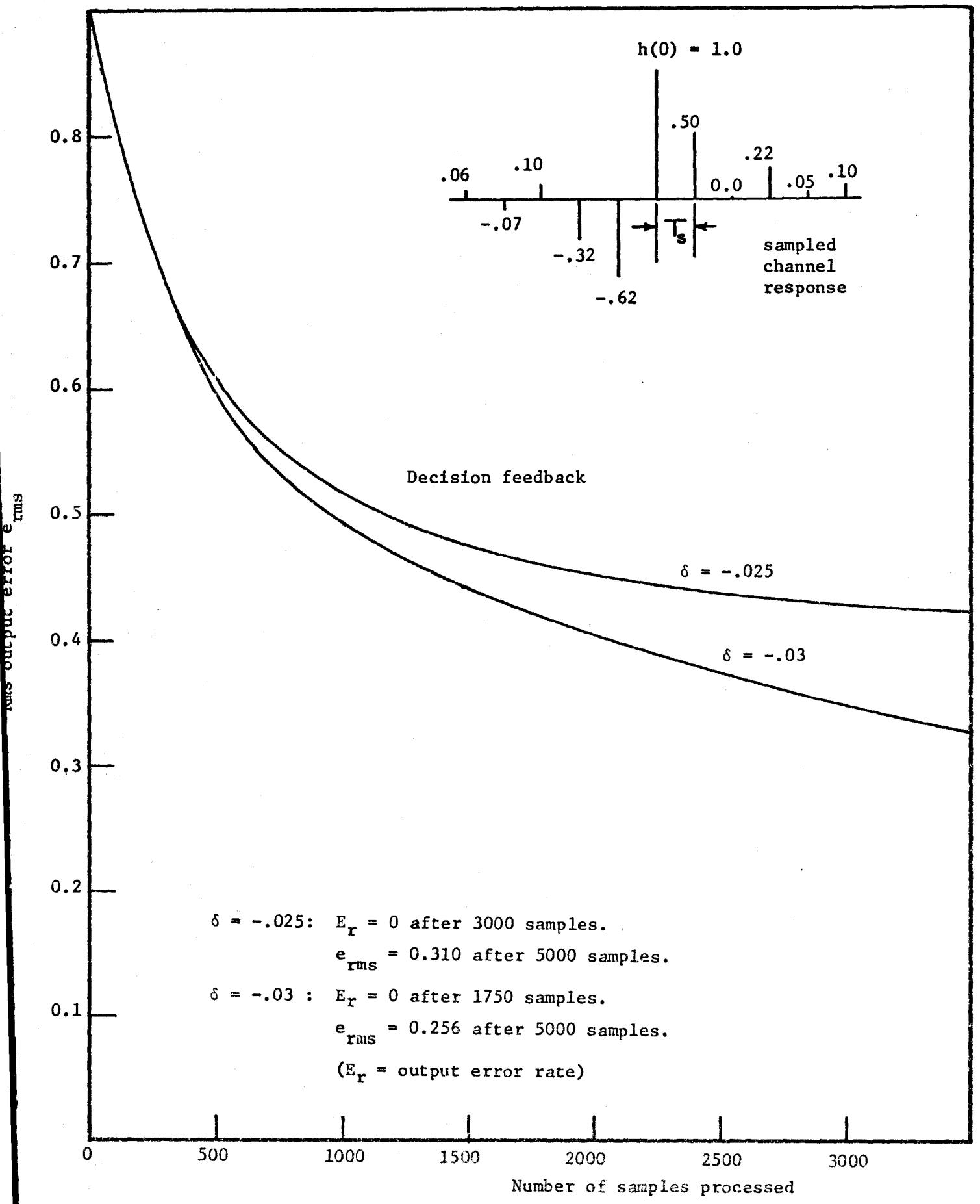

δ = -.025: E_r = 0 after 3000 samples.
e_{rms} = 0.310 after 5000 samples.

δ = -.03 : E_r = 0 after 1750 samples.
e_{rms} = 0.256 after 5000 samples.

(E_r = output error rate)

Figure 5.15 Decision directed convergence curves for channel response shown for 2 values of δ.

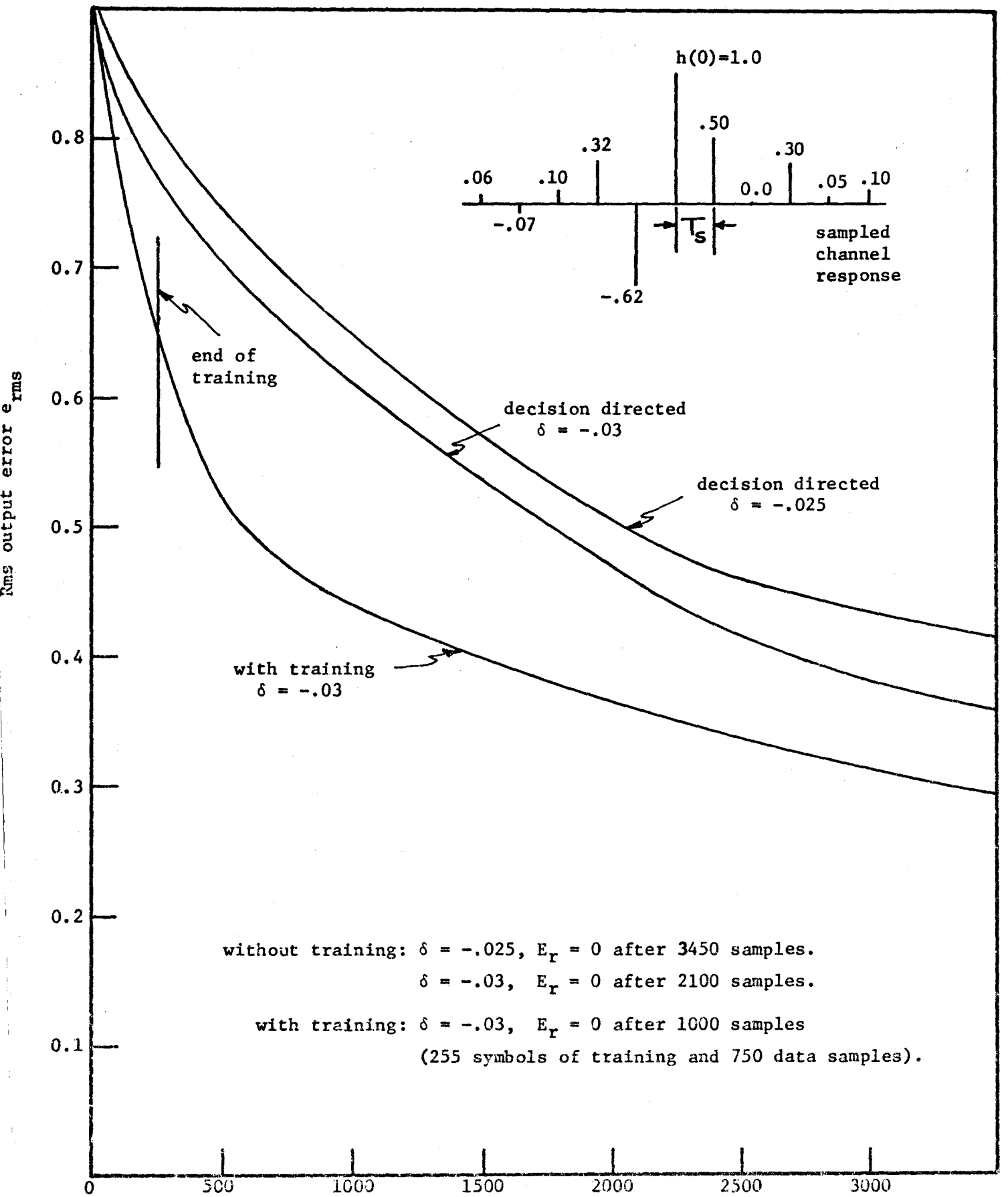

Figure 5.16 Estimate feedback convergence curves showing the effect of a 255 symbol training sequence.

the same value of rms error was eventually obtained in both the trained and the untrained case. We also tried this test using the decision feedback equalizer and similar results were obtained as shown in figure 5.17.

We also investigated the effect of training on the convergence properties of the equalizer when the channel response was that shown in figure 5.9. For this channel, the decision feedback equalizer did not converge when the adaptive algorithm was operating in the decision-directed mode, whereas the estimate feedback equalizer did. We first tried a 255 symbol training sequence. We found that for the estimate feedback equalizer, we obtained results similar to those shown in figure 5.16, but that the decision feedback equalizer did not always converge to an error-rate of essentially zero (E_r=0). For the decision feedback equalizer, we then tried a 510 symbol training sequence (formed by transmitting the 255 symbol sequence twice). In this case we found that the decision feedback equalizer always converged to zero error-rate and to a low value of the rms error, typically $e_{rms} = 0.25$, within a few hundred samples after the cessation of the training sequence.

5.3 Performance in the Presence of Noise

In the preceding discussion we have investigated the convergence properties of the estimate feedback equalizer, and have to some extent compared them to the corresponding properties of the known decision feedback equalizer. In all cases the equalizers were operated under the control of the adaptive algorithm derived in chapter 4. This investigation was conducted by means of computer simulations and a variety of channel

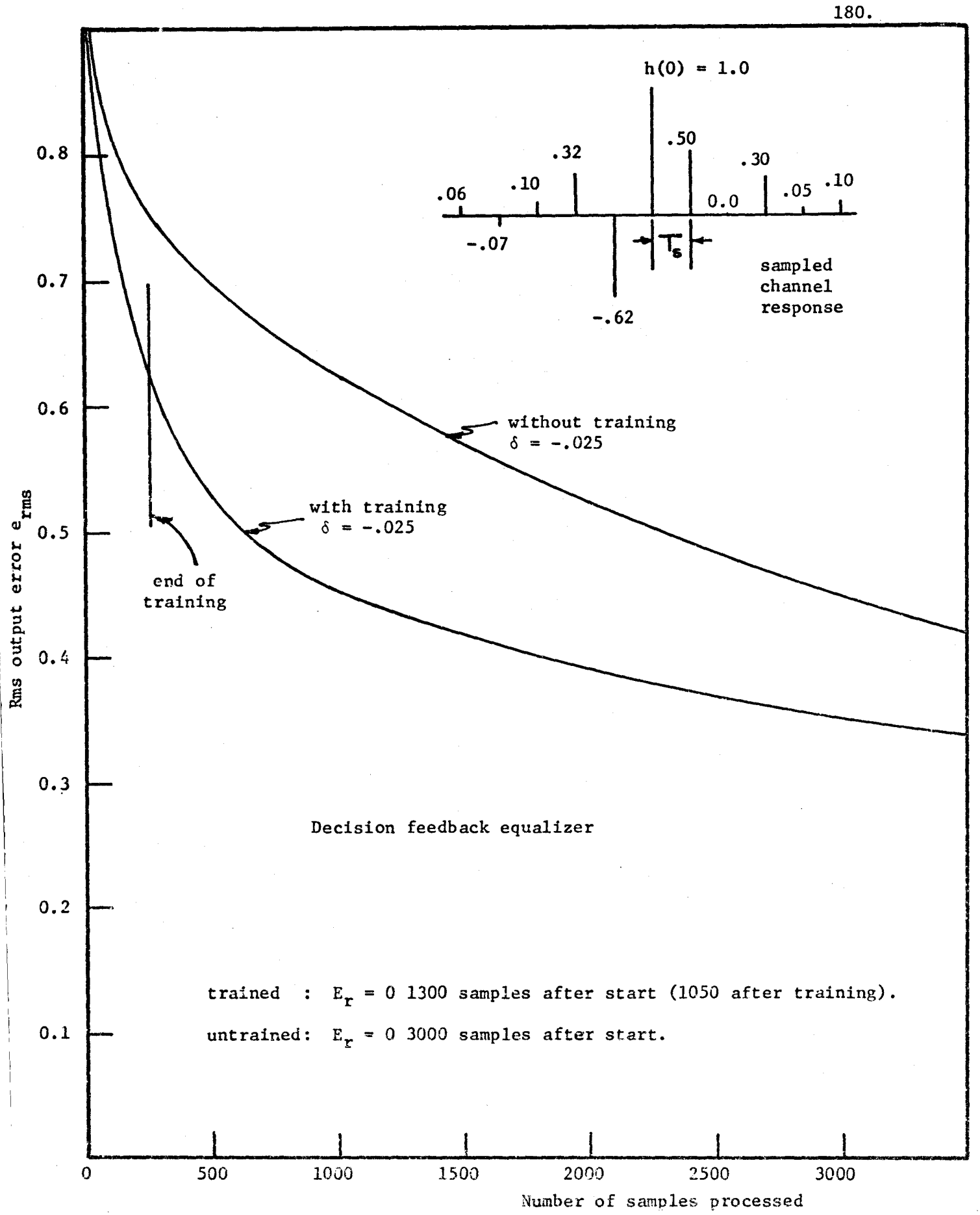

Figure 5.17 Convergence curves for channel response shown showing the effect of a 255 symbol training sequence.

impulse responses were used to test the equalizer. We found that the estimate feedback equalizer can be adapted, albeit quite slowly in a few cases, to each of these channel impulse responses using a decision directed adaptive algorithm, but that the decision feedback equalizer would not adapt in the decision directed mode to the channel of figure 5.9. We then showed how a relatively short training sequence could be used to obtain quite rapid convergence of the estimate feedback structure on all channels. All of this investigation was conducted at a high signal to additive noise ratio (ρ_n = 30db). We must now consider the properties of the estimate feedback equalizer as a function of the additive noise level (or signal to noise ratio ρ_n).

As the additive noise level is increased (the signal to noise ratio ρ_n is decreased) decision errors at the equalizer output, even when the equalizer has converged to its optimum operating point, will become more frequent. This occurs because the minimum attainable mean square error is increased by the presence of noise. We must, therefore, evaluate the performance of the equalizer as a function of the additive noise level.

Because of the tanh(·) nonlinearity within the feedback path, and because of the adaptive nature of the equalizer, the analytical evaluation of the output probability of error P_e is an extremely difficult task. It is much simpler to estimate it by means of Monte Carlo simulation. However, before discussing this we shall consider the optimum non-adaptive decision feedback equalizer. Under certain restrictive assumptions, it is possible to obtain some feel, at least in a qualitative

sense, for how the additive noise affects its performance, and this will provide some indication of the effect of additive noise on the estimate feedback equalizer.

5.3a Theoretical Considerations

From equation (4-7), we may write the output of the fixed decision feedback equalizer at the nth sampling time as

$$\hat{s}_n = \sum_{i=0}^{M} g_i(n)x(n+i) - \sum_{j=1}^{L} f_j(n)\tilde{s}_{n-j} \qquad (4\text{-}7)$$

where the $\{\tilde{s}_{n-j};\ j=1,\ldots,L\}$ are the outputs of the threshold detector or hard limiter defined by equation (4-63). From equations (4-13) and (4-14) the optimum values of the tap gains $\{g_i(n);\ i=1,\ldots,M\}$ and $\{f_j(n);\ j=1,\ldots,L\}$ are defined by

$$\sum_{i=0}^{M} g_i(n)E\{x(n+i)x(n+k)\} - \sum_{j=1}^{L} f_j(n)E\{\tilde{s}_{n-j}x(n+k)\} = E\{s_n x(n+k)\}$$

$$(k=0,1,\ldots,M) \qquad (4\text{-}13)$$

and

$$\sum_{j=1}^{L} f_j(n)E\{\tilde{s}_{n-j}\tilde{s}_{n-m}\} - \sum_{i=0}^{M} g_i(n)E\{x(n+i)\tilde{s}_{n-m}\} = E\{s_n\tilde{s}_{n-m}\}$$

$$(m=1,\ldots,L) \qquad (4\text{-}14)$$

In order now to simplify our analysis in this section, let us make the following assumptions:

(a) The L previous decisions $\{\tilde{s}_{n-j};\ j=1,\ldots,L\}$ used in the formation of $\hat{s}_n$ are correct - that is

$$\tilde{s}_{n-j} = s_{n-j} \qquad (j=1,\ldots,L)$$

(b) The data symbols $\{s_k\}$ are binary and uncorrelated with zero mean and unit variance, i.e.,

$$E\{s_i s_j\} = \delta(i-j) = \begin{cases} 1 & (i=j) \\ 0 & (i\neq j) \end{cases}$$

(c) The number of taps on the recursive and non-recursive delay lines are equal, i.e., M=L.

The second of the above optimization equations may then be written as

$$f_m(n) - \sum_{i=0}^{M} g_i(n) E\{x(n+i)s_{n-m}\} = 0 \qquad (m=1,\ldots,L) \qquad (5\text{-}18)$$

Now from equation (4-5) we may write at the nth sampling time

$$x(n) = \sum_{k=n-L}^{n+L} s_k h(n-k) + n_c(n) = \sum_{k=-L}^{L} s_{n-k} h(k) + n_c(n)$$

for each input sample, where $n_c(n)$ is a sample of the additive background noise which we shall assume to be independent of the symbols $\{s_k\}$ and to be sample to sample uncorrelated, i.e.,

$$E\{n_c(m)n_c(n)\} = N_o\delta(m-n)$$

where N_o is the noise variance. Now let us find, explicitly, the various correlations in equations (4-13) and (5-18). First we may write

$$E\{x(n+i)x(n+k)\} = \sum_{p=-L}^{L} \sum_{j=-L}^{L} h(p)h(j)E\{s_{n+i-p}s_{n+k-j}\} + E\{n_c(n+i)n_c(n+k)\}$$

$$(k,i = 0,1,\ldots,L)$$

which by the use of assumption (b) may be reduced to

$$E\{x(n+i)x(n+k)\} = \sum_{p=-L}^{L} \sum_{j=-L}^{L} h(p)h(j)\delta(i-k+j-p) + N_o\delta(k-i)$$

$$(k,i = 0,1,\ldots,L)$$

This last equation may be written in the simpler form

$$E\{x(n+i)x(n+k)\} = \sum_{p=-L}^{L} h(p)h(p+k-i) + N_o\delta(k-i) \qquad (i,k=0,1,\ldots,L)$$

$$|p+k-i| \leq L$$

$$= 0 \quad \text{otherwise} \qquad (5\text{-}19)$$

If we then define

$$\psi(i,k) = \sum_{p=-L}^{L} h(p)h(p+k-i) \qquad |p+k-i| \leq L$$

$$(i,k=0,1,\ldots,L)$$

$$= 0 \quad \text{otherwise}$$

we may write equation (5-19) in the compact form

$$E\{x(n+i)x(n+k)\} = \psi(k,i) + N_o\delta(k-i)$$

$$(i,k=0,1,\ldots,L)$$

$$= \psi(i,k) + N_o\delta(i-k) \qquad (5\text{-}20)$$

Next let us consider the correlation $E\{x(n+i)s_{n-m}\}$ which may be written as

$$E\{x(n+i)s_{n-m}\} = \sum_{k=-L}^{L} h(k)E\{s_{n+i-k}s_{n-m}\} \qquad i=0,1,\ldots,L$$

$$m=1,\ldots,L$$

and this may readily be reduced to the form

$$E\{x(n+i)s_{n-m}\} = h(i+m) \qquad \begin{matrix} i=0,1,\ldots,L \\ m=1,\ldots,L \\ |i+m| \leq L \end{matrix} \qquad (5\text{-}21)$$

Then setting m=0 in equation (5-21) we at once obtain the correlation

$$E\{s_n x(n+k)\} = h(k) \qquad (k=0,1,\ldots,L) \qquad (5\text{-}22)$$

Using equations (5-20) to (5-22), we may now rewrite the optimization equations (4-13) and (5-18) as

$$f_m(n) = \sum_{i=0}^{L} g_i(n)h(i+m) \qquad (m=1,\ldots,L) \qquad (5\text{-}23)$$

and

$$\sum_{i=0}^{M} g_i(n)[\psi(i,k) + N_o\delta(i-k)] - \sum_{j=1}^{L} f_j(n)h(k+j) = h(k) \qquad (k=0,1,\ldots,L) \qquad (5\text{-}24)$$

Then substituting equation (5-23) into equation (5-24) we obtain

$$\sum_{i=0}^{L} g_i(n)\{\sum_{p=-L}^{L} h(p)h(p+k-i) - \sum_{j=1}^{L} h(i+j)h(k+j)\} + \sum_{i=0}^{L} g_i(n)N_o\delta(i-k) = h(k) \qquad (k=0,1,\ldots,L) \qquad (5\text{-}25)$$

and with a little manipulation, this may be rewritten as

$$\sum_{i=0}^{L} g_i(n)\{\sum_{p=-L}^{i} h(p)h(p+k-i) + N_o\delta(i-k)\} = h(k) \qquad (k=0,1,\ldots,L)$$

or

$$\sum_{i=0}^{L} g_i(n)\{\theta(i,k) + N_o\delta(k-i)\} = h(k) \qquad (k=0,1,\ldots,L) \qquad (5\text{-}26)$$

where we have defined

$$\theta(i,k) = \sum_{p=-L}^{i} h(p)h(p+k-i) \qquad (i,k=0,1,\ldots,L) \qquad (5\text{-}27)$$

Now we may readily show that

$$\theta(i,k) = \theta(k,i) \qquad \text{and} \qquad \theta(i,i) \geq 0 \quad ,$$

and thus the matrix

$$[\theta(i,k)] \qquad (i,k=0,1,\ldots,L)$$

is positive semidefinite. The matrix

$$R = [r(i,k)] = [\theta(i,k) + N_o\delta(i-k)] \quad (i,k=0,1,\ldots,L)$$

is therefore positive definite, and there is a unique solution of equation (5-26) for the optimum values of the gains $\{g_i(n);\ i=0,1,\ldots,L\}$. If we define the vectors

$$G(n) = \begin{bmatrix} g_o(n) \\ g_1(n) \\ \vdots \\ g_L(n) \end{bmatrix} \qquad \text{and} \qquad H = \begin{bmatrix} h(0) \\ h(1) \\ \vdots \\ h(L) \end{bmatrix}$$

we may write this solution in the form

$$G_o(n) = R^{-1}H \qquad (5\text{-}28)$$

where the subscript "o" denotes the optimum values of the gains.

If we now substitute equations (5-23) and (4-5) into the estimate $\hat{s}_n$, then after a little algebraic manipulation we may write

$$\hat{s}_n = [\sum_{i=0}^{L} g_{i_o}(n)h(i)]s_n + \sum_{i=0}^{L} g_{i_o}(n) \sum_{k=-L}^{i-1} h(k)s_{n+i-k} + \sum_{i=0}^{L} g_{i_o}(n)n_c(n+i)$$

. . . . (5-29)

where the gains $\{g_{i_o}(n);\ i=0,1,\ldots,L\}$ are the optimum gains defined by equations (5-26). The first term of equation (5-29) represents the desired signal component of the estimate $\hat{s}_n$. The second term is the residual intersymbol interference at the equalizer output and the third term is the contribution to $\hat{s}_n$ due to the additive background noise. We note that each of the three terms in equation (5-29) is uncorrelated with the other two.

Let us now find the mean-square value of each of the components of $\hat{s}_n$:

(i) the signal component

$$E\{\sum_{i=0}^{L} g_{i_o}(n)h(i)s_n \sum_{j=0}^{L} g_{j_o}(n)h(j)s_n\} = [\sum_{i=0}^{L} g_{i_o}(n)h(i)]^2 \qquad (5\text{-}30)$$

(ii) the residual intersymbol interference

$$\sum_{i=0}^{L} \sum_{j=0}^{L} g_{i_o}(n)g_{j_o}(n)E\{\sum_{k=-L}^{i-1} h(k)s_{n+i-k} \sum_{p=-L}^{j=1} h(p)s_{n+j-p}\}$$

With a little manipulation of this expression and the use of assumption (b), we obtain the result

$$\sum_{i=0}^{L} \sum_{j=0}^{L} g_{i_o}(n)g_{j_o}(n) \sum_{k=-L}^{i-1} h(k)h(k+j-i)$$

and if we then make the definition

$$\rho(i,j) = \sum_{k=-L}^{i=1} h(k)h(k+j-i) \qquad (j,i=0,1,\ldots,L)$$

we obtain the residual intersymbol interference as

$$\sum_{i=0}^{L} \sum_{j=0}^{L} g_{i_o}(n) g_{j_o}(n) \rho(i,j) \tag{5-31}$$

(iii) the additive noise component

$$E\{ \sum_{i=0}^{L} g_{i_o}(n) n_c(n+i) \sum_{j=0}^{L} g_{j_o}(n) n_c(n+j) \} = N_o \sum_{i=0}^{L} g_{i_o}^2(n) \tag{5-32}$$

Next let us define a signal to interference ratio at the equalizer output as

$$\rho_o = \frac{(\text{Output signal energy})}{(\substack{\text{Residual ISI} \\ \text{energy}}) + (\substack{\text{Output noise} \\ \text{energy}})} \tag{5-33}$$

Substituting equations (5-30) to (5-32) into this we obtain

$$\rho_o = \frac{[\sum_{i=0}^{L} g_{i_o}(n) h(i)]^2}{\sum_{i=0}^{L} \sum_{j=0}^{L} g_{i_o}(n) g_{j_o}(n) \rho(i,j) + N_o \sum_{i=0}^{L} g_{i_o}^2(n)} \tag{5-34}$$

where the optimum gains $\{g_{i_o}(n)\}$ are defined by equations (5-26). We may make the following observations concerning ρ_o:

(i) It is similar in form to the input signal to interference ratio

$$\rho_{in} = \frac{h^2(0)}{\sum_{\substack{k=-L \\ k \neq 0}}^{L} h^2(k) + N_o}$$

defined in equation (5-10).

(ii) Because of equalization, the intersymbol interference has been reduced. That is, it may be shown (George et al., 1971) that

$$\sum_{i=0}^{L}\sum_{j=0}^{L} g_{i_o}(n)g_{j_o}(n)\rho(i,j) < \sum_{\substack{k=-L \\ k\neq 0}}^{L} h^2(k)$$

(iii) The input additive noise energy N_o has been multiplied by the factor $\sum_{i=0}^{L} g^2_{i_o}(n)$. Depending on the sampled impulse response $\{h(k)\}$ of the particular channel being equalized, this may cause the additive noise to be enhanced relative to the desired signal components at the equalizer output and this may lead to increased output error-rates. This is particularly true at low values of the input signal to noise ratio ρ_n.

In principle we could use the results in equations (5-29) and (5-34) along with the error probability expression in equation (5-13), which was developed by Shimbo et al. (1971) to compute the output probability of error for the optimum, non-adaptive, decision feedback equalizer. However, in practice decision errors will occur especially at low values of the signal to noise ratio ρ_n. The errors are used in the recursive portion of the equalizer with the result that the intersymbol interference due to previous symbols may be enhanced instead of being cancelled as indicated in the above analysis. This means that the actual output signal to interference ratio may be quite different from the calculated value in equation (5-34). Any analytical evaluation of the output probability of error will tend, therefore, to be a rather optimistic estimate of the actual probability of error. This will be

especially true at low values of the signal to noise ratio ρ_n. The output signal to interference ratio does, however, indicate how the additive noise is affected by the equalizer, and this is the main result of this section.

Let us consider now the estimate feedback equalizer which is the main concern of this thesis. In a rather rough way, equation (5-34) may be applied to this structure in that the multiplication of the additive noise energy N_o by the factor $\sum_{i=0}^{L} g_{i_o}^2(n)$ will still occur, and as noted above for the decision feedback equalizer, this may lead to increased output error-rates. That is, for any channel response which causes the additive noise to be enhanced relative to the desired signal, we would expect the error-rate performance of the estimate feedback structure to become worse in the same manner as that of the decision feedback structure. However, in chapter 3, we showed that the decision feedback equalizer is a high signal to noise ratio approximation to the estimate feedback equalizer. We would, therefore, expect, at least at low signal to noise ratios, the output error-rate of the estimate feedback equalizer to be lower than that of the decision feedback equalizer. In practice, we shall find that this is true for many channels at all signal to noise ratios.

5.3b Results of Simulation

In this section, we shall describe the measurement, by means of Monte Carlo simulation, of the output error-rate or probability of error of the estimate feedback equalizer as a function of the input signal to noise ratio ρ_n. We shall compare these results to the corresponding

results for the decision feedback equalizer. The output error-rate is also a function of the particular channel being equalized, and therefore we have conducted our measurements using four of the nine channels* used in section 5.2. These four channels were selected on the following basis:

(i) The channels of figures 5.3 and 5.9 were selected because they are typical of a coaxial cable link and a schedule 4 data line respectively. Also the channel of figure 5.9 was chosen because error-rate measurements using a linear equalizer (Proakis, 1969) have been made on it, and these provide a standard to which we may compare the estimate feedback equalizer's performance.

(ii) The channel of 5.11 was chosen because it illustrates the situation where a matched filter precedes the equalizer. The channel of figure 5.10 was used because it is unsymmetric about h(0) but is otherwise equivalent to the response of figure 5.11.

Our main interest here is the steady state error-rate, namely the output probability of error after the adaptive algorithm has adjusted the equalizer to within a small neighborhood of its optimum operating point. We, therefore, used in each of the tests, a training sequence of 510 symbols so as to obtain rapid initial convergence of the equalizer. We then waited for about 2000 samples after the cessation of the training sequence in order to allow ample time for the equalizer to reach its

---

*namely those of figures 5.3, 5.9, 5.10 and 5.11.

steady state. We then measured the output error-rate by counting the number of errors. This count was continued until approximately 100 errors had been counted, and the procedure was repeated for each channel over a range of signal to noise ratios of from 6db to 30db.

The results of the error-rate simulations are shown in figures 5.18 to 5.21, where we have plotted the estimated output probability of error or error-rate

$$E_r = \frac{\text{number of errors counted}}{\text{total number of symbols processed}}$$

for the estimate feedback equalizer as a function of the input signal to noise ratio ρ_n. We have also plotted in each of these figures the following curves:

(i) the probability of error as a function of the signal to noise ratio for a non-dispersive channel (see equation (5-15)) which is a lower bound on the attainable probability of error.

(ii) the error probability at the equalizer input for the particular channel being measured. This is calculated from equation (5-13) and is the probability of error which would be obtained if no equalization were performed.

(iii) the corresponding output probability of error obtained by simulating the decision feedback equalizer.

Based on figures 5.18 to 5.21, we may make the following observations concerning the estimate feedback equalizer:

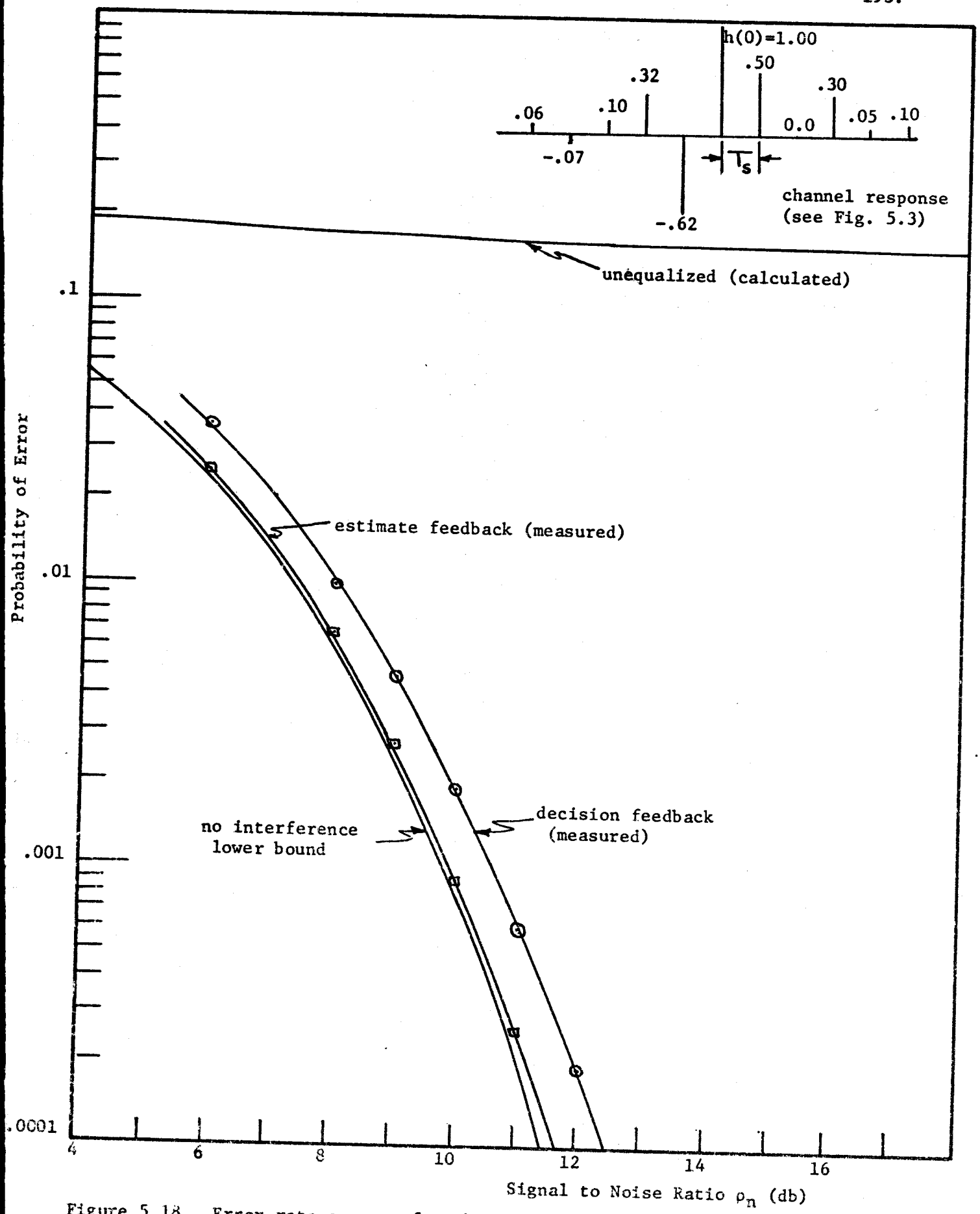

Figure 5.18 Error-rate curves, for channel response shown, illustrating the effects of equalization on the output error-rate.

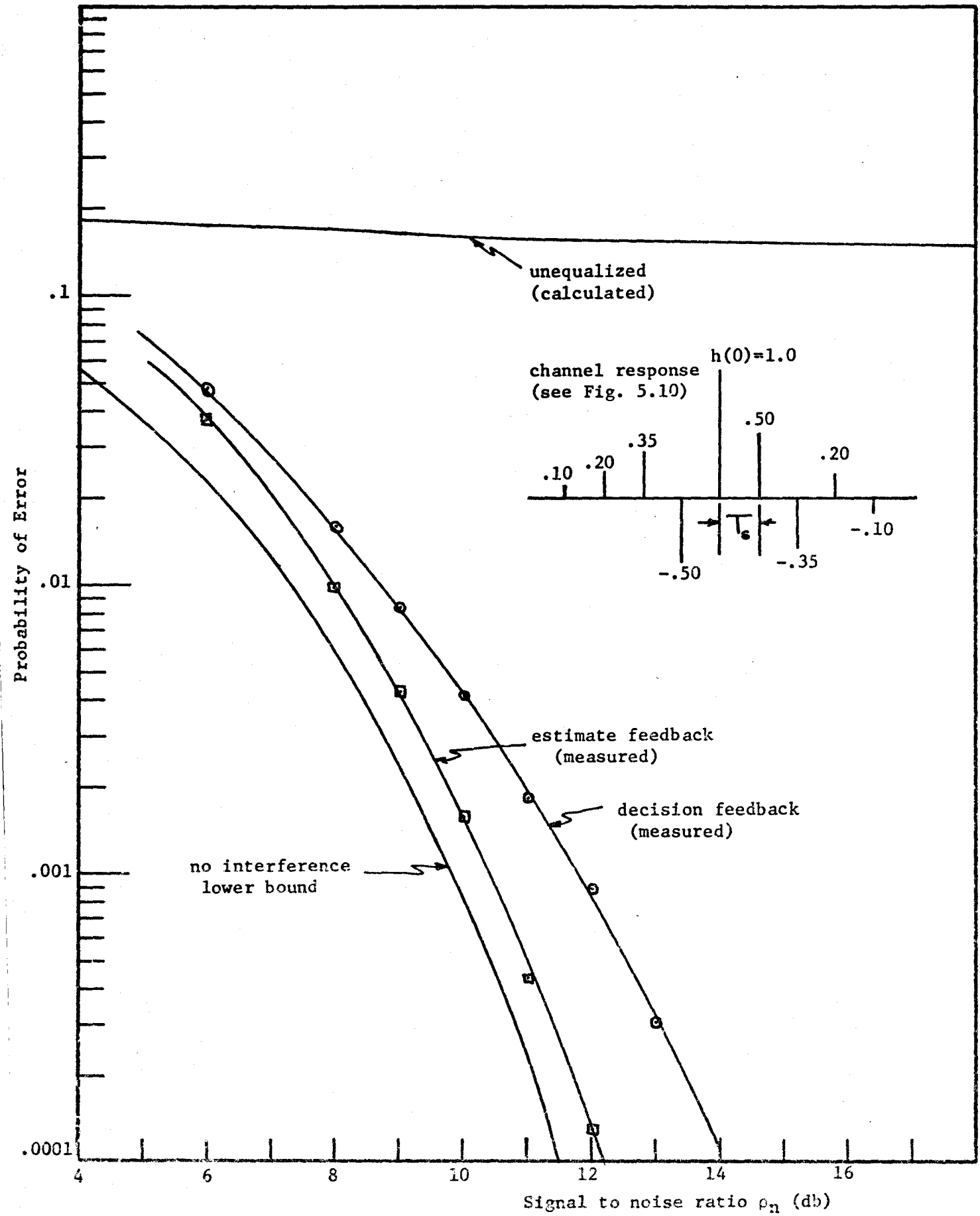

Figure 5.19 Error-rate curves, for channel response shown, illustrating the effects of equalization on the output error-rate.

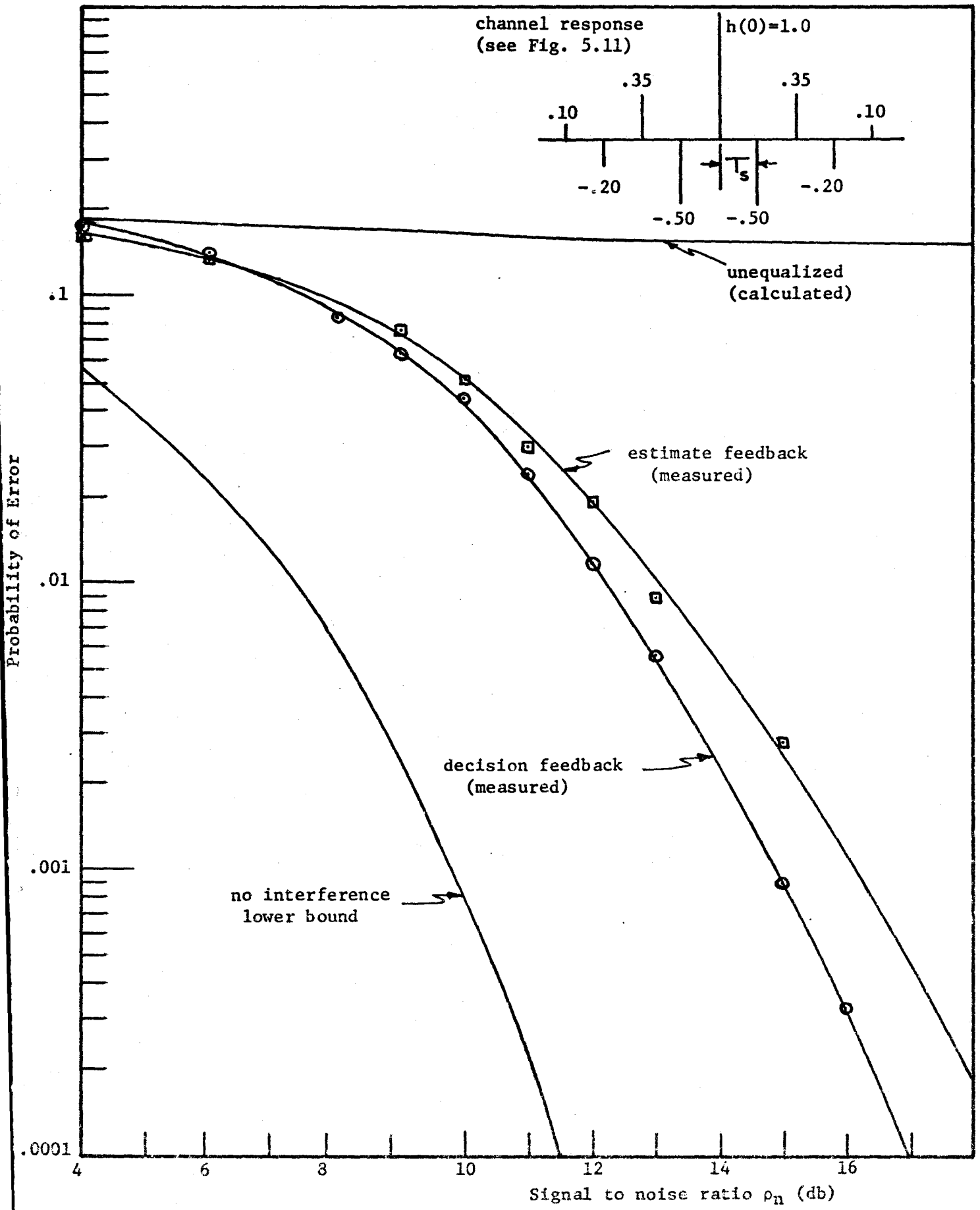

Figure 5.20 Error-rate curves, for channel response shown, illustrating the effects of equalization on the output error-rate.

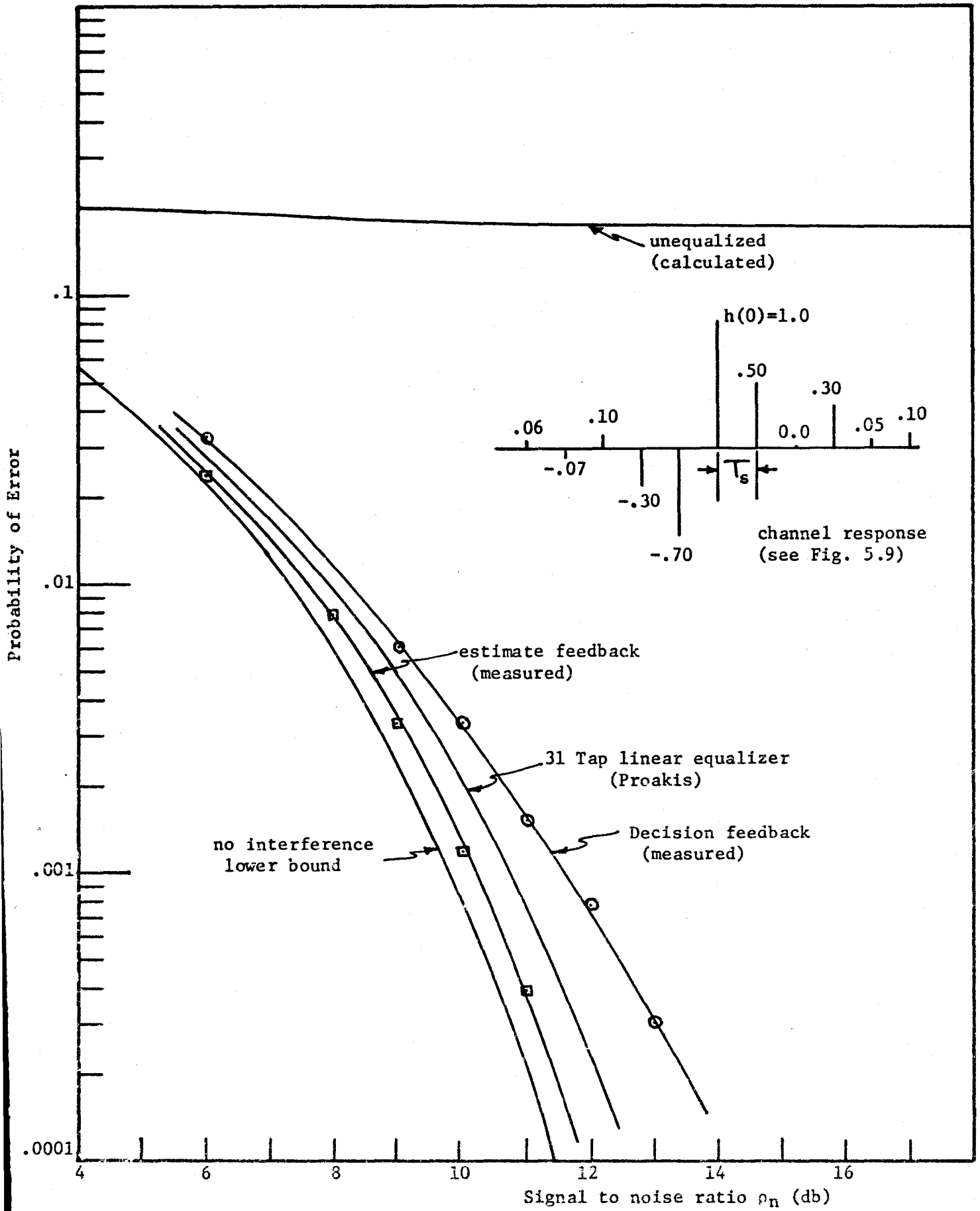

Figure 5.21 Error-rate curves, for channel response shown, illustrating the effects of equalization on the output error-rate.

(i) Depending on the sampled channel impulse response {h(k); k=-L,...,0,...,L}, there is a variation of up to about 6db in the signal to noise ratio ρ_n at which a given output error-rate is obtained.

(ii) Because the curves in figures 5.18 to 5.21 are empirical in that they are obtained by counting errors, they depend to some extent on when this counting begins. We have made the effect of this quite small by waiting until the equalizer is operating in steady state and by then counting errors over a large number of received symbols.

(iii) The curve in figure 5.20 for the decision feedback equalizer is consistent with one obtained by George et al. (1971) using a similar channel.

(iv) For the channels of figures 5.18, 5.19 and 5.21 the estimate feedback equalizer yielded better performance at all values of the signal to noise ratio ρ_n than did the decision feedback equalizer.

(v) For the sampled channel impulse response of figure 5.20 the performance of both the estimate and the decision feedback equalizers is much worse than for any of the other three channels which we used for our tests. At signal to noise ratios greater than about 6db the performance of the estimate feedback equalizer was slightly worse than that of the decision feedback equalizer,

but at lower values of the signal to noise ratio it was slightly better.

For all the channels which we tested, there was some tendency for errors to occur in bursts. We found that most of these bursts were only 2 or 3 symbols long but that the occasional burst 5 or 6 symbols long occurred. This tendency was more pronounced for the decision feedback equalizer than for the estimate feedback equalizer, and was always more severe at low signal to noise ratios (ρ_n < 6db). For both equalizer structures, it was most pronounced for the channel impulse response of figure 5.20.

Previous investigators (Austin, 1967 and George et al. 1969 and 1971) have noted this effect and discussed it in connection with the decision feedback equalizer. They have termed it the error propagation effect because in a decision feedback structure the occurrence of one decision error tends to cause another to occur thus leading to the creation or propagation of a burst of errors. In some recent tests, Keeler (1971) has shown that for error-rates less than 10^{-1}, error propagation does not seriously degrade the performance of the decision feedback equalizer, but at higher values of the error-rate it tends to become the dominant cause of performance degradation with the number of bursts increasing both in frequency of occurrence and length.

The main reason for the much worse performance of both the decision and the estimate feedback equalizers when they are equalizing the channel of figure 5.20 appears to be the enhancement of the additive noise by the equalizer. To see this, let us begin by defining the signal

to additive noise ratio at the input ($\hat{s}_n$) to the nonlinearity (sgn(·) or tanh(·) respectively) in the feedback path as

$$\rho_{n_o} = \frac{\text{(desired signal energy in } \hat{s}_n)}{\text{(noise energy in } \hat{s}_n)} \tag{5-35}$$

When the equalizer is both nonlinear and adaptive, as in the present case, ρ_{n_o} is very difficult to evaluate. However, by considering the non-adaptive decision feedback equalizer under the restrictive assumptions of section 5.3a, we may calculate an ideal output signal to noise ratio $\rho^*_{n_o}$. It will be only an approximation but it will provide some insight into the effect of the estimate and decision feedback equalizers on the additive noise.

Now substituting equations (5-30) and (5-32) into equation (5-35), we obtain the ideal output signal to noise ratio as

$$\rho^*_{n_o} = \frac{\left[\sum_{i=0}^{L} g_{i_o}(n)h(i)\right]^2}{N_o \sum_{i=0}^{L} g^2_{i_o}(n)} \tag{5-36}$$

where the $\{g_{i_o}(n)\}_{i=0}^{L}$ are the ideal, optimum, non-recursive gain values for the decision feedback equalizer obtained by solving equation (5-28) and the $\{h(i)\}_{i=0}^{L}$ are samples of the channel impulse response. As in the case of ρ_o in equation (5-34), the input noise variance (energy or power measure) has been multiplied by the factor $\sum_{i=0}^{L} g^2_{i_o}(n)$. Also, in the decision feedback equalizer, $\rho^*_{n_o}$ depends only on the non-recursive gains $\{g_{i_o}(n)\}$ and not on the recursive gains $\{f_{j_o}(n)\}$. Now the signal to noise ratio at the equalizer input is given by equation (5-11) as

$$\rho_n = \frac{h^2(0)}{N_o}$$

and comparing this to $\rho^*_{n_o}$, we see that when

$$\frac{\left[\sum_{i=0}^{L} g_{i_o}(n)h(i)\right]^2}{\sum_{i=0}^{L} g^2_{i_o}(n)} < h^2(0) \qquad (5\text{-}37)$$

the decision feedback equalizer will enhance the additive noise. The reverse is of course also true.

Using a computer program, we next solved equation (5-28) to obtain the ideal optimum gain values $\{g_{i_o}(n)\}$ for each of the channels in figures 5.18 to 5.21 over a range of values of the input signal to noise ratio ρ_n. In all cases we found that these calculated values were close to the average values* of the non-recursive gains after convergence in both the adaptive estimate and decision feedback equalizers. Therefore, the ideal signal to noise ratio $\rho^*_{n_o}$ will be, for the decision feedback equalizer, a reasonably good approximation to the actual value, neglecting of course the effect of decision errors appearing in the recursive section of the equalizer. For the estimate feedback equalizer, $\rho^*_{n_o}$ will only be indicative in a qualitative way of the effect of the equalizer on the additive noise because the previous estimates used in the recursive section will contain a noise component which contributes to the noise enhancement caused by the equalizer.

---

*Because we are considering adaptive systems, the actual gain values will, after convergence, always exhibit small fluctuations about their optimum values.

The ideal output signal to noise ratio $\rho^*_{n_o}$ and the difference $(\rho^*_{n_o} - \rho_n)$ between it and the input signal to noise ratio ρ_n were then calculated. They are tabulated in Table 5.2 for each of the channels of figures 5.18 to 5.21.

For the decision feedback equalizer, the difference $(\rho^*_{n_o} - \rho_n)$ provides a direct measure of the amount of noise enhancement or suppression. For the channels of figures 5.18, 5.19 and 5.21, it indicates that the additive noise is suppressed by a small amount, but for the channel of figure 5.20 it indicates that the decision feedback equalizer enhances the noise by between 2 and 4 db. From the measured error-rate curves of figures 5.18 to 5.21, we see that for the output error-rate of the decision feedback equalizer to have a given value, the signal to noise ratio ρ_n must be between 2 and 4 db greater for the channel of figure 5.20 than for any of the other three channels which we tested. It, therefore, appears to be mainly the enhancement of the additive noise which causes the much worse performance of the decision feedback equalizer when it is equalizing the channel of figure 5.20.

This same effect is also largely responsible for the error-rate performance of the estimate feedback equalizer being worse when it is equalizing the channel of figure 5.20. However, at values of ρ_n greater than about 6db, its performance is slightly worse than that of the decision feedback equalizer. This is caused by the fact that in the estimate feedback case estimates which are inherently noisy rather than noiseless decisions are used in the recursive section to compensate for intersymbol interference due to previous symbols. The noise component of these

Table 5.2: Illustration of noise enhancement and suppression.

Channel (Numbers refer to figures)	Input SNR ρ_n (db)	Output SNR ρ_{n_o} (db)	Noise enhancement $(\rho_{n_o} - \rho_n)$db
Fig. 5.18	6.53	7.29	0.76
(causes amplitude	10.05	10.56	0.50
and phase	15.33	15.79	0.46
distortion)	18.85	19.30	0.45
Fig. 5.19	6.53	7.79	1.26
(causes amplitude	10.05	10.75	0.70
and phase	15.33	16.04	0.71
distortion)	18.85	19.47	0.62
Fig. 5.20	6.53	4.59	-1.94
(causes only	10.05	7.41	-2.64
amplitude	15.33	12.41	-3.19
distortion)	18.85	15.45	-3.40
Fig. 5.21	6.53	7.34	0.81
(causes amplitude	10.05	10.74	0.69
and phase	15.33	15.95	0.62
distortion)	18.85	19.46	0.61

estimates contributes to the equalizer output noise and this increases the noise enhancement caused by the estimate feedback equalizer. The result is that, for the channel of 5.20 for which the non-recursive section of the equalizer causes noise enhancement, the resulting error-rate performance is slightly worse (approximately 1db) than in the decision feedback case.

At error-rates greater than about 10^{-1}, the error propagation effect in the decision feedback equalizer becomes much more severe. In fact for the channel of figure 5.20, its effect becomes worse than the abovementioned extra noise enhancement occurring in the estimate feedback equalizer. This causes the estimate feedback equalizer to have somewhat better performance for this channel when the error-rate is greater than about 10^{-1}, and accounts for the cross-over of the measured error-rate curves in figure 5.20. In chapter 3, we showed that both the estimate and the decision feedback equalizers are sub-optimum in that they are both approximations to the Conditional Bayes estimator. We also showed that the decision feedback equalizer is a high signal to noise ratio approximation to the estimate feedback equalizer. We, therefore expect that, at least at low values of ρ_n, the estimate feedback equalizer will always yield better performance, and this has indeed been observed.

This same cross-over of the error-rate curves has been observed by George et al. (1969, 1971) in comparing the decision feedback equalizer to a linear (transversal filter) equalizer, and a similar explanation to that given above holds in this case.

From Table 5.2, it can be seen that noise enhancement* occurs only for the channel of figure 5.20, but for the other three channels which we tested the additive noise appears to have been suppressed by a small amount, and as the measured error-rate curves indicate the decision feedback equalizer yields better performance on these three channels. More importantly, we have found that for any channel for which the additive noise appears to be suppressed, the estimate feedback equalizer yields better performance than the decision feedback equalizer at all values of the signal to noise ratio ρ_n.

To see why this is so, let us begin by considering the sampled channel impulse response $\{h(k);\ k=-L,\ldots,0,\ldots,L\}$ where, as in all of our simulation work, the sampling or symbol period has been normalized to unity. We may readily write it as a sampled function of delay τ in the form

$$h(\tau) = \sum_{k=-L}^{L} h(k)\delta(\tau-k) \tag{5-38}$$

where $\delta(\tau)$ is the Dirac delta function. Then taking the Fourier transform of $h(\tau)$ with respect to τ, we obtain, at least in a formal sense, the sampled channel transfer function

$$H(\omega) = \sum_{k=-L}^{L} h(k)e^{-j\omega k} \tag{5-39}$$

This function is periodic in ω with period 2π, but we shall be interested only in the primary interval

---

*As calculated by comparing the ideal output signal to noise ratio $\rho^*_{n_o}$ of equation (5-36) to the input signal to noise ratio ρ_n.

$$-\pi < \omega < \pi$$

which is the normalized Nyquist bandwidth.

Now we may readily rewrite $H(\omega)$ in the form

$$H(\omega) = h(0) + \sum_{k=1}^{L} (h(k)+h(-k))\cos\omega k - j \sum_{k=1}^{L} (h(k)-h(-k))\sin\omega k$$

$$= h(0) + K(\omega) \qquad (5\text{-}40)$$

In this equation $h(0)$ represents the distortion-free component of the channel response and

$$K(\omega) = \sum_{k=1}^{L} (h(k)+h(-k))\cos\omega k - j \sum_{k=1}^{L} (h(k)-h(-k))\sin\omega k \qquad (5\text{-}41)$$

represents the dispersive component which distorts the signal and causes intersymbol interference. From equation (5-40), we may distinguish the following limiting cases:

(i) $h(k) = 0 \qquad (k \neq 0)$ (5-42)

The transfer function then becomes

$$H(\omega) = h(0) \qquad (5\text{-}43)$$

implying that the channel is non-dispersive. There is no intersymbol interference and no equalization required.

(ii) $h(k) = -h(-k) \qquad (k \neq 0)$ (5-44)

and the channel transfer function becomes

$$H(\omega) = h(0) + K(\omega) = h(0) - 2j \sum_{k=1}^{L} h(k)\sin\omega k$$

In this case the distortion term $K(\omega)$ is purely imaginery. It can then be shown using paired echo theory (Lucky, 1968) that this corresponds to a channel which causes only phase or delay distortion of the transmitted signal. This distortion causes intersymbol interference and equalization is required.

(iii) $h(k) = h(-k) \qquad (k \neq 0)$ (5-45)

and the channel transfer function becomes

$$H(\omega) = h(0) + K(\omega) = h(0) + 2 \sum_{k=1}^{L} h(k)\cos\omega k$$

Here the distortion term $K(\omega)$ is purely real and (again using paired echo theory) we can show that such a channel causes only amplitude distortion. This of course causes intersymbol interference and equalization is again required.

Obviously, the ideal channel transfer function is that given by equation (5-43) where there is no distortion. However, in almost all realistic situations, a communications channel causes both amplitude and phase distortion of the transmitted signal, and some form of equalization is required.

Now let us consider the action of the decision feedback equalizer as a function of the channel response. A number of previous investigators (Austin, 1967; George et al., 1969, 1971 and Monsen, 1971) have indicated that a decision feedback equalizer always yields superior performance to a linear (transversal filter) equalizer for all values of the output error-rate less than about 10^{-1}, where error propagation does not seriously degrade the performance of the decision feedback equalizer. However,

all of their investigations have been confined to the case in which a filter matched to the channel impulse response precedes the equalizer. This matched filter completely equalizes or compensates for any phase distortion caused by the channel, and the equalizer thus sees an effective channel which causes only amplitude distortion (see equation (5-45)).

Now the decision feedback equalizer uses noiseless decisions in the recursive section to coherently cancel or subtract out intersymbol interference due to previous symbols. Thus if the sampled channel impulse response at its input is given by equation (5-38) with corresponding transfer function given by equation (5-40), this cancellation process leaves an effective, sampled channel impulse response

$$h'(\tau) = \sum_{k=-L}^{0} h(k)\delta(\tau-k) \tag{5-46}$$

with corresponding transfer function

$$H'(\omega) = h(0) + \sum_{k=1}^{L} h(-k)\cos\omega k - j\sum_{k=1}^{L} h(-k)\sin\omega k \tag{5-47}$$

which must be equalized by the linear, non-recursive section of the equalizer. The linear section does this by adapting to become essentially the inverse of $h'(\tau)$. On the other hand, the linear (transversal filter) equalizer must adapt to become the inverse of the original input impulse response $h(\tau)$ of equation (5-38).

By adapting to become the inverse, we mean that both the linear portion of the decision feedback equalizer and the linear equalizer attempt to adjust themselves so that the overall transfer function of the

equalizer and channel in cascade has the ideal all-pass form of equation (5-38) over the Nyquist bandwidth. This means that those frequencies in the received signal which are weak must be amplified and those which are strong must be attenuated. Now for any linear filter, we have the well known result that

$$S_y(\omega) = S_x(\omega)\,|G(\omega)|^2 \tag{5-48}$$

where $S_y(\omega)$ is the filter output power spectral density, $S_x(\omega)$ is the input power spectral density and $G(\omega)$ is the filter transfer function. It is clear from this that only the filter's amplitude characteristic $|G(\omega)|$ and not its phase characteristic $\arg(G(\omega))$ will affect the (noise) power appearing at its output. This implies that an equalizer will cause noise enhancement only when it must compensate for amplitude distortion caused by the channel, that is only when it must adjust the overall amplitude characteristic of channel and equalizer in order to approach the ideal form of equation (5-43).

Now when the channel impulse response $h(\tau)$ of equation (5-38) is symmetric about $h(0)$, so that it causes only amplitude distortion, the coherent cancellation process in the decision feedback equalizer removes one half the amplitude distortion in $h(\tau)$ to produce the effective impulse response $h'(\tau)$ of equation (5-46). This is done at the expense of causing $h'(\tau)$ to contain phase distortion which will, of course, have no effect on the noise power appearing at the equalizer output. Thus when $h(\tau)$ is symmetric, a linear equalizer must equalize twice as much amplitude distortion as the linear non-recursive portion of the decision feedback equalizer. That is the linear equalizer must provide more

amplification (and usually over a wider band of frequencies) of the frequency components in its input signal in order to make the overall characteristic approach the ideal form of equation (5-43). An example of this is given by the channel of figure 5.20 whose transfer function is plotted over the normalized Nyquist band in figure 5.22. The linear equalizer will, therefore, cause more noise enhancement with the result that on this type of channel, its performance will be inferior to that of the decision feedback equalizer.

In some recent work, Keeler (1971) has found that when the channel response $h(\tau)$ contains significant phase as well as amplitude distortion*, a linear (transversal filter) equalizer yields better performance by between $\frac{1}{2}$ and 1 db than the decision feedback equalizer. In the present work, we have found that for such channels the decision feedback equalizer tends to suppress the noise and to yield better performance than when the channel response $h(\tau)$ is symmetric about $h(0)$. This is readily seen from Table 5.2 and figures 5.18 to 5.21. We have partially corroborated Keeler's finding. In figure 5.21, we have shown an error-rate curve obtained for this channel by Proakis (1969) using a 31 tap linear equalizer. Comparing this curve to our measured curve for the decision feedback equalizer, we see that the linear equalizer is between $\frac{1}{2}$ and 1 db better. We would expect a similar result for the channels of figures 5.18 and 5.19.

---

*This is the usual type of channel which must be equalized, because in most cases of interest, it is impractical and uneconomic to match a filter to the channel response in order to obtain phase equalization. This occurs because the channel response is usually unknown and time-varying.

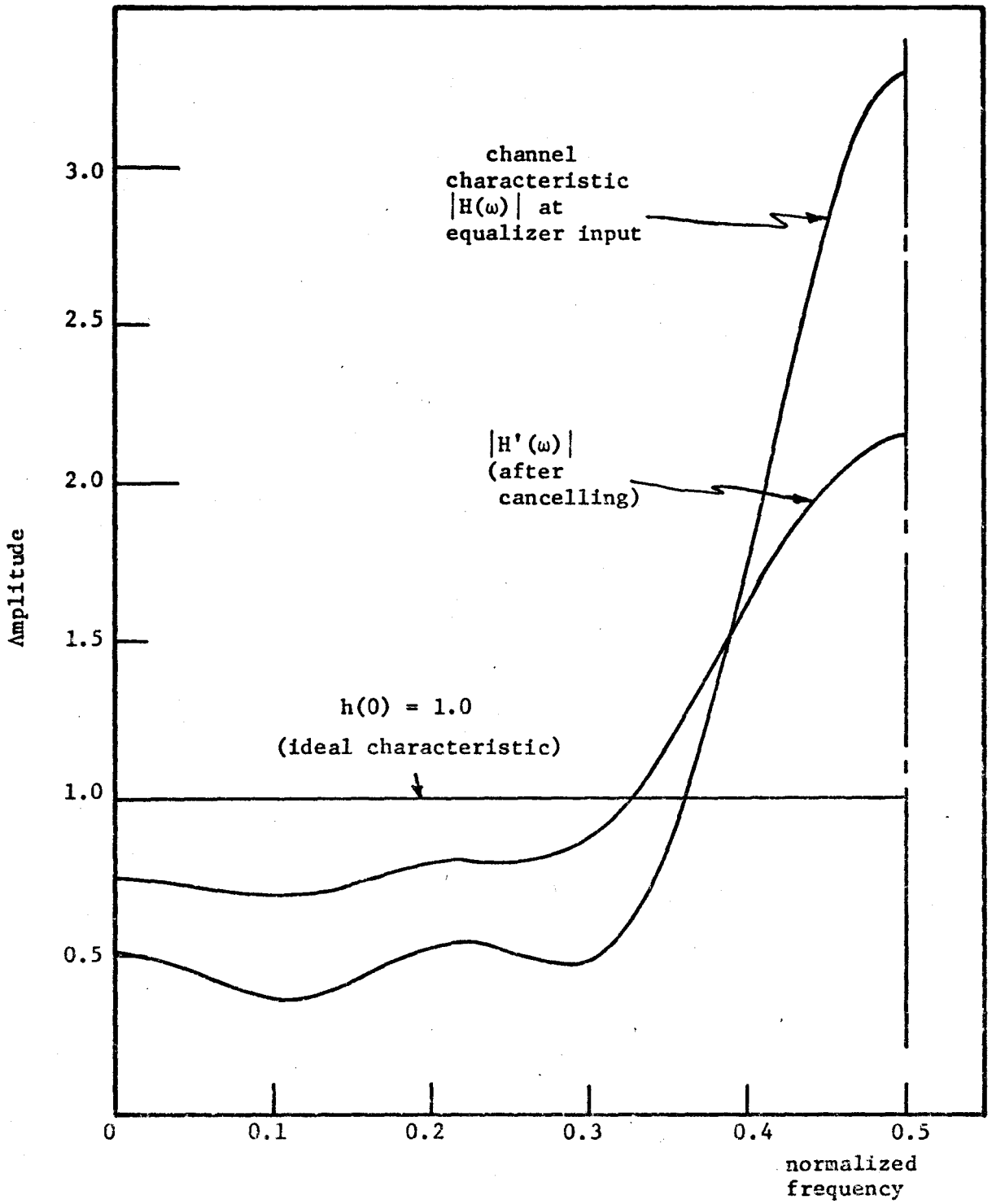

Figure 5.22 Amplitude characteristic for channel of figure 5.20 before ($|H(\omega)|$) and after ($|H'(\omega)|$) decision feedback action has taken place. Curves are plotted over the normalized Nyquist bandwidth.

This difference in performance arises because the coherent concellation process by which the decision feedback equalizer reduces the received channel impulse response $h(\tau)$ of equation (5-38) to the effective impulse response of equation (5-46) cancels the intersymbol interference due to previous symbols, but at the same time it induces additional amplitude and phase distortion into $h'(\tau)$. This additional distortion must be correlated by the linear non-recursive section of the decision feedback equalizer.

The additional amplitude distortion in $h'(\tau)$ causes the noise enhancement to be greater (or equivalently the noise suppression to be less) for the decision feedback equalizer than for the linear equalizer. Thus on this type of channel the linear equalizer yields better performance than the decision feedback equalizer. Examples of this effect are provided by the channels of figures 5.18, 5.19 and 5.21. In figures 5.23 to 5.25, we have plotted the amplitude and phase characteristics $|H(\omega)|$ and $\arg(H(\omega))$ over the normalized Nyquist bandwidth for each of these channels. We have also shown in each case the effective amplitude characteristic $|H'(\omega)|$ which results after the coherent cancellation process of decision feedback takes place. In each case, the fraction of the Nyquist bandwidth

$$-\pi < \omega < \pi \qquad \text{or} \qquad -\frac{1}{2} < f < \frac{1}{2}$$

over which an equalizer must amplify rather than attenuate the frequency components of the input signal in order to approach the ideal characteristic is greater after the coherent cancellation process of the decision feedback equalizer has taken place. Also the gain required in each case is

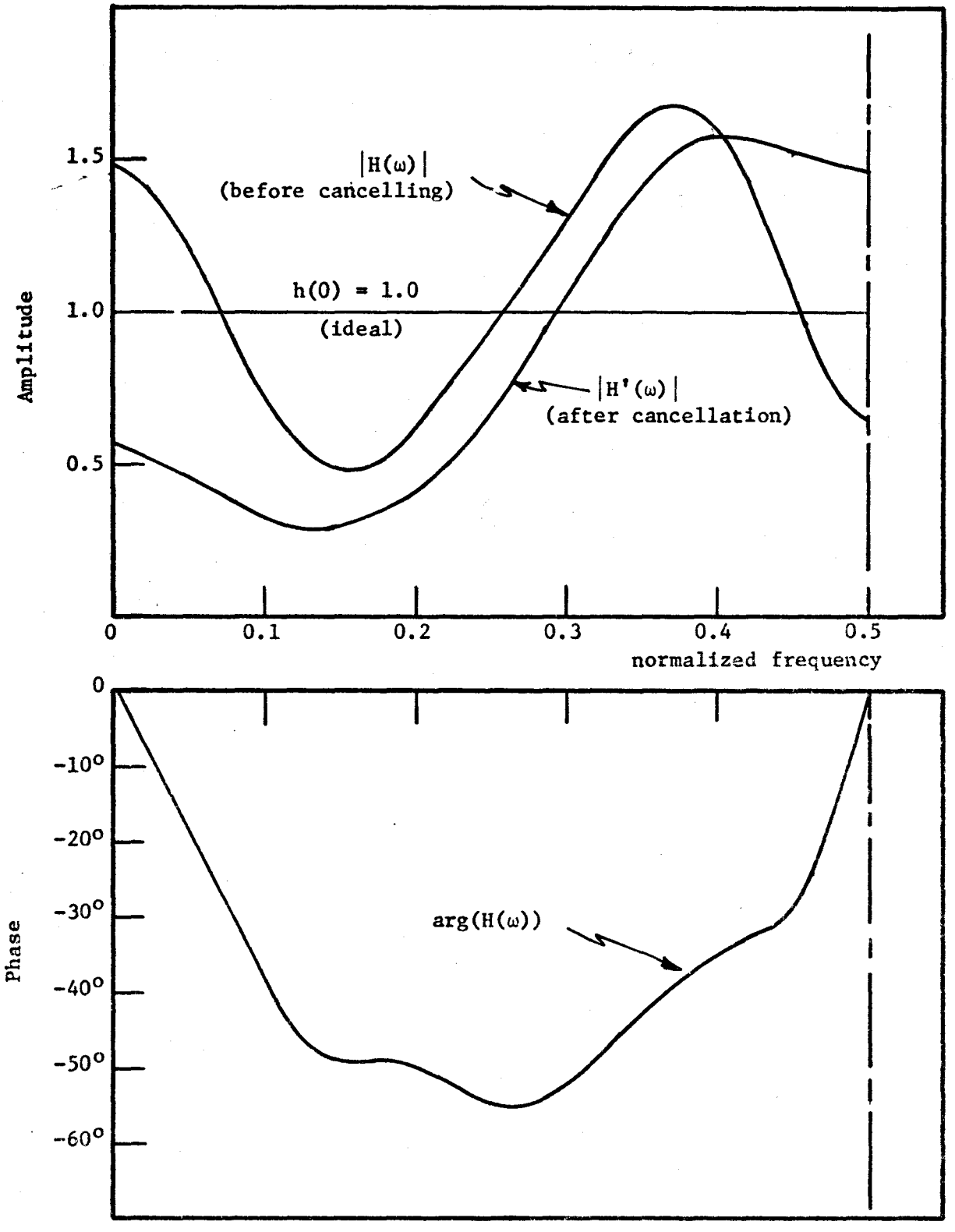

Figure 5.23 Transfer characteristics of channel of figure 5.18 showing effect of coherent calcellation on the amplitude characteristic. The curves are plotted over the normalized Nyquist bandwidth.

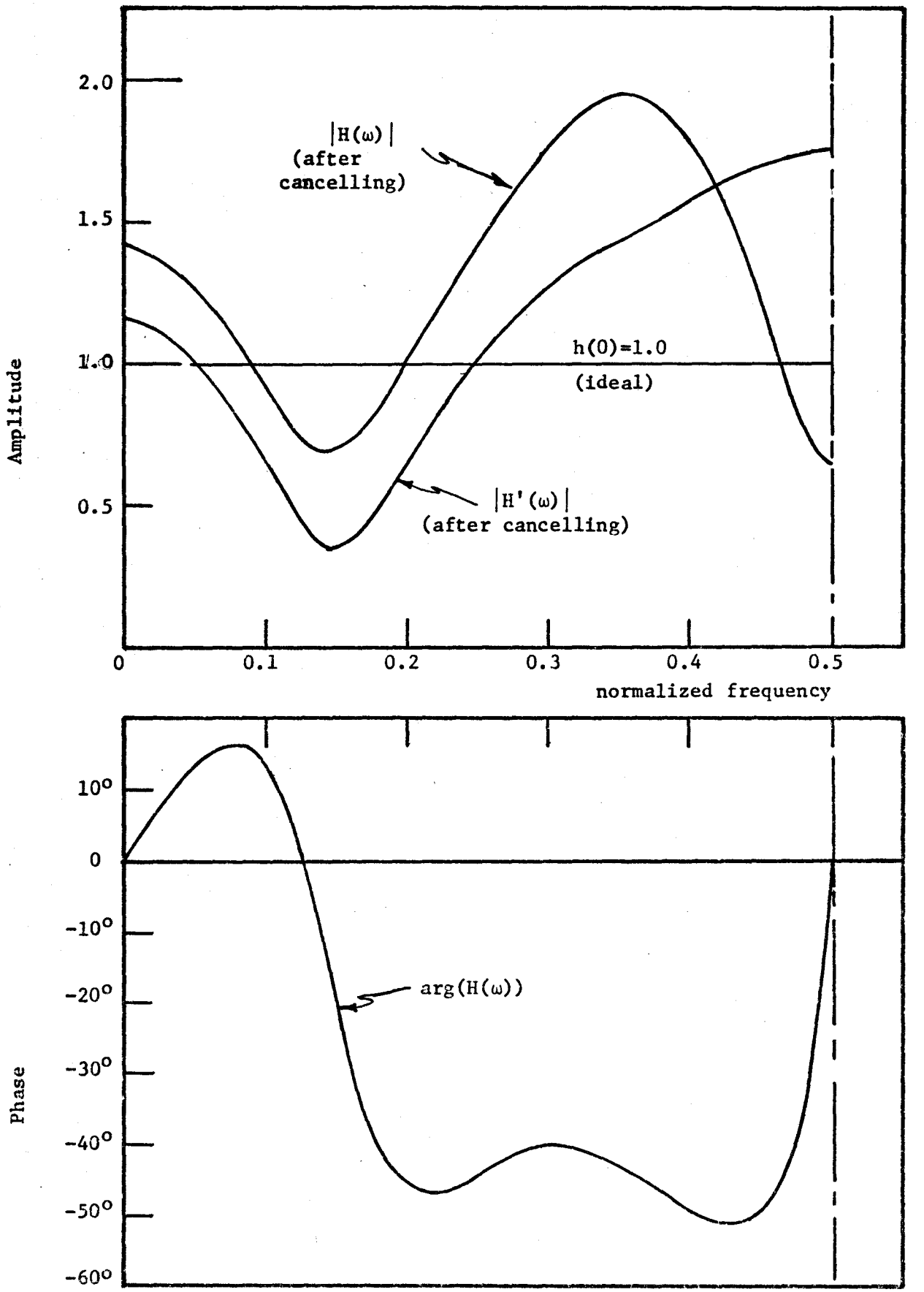

Figure 5.24 Transfer characteristics of channel of figure 5.19 showing effect of coherent cancellation on the amplitude characteristic. The curves are plotted over the normalized Nyquist bandwidth.

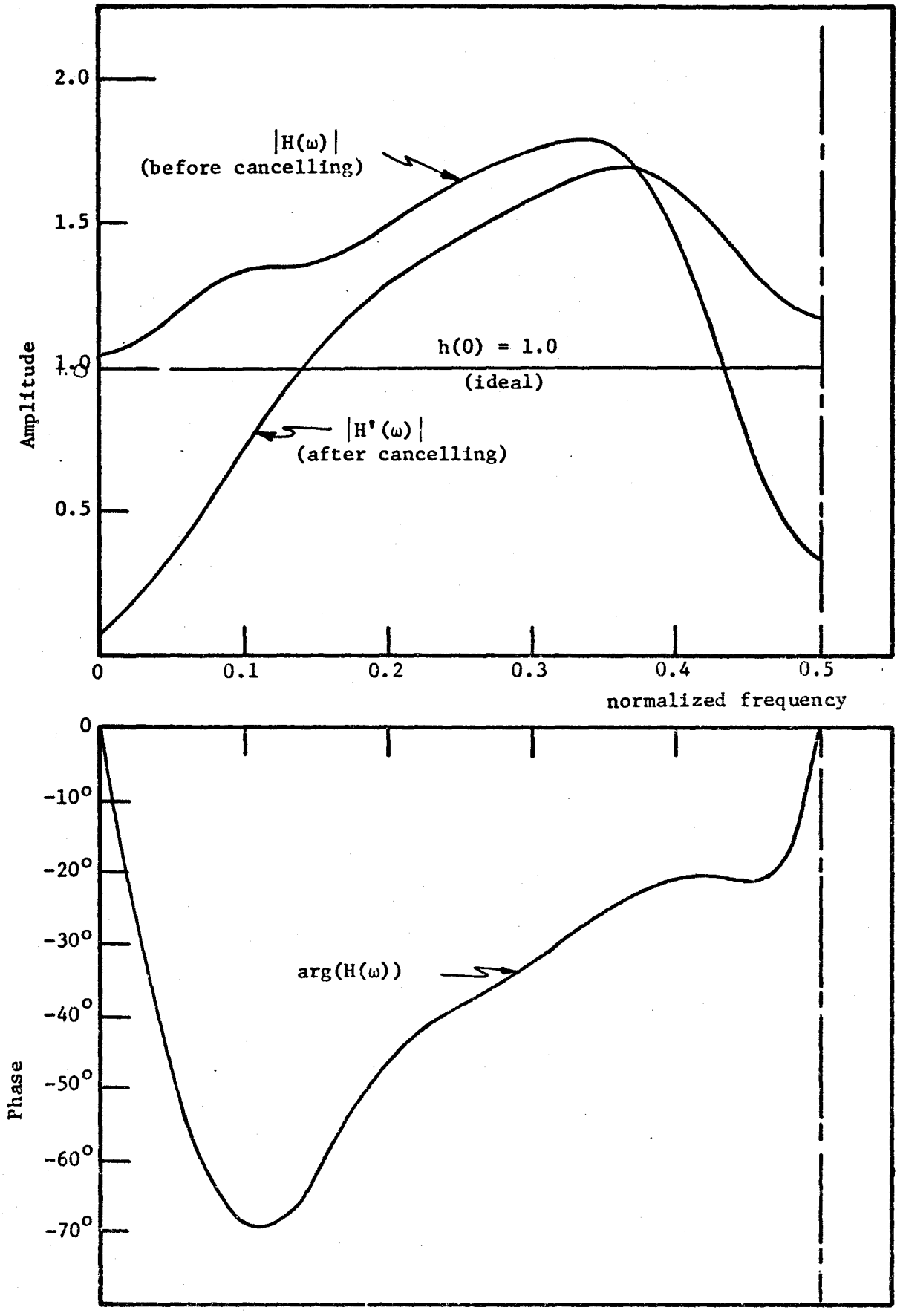

Figure 5.25 Transfer characteristics for channel of figure 5.21 showing effect of coherent cancellation on the amplitude characteristic. The curves are plotted over the normalized Nyquist bandwidth.

greater for the decision feedback equalizer. This means that the decision feedback equalizer will not on these channels suppress the noise as much (or equivalently, will enhance it more) than the linear (transversal filter) equalizer. We can, therefore, expect the performance of the linear equalizer to be better than that of the decision feedback equalizer on channels containing significant phase as well as amplitude distortion (as indicated by Keeler, 1971).

Turning now to the estimate feedback equalizer which is the main concern of this thesis, we showed in chapter 3 that its mean-square estimation error is always smaller than that of the linear equalizer. We, therefore, expect that its error-rate performance will always be better than that of the linear equalizer. On channels containing significant phase as well as amplitude distortion this also implies that the estimate feedback equalizer should yield better performance than the decision feedback equalizer. This is indeed the performance which we have obtained. For the channel of figure 5.21, where we have available the curve (Proakis, 1969) for the 31 tap linear equalizer, we find that the estimate feedback equalizer yields performance about $\frac{1}{2}$ db better than the linear equalizer and between 1 and 2 db better than the decision feedback equalizer. For the two channels of figures 5.18 and 5.19 we found the error-rate performance of the estimate feedback equalizer to be between 1 and 2 db better than that of the decision feedback equalizer.

5.4 The Saturating Limiter Equalizer

In chapter 3, we indicated that in some situations, it might be useful to be able to replace the tanh(·) nonlinearity of the estimate feedback equalizer with a simpler and more easily implementable nonlinearity. We then suggested, for the case of binary symbols, a saturating limiter defined by the relationship

$$\tilde{s}_n = \begin{cases} -1 & \hat{s}_n \leq -\alpha_s \\ \hat{s}_n & -\alpha_s < \hat{s}_n < \alpha_s \\ +1 & \hat{s}_n \geq \alpha_s \end{cases} \qquad (0 \leq \alpha_s \leq 1)$$

where $\hat{s}_n$ is the limiter input, $\tilde{s}_n$ is its output and α_s is a threshold or saturation value which must be suitably defined. It is of interest to note that for $\alpha_s = 0$

$$\tilde{s}_n = \text{sgn}(\hat{s}_n)$$

and the decision feedback equalizer results.

In this section, we shall describe the results of simulating the saturating limiter equalizer and will compare our results to those of the preceding section.

5.4a Convergence Properties

Our first tests of the saturating limiter equalizer were made in order to determine an optimum or near optimum value for the limiter saturation value α_s. To do this, we ran convergence and probability of error tests for several different values of α_s between 0 and 1 and for several different channels. In all the cases which we tried, we found

that the best results were obtained for α_s=1 which is the transmitted symbol magnitude. We, therefore, tried some further tests using the anti-podal symbol values $\pm\beta$ ($\beta \neq 1$), and in this case found that the best value for α_s appeared to be $\alpha_s = \beta$. Therefore, in all further tests of the saturating limiter equalizer, we used the transmitted symbol values ± 1 and the limiter saturation value $\alpha_s = 1$ (Taylor, 1971).

Using the same group of 9 channels as in section 5.3a, we next carried out decision directed convergence tests of the adaptive saturating limiter equalizer using the adaptive algorithm discussed in chapter 4. The results of these tests are shown in figures 5.26 to 5.34, where we have plotted the rms output error e_{rms} as a function of the number of samples or symbols processed. Each of these curves represents, as previously, the average over five separate runs. In order to facilitate comparisons, we have also plotted in these figures the corresponding curves for the estimate and decision feedback equalizers.

From the curves of figures 5.26 to 5.34, we may make the following observations:

(i) For all the channels which we tested, the saturating limiter equalizer exhibited convergence toward some minimal value of the rms estimation error e_{rms}.

(ii) For any given channel, the convergence speeds and the values of the rms estimation error after 5000 samples had been processed are comparable for all three equalizer structures.

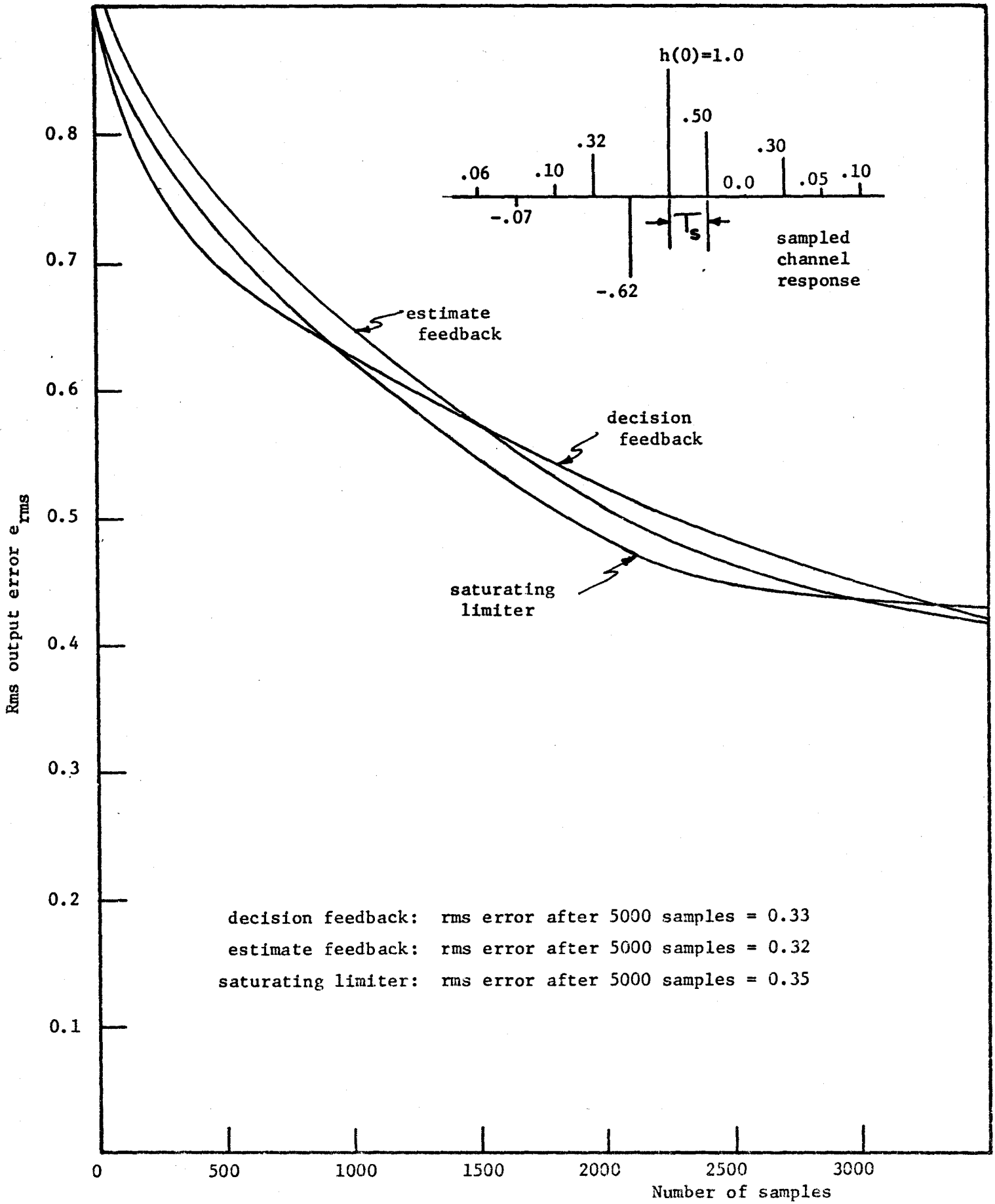

Figure 5.26 Decision directed convergence curves for channel response shown. Initial peak distortion D-2.12 and signal to interference ratio $\rho_{in} = 1.17$.

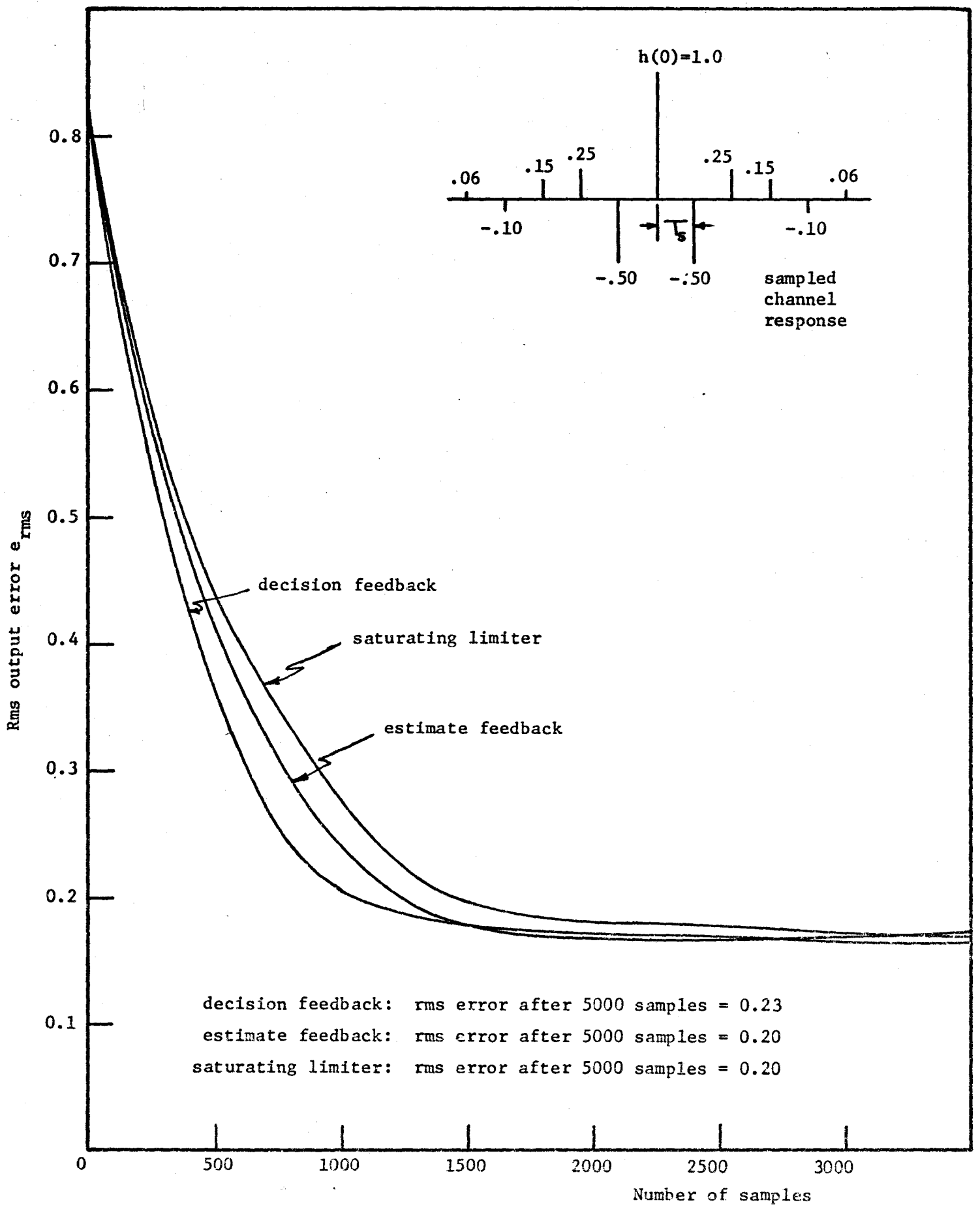

Figure 5.27 Decision directed convergence curves for channel response shown. D=2.12 and ρ_{in}=1.487.

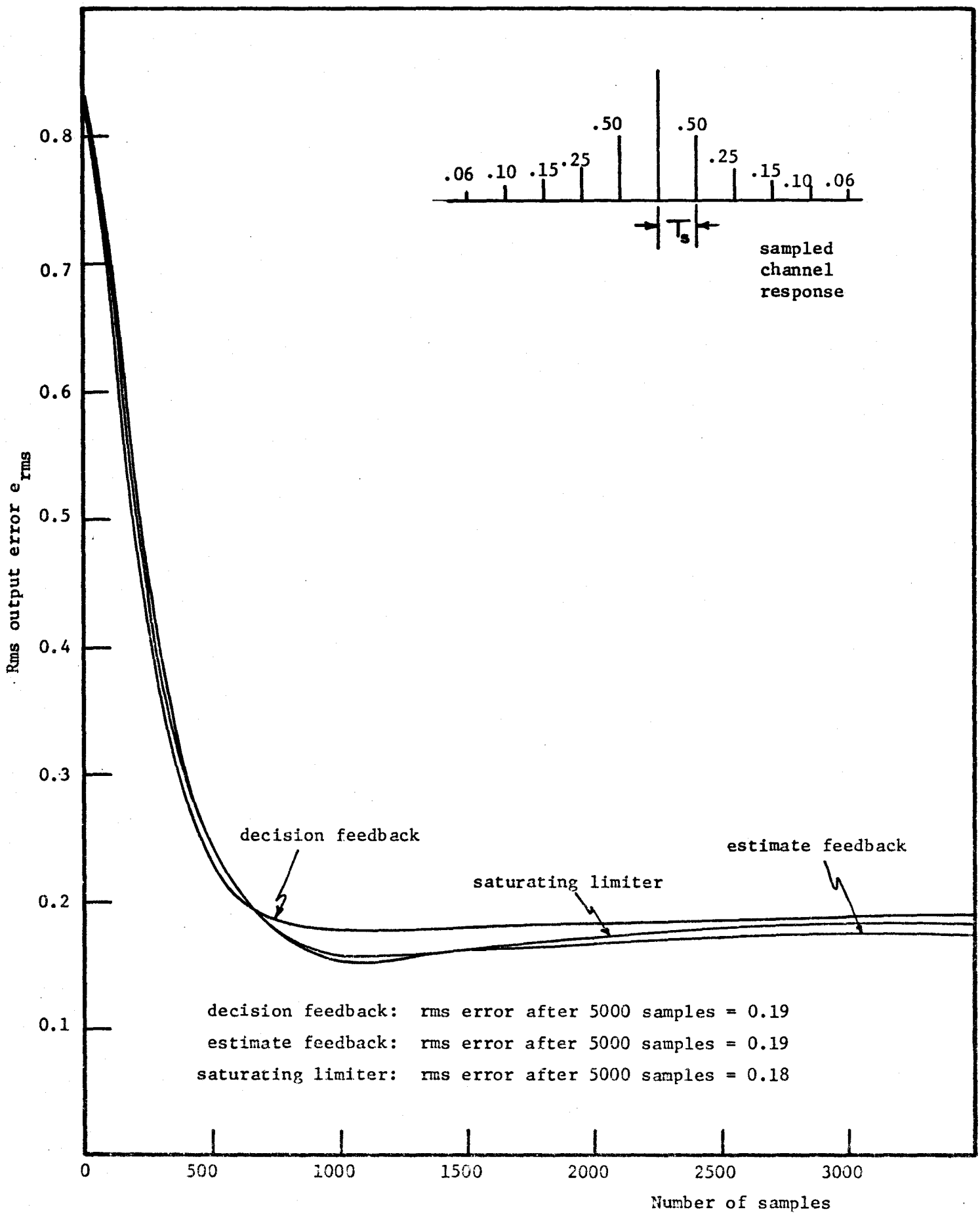

Figure 5.28 Decision directed convergence curves for channel shown.

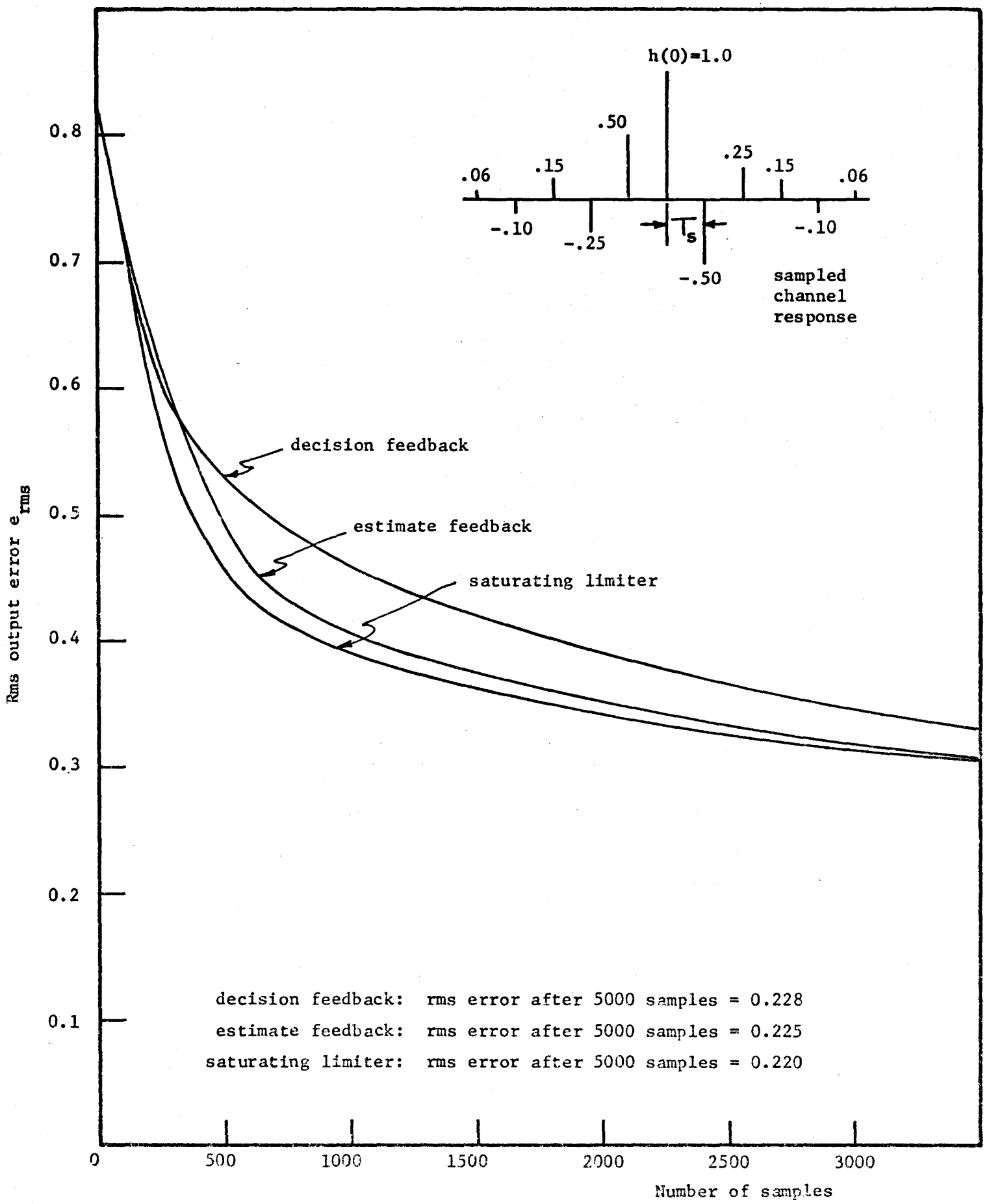

Figure 5.29 Decision directed Convergence curves for channel shown.

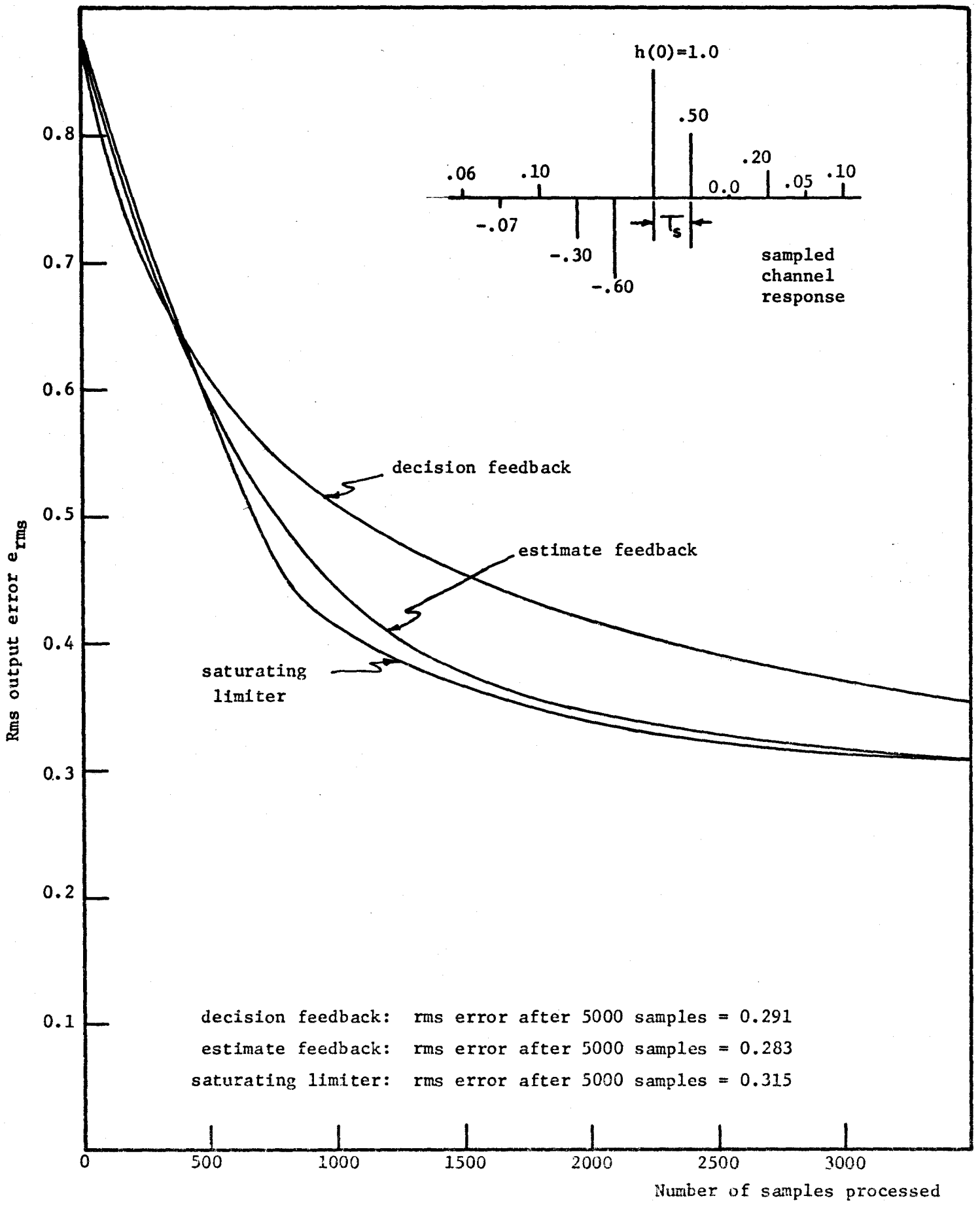

Figure 5.30 Decision directed convergence curves for channel response shown.

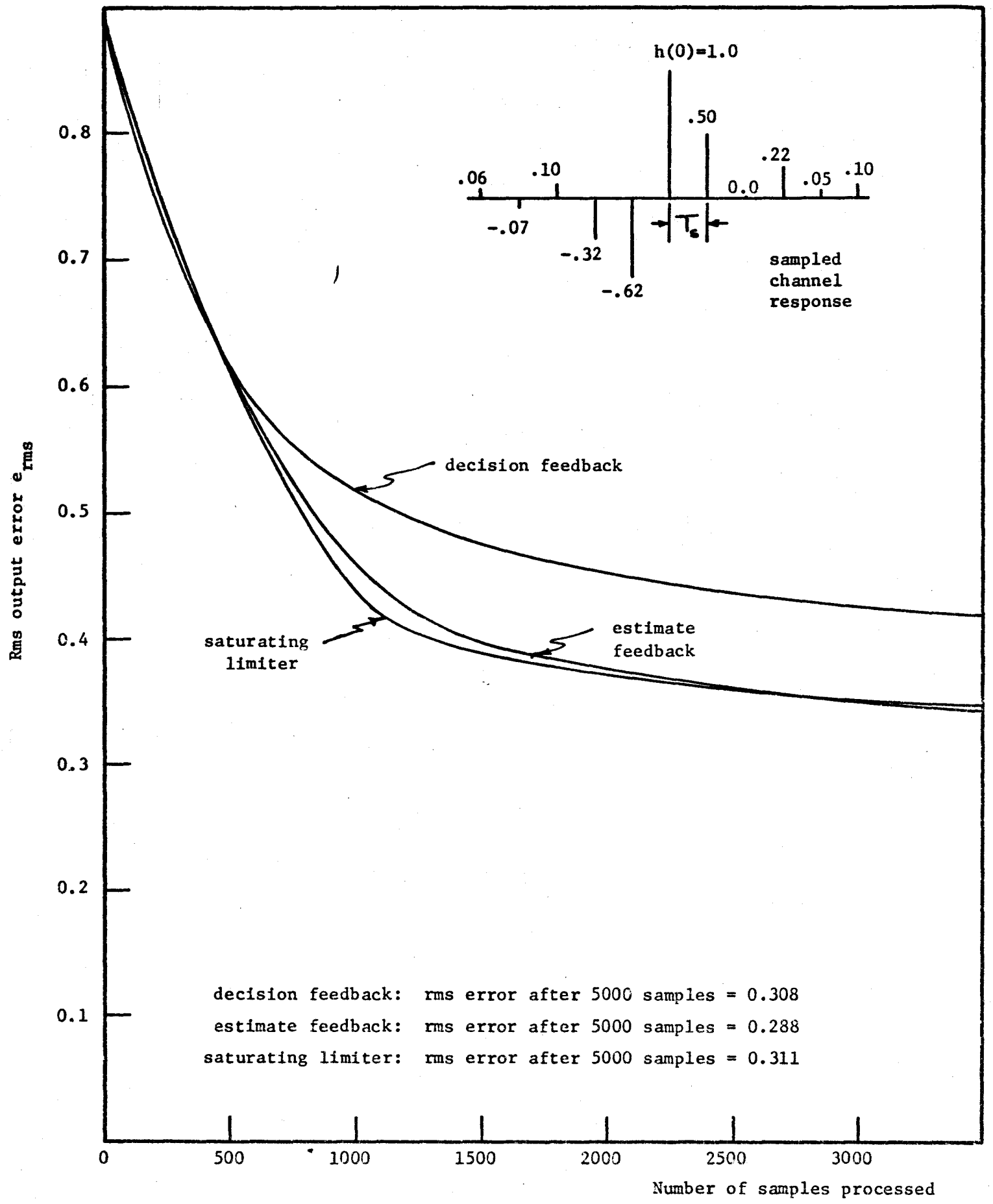

Figure 5.31 Decision directed convergence curves for channel response shown.

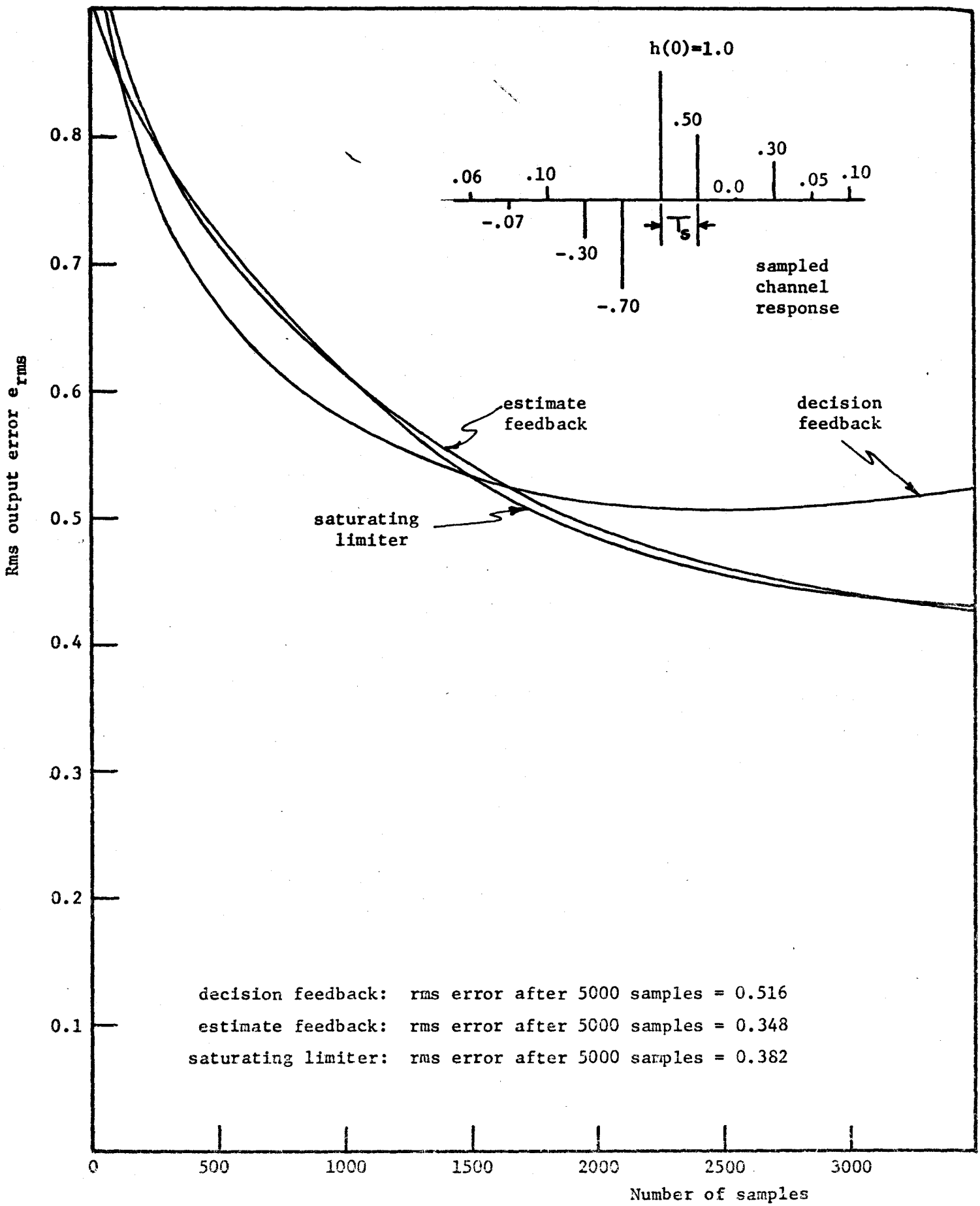

Figure 5.32 Decision directed convergence curves for channel response shown.

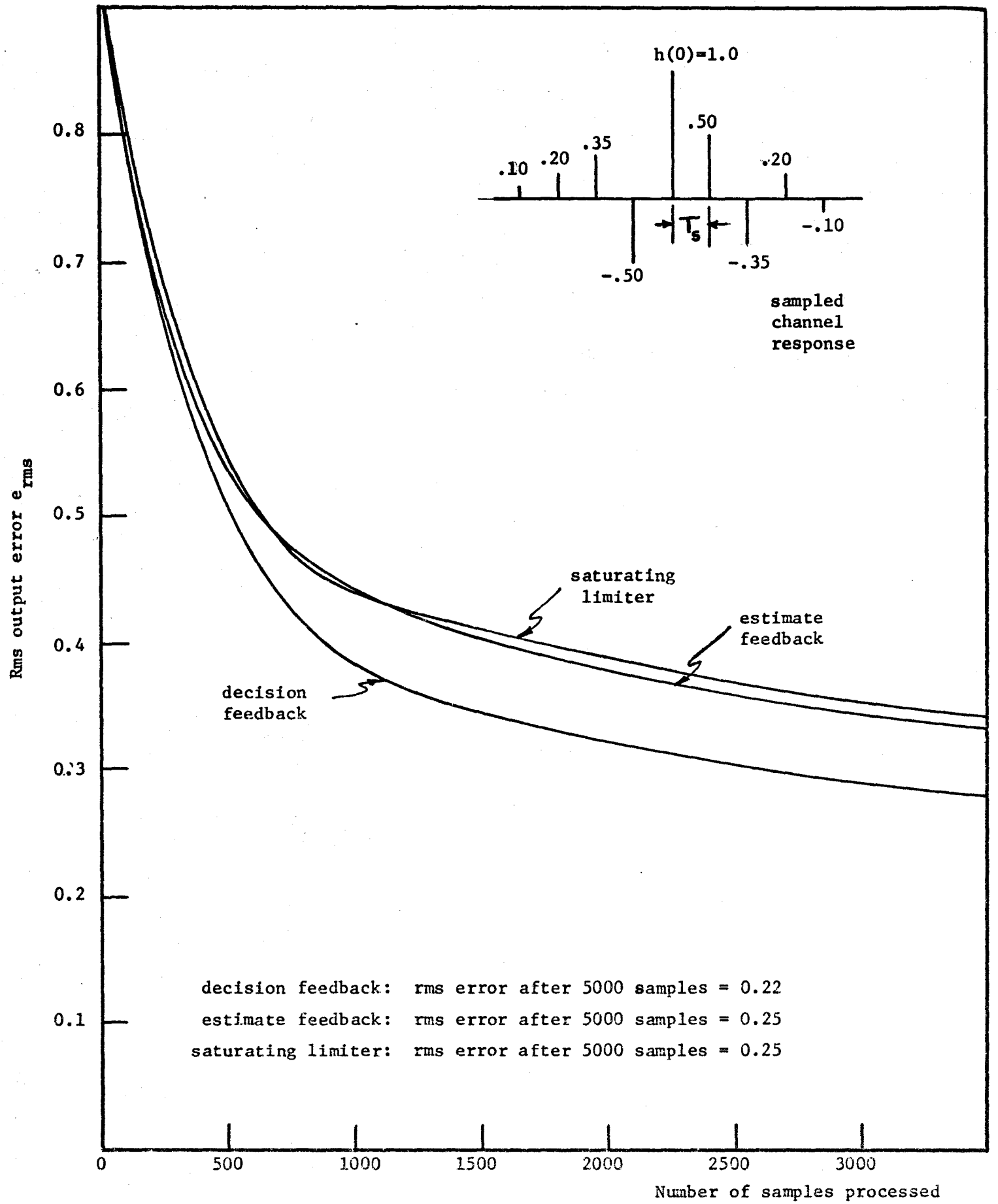

Figure 5.33 Decision directed convergence curves for channel response shown.

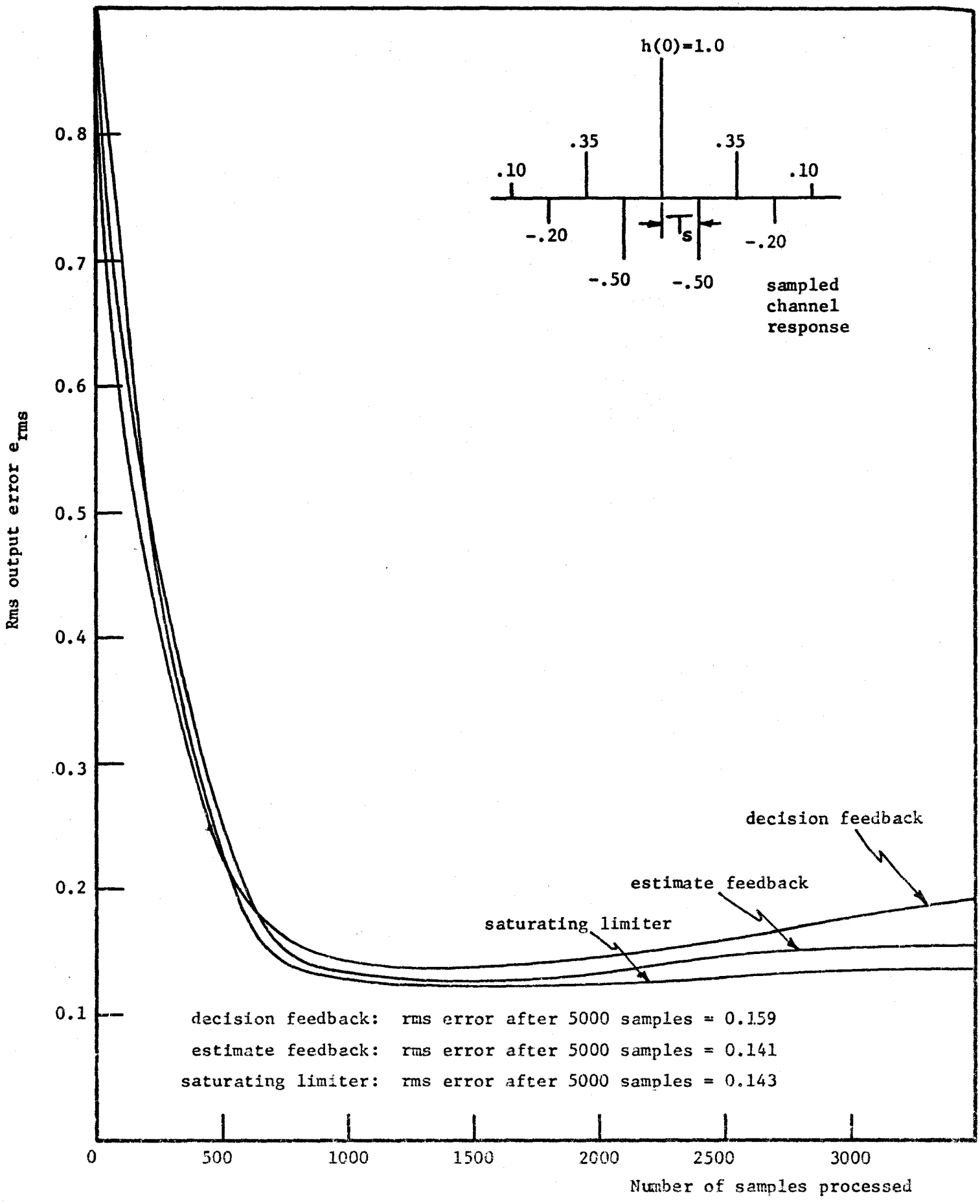

Figure 5.34 Decision directed convergence curves for channel shown.

(iii) All of the curves in figures 5.26 to 5.34 were obtained using the values $\alpha = -.004$, $\delta = -.025$ and $\gamma = -.005$ for the iteration constants. In general, we found that for the saturating limiter equalizer, the best convergence results were obtained with these constants lying in the same ranges as discussed in the preceding section for the estimate feedback equalizer.

(iv) From the curves, the convergence properties of the three adaptive equalizers can be seen to be comparable. For each channel, the three convergence curves lie quite close together, and the values of the rms output error after 5000 samples or symbols have been processed are quite close together.

We next conducted some tests to determine the effect of the interpolation constant δ. Typical results of these tests are shown in figures 5.35 and 5.36 for two values of δ. In each case we see that convergence is faster for a larger value of δ and that the rms error after 5000 symbols is smaller. This same behaviour was observed for both the estimate and the decision feedback equalizers, and it, therefore appears that the improved adaptive behaviour with larger values of the interpolation constant δ is characteristic of the adaptive algorithm developed in chapter 4.

We also conducted some tests to determine the effect of a training sequence on the convergence properties of the saturating limiter equalizer. For each channel which we tested, we found that we obtained results which were very close to those which we obtained using the estimate feedback equalizer.

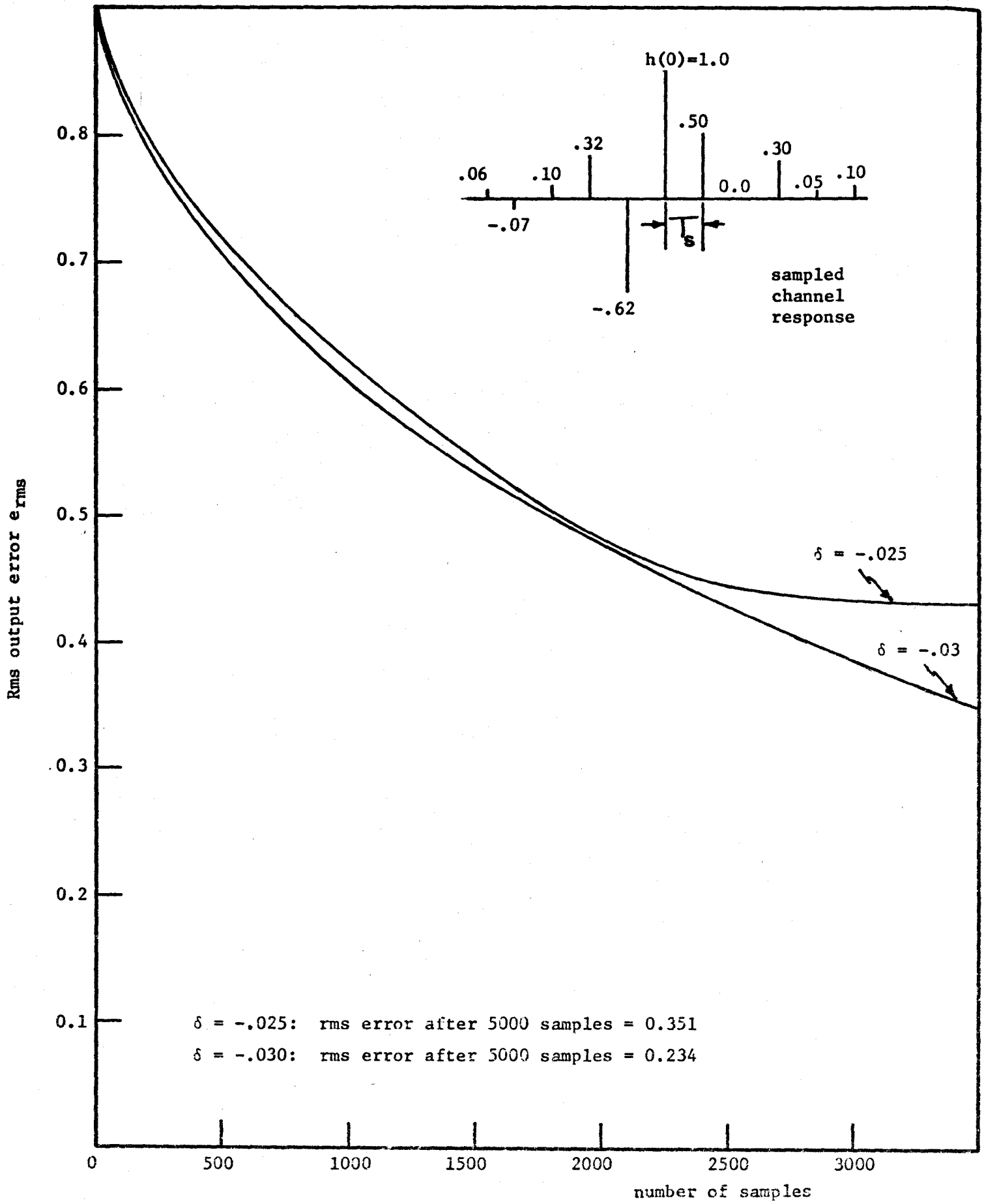

Figure 5.35 Decision directed convergence curves for channel response shown, illustrating the effect of the learning constant δ.

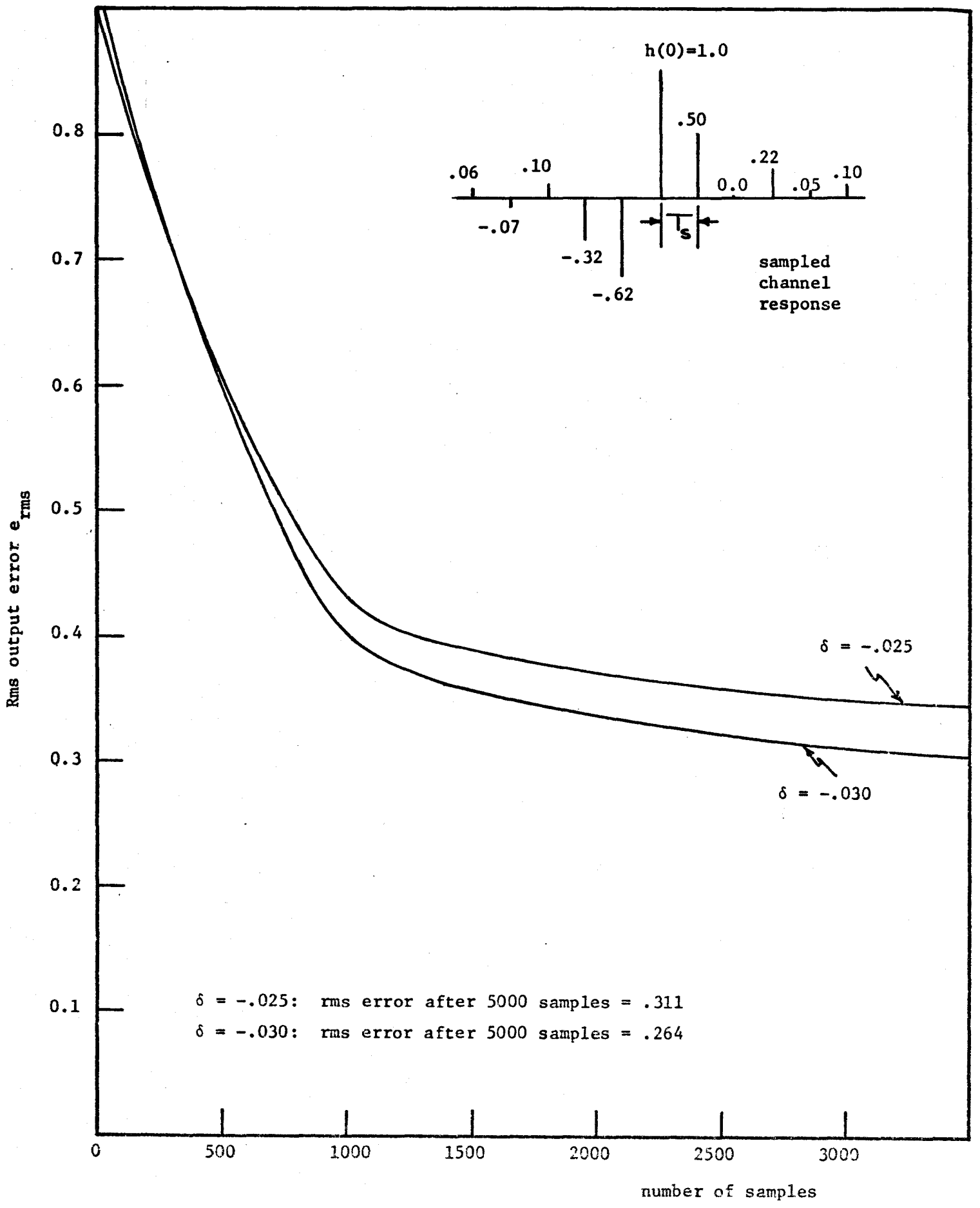

Figure 5.36 Decision directed convergence curves for channel response shown, illustrating effect of the learning constant δ.

In conclusion, it appears that the convergence properties of the adaptive saturating limiter equalizer are comparable to those obtained in the preceding section for the estimate and decision feedback equalizers.

5.4b Performance in the Presence of Noise

We next conducted a series of tests (by means of Monte Carlo simulation) to investigate the steady-state error-rate performance, as a function of the additive noise level. These tests were carried out using the same sampled channel impulse responses that we used for similar tests of the estimate and decision feedback equalizers. The resulting measured error-rate curves are plotted in figures 5.37 to 5.40 as a function of the signal to noise ratio ρ_n. We have also plotted in these figures, for purposes of comparison, the curves obtained in section 5.3b for the estimate and decision feedback equalizers.

From the curves of figures 5.37 to 5.40, we see that for every channel which we tested, the error-rate performance of the saturating limiter equalizer is only marginally worse than that of the estimate feedback equalizer. Therefore, it appears that in many situations the saturating limiter equalizer will serve as a very satisfactory and relatively simple approximation to the estimate feedback equalizer.

5.5 Summary

In this chapter, we have investigated, by means of Monte Carlo simulation, the performance characteristics of an adaptive, nonlinear estimate feedback equalizer which is controlled by the adaptive algorithm

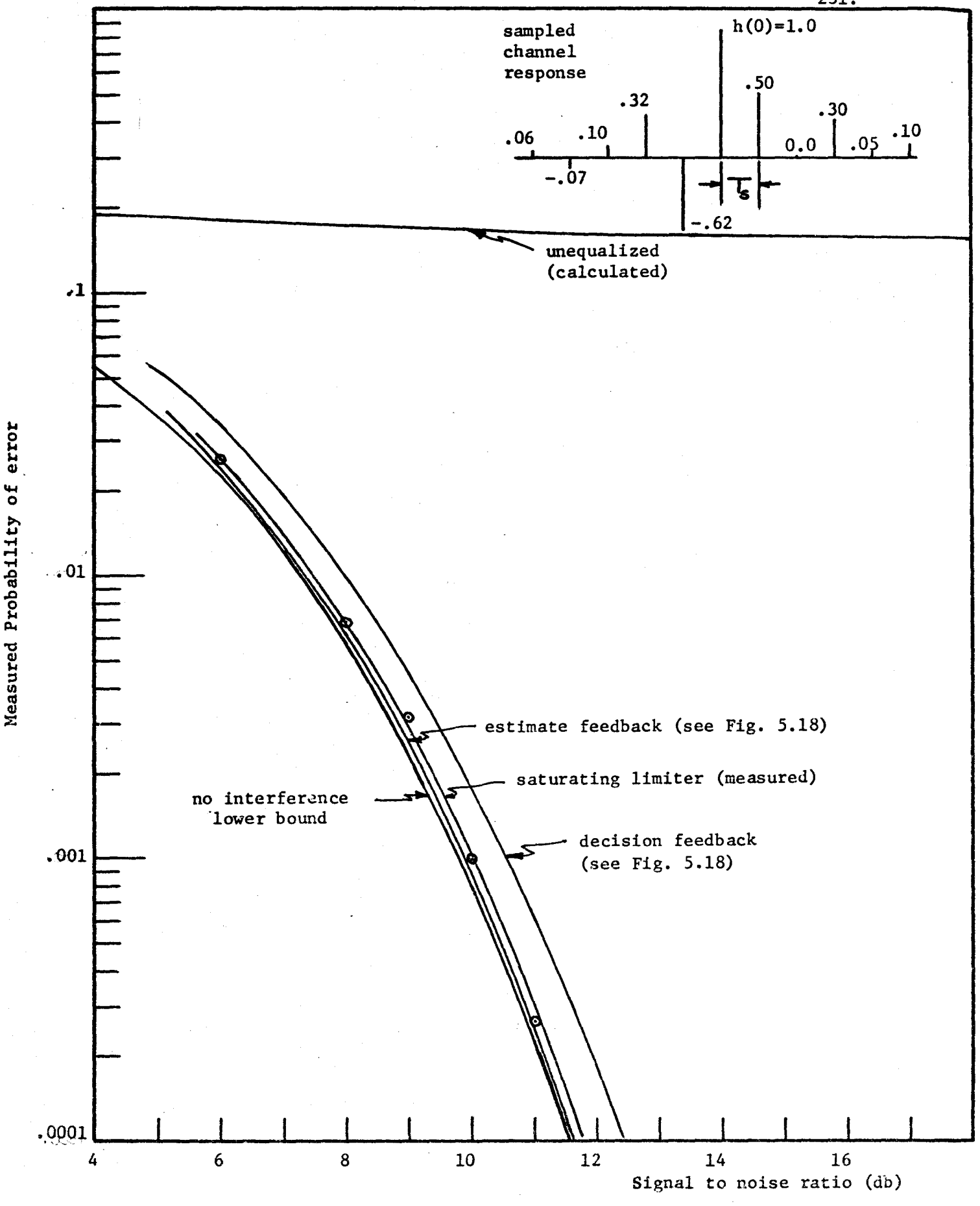

Figure 5.37 Error-rate curves for given channel response showing effects of different equalizers.

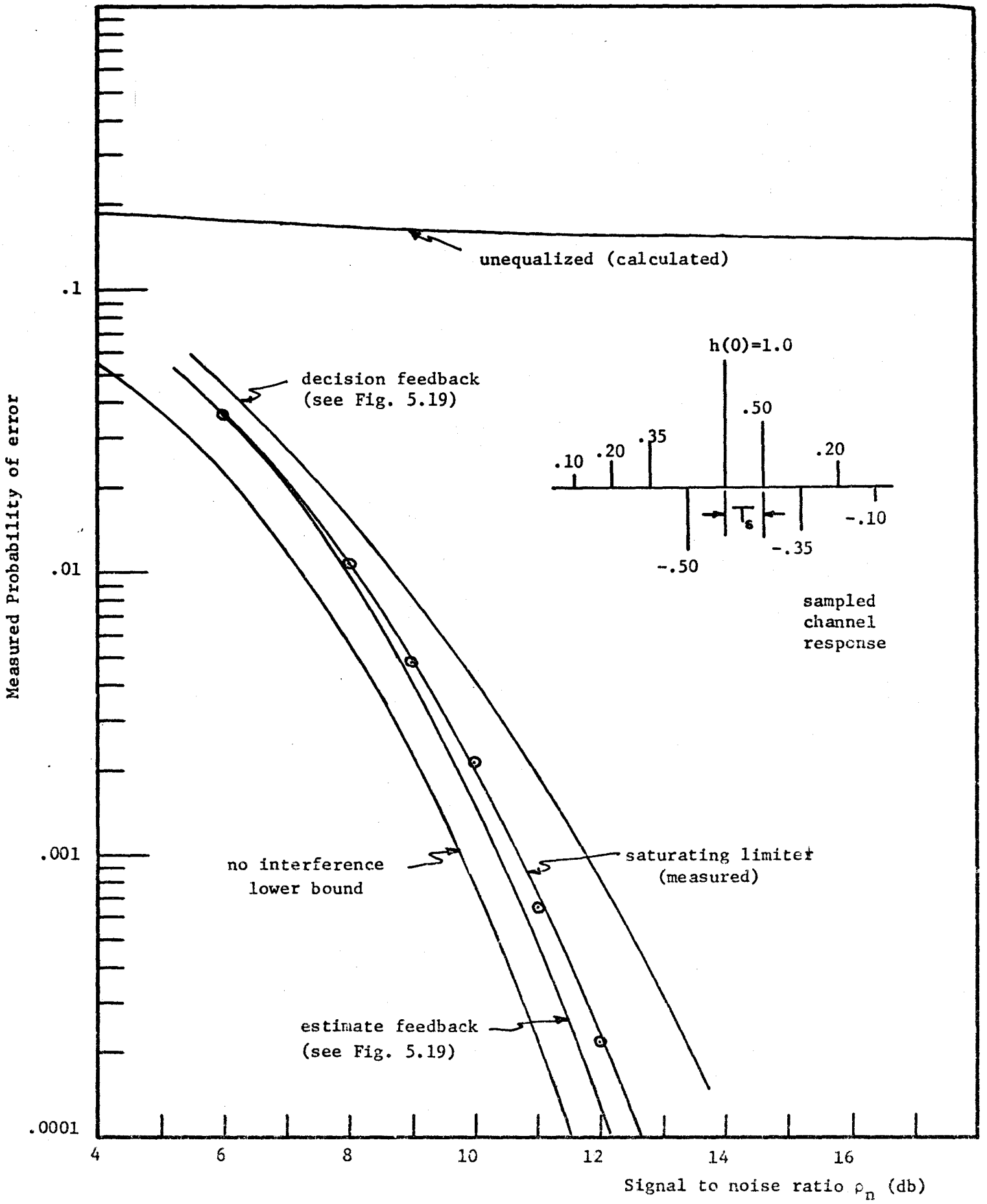

Figure 5.38 Error-rate curves for given channel response showing effects of different equalizers.

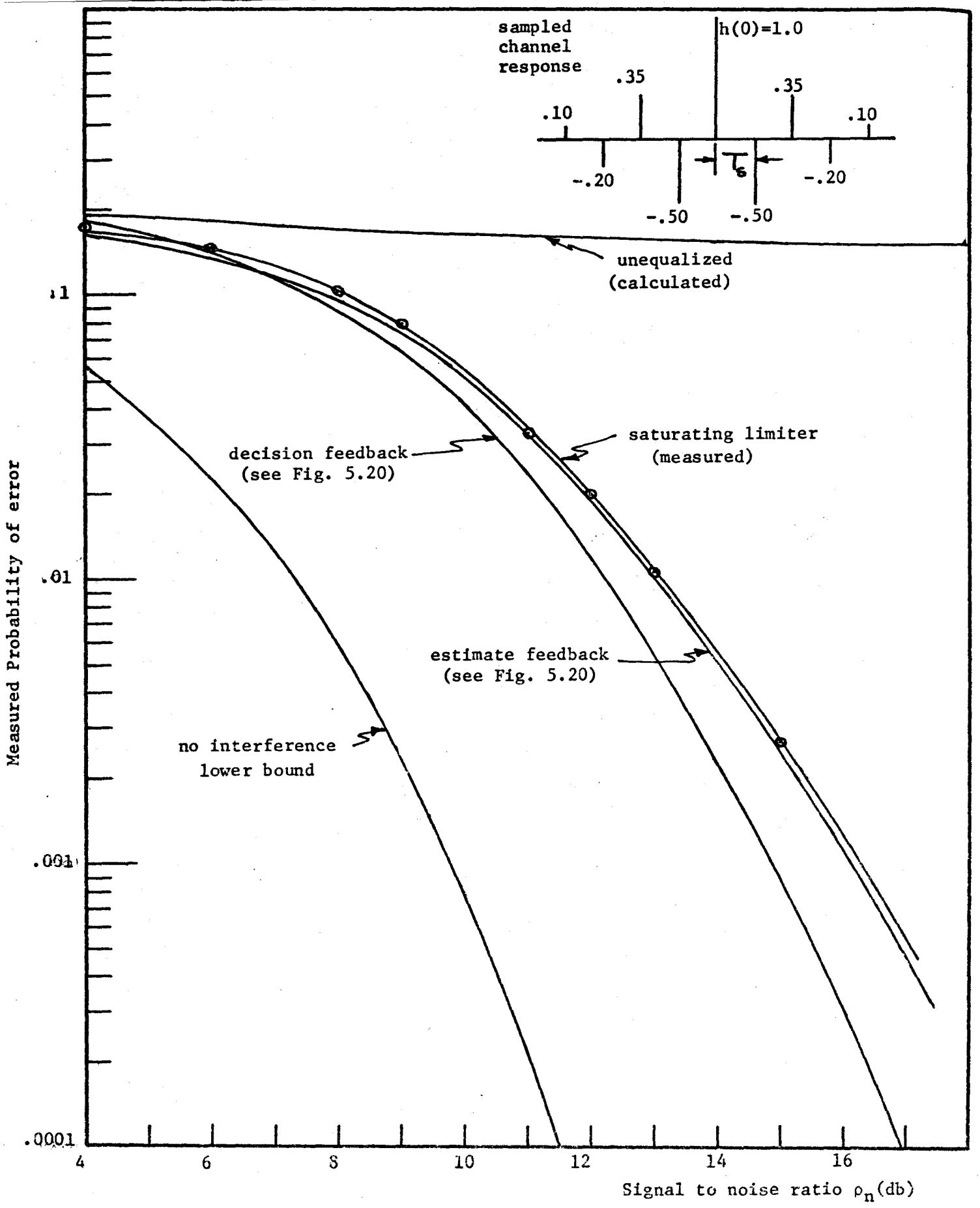

Figure 5.39 Error-rate curves for given channel response showing effects of different equalizers.

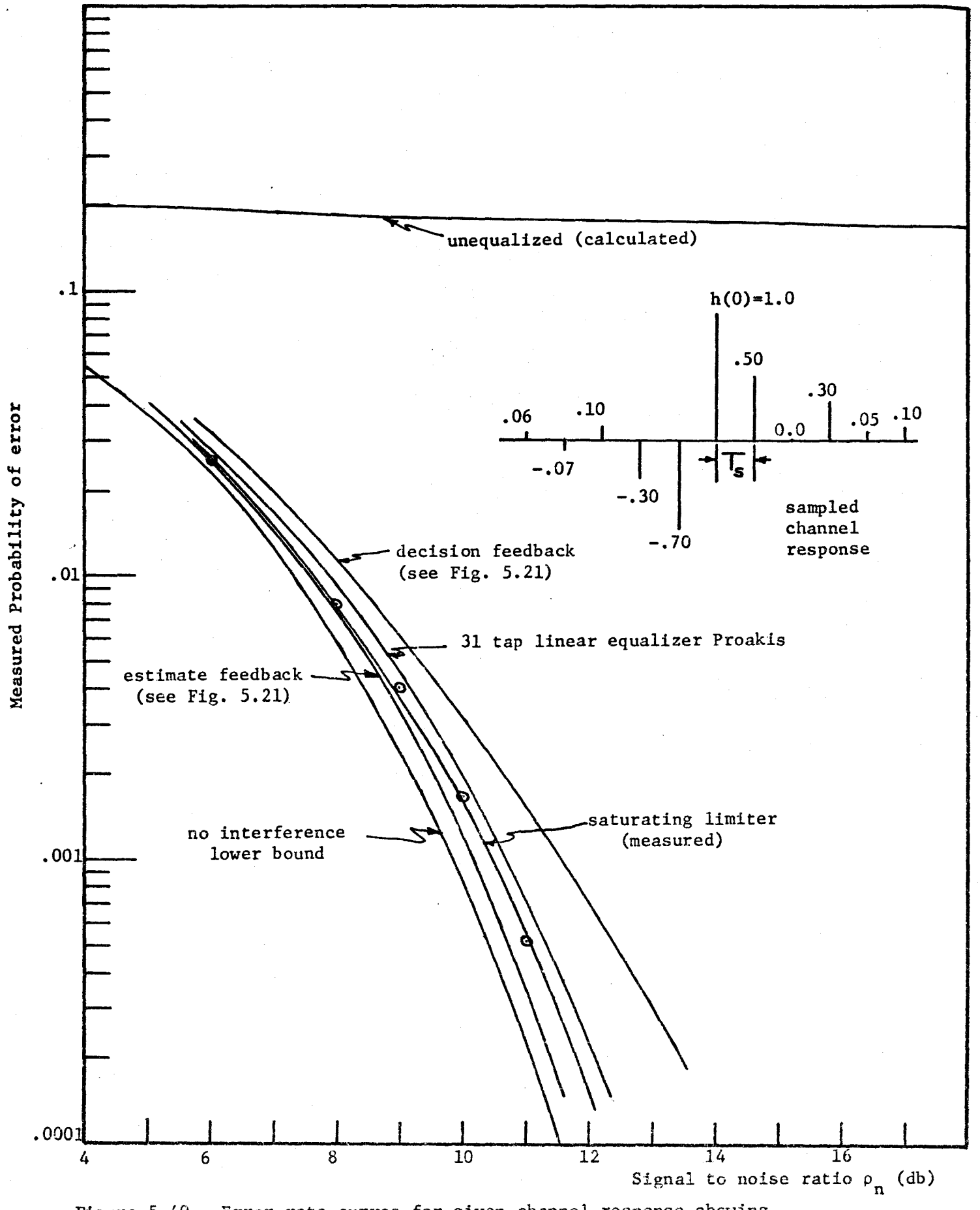

Figure 5.40 Error-rate curves for given channel response showing effects of different equalizers.

developed in chapter 4. We have compared its performance characteristics with those of the well known decision feedback equalizer, and have found that, when the channel causes both amplitude and phase distortion, the estimate feedback equalizer yields considerably better error-rate performance than either the decision feedback equalizer or a linear equalizer. We also found that the convergence characteristics of the two equalizers are comparable.

We then briefly described an approximation to the estimate feedback equalizer which uses a saturating limiter in the feedback path. Its convergence characteristics were seen to be comparable to those of the estimate feedback equalizer and its error-rate performance was seen to be only marginally worse than that of the estimate feedback equalizer.

CHAPTER 6

Conclusions and Suggestions for Further Work

6.1 Conclusions

In this thesis, we have applied Bayes estimation theory to derive a novel, unrealizable, nonlinear receiver structure for the reception of baseband digital signals. We have termed this unrealizable structure the conditional Bayes estimator or receiver and have derived the following two realizable approximations to it:

(i) A receiver consisting of a non-recursive linear filter followed by a nonlinear feedback system incorporating a soft limiter (hyperbolic tangent characteristic) in the feedback path. This is known as the estimate feedback receiver.

(ii) A receiver consisting of a nonlinear, non-recursive filter followed by the same nonlinear feedback system as in (i).

We then showed that the well known decision feedback system is a high signal to noise ratio approximation to the conditional Bayes receiver.

The second contribution of the present work was the development of a new adaptive algorithm for the iterative control of the nonlinear receiver. This algorithm was applied specifically to the structure in (i) above, and an evaluation of the performance characteristics of the resulting receiver was carried out. We found that the estimate feedback receiver yielded better performance than either the decision

feedback receiver or a linear (transversal filter) receiver, when the channel caused both amplitude and phase distortion of the signal (the typical situation on most telephone or coaxial cable channels and many radio channels). It therefore appears that the estimate feedback equalizer would be a suitable replacement for a linear or a decision feedback equalizer in any situation where it is not feasible to precede the equalizer with a filter matched to the channel response to obtain phase equalization.

We also derived a simple saturating limiter equalizer as an approximation to the estimate feedback equalizer. Its performance was evaluated and found to be comparable to, although marginally worse than that of the estimate feedback equalizer.

6.2 Suggestions for Further Work

In the present work we have derived and evaluated the estimate feedback receiver mentioned in (i) above. We have shown that its performance on channels containing both phase and amplitude distortion is superior to that of existing equalizers. However, all of this work has been confined to analysis and computer simulation, and the results which we have obtained should be verified experimentally in a carefully controlled implementation of the adaptive estimate feedback equalizer.

Also beyond deriving the basic structure, we have not pursued further any investigation into the nonlinear equalizer structure mentioned in (ii) above. More work should be conducted on this receiver with a view to making it adaptive and to evaluating its performance.

It is felt that its performance may approach quite closely to that of the optimum Bayes receiver derived by Bowen (1969).

The implementation of a complete receiver structure utilizing these nonlinear equalizers also warrants further careful study both of a theoretical and an experimental nature.

APPENDIX A

Circuit Model for a Time-Varying Channel Using a Power Series Expansion

In this appendix we briefly describe a circuit model for a time-varying channel. This model is obtained by forming a power series expansion of the equivalent low-pass channel transfer function G(t,f). This model was originally obtained by Bello (1963), and we shall make use of it in chapter 2 of the thesis where it provides a way to obtain measures of the dispersion characteristics of the channel.

Let us begin by recalling equation (2-17), namely,

$$n(t) = \int M(f)\ G(t,f)e^{j2\pi ft}df \qquad \text{(A-1)}$$

where M(f) is the amplitude spectrum of the transmitted signal m(t) and n(t) is the channel output. We now propose to expand G(t,f) in a power series in the frequency variable f, where from euqation (2-18) we have

$$G(t,f) = \int g(t,\xi)e^{-j2\pi f\xi}d\xi\ , \qquad \text{(A-2)}$$

$g(t,\xi)$ being the channel impulse response.

In all physical channels, there is some value ξ_o of the delay variable ξ about which the impulse response $g(t,\xi)$ may be assumed to be centered. In equation (A-2), let us make the transformation $\mu = \xi-\xi_o$ to obtain

$$G(t,f) = e^{-j2\pi f\xi_o} \int g(t,\mu+\xi_o)e^{-j2\pi f\mu}d\mu \qquad \text{(A-3)}$$

Then making the definition

$$g_o(t,\mu) = g(t,\mu+\xi_o) \ , \qquad \text{(A-4)}$$

which is the channel impulse response centered on the mean delay ξ_o, we may write the channel transfer function G(t,f) in the form

$$G(t,f) = e^{-j2\pi f\xi_o} \int g_o(t,\mu)e^{-j2\pi f\mu}d\mu$$

$$= e^{-j2\pi f\xi_o} G_o(t,f) \qquad \text{(A-5)}$$

From equation (A-5) we see that the presence of the mean delay ξ_o causes an exponential factor $\exp(-j2\pi f_o\xi)$ to appear in G(t,f). This factor may fluctuate very rapidly with f and would therefore cause a power series expansion of G(t,f) to converge very slowly. To avoid this problem we shall expand the function $G_o(t,f)$ in a power series in f.

Now let us assume that the signal spectrum M(f) is centered on f=0, and then let us expand the function $G_o(t,f)$ in a Taylor series in f about f=0 to obtain

$$G_o(t,f) = \sum_{n=0}^{\infty} \frac{1}{n!} \left[\frac{\partial^n G_o(t,f)}{\partial f^n} \bigg|_{f=0} \right] f^n \qquad \text{(A-6)}$$

where the derivatives are assumed to exist at least in the mean-square sense. Then using equation (A-5) we may, at least in a formal sense, evaluate these derivatives. The nth derivative in equation (A-6) may

be written, using equation (A-5), in the form

$$\frac{\partial^n G_o(t,f)}{\partial f^n} = \frac{\partial^n}{\partial f^n} \int g_o(t,\xi) e^{-j2\pi f\xi} d\xi$$

and this may readily be rewritten in the form

$$\frac{\partial^n G_o(t,f)}{\partial f^n} = (j2\pi)^n \int (-\xi)^n g_o(t,\xi) e^{-j2\pi f\xi} d\xi \qquad \text{(A-7)}$$

Then evaluating equation (A-7) at f=0, we obtain

$$\left.\frac{\partial^n G_o(t,f)}{\partial f^n}\right|_{f=0} = (j2\pi)^n \int (-\xi)^n g_o(t,\xi) d\xi \qquad \text{(A-8)}$$

We may then write the series of equation (A-6) in the form

$$G_o(t,f) = \sum_{n=0}^{\infty} \Gamma_n(t) (j2\pi f)^n \qquad \text{(A-9)}$$

where we have defined the coefficients $\Gamma_n(t)$ as

$$\Gamma_n(t) = \frac{1}{n!} \int (-\xi)^n g_o(t,\xi) d\xi \qquad \text{(A-10)}$$

Substituting equation (A-9) into equation (A-5), we obtain the time-varying transfer function G(t,f) as

$$G(t,f) = e^{-j2\pi f\xi_o} \sum_{n=0}^{\infty} \Gamma_n(t) (j2\pi f)^n. \qquad \text{(A-11)}$$

Now it can readily be shown that the factor $(j2\pi f)^n$ is the transfer function of an nth order differentiator. Thus if we substitute

equation (A-11) into equation (A-1), we can readily show that the complex low-pass channel output signal $\eta(t)$ may be written in the form

$$\eta(t) = \sum_{n=0}^{\infty} \Gamma_n(t) \frac{d^n}{dt^n} \{m(t-\xi_o)\} . \qquad \text{(A-12)}$$

Equations (A-11) and (A-12) are the defining equations for the circuit model of the channel. From equation (A-11) we see that the channel may be represented as the parallel combination of an infinite number of elementary channels. Each elementary channel consists of a differentiator of some order, followed by a time varying gain, and the overall circuit is preceded by the mean delay ξ_o. A block diagram of this circuit is shown in figure A.1.

The convergence properties of the series in equation (A-10) and the value of the remainder term when only a finite number of terms of the series is used have been examined by Bello (1963).

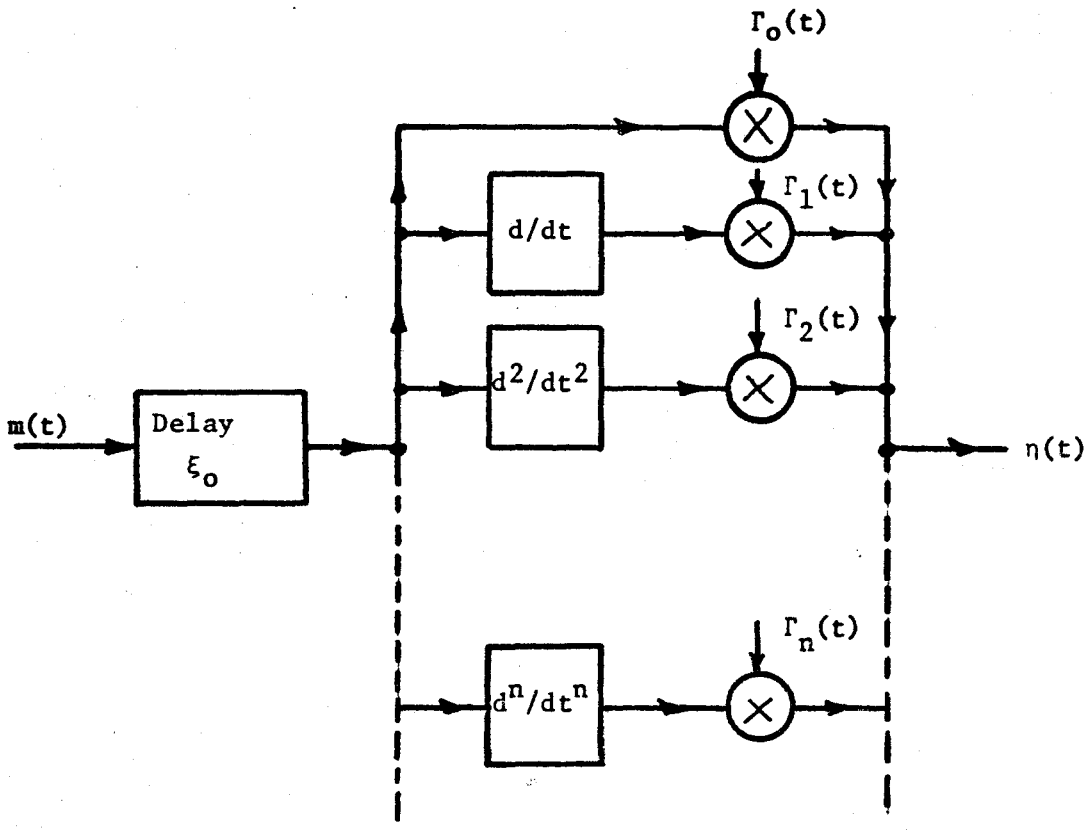

Figure A.1 Baseband circuit representation of time-varying dispersive channel obtained by power-series expansion of the channel transfer function.

APPENDIX B

A Simple Bayes Estimation Problem

In this appendix we consider a simple Bayes estimation problem. To wit, let us suppose that we sample the baseband input to a signal processing system at the times* $t=mT_s$ $(-\infty < n < \infty)$, and that these samples may be written in the form

$$x(m) = \alpha s_m + n_c(m) \qquad (-\infty < m < \infty) \qquad \text{(B-1)}$$

where the following conditions hold:

(i) The $\{s_m;\ -\infty < m < \infty\}$ are independent identically distributed binary random variables having the values ± 1 and the probability density function

$$p_s(s_m) = \frac{1}{2}\,\delta(s_m-1) + \frac{1}{2}\,\delta(s_m+1) \qquad \text{(B-2)}$$

(ii) α is some constant attenuation value. It may be regarded as the attenuation due to a channel.

(iii) The $\{n_c(m);\ -\infty < m < \infty\}$ are independent samples from a zero-mean Gaussian population with variance σ_n^2 and probability density function

$$p_n(n_c) = \frac{1}{\sqrt{2\pi}\,\sigma_n}\ \exp\left(-\frac{n_c^2}{2\sigma_n^2}\right) \qquad \text{(B-3)}$$

---

*T_s is an arbitrary sampling period which in a real situation corresponds to the transmission rate.

The problem now is to find the Baye's minimum mean square error estimate s_m^* of s_m at each time $t=mT_s$ $(-\infty < m < \infty)$ given the observation sequence $\{x(m);\ -\infty < m < \infty\}$.

At the time $t=mT_s$ (m arbitrary), the Bayes estimate may be written in the general form

$$s_m^* = E\{s_m|X\} \qquad (-\infty < n < \infty) \qquad \text{(B-4)}$$

where

$$X = \{x(m):\ -\infty < m < \infty\}$$

is a given realization (equivalent to a sample function) of the observation sequence. Because of assumptions (i) and (iii) above, the samples $\{x(m)\}$ are statistically independent, and equation (B-4) may be reduced to the simple form

$$s_m^* = E\{s_m|x(m)\} \quad . \qquad \text{(B-5)}$$

Under the further assumption that the conditional probability density function $p_s(s_m|x(m))$ exists, we may now write the required estimate s_m^* in the form

$$s_m^* = \int_{\underline{\xi}} s_n\ p_s(s_m|x(m))ds_m \qquad \text{(B-6)}$$

where the range of integration is the set $\underline{\xi}$ of all possible values of s_m (in this case 2). Applying Bayes rule, we may rewrite equation (B-6) in the form

$$s_m^* = \int_{\underline{\xi}} \frac{s_m p_x(x(m)|s_m) p_s(s_m) ds_m}{p_x(x(m))} \qquad (-\infty < m < \infty) \qquad \text{(B-7)}$$

and the problem of finding the estimate s_m^* has now been reduced to the finding of the probability density functions $p_x(x(m)|s_m)$ and $p_x(x(m))$.

Let us first find the conditional probability function $p_x(x(m)|s_m)$. From equation (B-1), the conditional random variable $x(m)|s_m$ is readily seen to be Gaussian with mean αs_m and variance σ_n^2. Its probability density function may then be written, using equation (B-3), in the form

$$p_x(x(m)|s_m) = \frac{1}{\sqrt{2\pi}\,\sigma_n} \exp\left(-\frac{(x(m)-\alpha s_m)^2}{2\sigma_n^2}\right) \qquad \text{(B-8)}$$

Now the joint probability density function $p(x(m),s_m)$ may be written in the form

$$p_{x,s}(x(m),s_m) = p_x(x(m)|s_m)\; p_s(s_m)$$

and using equations (B-2) and (B-8), this may be rewritten in the form

$$p_{x,s}(x(m),s_m) = \frac{1}{\sqrt{2\pi}\,\sigma_n} \exp\left(-\frac{(x(m)-\alpha s_m)^2}{2\sigma_n^2}\right) \cdot \left\{\frac{1}{2}\,\delta(s_m-1) + \frac{1}{2}\,\delta(s_m+1)\right\} \qquad \text{(B-9)}$$

The probability density function $p_x(x(m))$ of the received sample $x(m)$ may be written as

$$p_x(x(m)) = \int_{\xi} p_{x,s}(x(m),s_m)\,ds_m$$

If we than substitute equation (B-9) into this and carry out the required integration, we obtain the result

$$p_x(x(m)) = \frac{1}{2\sqrt{2\pi}\,\sigma_n} \exp\left[-\frac{(x(m)-\alpha)^2}{2\sigma_n^2}\right] + \frac{1}{2\sqrt{2\pi}\,\sigma_n} \exp\left[-\frac{(x(m)+\alpha)^2}{2\sigma^2}\right] \qquad \text{(B-10)}$$

We are now ready to find the required Bayes estimate. If we substitute equations (B-2), B-8) and (B-10) into equation (B-7), and carry out the indicated integration we obtain the result

$$s_m^* = \frac{\exp\left(\frac{\alpha x(m)}{\sigma_n^2}\right) - \exp\left(-\frac{\alpha x(m)}{\sigma_n^2}\right)}{\exp\left(\frac{\alpha x(m)}{\sigma_n^2}\right) + \exp\left(-\frac{\alpha x(m)}{\sigma_n^2}\right)} \qquad \text{(B-11)}$$

This may readily be written in closed form as

$$s_m^* = \tanh\left(\frac{\alpha x(m)}{\sigma_n^2}\right) \qquad \text{(B-12)}$$

which is the desired Bayes estimate. In the usual communications situation, α is normalized to unity by some form of gain control and the estimator takes on the simple form

$$s_m^* = \tanh\left(\frac{x(m)}{\sigma_n^2}\right) \qquad (-\infty < m < \infty) \qquad \text{(B-13)}$$

APPENDIX C

The Input Correlation Matrix

In the thesis the correlation matrix

$$[E\{x(m+i)x(m+j)\}] \qquad \begin{matrix}(-\infty < m < \infty)\\ (i,j = 0,1,\ldots,M)\end{matrix} \qquad \text{(C-1)}$$

of the set of input samples $\{x(m+i);\ i=0,1,\ldots,M\}$, stored in the non-recursive portion of the equalizer at any iteration time m, arises in several places. In this appendix, we will show that, under a quite general condition on the additive noise, this matrix is positive definite.

From equation (4-5), the input sample x(m) at any arbitrary iteration (or sampling) time m may be written as

$$x(m) = \sum_{k=-L}^{L} s_{m-k}h(k) + n_c(m) \quad (-\infty < m < \infty) \qquad \text{(C-2)}$$

where we assume

(i) The symbols $\{s_m\}$ are independent, identically distributed, binary random variables having the values ±1.

(ii) The $\{h(k)\}$ are samples of the received pulse shape or channel impulse response h(t) which is assumed to be non-random and of essentially finite duration.

(iii) The $\{n_c(m)\}$ are samples of stationary additive background noise. They are assumed to have zero mean, variance N_o and correlation function

$$E\{n_c(i)n_c(j)\} = N_o\rho(j-i) = N_o\rho(i-j) \qquad \text{(C-3)}$$

where $\rho(i-j)$ is a normalized correlation function with $\rho(0) = 1$.

Now let us compute the general term of the matrix defined in expression (C-1). Using equation (C-2), it may be written as

$$E\{x(m+i)x(m+j)\} = E\{\sum_{k=-L}^{L}\sum_{\ell=-L}^{L} s_{m+i-k}s_{m+j-\ell}h(k)h(\ell) + n_c(m+i)n_c(m+j)\}$$

$$i,j = 0,1,\ldots,M$$

$$-\infty < m < \infty)$$

which may at once be reduced to the form

$$E\{x(m+i)x(m+j)\} = \sum_{k=-L}^{L}\sum_{\ell=-L}^{L} E\{s_{m+i-k}s_{m+j-\ell}\}h(k)h(\ell) + N_o\rho(j-i) \qquad \text{(C-4)}$$

$$i,j = 0,1,\ldots,M$$

$$-\infty < m < \infty)$$

Let us consider the term $E\{s_{m+i-k}s_{m+j-\ell}\}$ in equation (C-4). With the use of assumption (i) above, we may write it as

$$E\{s_{m+i-k}\, s_{m+j-\ell}\} = \delta(\ell-k-j+i)$$

Then substituting this into equation (C-4) we obtain

$$E\{x(m+i)x(m+j)\} = \sum_{k=-L}^{L} h(k)h(k+j-i) + N_o\rho(j-i)$$

$$= \psi(j-i) + N_o\rho(j-i)\ . \qquad \text{(C-5)}$$

From equation (C-5), we see that the correlation matrix defined in expression (C-1) is composed of the sum of two component matrices

so that

$$[E\{x(m+i)x(m+j)\}] = [\psi(j-i)] + [N_o\rho(j-i)] \qquad i,j = 0,1,\ldots,M$$
$$-\infty < m < \infty)$$

Now let us consider the component matrix $[\psi(j-i)]$. First its diagonal terms are non-negative so that

$$\psi(i-i) = \psi(0) = \sum_{k=-L}^{L} h^2(k) \geq 0 \qquad (i = 0,1,\ldots,M)$$

and second it is symmetric since

$$\psi(j-i) = \sum_{k=-L}^{L} h(k)h(k+j-i) = \sum_{p=-L}^{L} h(p+i-j)h(p) = \psi(i-j)$$

Therefore the component matrix $[\psi(j-i)]$ is at least positive semidefinite. This means that, provided the additive noise correlation matrix $[N_o\ (j-i)]$ is positive definite*, which it is in almost all physical situations of interest, the input correlation matrix defined in expression (C-1) is positive definite and its inverse exists. This is the desired result.

---

*The only requirement needed for this to be true is that the noise power spectral density be non-zero over the bandwidth of interest. This condition holds in virtually all real communications situations.

APPENDIX D

Stability Properties of the Recursive Algorithms

DI The Algorithm for the Feedback Section

In equation (77) of the text the recursive algorithm for adaptive adjustment of the feedback gains $\{f_j(n)\}_{j=1}^{L}$ is stated as

$$f_j(n+1) = f_j(n) + \gamma E\{(s_n - y_n)\tilde{s}_{n-m}\} + \gamma \sum_{i=1}^{L} f_i(n) E\{\tilde{s}_{n-i}\tilde{s}_{n-m}\}$$

$$(j = 1,\ldots,L) \qquad (77)$$

and we now want to determine those values of the constant γ for which it is stable.

The quantity $(s_n - y_n)$ in (77) is just the error at the output of the non-recursive or forward section of the equalizer and we now define it as

$$\mu_n = s_n - y_n .$$

The algorithm may then be written as

$$f_j(n+1) = f_j(n) + \gamma E\{\mu_n \tilde{s}_{n-m}\} + \gamma \sum_{i=1}^{L} f_i(n) E\{\tilde{s}_{n-i}\tilde{s}_{n-m}\}$$

$$(j = 1,\ldots,L) \qquad (D\text{-}1)$$

For our present purposes, it is more convenient to work in matrix or vector notation, and we therefore make the following definitions:

$$\underline{F}(n) = \begin{bmatrix} f_1(n) \\ \vdots \\ f_L(n) \end{bmatrix} \tag{D-2}$$

the tap-gain vector at the nth iteration

$$\underline{K}(\mu_n,s) = \begin{bmatrix} E(\mu_n \tilde{s}_{n-1}) \\ \vdots \\ E(\mu_n \tilde{s}_{n-L}) \end{bmatrix} = \begin{bmatrix} K(\mu_n,\tilde{s}_{n-1}) \\ \vdots \\ K(\mu_n,\tilde{s}_{n-L}) \end{bmatrix}, \tag{D-3}$$

and

$$K(s,s) = \begin{bmatrix} E\{\tilde{s}_{n-1}\tilde{s}_{n-1}\} & \cdots & E\{\tilde{s}_{n-1}\tilde{s}_{n-L}\} \\ \vdots & & \vdots \\ E\{\tilde{s}_{n-L}\tilde{s}_{n-L}\} & \cdots & E\{\tilde{s}^2_{n-L}\} \end{bmatrix} \tag{D-4}$$

the positive definite correlation matrix. Using the definitions (D-2) to (D-4), the algorithm may now be written in vector form as

$$\underline{F}(n+1) = \underline{F}(n) + \gamma\underline{K}(\mu_n,s) + \gamma K(s,s)\underline{F}(n) \tag{D-5}$$

or as

$$\underline{F}(n+1) = [I + \gamma K(s,s)]\underline{F}(n) + \gamma K(\mu_n,s) \tag{D-6}$$

where I is the identity matrix. The last term on the right-hand side of (D-6) has no bearing on the stability of the algorithm, and therefore we neglect it and write

$$\underline{F}(n+1) = [I + \gamma K(s,s)]\underline{F}(n) \tag{D-7}$$

The system of (D-7) will be stable provided

$$|I + \gamma K(s,s)| < 1 \qquad \text{(D-8)}$$

Let Q be the normalized modal matrix of K(s,s). Then the following observations hold since K(s,s) is positive definite symmetric

$$Q^T = Q^{-1} \qquad \text{(D-9)}$$

$$Q^T Q = I \qquad \text{(D-10)}$$

and

$$K(s,s) = Q^T \Lambda Q \qquad \text{(D-11)}$$

where Λ is a diagonal matrix, the non-zero elements of which are the eigenvalues of K(s,s). The canonical linear transformation of (D-11) holds whether or not the eigenvalues are distinct. If there are multiple equal eigenvalues Λ is a Jordan Canonical form.

Using the transformation of (D-11) in (D-7), we obtain

$$\underline{F}(n+1) = [I + \gamma Q^T \Lambda Q]\underline{F}(n) \qquad \text{(D-12)}$$

or

$$\underline{F}(n+1) = Q^T[I + \gamma\Lambda]QF(n)$$

or

$$Q\underline{F}(n+1) = [I + \gamma\Lambda]QF(n) \qquad \text{(D-13)}$$

Making the linear transformation

$$\underline{F}'(n+1) = Q\underline{F}(n) \ , \qquad \text{(D-14)}$$

we obtain the algorithm in uncoupled form as

$$F'(n+1) = [I + \gamma\Lambda]F'(n)$$

and the stability condition (D-8) becomes

$$|[I + \gamma\Lambda]| < 1$$

or

$$|1 + \gamma\lambda_j| < 1 \qquad (j=1,\ldots,L) \qquad \text{(D-15)}$$

But K(s,s) is positive definite and thus $\lambda_j > 0$, (j=1,...,L) so that a sufficient condition for the algorithm to be stable is

$$|1 + \gamma\lambda_{max}| < 1 \qquad \text{(D-16)}$$

where λ_{max} is the maximum eigenvalue of K(s,s). From (D-16), we can at once deduce that the algorithm will be stable if γ lies in the range

$$\frac{-2}{\lambda_{max}} < \gamma < 0 \ . \qquad \text{(D-17)}$$

DII The Algorithm for the Reference Gain

The algorithm for adaptive adjustment of the reference gain $g_o(n)$ is given by equation (4-37) as

$$g_o(n+1) = g_o(n) + \frac{\alpha}{2}\frac{\partial E\{e_n^2\}}{\partial g_o(n)} \qquad \text{(4-37)}$$

where from equation* (4-24a)

$$\frac{\partial E\{e_n^2\}}{\partial g_o(n)} = -2E\{\eta_n x_n\} + 2\partial g_o(n)E\{\ _n x_n\} + 2\sum_{i=0}^{M} g_i(n)E\{x_{n+i}x_n\}$$

This algorithm may be extended to cover the entire non-recursive section of the equalizer. If we define the tap-gain vector

---

*η_n is the output of the recursive section at time n. Also in this appendix x_{n+i} is equivalent to x(n+i), (i=0,1,...,M).

$$G(n) = \begin{bmatrix} g_o(n) \\ \vdots \\ g_M(n) \end{bmatrix} \tag{D-18}$$

we may write

$$G(n+1) = G(n) + \frac{\alpha}{2} P(n) \tag{D-19}$$

where P(n) is the gradient vector

$$P(n) = -2\underline{K}_\eta + 2\partial g_o(n)\underline{K}_\epsilon + 2K(x,x)G(n) \tag{D-20}$$

with $\underline{K}_\eta$ = a column vector with entries $E\{\eta_n x_{n+j}\}$

$(j = 0,1,\ldots,M)$

$\underline{K}_\epsilon$ = a column vector with entries $E\{e_n x_{n+j}\}$

$(j = 0,1,\ldots,M)$

$K(x,x)$ = the correlation matrix $E\{x_{n+i}x_{n+j}\}$; $i,j = 0,1,\ldots,M$.

The algorithm (D-19) may then be written as

$$G(n+1) = G(n) - \alpha\underline{K}_\eta + \alpha\partial g_o(n)\underline{K}_\epsilon + \alpha K(x,x)G(n) \tag{D-21}$$

or as

$$G(n+1) = G(n) + \partial G(n) \tag{D-22}$$

where

$$\partial G(n) = \begin{bmatrix} \partial g_o(n) \\ \vdots \\ \partial g_M(n) \end{bmatrix} \tag{D-23}$$

so that

$$\partial G(n) = -\alpha \underline{K}_{\eta} + \alpha \partial g_o(n) \underline{K}_{\varepsilon} + \alpha K(x,x) G(n)$$

or

$$[\partial G(n) - \alpha \partial g_o(n) \underline{K}_{\varepsilon}] = \alpha K(x,x) G(n) - \alpha \underline{K}_{\eta} \qquad \text{(D-24)}$$

Now the identity

$$\partial g_o(n) \underline{K}_{\varepsilon} = K(\varepsilon,x) \partial G(n) \qquad \text{(D-25)}$$

holds if we define

$$K(\varepsilon,x) = \begin{bmatrix} E\{e_n x_n\} & 0 & \cdots & 0 \\ E\{e_n x_{n+1}\} & 0 & \cdots & 0 \\ \vdots & & & \vdots \\ E\{e_n x_{n+M}\} & 0 & \cdots & 0 \end{bmatrix}$$

Substititing (D-25) into (D-24) we obtain the result

$$[I - \alpha K(\varepsilon,x)] \partial G(n) = \alpha K(x,x) G(n) - \alpha \underline{K}_{\eta} \qquad \text{(D-26)}$$

Now consider the matrix

$$[I - \alpha K(\varepsilon,x)]$$

on the left-hand side of (D-26), about which we may make the following observations:

a) The identity matrix I is positive definite.

b) The second moment matrix $K(\varepsilon,x)$ is positive semi-definite.

(c) Properties (a) and (b) assure the existance of an inverse for the matrix $[I - \alpha K(\varepsilon,x)]$, provided $\alpha \leq 0$ which it must be.

(d) The last term on the right-hand side of (D-26) has no bearing on the stability of the algorithm and may be neglected from here on in order to simplify the algebra.

Thus, from (D-26), we now obtain the result

$$\delta G(n) = \alpha[I - \alpha K(\varepsilon,x)]^{-1} K(x,x)G(n)$$

or letting

$$[R_{ij}] = [I - \alpha K(\varepsilon,x)]^{-1} K(x,x)$$

we have

$$\delta G(n) = \alpha[R_{ij}]G(n) \tag{D-27}$$

Then substituting this result into equation (D-22) we obtain the result

$$G(n+1) = [I + \alpha[R_{ij}]]G(n) \tag{D-28}$$

which will be stable provided

$$|I + \alpha[R_{ij}]| < 1 \tag{D-29}$$

Now let M be the normalized modal matrix of $[R_{ij}]$. Then the following properties hold

$$M^T = M^{-1} \tag{D-30}$$

$$M^T M = I \tag{D-31}$$

and

$$[R_{ij}] = M^T \Gamma M \tag{D-32}$$

where Γ is a diagonal matrix whose non-zero values are the eigenvalues of $[R_{ij}]$, provided the eigenvalues are distinct. Otherwise Γ is a Jordan canonical form. Substituting (D-32) into (D-28) we obtain the result

$$G(n+1) = M^T[I + \alpha\Gamma]MG(n) \tag{D-33}$$

or

$$MG(n+1) = [I + \alpha\Gamma]MG(n) \tag{D-34}$$

and then letting

$$G'(n) = MG(n)$$

we obtain equation (D-34) in uncoupled form as

$$G'(n+1) = [I + \alpha\Gamma]G'(n)$$

The stability condition of equation (D-29) then becomes

$$|I + \alpha\Gamma| < 1$$

or equivalently

$$|1 + \alpha\lambda_j| < 1 \qquad (j = 0,1,\ldots,M) \tag{D-35}$$

where the $\{\lambda_j\}_{j=0}^{M}$ are the eigenvalues of $[R_{ij}]$. But these eigenvalues are all positive and therefore it is readily seen that a sufficient condition for stability is

$$|1 + \alpha\lambda_{max}| < 1 \tag{D-36}$$

where λ_{max} is the largest eigenvalue of $[R_{ij}]$. The sufficient condition (D-36) then constrains α to lie in the range

$$\frac{-2}{\lambda_{max}} < \alpha < 0 \tag{D-37}$$

in order to guarantee stability of the algorithm.

DIII The Algorithm for the Learning Weights

The recursive algorithm for adjusting the learning weights is given by equation (4-61) in the main text as

$$\alpha_i(n+1) = \alpha_i(n) + \delta \sum_{k=1}^{M} \alpha_k(n)\, E\{x_{n+k}x_{n+i}\} - \delta E\{x_n x_{n+i}\} \quad (i=1,\ldots,M)$$

. . . . (4-61)

and we now want to find those values of the constant δ for which it is stable.

As in our previous investigations of stability, it is easier to work in terms of matrices and vectors. Therefore defining

$\underline{A}(n)$ = vector of learning weights at the nth iteration

$\underline{K}_x$ = a column vector with entries $E\{x_n x_{n+i}\}$, i=1,...,M.

and

$C(x,x)$ = the MxM correlation matrix defined by

$$E\{x_{n+i}x_{n+j}\} \qquad (i,j = 1,\ldots,M)$$

we may write the algorithm of equation (4-61) in vector form as

$$\underline{A}(n+1) = \underline{A}(n) + \delta C(x,x)A(n) - \delta \underline{K}_x \qquad \text{(D-38)}$$

The last term in (D-38) has no bearing on the stability of the algorithm and thus may be dropped; so that the algorithm may be written as

$$\underline{A}(n+1) = [I + \delta C(x,x)]\, \underline{A}(n) \qquad \text{(D-39)}$$

This algorithm will thus be stable if

$$|I + \delta C(x,x)| < 1 \qquad \text{(D-40)}$$

Now let N be the normalized modal matrix of the positive-definite correlation matrix C(x,x). We then have the following properties for N

$$N^T = N^{-1} \qquad \text{(D-41)}$$

$$N^T N = I \qquad \text{(D-42)}$$

and

$$C(x,x) = N^T \sum N \qquad \text{(D-43)}$$

where $\sum$ is a diagonal matrix whose non-zero elements are the eigenvalues σ_j; j=1,...,M of C(x,x). Since C(x,x) is positive-definite

$$\sigma_j > 0 \qquad (j = 1,\ldots,M) \quad .$$

Using (D-42) and (D-43), we may now write (D-39) as

$$\underline{A}(n+1) = [I + \delta N^T \sum N]\, \underline{A}(n)$$

which may be rewritten as

$$\underline{A}(n+1) = N^T[I + \delta\sum]N\underline{A}(n)$$

or

$$N\underline{A}(n+1) = [I + \delta\sum]N\underline{A}(n) \qquad \text{(D-44)}$$

If we now let

$$\underline{A}'(n) = N\underline{A}(n)$$

we obtain the algorithm in uncoupled form as

$$\underline{A}'(n+1) = [I + \delta\sum]\underline{A}(n)$$

and the stability condition (D-36) becomes

$$|I + \delta\Sigma| < 1$$

or equivalently

$$|1 + \delta\sigma_j| < 1 \qquad (j = 1,\ldots,M)$$

If we now choose the largest of the eigenvalues σ_j and denote it σ_{max}, then a sufficient condition for the algorithm to be stable is

$$|1 + \delta\sigma_{max}| < 1$$

which constrains the constant δ to lie in the range

$$\frac{-2}{\sigma_{max}} < \delta < 0 \ .$$

BIBLIOGRAPHY

Austin, M,E, (August, 1967). Decision Feedback Equalization for Digital Communication over Dispersive Channels. M.I.T. Lincoln Lab., Lexington, Mass., Tech. Rept. 437.

Balakrishnan, A.V. (Dec., 1960). Estimation and Detection Theory for Multiple Stochastic Processes. J. Math. Analysis and Applications, vol. 1, pp. 386-410.

Bello, P.A. (Dec., 1963). Characterization of Randomly Time-Variant Linear Channels. IEEE Trans. on Comm. Systems. Cs-11, No. 4, pp. 360-393.

Bennett, W.R. and Davey, J.R. (1965). Data Transmission. McGraw-Hill Book Company, New York.

Bowen, R.R. (July, 1969). Bayesian Decision Procedure for Interfering Digital Signals. IEEE Trans. on Inform. Theory (Corresp.), vol. IT-15, No. 4, pp. 506-507.

Coll, D.C. (Dec., 1966). A System for the Optimum Utilization of Pulse Communication Channels. Defence Research Telecommunications Establishment DRTE Rept. No. 1168.

Costas, J.P. (Dec., 1956). Synchronous Communication. Proc. IRE, vol. 44, pp. 1713-1718.

Davenport, W.B. and Root, W.L. (1958). An Introduction to the Theory of Random Signals and Noise. McGraw-Hill Book Co. Inc., New York.

deBuda, R. (Aug., 1965). A Comment on the paper "Matched Filters for Interfering Signals" by D.A. George. Canadian General Electric technical memorandum RQ65EE29.

———— (Sept., 1970). Phaselock to a Suppressed Carrier in Additive Gaussian Noise. Canadian General Electric technical rept. RQ70EE7.

Deutsch, R. (1965). Estimation Theory. Prentice-Hall, Inc., Englewood Cliffs, N.J.

Di Toro, M.J. (Oct., 1968). Communication in Time-Frequency Spread Media Using Adaptive Equalization (invited Paper). Proc. IEEE, vol. 56, No. 10, pp. 1653-1679.

Dugundji, J. (March, 1958). Envelopes and Pre-envelopes of Real Waveforms. IRE Trans. on Inform. Theory, PGIT-14, No. 1, p. 53.

George, D.A. (Jan., 1965). Matched Filters for Interfering Signals. IEEE Trans. Inform. Theory (Corresp.), vol. IT-11, pp. 153-154.

George, D.A., Coll, D.C., Kaye, A.R. and Bowen, R.R. (1969). Channel Equalization for Data Transmission. A paper presented to the EIC Conference, Vancouver, B.C., September, 1969.

George, D.A., Bowen, R.R. and Storey, J.R. (June, 1971). An Adaptive Decision Feedback Equalizer. IEE Trans. Comm. Tech., vol. COM-19, pp. 281-293.

Gersho, A. (1968). Convergence Properties of an Adaptive Filtering Algorithm. Proc. Asilomar Conf. on Circuits and Systems.

———— (Oct., 1968a). Adaptation in a Quantized Parameter Space. Sixth Annual Allerton Conference on Circuit and System Theory. Monticello, Illinois.

———— (Jan., 1969). Adaptive Equalization of Highly Dispersive Channels for Data Transmission. Bell Syst. Tech. J., vol. 48, pp. 55-70.

———— (April, 1969a). Linear Adaptation. Proc. Polytechnic Inst. of Brooklyn Symposium on Computer Processing in Communications, April, 1969.

Gibby, R.A. and Smith, J.W. (Sept., 1965). Some Extensions of Nyquist's Telegraph Transmission Theory. Bell Syst. Tech. J., vol. 44, pp. 1487-1510.

Hancock, J.C. and Wintz, P.A. (1966). Signal Detection Theory. McGraw-Hill Book Company, New York.

Kailath, T. (June, 1960). Correlation Detection of Signals Perturbed by a Random Channel. IRE Trans. on Inform. Theory, vol. IT-6, pp. 361-366.

———— (1960a). Characterization of Time Variant Dispersive Channels. Lectures on Communication System Theory. E.J. Baghdady ed. McGraw-Hill Book Company, New York.

———— (1961). Optimum Receivers for Randomly Varying Channels. Fourth London Symposium on Inform. Theory. Butterworth Scientific Press, London.

Kalman, R.E. (March, 1960). A New Approach to Linear Filtering and Prediction Problems. Trans. ASME J. Basic Engrg. Ser. D., vol. 82, pp. 35-45.

Kalman, R.E. and Bucy, R.S. (March, 1961). New Results in Linear Filtering and Prediction Theory. Trans. ASME J. Basic Engrg. Ser. D., vol. 83, pp. 95-108.

Kaye, A.R. (April, 1968). Reception of Digital Signals over Randomly Time Variant Dispersive Channels. Ph.D. Thesis, Carleton University.

Kennedy, R.S. (1969). Fading Dispersive Communication Channels. John Wiley and Sons, New York.

Keeler, R.J. (1971). Construction and Evaluation of a Decision Feedback Equalizer. Proc. Internation. Communications Conf., Montreal.

Lang, G.R. and Brackett, P. (Aug., 1970). The Frequency Controlled Loop: A New Phase-Lock System. A paper presented to the fifth biennial Symposium on Communication Theory and Signal Processing, Queen's University, Kingston, Ontario.

Lender, A. (Oct., 1970). Decision-Directed Digital Adaptive Equalization Techniques for High-Speed Data Transmission. IEEE Trans. on Comm. Tech., vol. COM-18, pp. 625-632.

Lucky, R.W. (April, 1965). Automatic Equalization for Digital Communications. Bell Syst. Tech. J., vol. 44, pp. 547-588.

———— (Feb., 1966). Techniques for Adaptive Equalization of Digital Communication Systems. Bell Syst. Tech. J., vol. 45, pp. 255-286.

Lucky, R.W. and Rudin, H.R. (Nov. 1967). An Automatic Equalizer for General Purpose Communication Channels. Bell Syst. Tech. J., vol. 46, pp. 2179-2208.

Lucky, R.W., Salz, J. and Weldon, E.J. (1968). Principles of Data Communication. McGraw-Hill Book Co., New York.

Luenberger, D.G. (1969). Optimization by Vector Space Methods. John Wiley and Sons, Inc., New York.

Mark, J.W. (Aug., 1970). Adaptive Signal Processing for Digital Communication over Dispersive Unknown Channels. Ph.D. Thesis, McMaster University.

Monsen, P. (Jan., 1971). Feedback Equalization for Fading Dispersive Channels. IEEE Trans. on Inform. Theory, vol. IT-17, pp. 56-64.

Niessen, C.W. and Willim, D.K. (Aug., 1970). Adaptive Equalizer for Pulse Transmission. IEEE Trans. on Comm. Tech., vol. COM-18, pp. 377-395.

Nuttall, A.H. (July, 1962). Error Probabilities for Equicorrelated M-ary Signals Under Phase-Coherent and Phase-Incoherent Reception. IRE Trans. on Inform. Theory, vol. IT-8, pp. 305-314.

Nyquist, H. (1928). Certain Topics in Telegraph Transmission Theory. Trans. AIEE, vol. 47, pp. 617-644.

Peterson, W.W. (1961). Error-Correcting Codes. MIT Press, Wiley, New York.

Proakis, J.G. and Miller, J.H. (July, 1969). An Adaptive Receiver for Digital Signalling Through Channels with Intersymbol Interference. IEEE Trans. on Inform. Theory, vol. IT-15, pp. 484-497.

Proakis, J.G. (1970). Adaptive Digital Filters for Equalization of Telephone Channels. IEEE Trans. on Audio and Electroacoustics, vol. AU-18, pp. 195-200.

Richters, J.S. (Nov., 1967). Communication over Fading Dispersive Channels. MIT, Res. Lab. of Electronics, Tech. Report 464.

Schwartz, M., Bennett, W.R. and Stein, S. (1966). Communication Systems and Techniques. McGraw-Hill Book Company, New York.

Shannon, C.E. (1948). A Mathematical Theory of Communication. Bell Syst. Tech. J., vol. 27, pp. 379-423 and pp. 623-656.

Shimbo, O. and Celebiler, M.I. (April, 1971). The Probability of Error Due to Intersymbol Interference and Gaussian Noise in Digital Communication Systems. IEEE Trans. on Comm. Tech., vol. COM-19, pp. 113-119.

Taylor, D.P. (May, 1971). Nonlinear Feedback Equalizer Employing a Soft Limiter. Electronics Letters, vol. 7, pp. 265-267.

Tufts, D.W. (Sept., 1963). Nyquist's Problem in Pulse Transmission Theory. Cruft Lab. Tech. Rept. 425.

Tufts, D.W. and Berger, T. (April, 1967). Optimum Pulse Amplitude Modulation Part I: Transmitter-Receiver Design and Bounds from Information Theory. IEEE Trans. on Inform. Theory, vol. IT-13, pp. 196-208.

Turin, G.L. (1956). Communication Through Noisy Random Multipath Channels. IRE Conv. Rec., pt. 4, pp. 154-166.

———— (June, 1960). An Introduction to Matched Filters. IRE Trans. on Inform. Theory, vol. IT-6, pp. 311-329.

Ungerboeck, G. (Dec., 1971). Nonlinear Equalization of Binary Bipolar Signals in Gaussian Noise. IEEE Trans. on Comm. Tech., vol. COM-19, pp. 1128-1137.

Van Trees, H.L. (Mar., 1964). Optimum Power Division in Coherent Communication Systems. IEEE Trans., vol. SET-10, pp. 1-9.

———— (1968). Detection, Estimation and Modulation Theory, Part I. John Wiley and Sons, New York.

Vulikh, B.Z. (1963). Introduction to Functional Analysis for Scientists and Technologists. Pergamon Press. (1968, Addison-Wesley).

Widrow, B. (Dec., 1966). Adaptive Filters I: Fundamentals. Stanford Systems Theory Lab., Stanford University, Stanford, Calif., Tech. Rept. 6764-6.

Wiener, N. (Feb., 1942). The Extrapolation, Interpolation and Smoothing of Stationary Time Series. Report of the Services 19, Research Project DIC-6037, M.I.T. (also 1949, Wiley).

Zadch, L.A. and Ragazzini, J.R. (July, 1950). An Extension of Wiener's Theory of Prediction. Jour. Appl. Phys., vol. 21, pp. 645-655.